



HAL
open science

Urban growth simulations in order to represent the impacts of constructions and environmental constraints on urban sprawl

Mojtaba Eslahi

► **To cite this version:**

Mojtaba Eslahi. Urban growth simulations in order to represent the impacts of constructions and environmental constraints on urban sprawl. Modeling and Simulation. Université Paris-Est, 2019. English. NNT : 2019PESC2063 . tel-02493929

HAL Id: tel-02493929

<https://theses.hal.science/tel-02493929>

Submitted on 28 Feb 2020

HAL is a multi-disciplinary open access archive for the deposit and dissemination of scientific research documents, whether they are published or not. The documents may come from teaching and research institutions in France or abroad, or from public or private research centers.

L'archive ouverte pluridisciplinaire **HAL**, est destinée au dépôt et à la diffusion de documents scientifiques de niveau recherche, publiés ou non, émanant des établissements d'enseignement et de recherche français ou étrangers, des laboratoires publics ou privés.

THÈSE

Université PARIS-EST
Ecole Doctorale MSTIC

Discipline : Sciences et Technologies de l'Information Géographique

Mojtaba ESLAHI

Simulations de croissance urbaine pour représenter les impacts possibles des constructions et des contraintes environnementales sur l'étalement urbain - Constructibilité et application à l'étalement urbain

Urban growth simulations in order to represent the impacts of constructions and environmental constraints on urban sprawl - Constructibility and application to urban sprawl

École Spéciale des Travaux Publics (ESTP-Paris)
Institut de Recherche en Constructibilité (IRC)

Novembre 2019

Président du jury :	Monsieur Gilles GESQUIERE Professeur, Université de Lyon
Rapporteur :	Madame Myriam SERVIÈRES Maître de conférences, HDR, Ecole Centrale de Nantes
Rapporteur :	Monsieur Dominique BADARIOTTI Professeur, Université de Strasbourg
Examineur :	Monsieur Rani EL MEOUCHE Enseignant chercheur, IRC, ESTP-Paris
Examineur :	Monsieur Youssef DIAB Professeur, Université Paris-Est Marne-la- Vallée
Examineur :	Monsieur Matteo CAGLIONI Maître de conférences, Université Nice Sophia Antipolis
Directeur :	Madame Anne RUAS Professeur, Université de Marne-la-Vallée

Acknowledgements

I cordially thank Professor Dominique BADARIOTTI and Doctor Myriam SERVIÈRES for accepting to review this work from technical point of view. Many thanks to Professor Gilles GESQUIERE, Professor Youssef DIAB and Doctor Matteo CAGLIONI for being part of my thesis jury. I would like to thank my thesis director, Professor Anne RUAS, and my thesis co-director, Doctor Rani EL MEOUCHE, for all their supports and advices throughout this journey.

I would greatly thank the foundation of ESTP to finance this research. I wish to thank ESTP Paris and IRC for the opportunity they gave me. I would like to thank all my directors, colleagues and friends, for their companionship and supports.

My pure thanks to my lovely parents, and my beloved sisters, without the supports of whom I could not continue. Last but not least, I owe appreciation and sincere thanks to my incredible and lovely wife who has stood by me through all these years.

And to every person who has been there. Thank you all ...

This thesis is developed under the concept of constructibility in urban systems. Constructibility Research Institute (IRC), ESTP Paris has proposed the new concept of constructibility, in order to integrate performance-based approaches and process management methods. IRC develops its entire research themes based on constructability.

IRC defines the term of constructibility as an approach that aims to provide a reasoned insurance, from the beginning as to the achievement of the objectives of any construction project throughout its life cycle (Gobin, 2010). Constructibility is a new discipline that offers several methods and approaches in order to control the risks of a change in performance and provides a concrete response to the construction industry as well as their complexities. This concept originates from two terms of buildability and constructability which aims to reach and guarantee performance level of constructions and the process of modeling (Contrada, 2019). Buildability is described as the practice to be adopted by the designer for the purpose of facilitating the building construction (CIRIA, 1983). The term constructability enhance buildability extending the practice of sharing knowledge to the whole construction lifecycle (CII, 1986).

Cities are complex dynamic systems and several factors can affect the successful progress of the process of urban modeling. In the process of urban modeling, the model should respect several constraints and rules which may result in increasing its complexity. It is worth noting that this complexity of the cities can influence the performance of the modeling. Our proposed method in constructibility framework aims to improve our understanding of the urban growth simulations by representing the impacts of constructions and environmental constraints on urban sprawl. The purpose of this research is to give different images of the city of tomorrow for applying it to urban management and help the public policies decision making and constructibility can increase the performance level of the modeling in this process.

Table of Contents

Acknowledgements	i
Résumé	1
Abstract	3
Introduction	5
Chapter 1 : Urbanization and Urban Modeling	11
1.1. Urbanization	12
1.1.1. The Impacts of Urbanization	14
1.1.1.1. The Impacts of Urbanization on Environment	15
1.1.1.2. The Impacts of Urbanization on Agricultural Lands	16
1.1.1.3. Policies to Limit Agricultural Land Changes	16
1.1.2. Urbanization in France	16
1.1.2.1. Urbanization Measurements	18
1.1.2.2. Avoid or Reducing the Effects of Urbanization	20
1.2. Urban Modeling	21
1.2.1. Land Use Patterns	22
1.2.1.1. Concentric Zone Model	23
1.2.1.2. Sector Model	24
1.2.1.3. Multiple Nuclei Model	24
1.2.2. Sustainable Urban Modeling: An Overview on Different Techniques of Simulating Urban Growth and Land Use / Land Cover Change	25
1.2.2.1. Fractal Modeling	26
1.2.2.2. Artificial Neural Networks Modeling	27
1.2.2.3. Agent Based Modeling	29
1.2.2.4. Cellular Automata (CA) Modeling	31
1.2.2.4.1. SLEUTH CA Model	35
1.2.2.4.2. Advantages of SLEUTH	36
1.2.2.4.3. Limitation of SLEUTH	36
1.2.2.4.4. Some Evolutions and Applications of SLEUTH	37
1.3. Chapter Conclusion	38
Chapter 2 : Methodology and Fundamentals for Model Construction	41
2.1. Simulation Methodology to Investigate the Effects of Environmental Constraints and Constructions on Urban Sprawl	42
2.2. SLEUTH Urban Growth Model Structure	44
2.2.1. Growth Cycle	45
2.2.2. Growth Coefficients	46

2.2.3.	Growth Rules	46
2.2.3.1.	Spontaneous Growth	47
2.2.3.2.	New Spreading Center Growth	47
2.2.3.3.	Edge Growth	48
2.2.3.4.	Road Influenced Growth	48
2.2.4.	Self-Modification	49
2.3.	Urban Growth Modeling Considering Environmental Constraints Scenarios	50
2.3.1.	SLEUTH-3r Modifications to the SLEUTH	50
2.3.2.	Calibration of the SLEUTH-3r Model and Determining the Goodness of Fit	52
2.3.3.	Defining our Environmental-based Scenarios.....	56
2.3.3.1.	Scenario Protection Level 0 (Nearly No Environmental Protection - NEP)	57
2.3.3.2.	Scenario Protection Level 1 (Limited Environmental Protection - LEP).....	57
2.3.3.3.	Scenario Protection Level 2 (Moderate Environmental Protection - MEP).....	57
2.3.3.4.	Scenario Protection Level 3 (Extreme Environmental Protection - EEP).....	58
2.3.3.5.	Attraction-based Scenario Protection Level 1 (Attraction-based Limited Environmental Protection - ALEP).....	58
2.3.4.	Model Forecasting.....	59
2.3.5.	Model Evaluation and Investigation the Impacts of Urbanization Determinants on Model	60
2.4.	Integrate the Type of Buildings and Demography on Urban Sprawl Simulation	60
2.4.1.	Determinants and Impacts of Building Types on Urban Sprawl.....	61
2.4.1.1.	Building Type Classification.....	61
2.4.1.2.	Classifying the Existing Buildings	63
2.4.1.3.	Creating Building Type Matrix (Active Land Use Model).....	64
2.4.2.	Determinants and Impacts of Population Growth on Urban Sprawl.....	66
2.4.2.1.	Demographic Data	66
2.4.2.2.	Population Growth Estimation	67
2.5.	Urban Fabric Scenarios and Urban Configuration	67
2.6.	3D Representation of Prospective Urban Growth Simulations.....	69
2.7.	Chapter Conclusion.....	69
Chapter 3 : Application of the Model to Diversify the Simulations of Urban Sprawl		71
3.1.	General Presentation of Study Areas	72
3.2.	Developing Different Simulation Scenarios to Illustrate the Impacts of Environmental Constraints, Construction and Population on the Growth of a Metropolis - Toulouse Metropolis	73
3.2.1.	Data and Materials - Toulouse	76
3.2.2.	Environmental Constraints Scenarios - Toulouse	79
3.2.2.1.	Scenario Protection Level 0 (Nearly No Environmental Protection - NEP)	81
3.2.2.2.	Scenario Protection Level 1 (Limited Environmental Protection - LEP).....	83
3.2.2.3.	Scenario Protection Level 2 (Moderate Environmental Protection - MEP).....	85
3.2.2.4.	Scenario Protection Level 3 (Extreme Environmental Protection - EEP).....	86
3.2.2.5.	Attraction-based Scenario Protection Level 1 (Attraction-based Limited Environmental Protection - ALEP).....	89
3.2.3.	2D Urban Growth Simulations - Toulouse	91
3.2.4.	Urban Fabric Scenarios - Toulouse.....	100
3.2.4.1.	Building Type Classification.....	100
3.2.4.2.	Creating Building Type Matrix and Urban Weighting the Patches	103
3.2.4.3.	Demography and Population Management	103
3.2.4.4.	Implementation, Results and Discussion	104

3.3.	Developing Different Simulation Scenarios to Illustrate the Impacts of Environmental Constraints, Construction and Population on the Growth of a town - Saint Sulpice la Pointe peri-urban	109
3.3.1.	Data and Materials - Saint Sulpice la Pointe	110
3.3.2.	Environmental Constraints Scenarios - Saint Sulpice la Pointe	110
3.3.3.	2D Urban Growth Simulations - Saint Sulpice la Pointe	117
3.3.4.	Urban Fabric Scenarios - Saint Sulpice la Pointe.....	122
3.4.	Developing Different Simulation Scenarios to Illustrate the Impacts of Environmental Constraints, Construction and Population on the Growth of a small community - Rieucros rural area	125
3.4.1.	Data and Materials - Rieucros	126
3.4.2.	Environmental Constraints Scenarios - Rieucros	126
3.4.3.	2D Urban Growth Simulations - Rieucros	133
3.4.4.	Urban Fabric Scenarios - Rieucros.....	138
3.5.	The Impacts of Pixel Size and Calibration on Sustainability of Model	140
3.6.	Chapter Conclusion	143
Chapter 4 : Creation of Fictive 3D Buildings to Facilitate the Interpretation of Simulation Results and Differentiate Scenarios		145
4.1.	3D Urban Generating Applications and Procedure	146
4.2.	From Pixel to 3D Building Representation	149
4.2.1.	From Pixel to Polygon	151
4.2.2.	Positioning the Building footprints	153
4.2.3.	Configuration the Building footprints	156
4.2.4.	Building Footprints Generation.....	159
4.2.5.	Positioning Building Representations according to Urban Fabric Scenarios.....	161
4.3.	3D Visualization of the City of Tomorrow	165
4.4.	Chapter Conclusion	167
Chapter 5 : Conclusion and Perspectives		169
Annex A: Classified List of Researches and Applications of Simulating Urban Growth and Land Use / Land Cover Change.....		175
Annex B: SLEUTH Urban Growth Model Process Flow and the Scenario File Description		183
B.1.	Data Set Preparation	183
B.2.	Scenario File	184
B.3.	Model Execution	195
Annex C: Coefficients and Calibration		197
C.1.	Dispersion Coefficient Multiplier.....	197
C.2.	Best-Fit Coefficients.....	203
Annex D: Weighting Urban Patches Using Predefined Urban Land Use Models		209
D.1.	Toulouse Concentric Zone Model	209
D.2.	Toulouse Sector Model	210
D.3.	Toulouse Multiple Nuclei Model	211
D.4.	Toulouse Particular Complex Model.....	212

Annex E: INSEE Data Documentations.....	215
E.1. Number of Inhabited.....	215
E.2. List and Description of Variables - Table of Tiles	215
E.3. List and Description of Variables - Table of Rectangles	216
Publications	217
Bibliography.....	219

List of figures

<i>Figure 1. Structure of the thesis process flow</i>	8
<i>Figure 1. 1. Proportions of urban and rural world population, from 1950 to 2050; (United Nations, 2018)</i>	12
<i>Figure 1. 2. Total population, urban population and urbanization rates from 1950 to 2050; (United Nations, 2018)</i>	13
<i>Figure 1. 3. Urban sprawl physical patterns; (Galster et al., 2001)</i>	22
<i>Figure 1. 4. Concentric zone model (R. E. Park et al., 1925)</i>	23
<i>Figure 1. 5. Sector model (H. Hoyt, 1939)</i>	24
<i>Figure 1. 6. Multiple nuclei model; (Harris & Ullman, 1945)</i>	25
<i>Figure 1. 7. a: Sierpinski carpet construction, b: Design of fractal urban growth model development in the touristic village of Pogonia Etoloakarnanias, western Greece; (Triantakonstantis, 2012)</i>	27
<i>Figure 1. 8. a: hexagonal ANN, b: ANN neighborhood; (Weisner and Cowen, 1997)</i>	28
<i>Figure 1. 9. A comparison of the PSO-CA and the logistic-CA model; (Feng et al., 2011)</i>	33
<i>Figure 1. 10. The simulation accuracies of the PSO-CA model at different spatial scales using overall accuracy and kappa coefficient; (Feng et al., 2011)</i>	33
<i>Figure 1. 11. Components of agreement and disagreement for RF-CA using bootstrap aggregate, SVM-CA simulated land use map; and LR-CA simulated land use map (Kamusoko and Gamba, 2015)</i>	34
<i>Figure 1. 12. SLEUTH inputs data; (Clarke, K.C., 2008)</i>	35
<i>Figure 1. 13. State of cells according to four growth rules of SLEUTH; (Clarke, K.C., 2008)</i>	36
<i>Figure 2. 1. The proposed method procedure</i>	43
<i>Figure 2. 2. Worldwide Application of SLEUTH Land Use Change Model extracted from the published applications of SLEUTH until 2012 (Chaudhuri et al., 2013)</i>	44
<i>Figure 2. 3. Structure of the SLEUTH model (Chaudhuri et al., 2013)</i>	45
<i>Figure 2. 4. SLEUTH growth cycle</i>	46
<i>Figure 2. 5. Spontaneous growth example (Project Gigalopolis, 2018)</i>	47
<i>Figure 2. 6. New spreading center growth example (Project Gigalopolis, 2018)</i>	47
<i>Figure 2. 7. Edge growth example (Project Gigalopolis, 2018)</i>	48
<i>Figure 2. 8. Road influenced example (Project Gigalopolis, 2018)</i>	49
<i>Figure 2. 9. Self-modification (Project Gigalopolis, 2018)</i>	50
<i>Figure 2. 10. a: Illustration of the search algorithm in the original SLEUTH (Jantz et al., 2010); b: Illustration of the search algorithm in the original SLETH-3r</i>	52
<i>Figure 2. 11. Calibration, concept and procedure</i>	52

<i>Figure 2. 12. Process of creating the urban fabric scenarios</i>	60
<i>Figure 2. 13. Single dwellings (NSW Government, Australia, 2017)</i>	61
<i>Figure 2. 14. Low-rise housing (NSW Government, Australia, 2017)</i>	61
<i>Figure 2. 15. Shop top housing (NSW Government, Australia, 2017)</i>	62
<i>Figure 2. 16. Medium-rise housing and medium/high-rise housing (NSW Government, Australia, 2017)</i>	62
<i>Figure 2. 17. High-rise housing (NSW Government, Australia, 2017)</i>	63
<i>Figure 2. 18. Meaning of height attribute, content description (Content description of BD TOPO version 2.1, IGN)</i>	63
<i>Figure 2. 19. Building type matrix that is used in active land use pattern. The 3D matrix includes 9 maps. Each map corresponds to one type of building with specific height. The value of each layer is the average heights of the buildings with regards to the building type classification</i>	64
<i>Figure 2. 20. Urban map of 2017, prospective urban growth map of 2050 and the simulated growth area during the 33 years growth cycle for Toulouse.</i>	65
<i>Figure 2. 21. Checking the first loop of neighbors around the new urban pixels in building type matrix</i>	65
<i>Figure 2. 22. Calculating the likelihood of each value for each pixel in the building type matrix</i>	66
<i>Figure 3. 1. France population profile, 1950 - 2050 (United Nations, 2018)</i>	74
<i>Figure 3. 2. Location and extent of the urban area of Toulouse</i>	75
<i>Figure 3. 3. Population map (INSEE, 2011)</i>	77
<i>Figure 3. 4. Toulouse urban map contains the undifferentiated and industrial buildings, 2017, IGN</i>	78
<i>Figure 3. 5. Slope, hillshade, transportation, urban and exclusion maps of Toulouse</i>	79
<i>Figure 3. 6. NEP exclusion map generated for Toulouse, 2017. In all excluded maps, the common areas between urbanized and excluded areas are considered as urbanized areas</i>	82
<i>Figure 3. 7. LEP exclusion map generated for Toulouse, 2017. In all excluded maps, the common areas between urbanized and excluded areas are considered as urbanized areas</i>	84
<i>Figure 3. 8. MEP exclusion map generated for Toulouse, 2017. In all excluded maps, the common areas between urbanized and excluded areas are considered as urbanized areas</i>	86
<i>Figure 3. 9. EEP exclusion map generated for Toulouse, 2017. In all excluded maps, the common areas between urbanized and excluded areas are considered as urbanized areas</i>	88
<i>Figure 3. 10. ALEP exclusion/attraction map generated for Toulouse, 2017. In all excluded maps, the common areas between urbanized and excluded areas are considered as urbanized areas</i>	90
<i>Figure 3. 11. Historical urban maps of 2000 and 2017 and prospective urban maps that are simulated by different environmental protection scenarios for 2017, Toulouse</i>	93
<i>Figure 3. 12. Comparison of urban patches simulated by different environmental protection scenarios, 2017, Toulouse</i>	94
<i>Figure 3. 13. Comparison of the historical urban patch and corresponding prospective patch that is simulated by SLEUTH-3r through environmental protection scenario level 3 (EEP), Toulouse</i>	95
<i>Figure 3. 14. Urban map of 2050 and prospective urban maps for 2050, Toulouse</i>	97
<i>Figure 3. 15. Comparison of urban patches simulated by different environmental protection scenarios, 2050, Toulouse</i>	98

<i>Figure 3. 16. Illustration of the average heights and the average surfaces of undifferentiated buildings classified according to building types, Toulouse</i>	<i>102</i>
<i>Figure 3. 17. Simulated urban growth that are used in urban fabric scenarios, Toulouse.....</i>	<i>107</i>
<i>Figure 3. 18. Urban sprawl via the urban fabric scenarios to locate 55% urban population growth, Toulouse</i>	<i>108</i>
<i>Figure 3. 19. Location and extent of the urban area of Saint Sulpice la Pointe study area.....</i>	<i>109</i>
<i>Figure 3. 20. Slope, hillshade, transportation, urban and exclusion maps of Saint Sulpice la Pointe</i>	<i>111</i>
<i>Figure 3. 21. NEP exclusion map generated for Saint Sulpice la Pointe, 2017. The excluded areas include the remarkable buildings, cemeteries, airfields, sport grounds; railways stations, triage areas; activity areas (administrative, culture and leisure, education, water management, industrial or commercial, health, sports and transport) and national parks; that are shown in red and the water surfaces that are represented in blue. They take the value of 100 and the others take the value of 50.....</i>	<i>112</i>
<i>Figure 3. 22. LEP exclusion map generated for Saint Sulpice la Pointe, 2017. The excluded areas indicate the remarkable buildings, cemeteries, airfields, sport grounds; railways stations, triage areas; activity areas (administrative, culture and leisure, education, water management, industrial or commercial, health, sports and transport) and national parks that are shown in red, the water surfaces represented in blue and the closed forests areas (wood land, closed coniferous forest, closed deciduous forest, mixed closed forest and tree area) in dark green. They take the value of 100 and the others take the value of 50.....</i>	<i>113</i>
<i>Figure 3. 23. MEP exclusion map generated for Saint Sulpice la Pointe, 2017. The excluded map contains all parks, protected areas and water bodies have made from the database of the IGN for 2017 including the remarkable buildings, cemeteries, airfields, sport grounds; railways stations, triage areas; activity areas (administrative, culture and leisure, education, water management, industrial or commercial, health, sports and transport) and national parks that are shown in red, the water surfaces represented in blue, the close forest areas (wood land, closed coniferous forest, closed deciduous forest, mixed closed forest and tree area) in dark green (value 100) and the open forest, hedge, woody heath, peupleraie, orchard, vine in light green (value 75).</i>	<i>114</i>
<i>Figure 3. 24. EEP exclusion map generated for Saint Sulpice la Pointe, 2017. The excluded map contains the remarkable buildings, cemeteries, airfields, sport grounds; railways stations, triage areas; activity areas (administrative, culture and leisure, education, water management, industrial or commercial, health, sports and transport) and national parks that are shown in red, the water surfaces represented in blue, the close forest areas (wood land, closed coniferous forest, closed deciduous forest, mixed closed forest and tree area) in dark green and the open forest, hedge, woody heath, peupleraie, orchard, vine in light green. All excluded areas take the value of 100 and the others take the value of 50.</i>	<i>115</i>
<i>Figure 3. 25. ALEP exclusion/attraction map generated for Saint Sulpice la Pointe, 2017. Four concentric zones with different attraction rates, make attraction force to the center. The areas in distances of seven pixels (~ 210m) around water surfaces are considered as attraction areas for dwelling as well. The LEP exclusion map is used for the excluded areas.....</i>	<i>116</i>
<i>Figure 3. 26. Historical urban maps of 2000 and 2017 and prospective urban maps that are simulated by different environmental protection scenarios for 2017, Saint Sulpice la Pointe.....</i>	<i>118</i>
<i>Figure 3. 27. Comparison of the historical urban patch and corresponding prospective patch that is simulated by SLEUTH-3r through environmental protection scenario level 3 (EEP), Saint Sulpice la Pointe</i>	<i>119</i>
<i>Figure 3. 28. Urban map of 2050 and prospective urban maps for 2050, Saint Sulpice la Pointe.....</i>	<i>121</i>
<i>Figure 3. 29. Location and extent of the urban area of Rieucros study area.....</i>	<i>125</i>
<i>Figure 3. 30. Slope, hillshade, transportation, urban and exclusion maps of Rieucros</i>	<i>127</i>

<i>Figure 3. 31. NEP exclusion map generated for Rieucros, 2017. The excluded areas include the remarkable buildings, cemeteries, airfields, sport grounds; activity areas (administrative, culture and leisure, education, water management, industrial or commercial, health, sports and transport) and national parks; that are shown in red and the water surfaces that are represented in blue. They take the value of 100 and the others take the value of 50.....</i>	<i>128</i>
<i>Figure 3. 32. LEP exclusion map generated for Rieucros, 2017. The excluded areas indicate the remarkable buildings, cemeteries, airfields, sport grounds; activity areas (administrative, culture and leisure, education, water management, industrial or commercial, health, sports and transport) and national parks that are shown in red, the water surfaces represented in blue and the closed forests areas (wood land, closed coniferous forest, closed deciduous forest, mixed closed forest and tree area) in dark green. They take the value of 100 and the others take the value of 50.</i>	<i>129</i>
<i>Figure 3. 33. MEP exclusion map generated for Rieucros, 2017. The excluded map contains all parks, protected areas and water bodies have made from the database of the IGN for 2017 including the remarkable buildings, cemeteries, airfields, sport grounds; activity areas (administrative, culture and leisure, education, water management, industrial or commercial, health, sports and transport) and national parks that are shown in red, the water surfaces represented in blue, the close forest areas (wood land, closed coniferous forest, closed deciduous forest, mixed closed forest and tree area) in dark green (value 100) and the open forest, hedge, woody heath, peupleraie, orchard, vine in light green (value 75).....</i>	<i>130</i>
<i>Figure 3. 34. EEP exclusion map generated for Rieucros, 2017. The excluded map contains the remarkable buildings, cemeteries, airfields, sport grounds; activity areas (administrative, culture and leisure, education, water management, industrial or commercial, health, sports and transport) and national parks that are shown in red, the water surfaces represented in blue, the close forest areas (wood land, closed coniferous forest, closed deciduous forest, mixed closed forest and tree area) in dark green and the open forest, hedge, woody heath, peupleraie, orchard, vine in light green. All excluded areas take the value of 100 and the others take the value of 50.</i>	<i>131</i>
<i>Figure 3. 35. ALEP exclusion/attraction map generated for Rieucros, 2017. Four concentric zones with different attraction rates, make attraction force to the center. The areas in distances of seven pixels (~140m) around water surfaces are considered as attraction areas for dwelling as well. The LEP exclusion map is used for the excluded areas.</i>	<i>132</i>
<i>Figure 3. 36. Historical urban maps of 2000 and 2017 and prospective urban maps that are simulated by different environmental protection scenarios for 2017, Rieucros</i>	<i>134</i>
<i>Figure 3. 37. Comparison of the historical urban patch and corresponding prospective patch that is simulated by SLEUTH-3r through environmental protection scenario level 3 (EEP), Rieucros</i>	<i>135</i>
<i>Figure 3. 38. Urban map of 2050 and prospective urban maps for 2050, Rieucros</i>	<i>137</i>
<i>Figure 3. 39. Urban growth simulation of Saint Sulpice la Pointe study area according to two different pixels size</i>	<i>142</i>
<i>Figure 4. 1. The five LoDs of the OGC CityGML (source: KIT Karlsruhe, K.-H. Häfele, Gröger et al., 2012)</i>	<i>147</i>
<i>Figure 4. 2. The 3D building representation procedure</i>	<i>150</i>
<i>Figure 4. 3. An example of geo-referencing the SLEUTH output map Saint Sulpice la Pointe (EEP simulation scenario, 2050)</i>	<i>152</i>
<i>Figure 4. 4. A schema of eliminating the null pixels.....</i>	<i>153</i>
<i>Figure 4. 5. Orientation of a polygon, R_1 and R_2 are the local and overall references respectively</i>	<i>154</i>
<i>Figure 4. 6. Python code used for orientation</i>	<i>155</i>
<i>Figure 4. 7. An example of subdividing a polygon to smaller squares</i>	<i>156</i>
<i>Figure 4. 8. Python code used for subdividing a polygon.....</i>	<i>156</i>

<i>Figure 4. 9. Definition of river proximity constraint</i>	<i>157</i>
<i>Figure 4. 10. Removed overlap areas of the polygons</i>	<i>158</i>
<i>Figure 4. 11. An example of the polygons and the squares identifiers, case study of Toulouse.....</i>	<i>159</i>
<i>Figure 4. 12. Assembling sub pixels respecting the roads</i>	<i>161</i>
<i>Figure 4. 13. Create the building footprints by making different erosion to each polygon according to the scenarios, Rieucros</i>	<i>162</i>
<i>Figure 4. 14. Create the building footprints by making different erosion to each polygon according to the scenarios, Saint Sulpice la Pointe.....</i>	<i>162</i>
<i>Figure 4. 15. Create the building footprints by making different erosion to each polygon according to the scenarios, Toulouse.....</i>	<i>163</i>
<i>Figure 4. 16. Searching for the nearest neighbor</i>	<i>164</i>
<i>Figure 4. 17. The algorithm of calculating the probability of the height for each building according to the building types and urban fabric scenario</i>	<i>165</i>
<i>Figure 4. 18. 2D and 3D views, medium/high dense fabric scenario (13 growth cycle), Rieucros</i>	<i>166</i>
<i>Figure 4. 19. 2D and 3D views, medium dense urban fabric scenario (18 growth cycle), Rieucros</i>	<i>166</i>
<i>Figure 4. 20. 2D and 3D views, low dense urban fabric scenario (23 growth cycle), Rieucros</i>	<i>167</i>
<i>Figure D. 1. Giving weight to the urban area using concentric zone model, Toulouse</i>	<i>210</i>
<i>Figure D. 2. Giving weight to the urban area using sector model, Toulouse</i>	<i>211</i>
<i>Figure D. 3. Giving weight to the urban area using multiple nuclei model, Toulouse</i>	<i>212</i>
<i>Figure D. 4. The urban maps with different height that used to create particular complex pattern.....</i>	<i>213</i>
<i>Figure D. 5. Giving weight to the urban area using particular complex pattern for Toulouse</i>	<i>213</i>

List of tables

<i>Table 1. 1. Distribution of the area of mainland France by nature of occupancy according to Corine Land Cover 2006 (corrected data) and 2012. (ESCo, 2017, section 1, p. 20; Source: SOeS, MTES).....</i>	<i>19</i>
<i>Table 1.2. Distribution of the area of mainland France by nature of occupancy according to Teruti-Lucas surveys 2006 and 2014. (ESCo, 2017, section 1, p. 22; Source: SSP (Service de la Statistique et de la Prospective) – MAA (Ministère de l'Agriculture et de l'Alimentation)).....</i>	<i>19</i>
<i>Table 1. 3. Description of the collected geospatial and socio-economic data; (Arsanjani et al., 2013).....</i>	<i>30</i>
<i>Table 1. 4. Compare the validity of simulation models; (Kamusoko and Gamba, 2015).....</i>	<i>34</i>
<i>Table 2. 1. Metrics that can be used to evaluate the goodness of fit of the basic SLEUTH model (Dietzel and Clarke, 2007)</i>	<i>54</i>
<i>Table 2. 2. New fit metrics available in SLEUTH-3r (Jantz et al., 2010)</i>	<i>55</i>
<i>Table 2. 3. The percentage of the environment protection for excluded areas and the attractive areas considered in the environmental protection scenarios</i>	<i>59</i>
<i>Table 2. 4. Primary urban fabric scenarios for Toulouse study area.</i>	<i>68</i>
<i>Table 3. 1. Percentage of the urban population residing in Toulouse, (United Nations, 2018)</i>	<i>76</i>
<i>Table 3. 2. Changes in physical occupation between 2006 and 2014 in Midi-Pyrénées region (309080 points), Teruti-Lucas.....</i>	<i>81</i>
<i>Table 3. 3. Dispersion coefficient (D_M) multiplier per environmental protection scenario, Toulouse.....</i>	<i>91</i>
<i>Table 3. 4. Best-fit coefficient values driven from calibration process of SLEUTH-3r, Toulouse.....</i>	<i>92</i>
<i>Table 3. 5. Urban growth simulated results obtained from different environmental protection scenarios and the comparison of the results to the observed map of 2017, Toulouse.....</i>	<i>96</i>
<i>Table 3. 6. Urban growth simulated results obtained from different environmental protection scenarios for 2050, Toulouse.....</i>	<i>99</i>
<i>Table 3. 7. Number, area and height of undifferentiated buildings according to our building classification, Toulouse.....</i>	<i>101</i>
<i>Table 3. 8. Number, area and height of industrial buildings, Toulouse.....</i>	<i>101</i>
<i>Table 3. 9. Estimation of the average number of inhabitant for each type of buildings, Toulouse</i>	<i>104</i>
<i>Table 3. 10. Comparing the population growth of four different primary urban fabric scenarios, Toulouse</i>	<i>105</i>
<i>Table 3. 11. Urban fabric scenarios comparison according to the growth cycle to have similar rate of increased population. The gray column represents the population increasing of low dense urban fabric scenario during 33-growth cycle that is closer to the existing urban fabric, Toulouse</i>	<i>106</i>
<i>Table 3. 12. Dispersion coefficient (D_M) multiplier per environmental protection scenario, Saint Sulpice la Pointe</i>	<i>117</i>

<i>Table 3. 13. Best-fit coefficient values driven from calibration process of SLEUTH-3r, Saint Sulpice la Pointe</i>	117
<i>Table 3. 14. Urban growth simulated results obtained from different environmental protection scenarios and the comparison of the results to the observed map of 2017, Saint Sulpice la Pointe</i>	120
<i>Table 3. 15. Urban growth simulated results obtained from different environmental protection scenarios for 2050, Saint Sulpice la Pointe</i>	122
<i>Table 3. 16. Number, area and height of undifferentiated buildings according to our building classification, Saint Sulpice la Pointe</i>	122
<i>Table 3. 17. Estimation of the average number of inhabitants for each type of buildings, Saint Sulpice la Pointe</i>	123
<i>Table 3. 18. Comparing the population growth of four different primary urban fabric scenarios, Saint Sulpice la Pointe</i>	123
<i>Table 3. 19. Urban fabric scenarios comparison according to the growth cycle to have similar rate of increased population. The gray column represents the population increasing of low dense urban fabric scenario during 33-growth cycle that is closer to the existing urban fabric, Saint Sulpice la Pointe</i>	124
<i>Table 3. 20. Dispersion coefficient (D_M) multiplier per environmental protection scenario, Rieucros</i>	133
<i>Table 3. 21. Best-fit coefficient values driven from calibration process of SLEUTH-3r, Rieucros</i>	133
<i>Table 3. 22. Urban growth simulated results obtained from different environmental protection scenarios and the comparison of the results to the observed map of 2017, Rieucros</i>	136
<i>Table 3. 23. Urban growth simulated results obtained from different environmental protection scenarios for 2050, Rieucros</i>	138
<i>Table 3. 24. Number, area and height of undifferentiated buildings according to our building classification, Rieucros</i>	138
<i>Table 3. 25. Estimation of the average number of inhabitant for each type of buildings, Rieucros</i>	139
<i>Table 3. 26. Comparing the population growth of five different primary urban fabric scenarios, Rieucros</i>	139
<i>Table 3. 27. Urban fabric scenarios comparison according to the growth cycle to have similar rate of increased population. The gray column represents the population increasing of low dense urban fabric scenario during 33-growth cycle that is closer to the existing urban fabric, Rieucros</i>	140
<i>Table 4. 1. Number and the area of the current buildings classified based on the building types</i>	155
<i>Table 4. 2. Pixel identifiers description</i>	159
<i>Table 4. 3. Area of the new building foot prints buildings classified based on the building types</i>	160
<i>Table A. 1. Examples of the applications of urban growth and LUCC models, divided into four groups including fractal modeling, artificial neural network modeling, agent-based modeling and cellular automata modeling</i>	175
<i>Table C. 1. Dispersion coefficient multiplier, scenario protection level 0 (Nearly No Environmental Protection - NEP), Toulouse</i>	198
<i>Table C. 2. Dispersion coefficient multiplier, scenario protection level 1 (Limited Environmental Protection - LEP), Toulouse</i>	198
<i>Table C. 3. Dispersion coefficient multiplier, scenario protection level 2 (Moderate Environmental Protection - MEP), Toulouse</i>	198

<i>Table C. 4. Dispersion coefficient multiplier, scenario protection level 3 (Extreme Environmental Protection - EEP), Toulouse</i>	199
<i>Table C. 5. Dispersion coefficient multiplier, attraction-based scenario protection level 1 (Attraction-based Limited Environmental Protection - ALEP), Toulouse</i>	199
<i>Table C. 6. Dispersion coefficient multiplier, scenario protection level 0 (Nearly No Environmental Protection - NEP), Saint Sulpice la Point</i>	199
<i>Table C. 7. Dispersion coefficient multiplier, scenario protection level 1 (Limited Environmental Protection - LEP), Saint Sulpice la Point</i>	200
<i>Table C. 8. Dispersion coefficient multiplier, scenario protection level 2 (Moderate Environmental Protection - MEP), Saint Sulpice la Point</i>	200
<i>Table C. 9. Dispersion coefficient multiplier, scenario protection level 3 (Extreme Environmental Protection - EEP), Saint Sulpice la Point</i>	200
<i>Table C. 10. Dispersion coefficient multiplier, attraction-based scenario protection level 1 (Attraction-based Limited Environmental Protection - ALEP), Saint Sulpice la Point</i>	201
<i>Table C. 11. Dispersion coefficient multiplier, scenario protection level 0 (Nearly No Environmental Protection - NEP), Rieucros</i>	201
<i>Table C. 12. Dispersion coefficient multiplier, scenario protection level 1 (Limited Environmental Protection - LEP), Rieucros</i>	201
<i>Table C. 13. Dispersion coefficient multiplier, scenario protection level 2 (Moderate Environmental Protection - MEP), Rieucros</i>	202
<i>Table C. 14. Dispersion coefficient multiplier, scenario protection level 3 (Extreme Environmental Protection - EEP), Rieucros</i>	202
<i>Table C. 15. Dispersion coefficient multiplier, attraction-based scenario protection level 1 (Attraction-based Limited Environmental Protection - ALEP), Rieucros</i>	202
<i>Table C. 16. Calibration coefficients, scenario protection level 0 (Nearly No Environmental Protection - NEP), Toulouse</i>	203
<i>Table C. 17. Calibration coefficients, scenario protection level 1 (Limited Environmental Protection - LEP), Toulouse</i>	203
<i>Table C. 18. Calibration coefficients, scenario protection level 2 (Moderate Environmental Protection - MEP), Toulouse</i>	204
<i>Table C. 19. Calibration coefficients, scenario protection level 3 (Extreme Environmental Protection - EEP), Toulouse</i>	204
<i>Table C. 20. Calibration coefficients, attraction-based scenario protection level 1 (Attraction-based Limited Environmental Protection - ALEP), Toulouse</i>	204
<i>Table C. 21. Calibration coefficients, scenario protection level 0 (Nearly No Environmental Protection - NEP), Saint Sulpice la Point</i>	204
<i>Table C. 22. Calibration coefficients, scenario protection level 1 (Limited Environmental Protection - LEP), Saint Sulpice la Point</i>	205
<i>Table C. 23. Calibration coefficients, scenario protection level 2 (Moderate Environmental Protection - MEP), Saint Sulpice la Point</i>	205
<i>Table C. 24. Calibration coefficients, scenario protection level 3 (Extreme Environmental Protection - EEP), Saint Sulpice la Point</i>	205
<i>Table C. 25. Calibration coefficients, attraction-based scenario protection level 1 (Attraction-based Limited Environmental Protection - ALEP), Saint Sulpice la Point</i>	205

<i>Table C. 26. Calibration coefficients, scenario protection level 0 (Nearly No Environmental Protection - NEP), Rieucros</i>	<i>206</i>
<i>Table C. 27. Calibration coefficients, scenario protection level 1 (Limited Environmental Protection - LEP), Rieucros</i>	<i>206</i>
<i>Table C. 28. Calibration coefficients, scenario protection level 2 (Moderate Environmental Protection - MEP), Rieucros</i>	<i>206</i>
<i>Table C. 29. Calibration coefficients, scenario protection level 3 (Extreme Environmental Protection - EEP), Rieucros</i>	<i>206</i>
<i>Table C. 30. Calibration coefficients, attraction-based scenario protection level 1 (Attraction-based Limited Environmental Protection - ALEP), Rieucros</i>	<i>207</i>

Résumé

L'urbanisation est principalement due à la croissance démographique, à l'exode rural vers villes et au changement de mode de vie. Ce processus augmente les terres artificielles, qui affectent la biodiversité, les écosystèmes, le climat urbain et réduit les terres pour l'agriculture et les espaces naturels.

L'objectif de cette thèse est de proposer des solutions pour simuler divers scénarios d'urbanisation afin d'améliorer la prise de décision en matière de politiques publiques. Pour ce faire, le modèle SLEUTH est utilisé afin d'évaluer l'impact des types de bâtiments et des règles environnementales sur l'étalement urbain. Dans la méthode utilisée, SLEUTH intègre davantage des données topographiques, des données sur les tissus urbains et démographiques, y compris des caractéristiques géographiques et des contraintes environnementales. Le principal défi de cette recherche est de proposer différents scénarios d'étalement urbain pour plusieurs types de règles environnementales tout en tenant compte du besoin des habitants ou du moins d'une estimation de la croissance de la population.

Le modèle SLEUTH est l'un des modèles de simulation d'automates cellulaires bien connus, qui correspond à la simulation dynamique de l'expansion urbaine et s'adapte au modèle morphologique de la configuration urbaine. SLEUTH, comme beaucoup d'autres méthodes de simulation de la croissance urbaine, ne considère que les données historiques. Bien que les impacts de la croissance démographique et du tissu urbain soient implicitement pris en compte lors de la phase d'étalonnage sur les cartes urbaines historiques, il est impossible d'inclure les changements de taux de croissance démographique ou de types de bâtiments dans les simulations. De plus, les résultats de SLEUTH se limitent à des données matricielles difficiles à interpréter pour les décideurs. Les résultats sont des pixels, sur lesquels une urbanisation est supposée se produire, ce qui a peu de sens du point de vue de l'urbanisme. Par conséquent, notre recherche vise à diversifier les possibilités de simulation en intégrant explicitement le facteur des types de bâtiments en fonction de la croissance de la population et en fournissant des modèles de visualisation des résultats de scénarios de croissance urbaine en 2D et même en 3D.

Afin d'améliorer les résultats de SLEUTH, différents scénarios de simulation de croissance urbaine en 2D ont été définis sur la base du modèle SLEUTH en ajoutant le type de bâtiment et l'estimation de la croissance démographique en tant que facteurs du tissu urbain. Chaque simulation correspond à des politiques plus ou moins restrictives en espaces considérant ce que ces territoires peuvent accueillir en tant que type de bâtiment et en tant que population globale. De plus, les simulations peuvent aider l'utilisateur à protéger les terrains souhaités, tels que les espaces environnementaux, de l'urbanisation. Ces scénarios montrent la force de la simulation du modèle et permettent d'améliorer notre compréhension de l'étalement urbain.

Trois études de cas de tailles et de populations différentes sont utilisées, Toulouse Métropole, Saint Sulpice la Pointe et Rieucros, afin de donner une idée de l'efficacité de la méthode

proposée à plusieurs échelles. L'évaluation des résultats indique que la méthode proposée est capable d'effectuer différentes simulations correspondant à plusieurs priorités et contraintes foncières. Il est utile de voir quels terrains peuvent être protégés (où) et quel type de bâtiment peut être utilisé pour limiter l'étalement urbain (combien). Une représentation en 3D de chaque simulation de croissance urbaine est fournie afin de faciliter l'interprétation de la simulation SLEUTH et de différencier les scénarios. Les résultats permettent d'avoir plusieurs images de la ville de demain pour l'appliquer aux politiques urbaines.

Mots-clés: urbanisation, étalement urbain, simulation, modèle de SLEUTH basé sur des scénarios, tissu urbain, constructibilité, SLEUTH-3r, systèmes d'information géographique (SIG), politique de la ville

Abstract

The process of urbanization occurs mainly due to population growth, rural exodus to cities and life style that often induces the nearly irreversible changes. It increases the artificial lands, which affect the biodiversity, ecosystems, urban climate, and reduces land for agriculture and natural areas.

The focus of this thesis is to simulate diverse urbanization scenarios in order to improve public policies decision making. To do this, the SLEUTH model is used in order to investigate the impacts of building types and environmental rules on urban sprawl. In the method used, the SLEUTH model integrates more topographic data, urban tissue and demographic data, including geographical features and the environmental constraints. The main challenge in this research is to propose different urban sprawl scenarios for different kind of environmental rules while taking into account the population demand or at least population growth estimation.

The SLEUTH model is one of the well-known cellular automata simulation models, which matches the dynamic simulation of urban expansion and adapts to morphological model of the urban configuration. SLEUTH, like many other urban growth simulation methods, considers only the historical data. Although, the impacts of population growth and urban tissue are implicitly considered during the calibration phase on the historical urban maps, changes in population growth rate or in building types cannot be included in its simulations. Moreover, the SLEUTH results are limited to raster data that are difficult to interpret for decision makers. The results are some pixels on which urbanization is supposed to occur, which do not make much sense from urbanism point of view. Therefore, our research aims to diversify the simulation possibilities integrating explicitly factors of building types according to population growth and providing visual methods to view urban growth scenario results in 2D and even 3D.

In order to improve the SLEUTH results, different 2D urban growth simulation scenarios have been defined based on the SLEUTH model by adding buildings type and the estimation of the population growth as urban fabric factors. Each simulation corresponds to policies that are more or less restrictive of spaces considering what these territories can accommodate as a type of building and as a global population. In addition, the simulations can help the user to protect the desired lands such as the environmental spaces from urbanization. These scenarios show the simulation capabilities of the model and make it possible to improve our understanding of an urban sprawl simulation.

Three different case studies with various sizes and populations are used including Toulouse metropolitan, Saint Sulpice la Pointe and Rieucros to provide a view of the effectiveness of the proposed method on several scales. The results evaluation indicates that the proposed method makes different simulations that correspond to different land priorities and constraints. It helps to see which land can be protected (where) and how building type can be used to constrain

urban sprawl (how much). A 3D representation for each prospective urban growth simulations is provided in order to facilitate the interpretation of the SLEUTH simulation and differentiate the scenarios. The findings allow having different images of the city of tomorrow for applying it to urban policies.

Keywords: Urbanization, urban sprawl, simulation, scenario-based SLEUTH model, urban fabric, Constructability, SLEUTH-3r, Geographical Information Systems (GIS), Urban policy

Introduction

The process of urbanization occurs mainly due to population growth, rural exodus to cities and life-style which often induces the nearly irreversible changes because of the land take phenomena and increases the artificial lands. It affects the biodiversity, ecosystems, urban climate, and agriculture and natural areas. The balance between land protection and urbanization is an environmental and social concerns of the public authorities. This can be achieved by providing security, welfare and social services to residents, as well as respecting the environment and biodiversity. Although, the latter played a significant role in reducing pollution and physical and mental needs of the inhabitants as well. The main challenge in this research is to propose different urban sprawl scenarios for different kind of environmental rules while consider population demand or at least population growth estimation.

The compact cities preserve the soil, reduce some environmental impacts of urbanization and decrease greenhouse gas emissions by reducing travel as well as often decrease the construction cost. These objectives can be achieved by densification which increases the height of buildings. Land use densification is a specific target of many land use policies in most [OECD countries](#) (the Organization for Economic Co-operation and Development, 2017), however for many reasons it may effects on the urban environment and the population welfare e.g. decreasing the residential area, reducing sunlight, runoff problems, creating of heat islands, and reducing the amenities associated with open spaces as well as reducing the people privacy ([ESCo, Expertise Scientifique Collective, 2017, sections 5, p.78](#)).

The objective of this thesis is to generate diverse urbanization scenarios in order to improve public policies decision making. To do this, SLEUTH modeling improvement is proposed that integrates more topographic data, urban tissue and demographic data while respects geographical features and the environmental constraints. SLEUTH's acronym is derived from its data input requirements: Slope, Land use, Exclusion, Urban, Transportation and Hillshade. This model is used in order to investigate the impacts of building types and environmental rules on urban sprawl.

Many studies, using various modeling approaches and simulation tools have been made in the field of urban growth. Among all dynamic and spatially explicit models, those based on Cellular Automata (CA) are common for their applications in urban areas. This can be explained by the spatially explicit character and dynamic behavior of cellular automata models. Simplicity, flexibility, intuitiveness, transparency, the ability to incorporate the spatial, temporal dimensions of the processes and capability of modeling complex dynamic systems such as urban systems, are some features of CA modeling. CA can be easily integrated with Geographical Information Systems (GIS) to have a high spatial resolution model with

computational efficiency. In addition, nonlinearity of the iterative process of CA leads to regular fractal patterns, i.e. to regular and ordered spatial patterns that generate similar geometries at different scales. The SLEUTH model is one of the cellular automata models that can simulate the dynamic nature of urban expansion and can be compatible with urban environment modeling.

From geographical point of view, a city appears as an agglomeration of buildings and people, essentially different from agricultural lands. A city is composed of the agglomeration of geographical and social environment that is formed by structures and residents, and can be defined by the occupied space and the social relationships it creates. The constructions as spatial objects represent the coalescence and the social environment demonstrate the coherence of the city. These spatial and social agglomerations make an interesting indicator to understand the scale and the evolution of the cities ([Antoni, 2003](#)).

SLEUTH, like many other urban growth simulation methods, uses the historical data in order to calibrate the model. Although the impacts of population growth and urban tissue are implicitly considered during the calibration phase of SLEUTH, the changes in population growth rate or in building types cannot be included in its simulations. Moreover, the SLEUTH results are limited to some raster data that is difficult to interpret for decision makers. The results are some pixels on which urbanization is supposed to occur, which do not make much sense from urbanism point of view. The research presented in this thesis aims to challenge the results of the classical urban growth methods that are often independent from the factors of building types and population, and gives an improvement to provide a more reliable method.

In SLEUTH model, a simulation is made up of a series of growth cycles where each cycle represents a year of growth. The rhythm of growth is calibrated by means of historical data and the model is based on learning and therefore it will reproduce the same tendency as today (same type of building). Therefore, it seems interesting to integrate some new effective factors such as estimated population, building types and more topographic data in order to improve the number and location of simulated pixels per growth cycle. In order to integrate the demography and building types, the buildings are classified to different residential categories considering their height and configuration to study the Human Settlement Capacity (HSC). The results of the proposed method lead to different simulations that are related to different land priorities and constraints.

In this research, common data (such as topographic, buildings and demography data) are used in order to create different types of scenarios according to urban policies, while remaining realistic. Integrating the additional data leads hopefully to better parameterization of the model. Given that we know the prediction of urban growth is an indeterminate proposition, several prospective scenarios based on the new model parametrizations are defined related to different urban area (the Toulouse metropolitan, Saint Sulpice la Pointe that is a town around Toulouse, and Rieucros as a small community in a rural area), in order to query the simulation ability in different scale. These scenarios show the simulation capabilities of the model and make it possible to improve our understanding of an urban sprawl simulation. The simulation results of

the three different case studies with various sizes and populations provide a good view of the scalability of the proposed method and the findings allow having different images of the city of tomorrow to choose and reflect on urban policies. In urban modeling, proposing different simulation of urban sprawl is fundamental because it shows the possible impact of urban sprawl but also the capacity of urban settlement according to different scenario.

In this thesis, the prospective urban growth simulations are compared while keeping the same population growth rate for the desired forecasting date. Moreover, the demographic capacity in each scenario in both dense and sprawl cities are calculated and compared. The purpose of the thesis is to provide a way to simulate urban growth, with less semantic information loss, and to show the differences of sprawl and dense growth, by integrating topographic data, demographic, and building types with the CA model.

Least, a 3D representation for each prospective urban growth simulations is provided to facilitate the interpretation of the SLEUTH simulation, to better understand the SLEUTH simulation results and to differentiate the scenarios, in order to support the scientists and authorities in charge of urban planner and management.

In this research, we use SLEUTH model that sounds good, but from our perspective it's not good enough. SLEUTH produces square areas (raster files) on which urbanization is supposed to occur. There is no further information from these new urban areas, and their purposes and uses are unclear. In addition, we do not know their meaning in terms of urban fabric. We have faced many challenges in this research, though the most critical issue is how to propose different urban sprawl scenarios for different kind of environmental rules. In addition, considering population demand (or at least population growth estimates) is another important challenge.

With the objectives mentioned above, the thesis starts with raising the following questions about the evolutionary trajectory of urbanization as well as densification:

- What are the urbanization and densification?
- Why doing urban sprawl simulation, while we know that all simulations are fictions and they are based on some assumptions?

Achievements

- Urban sprawl phenomena is a big challenge for the authorities and urban planners.
- We have proposed a way to improve simulated urban sprawl using topographic data and population density for results analysis.
- The results demonstrate that the urban growth is widely dependent to building type (urban fabric) and population growth. Classification of the building types and the estimation of the population growth try to provide required amount of urban growth, and the protection rules attempt to regulate the location of growth areas.

In fact, urban growth simulations can be used to see what can happen in the future; how will be the housing, population growth and land cover changes and where can occur. These simulations

can help us find and protect some areas against artificialization and urbanization. Moreover, they can be used to think about future urbanization and make choices on urban policies.

Thesis Structure

This thesis consists of 5 chapters intended to explore the optimization of SLEUTH as an urban growth cellular automata. The work aims to obtain a better parameterization of urban growth in order to demonstrate the impacts of constructions and environmental constraints on urban sprawl by integrating more topographic data, urban fabric and demographic data. Major themes are developed in this work and an original contribution is proposed. A brief introduction is presented at the beginning of each chapter to guide the reader before tackling the main subject. In the same spirit, each chapter ends with a discussion of the content. The structure of the thesis process flow is illustrated in the figure I. Below, the structure of the thesis is presented with an overview of each subsequent chapter.

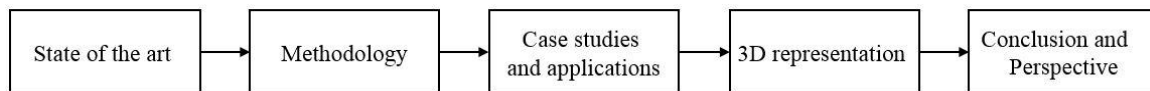


Figure I. Structure of the thesis process flow

Chapter 1 gives a brief overview of urbanization and land artificialization in order to understand the strengths and tendencies of the urbanization process. In this chapter, determinants and the impacts of urbanization are discussed. In addition, a brief review of the state-of-the-art in some academic research and urban planning practices is presented, to explore land use pattern and urban simulation techniques.

Chapter 2 describes the thesis methodology and fundamentals for model construction including the reason to choose the model, the scenarios considered, the factors used to optimize the model and the implementation of the proposed model.

Chapter 3 dedicates to the case studies and applications including the implementation of our model on three different study areas, providing the results, evaluating them and make a discussion of the obtained results.

Chapter 4 explores the 3D illustration of the urban growth scenarios in order to better understand the simulation results, to facilitate the interpretation of the SLEUTH simulation and to differentiate the scenarios. In this chapter, first the different 3D modeling tools and applications are reviewed. Next, a 3D proposal is represented in order to analyze the simulation model regarding to 3D.

Chapter 5 concludes the thesis by summarizing the results of the preceding research and discussing future work required in developing these methods.

Annex A represents, a list of methods in the domain of urban growth and land use and land cover changes (LUCC) modeling including their use cases, their applications and some of their capabilities and limitations.

Annex B describes the SLEUTH urban growth model process flow. One scenario file is represented in detail in this Annex.

Annex C illustrates the examples of the SLEUTH calibration files that are used to achieve dispersion coefficient multiplier and calibration best-fit coefficient.

Annex D represents the examples of weighting urban patches using predefined urban land use models. In this Annex, the examples of four predefined urban land use pattern contain concentric zone model, sector model, multiple nuclei model and particular complex model, for the study area of Toulouse are provided.

Annex E describes documentation of the National Institute of Statistics and Economic Studies (INSEE) data including the source, the generated information and the list and description of variables that are used in the population estimations and the urban fabric scenarios.

Chapter 1 : Urbanization and Urban Modeling

Contents

- 1.1. Urbanization
 - 1.2. Urban Modeling
 - 1.3. Chapter Conclusion
-

Urbanization is a process that leads to increase the size of cities. It occurs mainly due to population growth, rural exodus to cities and life style. The urbanization process often induces the nearly irreversible changes and increases the artificial lands. It affects the biodiversity, ecosystems, urban climate, and agriculture and natural areas. The balance between housing and land protection is one of the environmental and social concerns of the public authorities. This should be achieved by providing security, welfare and social services to residents as well as respecting the environment and biodiversity. The latter played a significant role in reducing pollution and physical and mental needs of the inhabitants as well.

Cities are shaped by urban expansion, migration, succession according to their geography and natural environments. In general, urban growth and mostly urban sprawl generates land artificialization and it changes the natural agricultural lands to residential housings. Urbanization is one of the most effective factors in expanding the artificialization the territories. This is why the tracking and controlling the artificial territories represent an important challenge for local authorities facing with objectives of sustainable development.

Many studies have been done in the field of urban growth, using various modeling approaches and simulation tools in order to spatially reconstruct the occupation and changes in land use. In this chapter, some different urban land use patterns are overviewed which can be considered as predefined patterns. Predefined patterns are static models that describe patterns of urban land use in a generic city. These patterns should be created manually for each study area according to the land use observations for that area.

In the last decades, various techniques have been predominantly used to simulate the urban growth and land use / land cover changes (LUCC). These techniques, their use cases and their applications are widespread. Therefore, choosing a well-fit method among them for a new case study is always a challenge for the urban planners and stakeholders. In the researches of this

thesis, an overview on some different techniques of urban growth and LUC modeling is presented, which seeks to understand and document the state of the art of different simulation techniques and investigate their applications. From all various techniques, the fractal modeling, artificial neural network modeling, agent-based modeling and cellular automata modeling have been categorized and their use cases, their applications; and their capability and limitations are discussed. The classified list of different researches in this field is proposed in Annex A that could be used to provide an appropriate view for urban planners in the field of urban planning development. Some more used techniques and applications are reviewed in detail in this chapter.

In this chapter, first, a brief overview on urbanization is provided in section 1.1. The urban sprawl and artificialized lands, their characteristics and their impacts on environment and the human life are reviewed in this section. Then in section 1.2, some land use patterns and different techniques of urban growth and LUC modeling are represented. The chapter is concluded in section 1.3.

1.1. Urbanization

The size of cities increased all over the world. The process, named urbanization is mainly due to population growth, rural exodus to cities and to life style. World urbanization prospects of department of economic and social affairs of [United Nations \(2018\)](#) demonstrate that in 2018, 55 % of the world’s population lived in urban areas and the coming decades the both global population growth and urbanization will continue in urban areas. Moreover, those projections show that urbanization and the population growth will cause to increase the urbanization to more than 66% in 2050 (see figure 1.1).

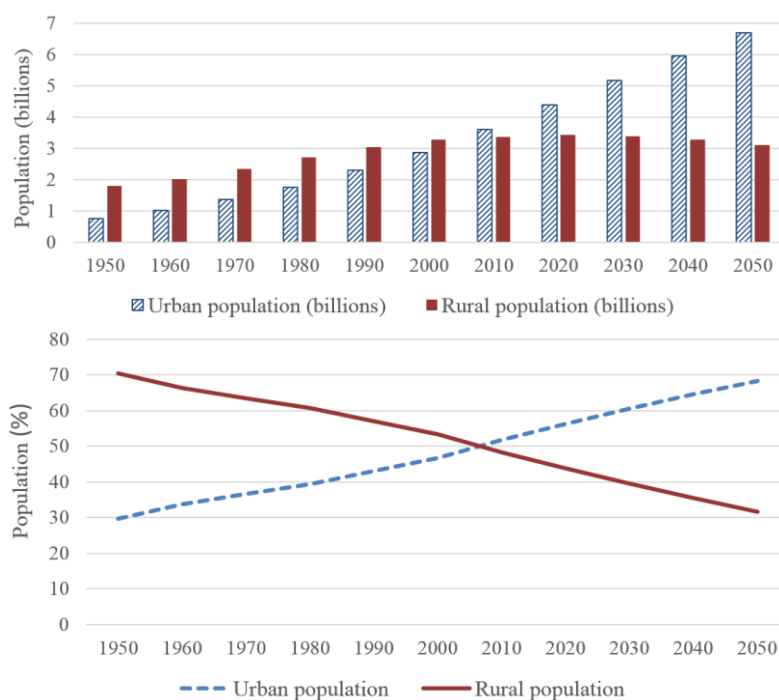


Figure 1. 1. Proportions of urban and rural world population, from 1950 to 2050; ([United Nations, 2018](#))

Migrating population from rural to urban area has proceeded rapidly during last six decades. Suburbanization refers to shifting the residential area to outward. Suburban sprawl demonstrates a balance between the forces that are pushing people together in cities and those pushing them out. Some researches show that suburbanization has gone so far to form new points of concentration outside the downtown (Sridhar, 2007).

Regarding to definition provided from INSEE (the National Institute of Statistics and Economic Studies collects, produces, analyzes and disseminates information on the French economy and society), since 1954 in France, an urban unit is generally defined as a municipality or a group of municipalities that combines the continuity of buildings where the distance of two buildings are less than 200 meters and it has at least 2000 inhabitants. The surrounding commune of an urban unit is considered as urban and the other communes are considered as the rural communes. Later in 2010, other words are defined called urban centers (Pôles urbains in French). The urban centers are the subset of urban units that presents 10 000 jobs and are not the crown of other urban centers. Since October 2011, the zoning in urban areas (ZAU) provides a vision of the influence areas of cities, in the sense of urban units, on the territory. It divides the territory into four major types of spaces. One of them demonstrates mainly the rural spaces (e.g. small urban units and rural municipalities) and others represent urban spaces including the urban centers, the suburban peripheries and the multi-centric municipalities (INSEE).

Almost half of the European population lives in urban areas of less than 500,000 inhabitants. In fact, according to the provided definitions, Europe is an area of small towns with the distance of fifteen kilometers from each other (ESCo, 2017, introduction, p. 9). Nowadays, most of the countries cannot avoid the urban population growth and their rate of urbanization is increasing rapidly. In France, nearly 55% of urban residents in 1950 lived in one unit while this rate was increased to around 80% in 2018 and it will continued to 88% in 2050 that is comparable to other industrialized countries (United Nations, 2018) (see figure 1.2).

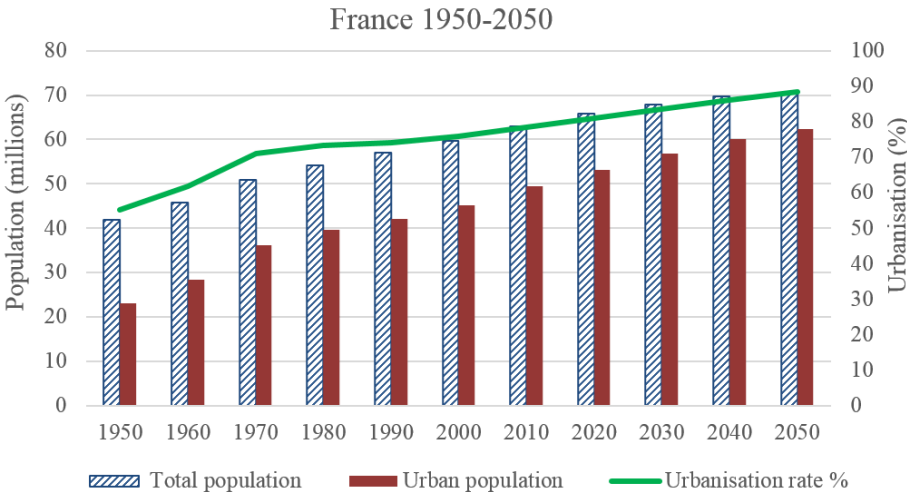


Figure 1. 2. Total population, urban population and urbanization rates from 1950 to 2050; (United Nations, 2018)

The long-term growth of real GDP (Gross Domestic Product) per capita can be considered as an index to measure the link between urbanization and development. The increasing of the agricultural productivities caused the cities developments where the people migrate more and more from the rural communes to the path of the communication routes and cities suburbs. Later, the Industrial Revolution caused the emergence of industrial firms in existing cities or around the required natural resources that attract the workers who had left the agricultural sector. This, as a reciprocal phenomenon, on the one hand, led to an exponential increase in urban migration and an increase in the size of local markets for goods, services and labor, and, on the other hand, attracts more firms. The agglomeration of populations and economic activities effect on the price of land. This increasing of the land price causes that the people with less income move from the city centers to the edge of the cities and the cities be spread. This urban sprawl can happened either by expanding the urban boundaries with new urban development adjacent to pre-existing facilities or by the discontinuous sprawl. In the latter case, in order to provide a good commute to working place, the populations or firms move to the communes close enough to the cities (ESCo, 2017, introduction, p.8 & 9). The apparent slowness of urban sprawl, often, hides its real speed and could not be seen in the short term. Urban sprawl is a complex cross-cutting phenomenon that each sector brings a different angle of observation (e.g. the transport studies identify a link between the progression of the building and the network of roads, land surveys show that farmland prices increase as urbanization progresses) (Antoni, 2010).

Urbanization, as a part of artificialization, is the main factor of urban expansion, which occurs by increasing the surface area of the city and the extensions of its borders. In some cases, the urban expansion happens outside the peripheral areas that are called peri-urban. Peri-urbans are closely linked to the urban and they are take place in communes outside the city. In France, the urban sprawl affected by peri-urbanization has slowed down before the 2000s, and it is always a demographic balances between urban and peri-urban areas and French landscapes (ESCo, 2017, introduction, p.11). Urbanization as an inevitable phenomenon often induces irreversible changes and can impress on biodiversity, ecosystems and urban climate and transforms agricultural and natural areas. Tracking and controlling the artificialized lands represent an important challenge for local authorities facing with transversal objectives of sustainable development and it is a pressing societal demand in environmental matters. Therefore, sustainable urban planning and management require reliable land change models, which can be used to improve decision-making (see section 1.2).

1.1.1. The Impacts of Urbanization

In December 2017, a collective scientific multidisciplinary report on artificialized land and artificialization processes including the drivers, impacts and potential responses in the French territory was published that was jointly conducted by IFSTTAR (*Institut français des sciences et technologies des transports, de l'aménagement et des réseaux*) and INRA (*Institut national de la recherche agronomique*) (ESCo, 2017). Their researches was requested and supported by CGDD/MTES (*Commissariat général au développement durable, Ministère de la Transition écologique et solidaire*), ADEME (*Agence de l'environnement et de la maîtrise de l'énergie*)

and DGPE (*Direction générale de la performance économique et environnementale des entreprises, Ministère de l'Agriculture et de l'Alimentation*). The concept of artificialized land is introduced by agronomists to identify changes in the French landscape by identifying various land uses and their changes (ESCo, 2017, introduction, p.7; source: Slak and Vidal, 1995). This land uses classifications leads to four main distinct types of land use, including agriculture, forestry, natural spaces and the artificialized land. Artificialization refers to the process of specific land use changes from the agriculture, forestry and natural spaces to the artificialized land. Artificialized lands include the constructed areas, the spaces that are affected and shaped by human activity and the green spaces associated with them e.g. residential, commercial, administrative, educational and industrial constructions, quarries, mines and dumps as well as parks and gardens, sports and leisure facilities (Barbe et al., ESCo, 2017, section 1).

Artificialization, and its effects can be studied from different aspects including the type of land cover after artificialization e.g. waterproofing, mineralization and plant cover; the positioning of the land in the urban fabric e.g. centers of dense cities, suburbs, zones extending the city's borders, peri-urban municipalities, municipalities outside urban influences; and the type of activities that take place there e.g. individual or collective housing, industrial activities and their nature, tertiary activities, commercial and logistical activities, transport infrastructure (ESCo, 2017, introduction, p.11).

1.1.1.1. The Impacts of Urbanization on Environment

With the growth of urbanization and as result urban sprawl and consequently increasing the artificialized lands, air and soil pollutions are increasing. For example, increasing inner city travels as well as long distances between home and workplace cause to burn more car fuel. Vehicle traffic causes pollution through the creation of airborne particles and toxins as well as pollution caused by brake pads. Furthermore, artificialization causes rising the lands occupied by mining and industrial sites around the cities that make both soil and air pollution. Mines and factories release large amount of dust, carbon monoxide, hydrocarbons and chemicals compounds into the air causing massive air pollution. Over the last three decades, the scientists have made more research on the impacts of artificialization on physical, chemical and biological properties of soils (Cornu et al., ESCo, 2017, sections 2). It turns back to the end of 20th century that they study the health and environmental risks of mining and industrial sites. In addition, the soil pollution affects urban hydrology. This is essential in the management of water and material flows and led to a reconsideration of the role of soils in urban areas. As mentioned earlier, attempts to investigate the impacts of increasing urbanization are made for various reasons, including environmental reasons e.g. limiting the losses of agricultural land and forest, reducing its effects on the lives of inhabitants, animals and plants and lessening the carbon impact by reducing the commute. Urbanization has a significant influence on local environmental features, vegetation and animal species. It impresses the habitats by fragmentation and connectivity between them. In this situation, the infrastructure, industrial areas and the mining areas usually have a negative effect on flora and fauna (Cohen et al., ESCo, 2017, sections 3). It, also affects the physical urban environment, the urban microclimate and noise and air pollution where some of these long-term impacts transfer the pollutants into water,

soil and the food chain (Musy et al., ESCo, 2017, sections 3). From other impacts of urbanization on environmental, we can mention the urban heat islands that are another concern arising from the expansion of urbanization and come from the heat that is produced by industrial and urban areas (Parker, 2006).

1.1.1.2. The Impacts of Urbanization on Agricultural Lands

As reviewed before, cities are shaped by various factors that one of them is the migration from rural to urban areas. This shifting from the rural to peri-urban or urban areas, on the one hand, extends the area of the cities and makes the urban sprawl and, on the other hand, causes the loss of the agricultural lands with changing to the built on lands. In fact, land takes impress agriculture in both terms of the production loss and agricultural environment considering the low reversibility of agricultural soils that have become polluted and impermeable. Agricultural land can easily be converted to the artificialized land while the reverse conversion is difficult, expensive and takes time. Referring to ESCo (Géniaux et al., ESCo, 2017, sections 4), almost 70% of urbanization takes place on the very good quality farmland where this category of land covers itself accounts for 68% of France territories in 2017. The income from agricultural land and the value of land are the other reasons of the land use changes in the agricultural areas.

1.1.1.3. Policies to Limit Agricultural Land Changes

Some policies can avoid, limit and compensate the agricultural land changes such as greenbelts, zoning, policies to address agricultural production and adjusting taxation on the sale of agricultural land. A green belt consists of a natural area that is designated by public authority to be protected from urbanization (Baumont and Guelton, ESCo, 2017, sections 4). The green belts exist in several countries such as United Kingdom (Baumont and Guelton, ESCo, 2017, sections 4; source: Schone, 2010). They aim to limit urban sprawl by promoting settlement in already equipped areas, reduce the impact on agricultural areas, and avoid peripheral displacement in rural areas (Baumont and Guelton, ESCo, 2017, sections 4; source: Gelan et al., 2008). Green belts can have an effect on the restriction of buildings and their price, the improvement of environmental amenities on and around the site and the effects of supply scarcity in relation to demand. The verification of these effects was carried out in France (Baumont and Guelton, ESCo, 2017, sections 4; source: Géniaux and Napoléone, 2011) and demonstrates the protective effect of a strict environmental zone and nearby, while the attractiveness is reinforced on a larger scale. At the same time, the scarcity effect causes prices to rise and changes housing demand by pushing it to other locations (Baumont and Guelton, ESCo, 2017, sections 4; source: Wu et al., 2004).

1.1.2. Urbanization in France

Between 1950 and 2018, the world urban growth rates were positive in almost all countries of the world (United Nations, 2018). In the last 30 years, the consumption of space per inhabitant has been multiplied by two or three in most French cities. However, the development and the

sprawl of the cities, their demographic growth and their economic developments will certainly not be sustainable in the long term and at such a sustained pace (Youssoufi and Antoni, 2009).

The public policies of the household location and the urban planning strategies attempts to manage the housing demand. In these policies, various factors are considered such as the housing price and the distance from the center, household density and spatial distribution and the transport policy. In most cases, the price of housing decreases when the distance from the city center increases, and vice versa. On the other hand, the density decreased with distance from the center and the housing area per person increased. Public policies can also play an important role in the form of land acquisition and development projects (Aguilera and Bonin, ESCo, 2017, sections 5).

In addition to the urbanization determinants discussed before in this chapter, such as population growth and migrating population from rural to urban area, there are some other particular factors that impact the amount of urbanization in France. In urban planning, the development of natural amenities can limit the environmental impacts of urbanization. However, natural amenities may attract people. They also effect on extensive development of second homes. The natural and climatic amenities, water-related recreation, and the amenities associated with sports as well as the growth in the proportion of forest cover are some other factors that have a great impact on local population growth and increases incoming migration. Local population growth leads the extensive development of second homes and more facilities. France is a destination for international migrants due to the vastness, water resources, climate diversity, and historical, cultural and investment attractions. This international migration, in turn, causes the demand for residential land and thus, the expansion of the urbans and peri-urbans. The development of these spaces should optimize the accessibility to the facilities and to the zones of leisure while avoiding a fragmentation of the natural and agricultural zones. Therefore, the public policy should take into account the housing and the facilities demand while limiting the environmental impacts and the spatial extension of urban areas (Aguilera and Bonin, ESCo, 2017, sections 5). The development of peri-urban spaces should optimize the accessibility to the facilities and to the zones of leisure while avoiding a fragmentation of the natural and agricultural zones (Frankhauser et al. 2007).

In France, like in other post-industrialized countries, the relationship between population growth and the expansion of urban spaces is not linear. Indeed, the increasing of the housing demand is often more than population growth. This comes from the life style and the characteristics of French households in terms of housing choice such as the preference of living in the detached houses or detached single-family homes, the lack of large houses and large apartments in the city centers or downtown (that leads to the preference for suburban areas), and the desires of children to live in separate homes from parents (Aguilera and Bonin, ESCo, 2017, sections 5).

Public transport policies are other factors that play a complex role in urban planning and development. Public transportation is one of the factors of reducing pollution and overall energy consumption. However, in the same time, it gives the possibility to the people to live with more

distance from the center, which leads to urban sprawl (Aguilera and Bonin, ESCo, 2017, sections 5). Construction of infrastructure and transportation networks are also important factors of the land artificialization. Based on the SOeS - MTES (*Service de l'Observation et des Statistiques, Ministère de la Transition Ecologique et Solidaire*) report, 20,970 km² equivalent to 3.8% of the French mainland dedicated to rail and road networks in 2012 (Thévenin and F-Mannone, ESCo, 2017, sections 6). Moreover, the economic importance in sector of housing and transportation construction is significant and millions of people directly and indirectly are employed in this sector with more than 1.3 million jobs in France, which does not always incite to limit this activities (Aguilera and Bonin, ESCo, 2017, sections 5).

1.1.2.1. Urbanization Measurements

The measurement of artificialized lands refers to the surfaces including the built land used, paved or stabilized land, artificial green spaces and the spaces that are affected and shaped by human activity and the urban footprints that defines the outline of urban expansion. There are different methods of measuring land-use changes including remote sensing, the statistical surveys, the value-adding to administrative files and databases and the retrospective or predictive modeling approaches (Barbe et al., ESCo, 2017, section 1).

According to CLC (*Corine Land Cover*) source, 5.5 % of France territory in 2012 was classified as artificial land while according to the Ministry of Agriculture (Teruti-Lucas source), this amount is almost 9.3 % in 2014 where more than 30% of them were artificial grassy lands (see tables 1.1 and 1.2). The differences of amounts come from their different ways of data extraction. Teruti-Lucas is a statistical data that is based on the original association of aerial photographs constituting the survey frame and field surveys by investigators and whereas CLC is an exhaustive source that is derived from the visual interpretation of satellite images but has some threshold. As mentioned before, urbanization as a major driver of artificialization, represents a large part of the artificial land. CLC shows that in 2012, 75% of artificialized lands were located in the continuous or non-continuous urban fabric, and the others contain the areas such as the railways and road networks, the industrial or commercial areas and the facilities (ESCo, 2017, introduction, p.8).

Housing along with economic activities and transport infrastructure are the main activities that take place on artificialized lands. Housing took 42% of the artificialized areas in 2014 and almost half of the newly artificialized areas from 2006 to 2014 were for individual or collective housing (Teruti-Lucas, source; ESCo, 2017, sections 5). Housing cause the urban sprawl and peri-urbanization, while at the same time the density of the urban areas are also increasing (Aguilera and Bonin, ESCo, 2017, sections 5). As illustrated in table 1.1, according to the Corine Land Cover, the land artificialization in France has increased 20% from 1990 to 2012, where 8% occurred from 1990 to 2000, 7% from 2000 to 2006 and the over 3% from 2006 to 2012. The statistics indicates the expansion of urbanization, which covers nearly 2.3 million hectares in 2012 mention that the urban areas increasing rate was 2 % between 2006 and 2012 (Ruas et al., ESCo, 2017, section 1).

Table 1. 1. Distribution of the area of mainland France by nature of occupancy according to Corine Land Cover 2006 (corrected data) and 2012. (ESCo, 2017, section 1, p. 20; Source: SOeS, MTES)

	2006			2012		
	Mha	%	%	Mha	%	%
Continuous urban fabric	0.044	1.5	0.1	0.044	1.5	0.1
Discontinuous urban fabric	2.208	74.8	4.0	2.253	74.3	4.1
Industrial zones, commercial & public installations	0.359	12.2	0.7	0.385	12.7	0.7
Transport infrastructure	0.103	3.5	0.2	0.109	3.6	0.2
Other economic activities	0.098	3.3	0.2	0.098	3.2	0.2
Green spaces and recreational areas	0.141	4.8	0.3	0.143	4.7	0.3
Artificialized land	2.953	100.0	5.4	3.032	100.0	5.5
Agricultural land	32.696		59.6	32.619		59.5
Forested and natural land	19.202		35.0	19.192		35.0
Total surface	54.851		100.0	54.843		100.0

As mentioned above, according to Teruti-Lucas source, in 2014, almost 9.3 % of France lands in 2014 were artificialized. This source is also indicates an increase in the amount of artificial lands from 1984 to 2014. Table 1.2 illustrates the distribution of the area of mainland France by nature of occupancy obtained from Teruti-Lucas source. It shows that, in 2014, 1 million hectares out of 5.1 million hectares of the artificialized lands, were built-on lands, 2.5 million hectares of them were linear or non-linear coated and stabilized surfaces, e.g. the road or rail infrastructure, municipal roads and car parks, and the rest were other artificialized lands including the grassed and non-vegetated lands (Ruas et al., ESCo, 2017, section 1).

Table 1.2. Distribution of the area of mainland France by nature of occupancy according to Teruti-Lucas surveys 2006 and 2014. (ESCo, 2017, section 1, p. 22; Source: SSP (Service de la Statistique et de la Prospective) – MAA (Ministère de l'Agriculture et de l'Alimentation))

	2006			2014		
	Mha	%	%	Mha	%	%
Built-on land	0.756	16.5	1.4	0.923	18.1	1.7
Coated or stabilized surfaces	2.159	47.3	3.9	2.456	48.1	4.5
non-linear areas	0.719	15.7	1.3	0.841	16.5	1.5
linear areas	1.441	31.5	2.6	1.615	31.6	2.9
Other artificial lands	1.653	36.2	3.0	1.725	33.8	3.1
Grassed land	1.465	32.1	2.7	1.583	31.0	2.9
Unvegetated land	0.188	4.1	0.3	0.142	2.8	0.3
Total artificialized land	4.568	100.0	8.3	5.104	100.0	9.3
Agricultural land	28.591		52.1	28.029		51.0
Forested land	17.042		31.0	17.033		31.0
Other uses	4.718		8.6	4.752		8.7
Total surface	54.919		100.0	54.919		100.0

Although, the two source above give some information about the artificial land and the urbanization areas, neither Corine Land Cover nor Teruti-Lucas could not provide more precise

information in terms of the increase the artificialization in peri-urban and rural areas ([Barbe et al., ESCo, 2017, section 1, p.24](#)). In Europe the urban sprawl often occur with the extension of urban areas on the periphery of the zones already built rather than more distant areas and also by the peri-urban development, however the concentration of populations and employments are in urban areas. In the context of biodiversity loss and climate changes, Europe is very concerned by the continuous increase of its artificialized soils. Similar to France, the rate of land take in Europe increased 2.7% from 2000 and 2006 according to the Corine Land Cover statistics (107,800 ha per year). Given the statistics presented above, it seems necessary to optimize the land take measurement to obtain the information more precise within urban, peri-urban and rural areas and to differentiate the types of artificial land covers and their relations.

1.1.2.2. Avoid or Reducing the Effects of Urbanization

According to [ESCo \(2017, section 8\)](#), the term of artificialization is not defined in French law, which makes a legal controversies over it. In fact, there is no general policy against it, except in some agricultural land or the natural protected environments such as national parks. Therefore, [ESCo](#) attempts to provide some effective mechanisms to prevent, reduce and compensate of artificialized lands. In order to prevent artificialization, there is always some propositions such as stopping to promote new settlements on new artificialized land. [ESCo \(2017, section 8\)](#) provides some other propositions as follow:

- Zoning as an efficient way make it possible to control the residential densities and the land market effectively.
- Approval of law and taxation for the particular sensitive areas such as rural areas, agricultural lands and the coastlines can efficiently help to avoid urbanization, and artificialization in general, in these areas.
- Rehabilitation and densification of the current urban areas can be another way to prevent urbanization, however, the required space for amenities should also be considered in densification process.

To reduce and compensate the effects of artificialization, which come partly from urbanization, [ESCo \(2017, section 8\)](#) gives some suggestions such as:

- Studying the characteristics of the soils and environment over which the transformation is projected. This requires more investment in water, soil and environment consulting.
- Recycling the artificial lands in order to rehabilitate of polluted sites and soils.
- Limiting the sealing surfaces in urban areas e.g. increasing the soil's absorption capacity in the car parks surfaces and paving stones.

In rural code and forest code there are some agricultural and forestry compensation mechanism, respectively. However, there is no specific compensation mechanisms neither for the artificialized land nor for their impacts such as biodiversity, hydrology, soil pollution and urban climate, in France ([ESCo, 2017, section 8](#)).

In addition to the mechanisms discussed above, urban growth management strategies (GMS) (Pollock P., 2008) are needed to keep a balance between housing and land protection. GMS attempts to manage the growth rate of the cities by considering some factors such as:

- The amount, type, extent, rate, and quality of urban development,
- Protection of natural spaces, sufficient and affordable housing, delivery of utilities, preservation of buildings and places of historical value, and sufficient places for the conduct of business,
- Impact fees (e.g. transportation improvements, new parks, and expansion of schools),
- Application of zoning to reduce the cost of service delivery such as fire protection and emergency medical response services ,
- Preventing suburban densities from affecting a large area,

Yousoufi and Antoni (2009) proposed two solutions to answer the demand for housing relative to the increase of the number of households, in the case of an agglomeration like Besançon as follow:

- Occupying vacant dwellings or invest urban spaces in rehabilitation if the supply is sufficient. This can revitalizes urban spaces that are sometimes abandoned without any spreading effect. However, it probably cannot completely provide the housing demands.
- Opening the urbanization of non-built spaces in any possible spaces (that may happen often in the periphery). This solution may satisfy demand, however, it increases the consumption of residential space and encourages urban sprawl.

1.2. Urban Modeling

Given the phenomenon of urbanization, the urban planning process seems inevitable. Urban planners use different models of urban growth and land use change for various tasks such as estimating population growth, land use changes, analyzing their impacts, and creating demographic and geographic urban patterns. In this section, we review some different land use patterns, different techniques of simulating urban growth and land use and their applications.

The predictive or prospective models of urban growth and land use changes attempt to represent different scenarios of the urban expansions in terms of space consumption, the urban sprawl configuration, density and demography, and the socio-economic and environmental effects of urbanization (Barbe et al., ESCo, 2017, section 1, p.16).

Urban sprawl and urban growth are somehow related and the cities mainly get bigger by expanding around their peripheries. Although, sometimes cities get bigger by increasing their central densities leading to the formation of a compact city. In general, cities grow in various forms and different factors have impact on the urban growth such as economic, environmental and social factors (Ewing, 1994; Tabourin, 1995; Galster et al., 2001, Gober et Burns, 2002, Antrop, 2004). These factors make the cities develop by different patterns. Figure 1.3, illustrates five different patterns considered as the urban sprawl patterns (Galster et al., 2001).

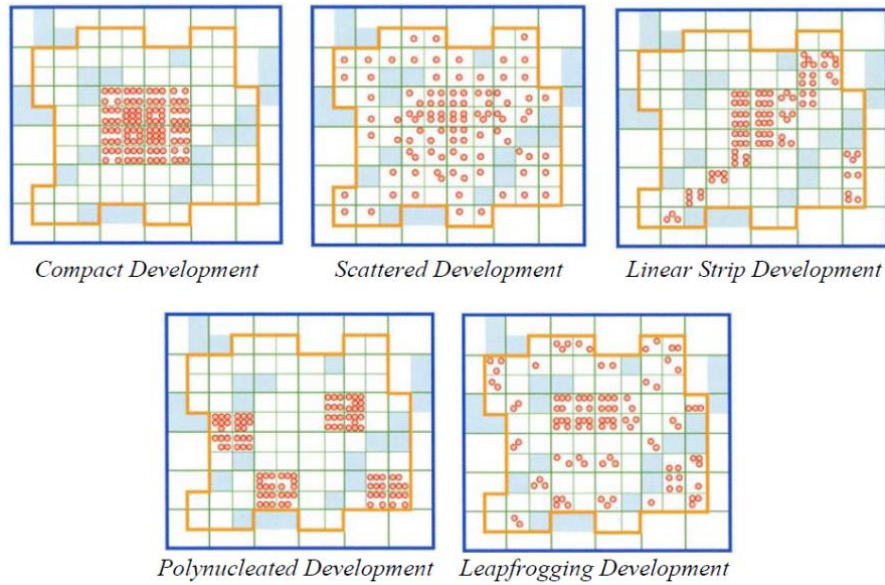


Figure 1.3. Urban sprawl physical patterns; (Galster et al., 2001)

In most classical urban models, cities spread continuously by expansion of their borders through the concentric circle zones where the density decrease with the distance to the center. However, this continuous growth can occur along the linear attractive zones such as the roads or/and the rivers which makes the linear strip development. In case of non-continuous urban pattern, the growth often happens as a fragmented and disjointed peri-urban development. This fragmented development, which is the case of most European cities as well as French cities, leads to sprawl development where the buildings are dispersed in the middle of agricultural, forested or natural areas like the scattered pattern (Coisnon and Oueslati, ESCo, 2017, section 5). The fragmented development can take place in the form of satellite clusters or the discrete strip development over the entire periphery of the city or dispersed areas similar to polynucleated and leapfrogging pattern (see figure 1.3).

1.2.1. Land Use Patterns

Land use patterns can give a view of the form of cities. Urban patterns often contain spatial structure of the urban area such as buildings, open spaces and human activities. In general, the physical form of cities is shaped by their social and topographic features, etc., which leads to the creation of different urban areas such as residential, industrial and commercial. Land use and urban growth patterns give an idea to forecast the effects of human behavior as well as natural phenomenon and vice versa. The knowledge on the urban growth patterns and land use change is essential for the stakeholders including city planners, resource managers, environmentalists, and policy makers. This information allows them to engage in knowledgeable and productive planning, policy, and informed decision making (Hedge et al., 2008). In this section, three famous urban land use models including concentric zone model, sector model and multiple nuclei model are defined. These classical land use patterns were developed to generalize the urban land use patterns of the industrial cities of United States that we call hereafter predefined patterns. Predefined patterns are static models that should be created manually for each study area according to the land use observations for that area. In this

thesis, a method of producing land use pattern is proposed that can be adapted to any study area and automatically updated considering the current land use. This pattern, hereinafter referred to as the active pattern, is presented in next chapter (section 2.4.1.3).

1.2.1.1. Concentric Zone Model

The Concentric zone model is a theoretical model to explain urban social structures that applied on Chicago by Burgess (R. E. Park et al., 1925). Burgess theorized that social structures extend outward from the one central business area. This model depicts the use of urban land as a set of concentric rings where each ring devoted to a different land use. Figure 1.4 illustrates the general form of the model.

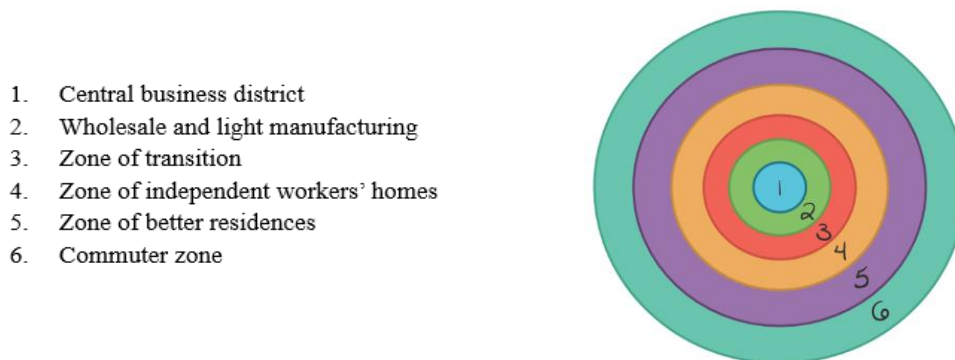


Figure 1. 4. Concentric zone model (R. E. Park et al., 1925)

The center ring is central business district that is the most accessible location in the city. The second zone is considered as wholesale and light manufacturing. The transition area includes rooming houses and mostly the workers who work in the second zone and the low-income families are living there. Working class zone is established for middle class families to escape the transitional second zone to maintain convenient access to their work. The fifth Zone contains the more expensive apartments, hotels and single-family homes. The last zone is for commuters and consists of suburbs or satellite cities that are located around transportation routes. The concentric zone model represents the population density decrease towards outward zones. The relation between economic status and distance from the center is visible in this model. The concentric zone model represent the older and compact city of Chicago (R. E. Park et al., 1925). This model is based on cities of U.S. of early 20 century and does matched neither the foreign cities, nor the modern cities.

In general, the household income and their social preferences can shape the residential urban zones. In the cities where the citizens, with similar social preferences, have different incomes, low-income households live in a central circle close to the employment center. In these cases, the middle and higher income households inhabit in the zone around and farther from center in the more expensive apartments and single-family homes. But if their socio-economic preferences are different, the households with different incomes live in or around the center. In non-homogeneous spaces, the residential zones depend to the presence of natural, historical or modern amenities or the social neighborhoods. In some cities like Paris or other European

metropolises, which have these attractive spaces in the center, the higher income households live in the center and the zone of the disadvantaged households is located in more distance from the center. The residential zoning in these European metropolises is different from the industrial cities of United States that presented in concentric zone (Baumont and Guelton, ESCo, 2017, section 5).

1.2.1.2. Sector Model

Homer Hoyt (1939) developed the sector or wedge-shaped model on 1939, which is a modified version of the concentric zone model. He found that most major cities are developed around the nexus of several important transport facilities such as railroads, seaports, and the other transportation routes that emanate from the city's center. This model takes into account transportation developments where the city expands outwards, but along railways, highways, and water. Figure 1.5 illustrates the sector model pattern.

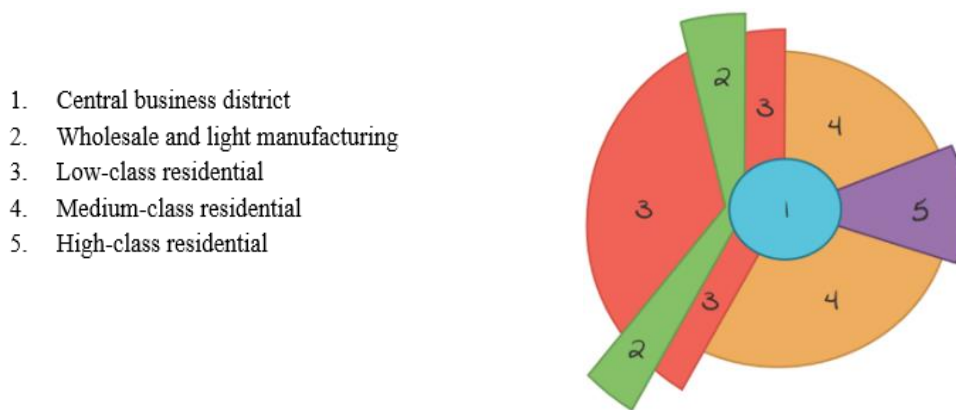


Figure 1. 5. Sector model (H. Hoyt, 1939)

The core of the city is the central business district. The second sector contains of the wholesales and light manufacturing. In general, the low-income households are in close proximity to railroad lines, and commercial establishments are along business thoroughfares. In sector model, the city tends to grow in wedge-shaped patterns, connected to the central business district and centered on major transportation routes. Sectors of middle and higher income households located away from industrial sites. The commuter zone can be consider all around the sectors.

1.2.1.3. Multiple Nuclei Model

Many cities did not fit the traditional concentric zone or sector model. Harris and Ullman (1945) proposed a model in which the growth of a city depends on different centers of each specific area called nuclei. The multiple nuclei model considers the increasing of car ownership and transportation access and so the greater movement.

In this model, the areas with similar activities are gathered; therefore, the land use is similar in adjacent areas. Figure 1.6 illustrates the multiple nuclei model. In this model, the central

business district is the major center of commerce and the model can still develop multiple smaller business districts. Light manufacturing and wholesaling located along transport routes.

Mostly the newer and modern cities with large land area in U.S. (e.g. Houston and Los Angeles) can be considered as the multiple nuclei pattern.

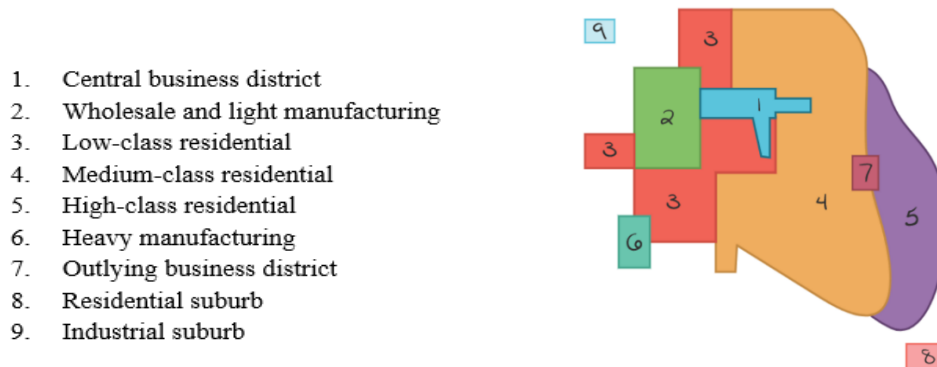


Figure 1. 6. Multiple nuclei model; (Harris & Ullman., 1945)

1.2.2. Sustainable Urban Modeling: An Overview on Different Techniques of Simulating Urban Growth and Land Use / Land Cover Change

Many recent studies, using diverse modeling approaches and simulation tools of varying complexity have been conducted in the field of urban growth. A significant number of researches have been carried out on urban growth and land use changes, including the linear and non-linear behavior of urban systems. Researches show that the urban growth is a dynamic system and therefore it is highly complex and non-linear in nature (Pumain and Reuillon, 2017). From all existing approaches, the cellular automata modeling (Clarke et al., 1996; Clarke et al., 2001), agent-based modeling (Robinson et al., 2012; Arsanjani et al., 2013), artificial neural network modeling (Pijanowski et al., 2009; Mohammady et al., 2014) and fractal modeling (Herold et al., 2002; Triantakoustantis, 2012) are the most used in the last two decades. Among all dynamic models spatially explicit, those based on CA are more common for their applications in urban areas. CA can be integrated with GIS to have a high spatial resolution model with computational efficiency. The CA models are used to simulate urban growth and land use changes (Al-shalabi et al., 2013; Deng et al., 2015; Nourqolipour et al., 2014), project future scenarios of urban landscape (Maeda et al., 2011; Yin et al., 2011) and investigate urban ecological security (Gong et al., 2009; Mao et al., 2013).

The prospective modeling of urban growth and LUCC is rapidly expanding practice designed to inform decision-makers about the possible impacts in terms of space consumption, future forms of urban sprawl and their socio-economic and environmental consequences. Analyses of past changes are a prerequisite for exploring future urbanization using spatial simulation models. Most of these models, use the historical land cover data in order to simulate the future urbanization. The calibration process of the model analyses the past land use changes. Next, the model validation is performed by simulating urbanization over a past period. In validation process the results and the observed data are compared. In most of the researches the models

are based cellular automata (CA) approaches e.g. SLEUTH and CA-Markov model ([Barbe et al., ESCo, 2017, section 1](#)). In most of urban growth and LUCC simulations, the impacts of population growth and building types are implicitly considered during the calibration phase, however, changes in population growth rates or urban tissue are usually not included in their simulations. This makes it difficult to use the results in order to make reasonable decision for sustainable urban planning and management.

In this section, some techniques that are used in the domain of urban growth and LUCC modeling including fractal modeling, artificial neural network modeling, agent-based modeling and cellular automata modeling are represented and a classified list of different researches and their applications are prepared. The classified list could be used to provide an appropriate view for urban planners in the field of urban planning development (see Annex A). The methodology of our survey is based on a literature review on the articles that are concentrated on simulating the urban growth and LUCC model. The objective is to provide an appropriate view in the field of urban modeling by presenting and classifying the different simulation techniques. The urban and LUCC modeling techniques, their use cases and their applications are widespread, so many scientific articles, project reports as well as online resources have been studied. During the screening and review process, it was found that each method has some general characteristics that make it possible to fit better to a study area according to the availability of data, the use case, application and operation. For some of articles, the required data, their constraints, and their interoperability to other data and systems e.g. RS (Remote Sensing) data, GIS are also presented.

1.2.2.1. Fractal Modeling

[Mandelbrot \(1983\)](#) has firstly developed the fractal geometry. Unlike Euclidean geometry, the mathematical objects in fractal geometry can take intermediate dimensions. [Frankhauser \(1990\)](#) has investigated the application of fractals in urban structures, e.g. spatial distribution of buildings or different uses. In this research, he introduced the fractal growth processes, their simulation and growth dimensions regarding the urban growth simulation. Analysis of the built-up area of some agglomerations at the scale of the metropolitan areas shows that urban tissues follow an internal order that corresponds to a fractal geometry ([Frankhauser, 1994](#)). Fractals are dynamic objects and their self-similarity and scale dependency can characterize the complexity of spatial objects ([Barredo et al., 2003](#)). The geometry of the fractals depends on an evolutionary process. As mentioned before, urban areas can be considered as complex dynamic systems. The spatial patterns of urban areas can be determined by land use dynamics within the self-organized urban system. Despite urban fabric irregular form, it is possible to describe their development using fractal analysis, by comparing the fractal behavior of an urban fabric at different dates ([Frankhauser, 2005](#)).

[Herold et al. \(2002\)](#) used the landscape metrics including the fractal dimension, in order to detect urban land use changes. [Triantakonstantis \(2012\)](#) applied fractals and theory of Chaos for urban growth prospective modeling in the touristic village of Pogonia Etoloakarnanias, western Greece, where a large percentage of urban growth of 57.5% has been occurred during

8 years from 2003 to 2011. Chaos theory focuses on the behavior of dynamical systems that are highly sensitive to initial conditions. Small differences in these conditions yield widely diverging outcomes especially for dynamical systems. The Sierpinski carpet is used to find areas suitable for urban development (see figure 1.7). The Sierpinski carpet is a fractal construction developed by Sierpinski in 1916. The construction of the Sierpinski carpet begins with a square. The square is divided to a 3-by-3 grid to have 9 equal sub-squares, abstracting the middle one. The same procedure is then applied recursively to the remaining eight sub-squares and these continue (see figure 1.7a). After Sierpinski carpet abstraction iterations, the remaining areas have the potential to be urbanized considering their fractal distributional principle. Several shapes of Sierpinski carpets were tested. After fifth iteration of Sierpinski carpet tessellation, the most appropriate shape was found for their case study. The model has produced an accuracy percentage of 70.6% for training set and 81.8% for validation set where the majority of buildings were situated within Sierpinski carpet (see figure 1.7b).

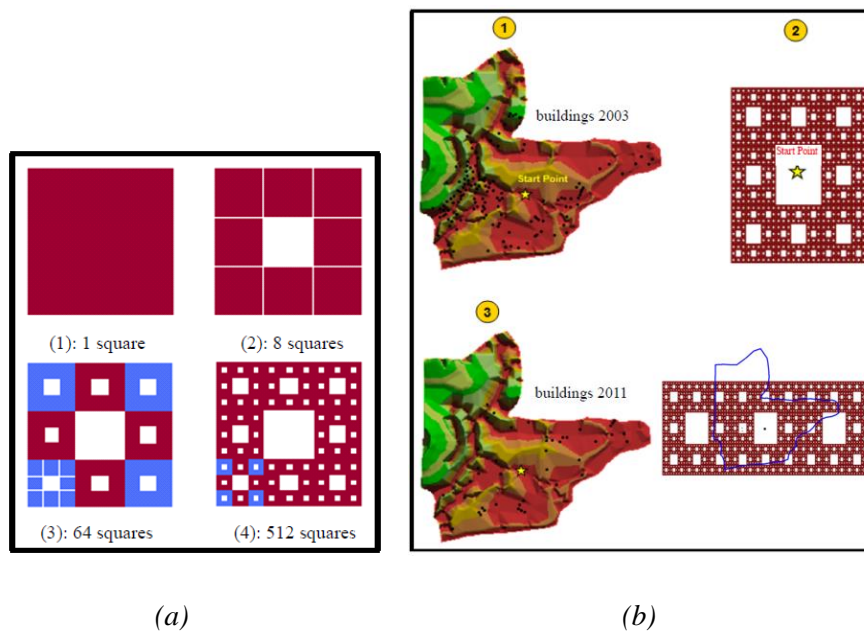


Figure 1. 7. a: Sierpinski carpet construction, b: Design of fractal urban growth model development in the touristic village of Pogonia Etoloakarnanias, western Greece; (Triantakonstantis, 2012)

1.2.2.2. Artificial Neural Networks Modeling

Many dynamic systems and forecasting time series have used artificial neural networks (ANN) modeling (Vemuri and Rogers, 1994). In some researches, this technique is used as a tool for simulating urban growth pattern that is complex, non-linear and dynamic process system. ANN models are knowledge-based models that use a machine learning approach to quantify and to model complex behavior of urban development. ANN uses a process of learning from the provided samples, which works well in dealing with imprecise data (Weisner and Cowen, 1997; Pijanowski et al., 2002; Tayyebi et al., 2009; Tayyebi et al., 2011).

Weisner and Cowen (1997) have applied ANN and GIS for modeling urban growth in sub-regions of a metropolitan area, considering the spatiotemporal database of single-family

residential building permits for an eleven-year period. This model assumes that the time of occurrence and magnitude of urban growth in a sub-region of a metropolitan area is a function of the development already occurred in the sub-region and within the neighboring areas. Indeed, ANN models the time series of nonlinear dynamic systems by mapping the state of the system at time t , $x(t)$, to some future state, $x(t + \Delta t)$ where the networks are composed of input layers, intermediate layers and output layers. Each layer can apply any function to the previous layer in order to produce an output, and the hidden layer transforms the inputs into something that the output layer can use. Spatial temporal database of this research defines tessellation regular hexagons covering two counties of Columbia SC study area. Using regular hexagon tessellations makes the neighborhoods relations, shapes and sizes uniform throughout the surface (see figure 1.8). The building data from the years 1981 and 1989 are used as training set and the test set contains the data from 1990 and 1991. By comparing this model to a linear regression model, ANN performs more accurate as a non-linear model of dynamic urban systems.

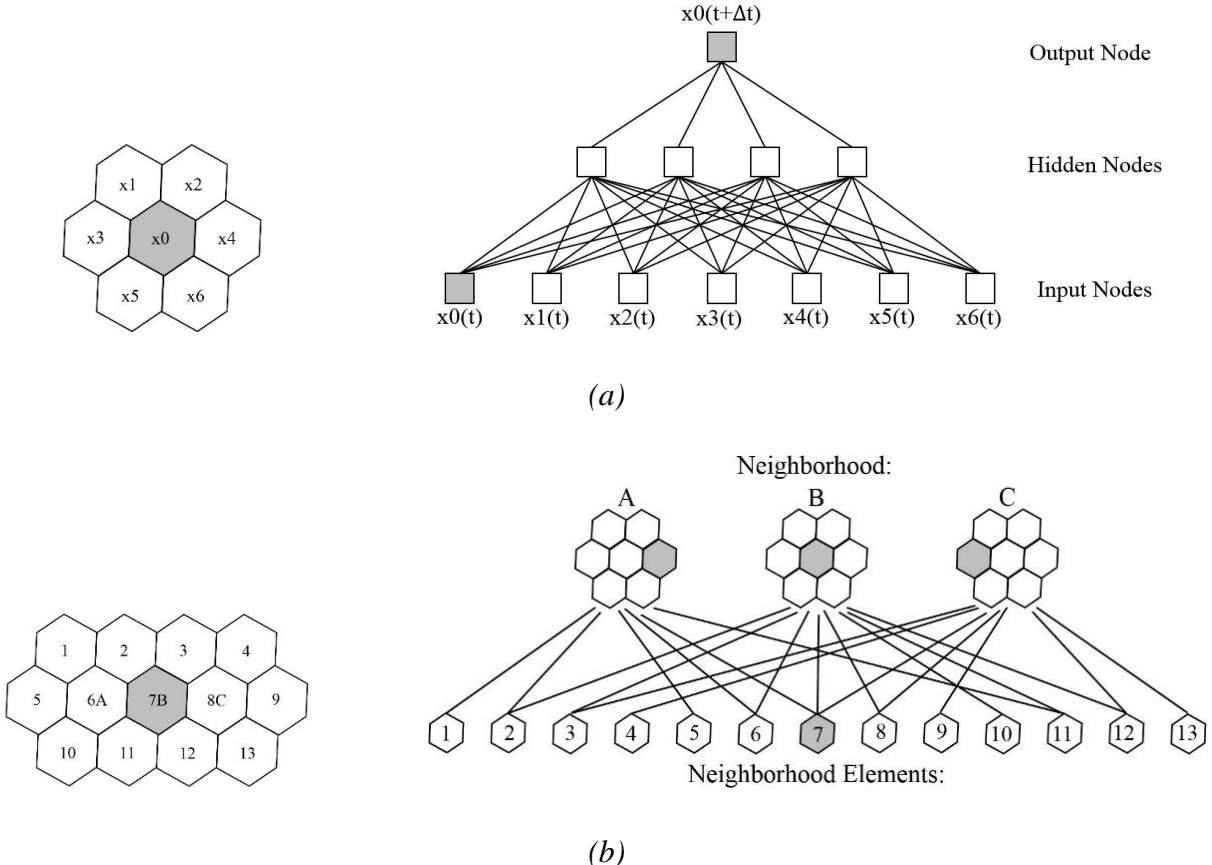


Figure 1. 8. a: hexagonal ANN, b: ANN neighborhood; (Weisner and Cowen, 1997)

Mohammady et al. (2014) used ANN for urban growth modeling in Sanandaj metropolitan, Iran. The dataset is the collection of the Landsat imageries of 2000 and 2006 including the distance to principle roads, distance to residential areas, elevation, slope, distance to green spaces and distance to region centers. They have integrated the Remote Sensing (RS) data and GIS to ANN. Percent Correct Match (PCM) is a way to evaluate an urban development model (Pontius and Schneider, 2001) and figure of merit is a method to evaluate resemblance between

actual and simulated map (Pontius et al., 2008). If simulated map has a high goodness of fit to actual map, figure of merit will be high. These two evaluation methods are used in this research. They show that the accuracy of urban growth modeling for the case study region is at a reasonable level. Overall accuracy and kappa coefficient of these imageries were 92.57% and 89.17% for 2000 and 94.71% and 92.68% for 2006, respectively.

1.2.2.3. Agent Based Modeling

Multi-agent system is a combination of multiple agents. An agent is something that perceive and act on environment (Russell and Norvig, P. 54, 2003). Basically, agents are computational entities that are able to communicate and to act in a sort of autonomous way while all interacting in a shared environment. In 1995, Ferber has provided a coherent overview on multi-agent systems. Multi-agent systems are based on the idea that it is possible to represent the behavior of the entities. Multi-agent systems provide a new solution to the concept of modeling and simulation in the environmental sciences, offering the opportunity to directly represent individuals, their behaviors and their interactions. For example, in a multi-agent population model, individuals will be represented directly in the form of agents and the quantity of individuals of a given species will be the result of confrontations, e.g. co-operation, struggle and reproduction, of the behavior of all the individuals of the system. The multi-agent systems allow to model the complex situations whose global structures emerge from interactions between individuals. The multi-agent system simulations are able to consider both quantitative parameters and qualitative parameters such as individual behaviors. Many sciences such as physics, chemistry, biology, ecology, geography and social sciences use multi-agent simulations in order to explain and forecast natural phenomena (Ferber, 1995).

The agent-based models can be used to simulate the effects of the non-linear behavior of individuals on land change and the complex urban systems. Agent-based model is suited to overcome the problem of some other models in the inability of integrating human, social and economic factors (Manson, 2005; Crooks et al., 2008; Rousseaux et al., 2011; Robinson et al., 2012). Since agent-based models are linked to the possibility of representing movement independently of scale, they can be used as a micro-simulation technology for a wide range of spatial applications in order to simulate the urban growth and land use changes.

As mentioned, an urban system is a dynamic complex system. Perret et al. (2010) have presented a multi-agent system, which is a hierarchy of topographic agents, to model the urban dynamics as a complex system. The high-level evolution rules control the dynamics of the model considering the environment of each sub-system. They combined the rules with a constraint-based approach in order to achieve the target values fixed by the rules.

Arsanjani et al. (2013) have made an effort to monitor the spatiotemporal patterns of Tehran (Iran) in order to distinguish the biophysical, social, and economic driving forces of the recent expansions as the major predictors of future growth and modeling urban growth based on the simulation capabilities of agent-based model. They have used a geo-simulation approach that couples agent-based modeling with multi criteria analysis for the period between 1986 and 2006

in order to simulate spatiotemporal patterns of urban growth. They have collected a set of environmental features (e.g., land use map of 1986, 1996, 2006, topography, recreation areas, and the transport network), socio-economic data (e.g., population and land and housing prices), and temporal multi-spectral satellite images (see table 1.3). Because of rapid population growth and urbanization in some developing countries such as Iran, land developers are involved in the construction of massive housing projects. Therefore, to control urban growth, three different types of agents are presented, including developer agents, government agents, and resident agents. The interactions of the agents are combined through overlay functions within a geographic information system. Then, Markov chain model and a concise statistical extrapolation are used to determine the amount of probable future expansion in Tehran for 2016 and 2026. To evaluate the results of this expansion, the model is estimated using data of 2011 and then validated based on urban expansion in 2013. Kappa indices of 0.8463 and 0.8241 are obtained respectively from the simulated map of urban developments for 2011 for each approach. One advantage of the agent-based models is the ability to integrate human, social and economic factors and to consider the interactions of the behavior of individuals on different scales. This capability make it possible to produce more accurate simulation, comparing to other methods. By analyzing the obtained results, they found that the behavior of developer agents can affect the results. They proposed to simulate the urban growth in the greater metropolitan area in order to retain the effectiveness of the agents.

Table 1. 3. Description of the collected geospatial and socio-economic data; (Arsanjani et al., 2013)

Data type	Dataset	Source
(1) Environmental features	Building blocks	Tehran GIS Center, Iranian National Cartographic Center
	Suburb cities	
	Transport network	
	Public parks	
	Protected parks	
	River stream	
	Tehran districts	
	Land use maps (1986, 1996, 2006)	
	Digital elevation model	
	Population	
(2) Sosio-economic data	Land price	Iranian National Cartographic Center, Own survey
	House price	
	Landsat images (Path/Row:164/35;	
(1) Satellite images	June 1986, July 1996, July 2006, June 2011)	U.S. Geological Survey

Curie et al., (2011) have applied an agent-based simulation on densification of urban system from the morphological view using a formalization of island densification process. First, they developed and tested the basic densification methods (industrial zones, collective and individual housing). Then, they combined the developed elementary methods to produce mixed densification methods using different types. Finally, they make it possible to emphasize the importance of mixed densities in simulation and the lack of specialized densification methods for certain types.

Fosset et al., (2016) have used agent based modeling in order to simulate individual daily mobility within an urban environment and simulated the evolving traffic and its impact on air

quality. The aim of this model is to explore the impact of individual behaviors on the dynamics of the city and the impact of global measures on individual behaviors. Moreover, their model focuses on LEZ (Low Emission Zone) impact pollution and population.

1.2.2.4. Cellular Automata (CA) Modeling

Cellular automata models are bottom-up and discrete dynamic spatial models, which are originally discovered by Ulam and von Neumann in 1940, in order to understand the behavior of complex systems. A cellular automata is a discrete model that is used in different sciences such as computer science, mathematics, physics and microstructure modeling (Wolfram, 1983). The cellules are very simple agents and are usually located in a regular grid of cells that covers a space. Each cell have a finite number of states. The state of a cell at time (t+1) depends on the state of the cell at time (t) and its neighbors states. There are some transition rules that represent the process of changing each cell state according to the current state of the cell and the states of the cells in its neighborhood (Schiff, 2011; Santé et al., 2010). Tobler (1970; 1979) used the cellular space for geographic modeling. He developed a demographic model that could be used for forecasting. This model describes only population growth with particular emphasis on the geographical distribution of this growth. Afterward, CA-based models are widely applied for the simulating spatial dynamics (Couclelis, 1985; White and Engelen, 1993; Batty and Xie, 1994; Itami, 1994). CA can be well integrated with GIS and RS data. These integrations have been used in urban sprawl mechanisms, urban planning theories and urbanization effects (Clarke et al., 1996; Wagner, 1997; Clarke and Gaydos, 1998; Batty et al., 1999; Clarke et al., 2001; Li and Yeh, 2001; Li and Yeh, 2002).

In general, CA models represent the temporal as well as spatial process of changes. They dynamically update their transition rules, coupled either loosely or strongly with GIS. They have good spatial visualization capacity as well as the computational effectiveness. The CA models are used in order to simulate urban growth, sprawl and LUCC (Dubos-Paillard et al., 2003; Cheng and Masser, 2003; Alkheder et al., 2008; He et al., 2008; Almeida et al., 2008; Mitsova et al., 2011; Deng et al., 2015; Nourqolipour et al., 2014; Dubos-Paillard and Langlois, 2018, Antoni et al., 2019), project future scenarios of urban landscape (Barredo et al., 2003; Han et al., 2009; He et al., 2011; Maeda et al., 2011; Yin et al., 2011) and investigate urban ecological security (Gong et al., 2009; Mao et al., 2013).

Santé et al. (2010) has reviewed some cellular automata models applied to simulate of real-world urban processes. The main characteristics of urban CA models are as follows:

- Transition rules: These rules represent the processes of the model (e.g. strict transition rules, transition potential or probability, urban shape and form, artificial intelligence and fuzzy logic).
- Objective: e.g. descriptive models, predictive models, prescriptive models and multiple land use.
- Cell space: It is defined as a grid of cells with different resolution.
- Cell states: e.g. as non-urban and urban or active functions and passive functions.

- Neighborhood: It can be represented as a collection of cells based on adjacency (e.g. size and type).
- Growth constraint: It can be divided to the constraints that endogenously generated by the CA model and external constraint related to the other factors.
- Integration with other models: To calculate growth constraints, to define transition rules or to calibrate the model in order to improve the efficiency of the model in real-world processes.
- Calibration: It is used in obtaining the values of the transition rule parameters with the most accurate reproduction of the past evolution of land uses (e.g. methods based on trial and error and methods based on statistical techniques).
- Validation: The most used validation techniques are the ratio of simulated to real number of cells (or clusters) for a given land use, overall accuracy i.e. the percentage of correctly classified pixels, regression analysis between simulation results and real data, and confusion matrix and kappa index.

According to the characteristics of CA models, [Badariotti et al., \(2007\)](#) have proposed a formalization based on graph frame of geographic cellular automata, which allows to model the irregular and dynamic neighborhood of spatial entities. This formalization represents dynamics based on two types of proximities: an aerial proximity, based on Euclidean distance, and a functional proximity by the network. They have also proposed a cellular automation model to simulate the effect of different proximity in urban growth process which ameliorate the understanding of the role of proximities in urban dynamics. These criteria point out the three aspects of neighborhoods in the city, which play an important role in the structuring of urban space namely; built areas density, Euclidean distance from each cell to road network, and network distance to urban center ([Moreno et al., 2012](#)).

[Feng et al. \(2011\)](#) have applied a dynamic urban growth CA-based model using particle swarm optimization (PSO-CA) approaches with inertia weight in Fengxian District of Shanghai Municipality, eastern China. They have simulated the spatio-temporal process of urban growth from 1992 to 2008 at 30 meters spatial resolution. In order to reduce the simulation uncertainties and improve its locational accuracy in urban modeling, they introduced the incorporation of swarm intelligence that stochastically optimize the transition rules. They compared their model to the logistic-CA model by using the error budget method (see figure 1.9).

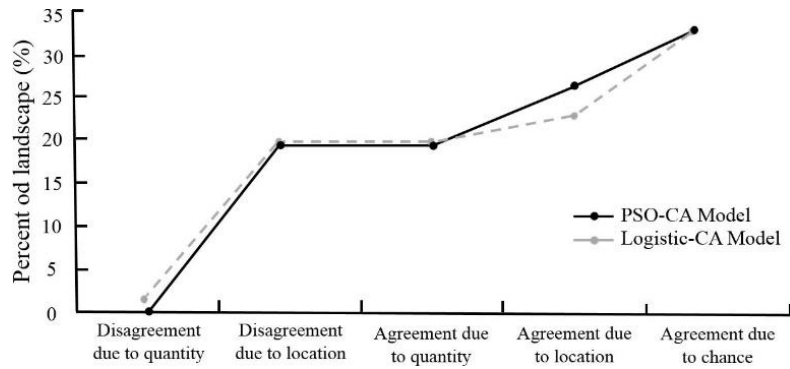


Figure 1. 9. A comparison of the PSO-CA and the logistic-CA model; (Feng et al., 2011)

The reference data are the classified map from the 2008 satellite imagery that demonstrate PSO-CA model outperform. The model was applied in different spatial scale to investigate the effects of the spatial resolution on the model (see figure 1.10).

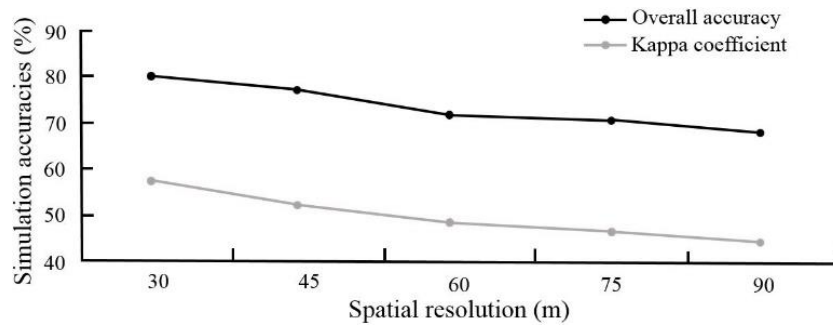


Figure 1. 10. The simulation accuracies of the PSO-CA model at different spatial scales using overall accuracy and kappa coefficient; (Feng et al., 2011)

The essential nature of CA modeling is to identify the complex nonlinear boundaries between urban and non-urban rural areas and their evolution over time. Kernel methods have been used to retrieve CA transition rules by mapping the original data into a high dimensional feature space. Yang et al. (2008) applied a Support Vector Machine-Cellular Automata (SVM-CA) model which is a type of kernel method to achieve higher accuracy and to overcome the limitations of neural networks and some constraint of CA models (e.g. harmful effects of inter-correlations between different driving factors). SVMs are sensitive to outliers and generally require more training time, especially if the dataset has many features (Resler et al., 2014).

Feng et al. (2015) proposed a GIS based cellular automata model that uses the Least Squares Support Vector Machine (LS-SVM) rules. This model is a modified version of SVMs, which is able to generate a direct solution by solving a set of linear equations instead of representing the optimization problem as one of quadratic programming. LS-SVM model can dynamically update the transition rules for each iteration of the model without needs of any arbitrary definition of a transition probability threshold. Using data from 1992 to 2008, Feng et al. (2015) made a simulation of urban growth in the Qingpu–Songjiang area of Shanghai, China. The proposed LS-SVM model consists of three modules including the LS-SVM model training, land use change decision rules and land map visualization. The LS-SVM model-training module

learns the CA transition rules. Based on the result from the LS-SVM model and subject to basic protective farmland constraints, the land use change decision rules module determines whether a nonurban cell will be converted to an urban cell or not. The map visualization module uses ArcGIS to visualize land change.

[Kamusoko and Gamba \(2015\)](#) proposed Random Forest-Cellular Automata (RF-CA) model, which combines RF and CA models for Harare Metropolitan Province, Zimbabwe. The RF models can handle a large database including the thousands of input numerical and categorical variables while quantify each input variable into an importance measure. Compared to other machine learning classifiers, these models require less training time. The RF models are robust in dealing with outliers and noises ([Rodriguez-Galiano et al., 2012](#)). Random forest uses bootstrap aggregate sample bagging to build many individual decision trees for a final prediction or classification ([Mellor et al., 2013](#)). [Kamusoko and Gamba \(2015\)](#) calculated multiple-step transition rates from land use/cover maps of 1984, 2002 and 2008. They simulated the land use/cover up to 2013, using multiple-step transition rates and a transition potential map based on the CA model. To validate the RF-CA model, the Kappa simulation, figure of merit, and components of agreement and disagreement statistics are calculated. They compared the RF-CA model with SVM-CA and Logistic Regression-Cellular Automata (LR-CA). In table 1.4, the validation statistics for all simulation models are shown. Figure 1.11, illustrates the components of agreement and disagreement for RF-CA using bootstrap aggregate, SVM-CA simulated land use map and LR-CA simulated land use map.

Table 1. 4. Compare the validity of simulation models; ([Kamusoko and Gamba, 2015](#))

Model	KSimulation	KTranslocation	KTransition	Figure of Merit (%)
RF-CA	0.51	0.51	0.99	47
SVM-CA	0.39	0.4	0.98	39
LR-CA	-0.22	-0.22	0.99	6

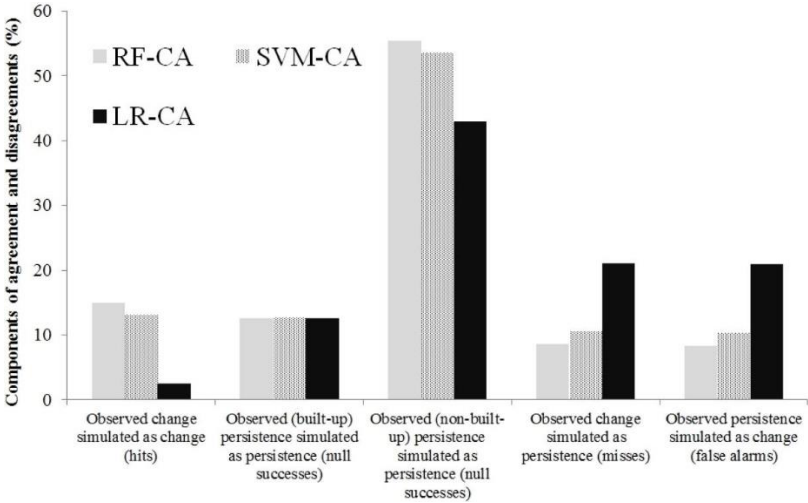


Figure 1. 11. Components of agreement and disagreement for RF-CA using bootstrap aggregate, SVM-CA simulated land use map; and LR-CA simulated land use map ([Kamusoko and Gamba, 2015](#))

Youssoufi and Antoni (2009) have applied three models including a potential, a cellular automata and a fractal model for the commune of Saône, located in the peri-urban area of Besançon in order to identify potentially developable spaces according to four urban planning constraints such as:

1. Ensure good accessibility to the urban and rural areas;
2. Avoid the fragmentation of built-up areas, natural or agricultural, in order to preserve the ecosystems and surrounding landscapes by maintaining a sustainable agricultural activity;
3. Avoid the creation of new roads;
4. Preserve or develop the installation of green flows within built-up areas to ensure the ventilation of dense central areas.

They have divided the study area to the cells of 80 meters resolution, and each cell has one of four states of built, non-built, service or road. The comparison of the three simulations shows that there is no strict overlap between the results from each of the models. The models have simulated the most interesting areas to be urbanized considering the constraints, however their configurations are very different.

1.2.2.4.1. SLEUTH CA Model

SLEUTH is an inductive pattern-based model that uses cellular automata and terrain mapping. This model applies of some growth rules to address UGM (Urban Growth Model) and DLM (Deltatron Land use Model) and evaluate the resulting growth rate. This model is widely used to simulate the urban growth (Clarke, 2008; Project Gigalopolis, 2018). SLEUTH's acronym is derived from its data input requirements: Slope, Land use, Exclusion, Urban, Transportation and Hillshade (See figure 1.12). As shown in Figure 1.12, several historical maps such as urban and transportation are needed for the SLEUTH model calibration.

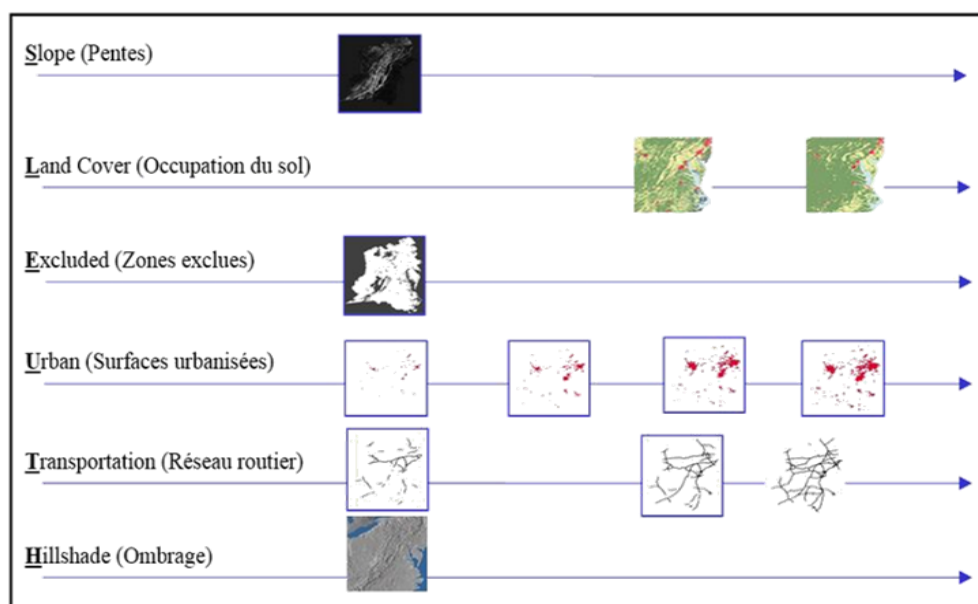


Figure 1. 12. SLEUTH inputs data; (Clarke, K.C., 2008)

The cell state is determined and updated based on four growth rules including the spontaneous new growth, diffusive or new spreading center growth, edge growth and road-influenced growth, which occur sequentially (See figure 1.13).

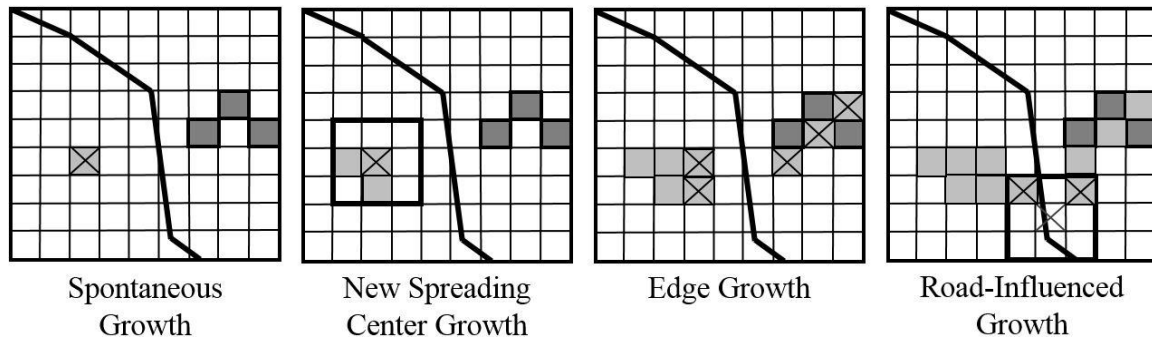


Figure 1. 13. State of cells according to four growth rules of SLEUTH; (Clarke, K.C., 2008)

The simulation rules are controlled by five coefficients including dispersion (diffusion), breed, spread, slope and road gravity coefficients. These parameters are defined in calibration process by comparing simulated land cover changes to the historical data of the study area.

1.2.2.4.2. Advantages of SLEUTH

The SLEUTH has been developed for modeling and forecasting the urban growth based on historical trends. This cellular automata-based model could explore the land cover change in order to model the urban dynamics within the area (Clarke, 1997). It can be used in a wide array of input data resolutions and can be applied to any geographic system at any extent and resolution, however the accuracy of the results will vary for different resolutions (Rafiee et al., 2009).

SLEUTH is an open source model that is available to all researchers and engineers who are interested in working with this model (project Gigapolis, 2018). Furthermore, there are some forums which help the users in their experiments. Another advantage of this model is that the different versions for various applications of this model has been developed by the researchers and developers, so it integrated improvements over the years.

1.2.2.4.3. Limitation of SLEUTH

The SLEUTH model forecasting accuracy in the near future is higher than those occurring in the more distant future, however it also depends on the historical data that are used for calibration (Chaudhuri and Clarke, 2014). This problem comes from the fact that the model has tendency to replicate the trend while the actual rate of change of growth may vary. Another limitation of the model is its scale dependency. The accuracy of the SLEUTH model depends on the spatial scale of the input data.

The SLEUTH results are limited to some raster data. The SLEUTH results are the raster graphics images with graphics interchange format (.gif file) consists of the combination of some

pixels (cells) on which urbanization is supposed to occur and it is difficult to interpret for decision makers.

The basic version of the model has some other limitation such as the required number of historical data, the restrictions of the memory and the problem of road search algorithm which leads time and memory consumption. The modified version of SLEUTH improves some limitations, which are explained more in Chapter 2. Moreover, SLEUTH tends towards edge growth, so it could not generate an appropriate level of dispersed growth. These limitations have been resolved or improved in the latest versions called SLEUTH-3r (SLEUTH 3.0beta_p01 Version R) (Jantz et al., 2010).

In SLEUTH, the rhythm of growth is calibrated by means of historical data. Therefore, it will produce the forecasting urban maps with the same tendency as today. As the model is based on historical maps, the impacts of population growth and urban tissue are implicitly considered during calibration. However, the changes in population growth rate or in building types cannot be included in its simulations.

In SLEUTH modeling the users have often some difficulty to properly calibrate and integrate the relevant variables. In calibration process, there is no clear consensus for choosing the appropriate matrices from the provided parameters (Silva and Clarke, 2002; Yang and Lo, 2003; Jantz et al., 2004; Dietzel and Clarke, 2007; Jantz et al., 2010). Different metrics and parameters that are often used in calibration process are discussed in Chapter 2.

1.2.2.4.4. Some Evolutions and Applications of SLEUTH

Dietzel and Clarke (2007) have developed an Optimal SLEUTH Metric (OSM) during the calibration phase. In OSM thirteen parameters are processed in order to determine the best goodness of fit measure of the run to the known historical input data. Guan and Clarke (2010) have developed a parallel version of SLEUTH called pSLEUTH that used an open source general-purpose parallel raster processing programming library (pRPL). pRPL make it possible to improve the computational performance of the model during the simulation and the calibration process by reducing the computation time for the calibration process with multiple processors. Actually in parallelizing model, the data parallelism and data task hybrid parallelism are used with both static and dynamic tasking as the load-balancing strategy (Chaudhuri et al., 2013). Goldstein et al. (2004) have developed the Genetic Algorithm (GA). The GA algorithm is used a new calibration mechanism instead of the traditional brute force that decrease in calibration time as well as keeping the goodness of fit (Chaudhuri and Clarke, 2013). Jantz et al. (2010) developed a new version of SLEUTH called SLEUTH-3r. In this version, four limitations of the model are resolved including the SLEUTH tendency towards edge growth, the inappropriate fit-statistics, the memory restrictions and the inability of the model to simulate the areas where growth is more likely to occur (Jantz and Goetz, 2005; Jantz et al., 2010). The improvements of this version make it suitable to be used in this thesis. The SLEUTH-3r will be represented in detail in the next chapter. All these modifications and evolutions of this model makes it popular, and nowadays it is used in many applications. SLEUTH-3r could be used as

a scenario-dependent model that aims to increase performance efficiency of model e.g. modifications to address scale sensitivity, calibration statistics, decreasing memory requirements and improving processing speed.

Jantz et al., (2010) used the SLEUTH-3r model in order to execute prospective scenario composed by sub-periods showing different spatial dynamics. Their simulations could determine the contribution of each urban growth patterns with respect to the scenario hypothesis. They defined a scenario that could add attractive factors to urban growth simulation.

Caglioni et al. (2006) have done a research on SLEUTH model coefficients growth. They have compared the growth coefficients values obtained from various case studies to describe different kinds of urban development. The coefficients, their combinations and their effects on each other and on the growth simulation are the most significant approach in simulation configuration and controlling urban dynamics. Combination of different parameter values could describe the urban dynamics for an urban complex typology. These combinations could results to recently developed metropolis, urban sprawl, well-established city, strongly restricted zone and metropolis with satellite cities.

KantaKumar et al. (2011) used the SLEUTH, GIS and RS data to anticipate urban growth in Pune Metropolitan Area. The 38 years (1973-2011) of multi-temporal data is used for the urban growth prediction in 2030. For the model calibration, the brute force method has been adopted to sequentially narrow down the ranges of coefficient values with respect to the increasing spatial resolution of datasets in three phases containing the coarse, fine and final calibration. Brute force calibration tests all possible combinations of the coefficient. At the end of each calibration run, the model produced 13 least squares regression metrics (e.g. population, cluster, edges and average slope).

The SLEUTH model is one of the cellular automata models, which model the dynamic simulation of urban expansion and could be adapted for 3D modeling of the urban environment. Da Silva et al. (2016 & 2018) made a research on SLEUTH cellular-automata to achieve a primary BIM-based 3D urban growth model. They developed new roads to connect the simulated urban footprints, which are partitioned into different building types before 3D visualization.

1.3. Chapter Conclusion

The balance between housing and land protection is one of the environmental and social concerns of the public authorities. Public policies are based on providing housing according to the demands while considering the effects of urbanization. Urban growth modeling attempts to represent different scenarios of the urban expansions in terms of space consumption, the urban sprawl configuration, density and demography, and the socio-economic and environmental effects of urbanization. A prospective simulation is interesting to explain the determinants of urbanization or to study the effects of new policies on artificialization.

Urban simulation techniques are willing to solve the various problems of urban growth modeling including the spatial resolution, the velocity of simulation processing times and the accuracy of urban growth simulations. Among all dynamic models and spatially explicit, those based on CA are more common for their applications in urban areas. This can be especially explained by the spatially explicit character and dynamic of cellular automata and easy integration with RS data in these models. CA can be easily integrated with GIS to have a high spatial resolution model with computational efficiency. In addition, nonlinearity of the iterative process of CA leads to regular fractal patterns, i.e. to regular and ordered spatial patterns that generate similar geometries at different scales. In this chapter, some previous works in the field of 2D urban growth have been reviewed.

In the course of urban modeling, many methods and algorithms have been used to forecast urban expansion, some of which are presented in this chapter. This chapter aims to give a general review from some of the existing approaches of urban growth modeling and compares their capability and limitations. The reliability and the accuracy of the model is depended on different factors and the results are not directly comparable due to the largely dependency on the land-use pattern of each area. Furthermore, the ability of the model to adapt to different real-world urban situations, data requirements and the availability of the software have to be considered in order to choose a suitable model. However, the micro simulation such as cellular automata simulation techniques, especially SLEUTH, offer greater potential for representing and simulating the complexity of the dynamic process, due to the increasing of computational power and greater availability of the spatial data.

SLEUTH uses the historical data in order to calibrate the model and therefore, it implicitly considers the impacts of population growth and urban tissue during the calibration phase of SLEUTH. But the changes in population growth rate or in building types cannot be included in its simulations. In addition, the interpretation of the SLEUTH results are difficult, because the results are limited to some cells (raster data). The objective of this research is to represent the impacts of constructions and environmental constraints on urban sprawl during an urban growth simulations. In next chapter, we represent the methodology and fundamentals of our proposed method in order to provide a more reliable modeling by improving the SLEUTH results that are often independent from the factors of building types and population. We add common data such as topographic data, buildings and demography data to the model in order to create different types of scenarios according to urban policies, while remaining realistic. The results of the proposed method lead to different simulations that are related to different land priorities and constraints.

Chapter 2 : Methodology and Fundamentals for Model Construction

Contents

- 2.1. Simulation Methodology to Investigate the Effects of Environmental Constraints and Constructions on Urban Sprawl
 - 2.2. SLEUTH Urban Growth Model Structure
 - 2.3. Urban Growth Modeling Considering Environmental Constraints Scenarios
 - 2.4. Impacts of Constructions and Demography on Urban Sprawl Simulation
 - 2.4.1. Determinants and Impacts of Building Types on Urban Sprawl
 - 2.4.2. Determinants and Impacts of Population Growth on Urban Sprawl
 - 2.5. Urban Fabric Scenarios and Urban Configuration
 - 2.6. 3D Representation of Prospective Urban Growth Simulations
 - 2.7. Chapter conclusion
-

Almost all urban growth and LUCC techniques use the historical geographic features such as urban, road and excluded maps to simulate the prospective maps. They can produce different results by varying the growth coefficients. However, in most of them, the changes of urban fabrics and their determinants such as changes in population growth rate or in building types are not considered explicitly, which renders it difficult to use the results in order to make reasonable decision for sustainable urban planning and management. The SLEUTH model is one of the CA models, which is used in this thesis and like many other urban growth simulation methods, considers only the historical data. Although, the impacts of population growth and urban tissue are implicitly considered during the calibration phase on the historical urban maps, changes in population growth rate or in building types cannot be included in its simulations. The proposed method tries to give more reliable urban growth simulation results by integrating the topographic data, buildings and the demography. The aim is to be able to propose a set of different simulations that correspond to different land priorities and constraints and to use common data (such as topographic data, buildings and demography) in order to improve the realism of each simulation and their adequacy with the real world.

This chapter focuses on the method that are applied in Chapter 3 and Chapter 4. This chapter discusses the principles of the proposed method, and in Chapters 3 and 4 the implementation

and results are presented and discussed. In this chapter, the methodology that is used in this thesis is briefly reviewed in section 2.1. In section 2.2, the SLEUTH urban growth CA model, its structure and its required data are described. In section 2.3, the environmental-based scenarios are defined. Determinants of construction types and demography, and their impacts on urban sprawl simulation are discussed in section 2.4. In section 2.5, the urban fabric scenarios are represented. In section 2.6, the objectives to 3D representation of the model are introduced. The process of creating of fictive 3D buildings and 3D illustration results are provided in Chapter 4. The chapter is concluded in section 2.7.

2.1. Simulation Methodology to Investigate the Effects of Environmental Constraints and Constructions on Urban Sprawl

In our research, SLEUTH urban growth model is used for simulating different scenarios from 2017 to 2050 for three different case study. A growth cycle is the basic unit of SLEUTH execution and therefore each scenario is composed of 33 growth cycle.

In the proposed method, first, different urban growth scenarios considering environmental constraints are defined. For the environmental scenarios, it is needed to defined different environmental constraints by altering the exclusion and attractiveness rates of some natural or artificial geographic features. These scenarios simulate various prospective urban growth considering different limitation rates of urbanization in particular spaces such as vegetation areas and forest. In addition, the scenarios simulate urban growth according to attractive areas. Attractive areas describe the spaces which urbanization is desired to occur, such as along roads and rivers. The exclusions and attractiveness are integrated into the model by altering the excluded input maps (see section 2.3).

The SLEUTH results are limited to raster data that are difficult to interpret for decision makers. The results are some pixels on which urbanization is supposed to occur, which do not make sense from urbanism point of view. Therefore, the proposed model aims to diversify the simulation possibilities integrating explicitly factors of building types according to population growth and providing visual methods to view urban growth scenario results in 2D and even 3D.

In most cases, the main factors of urban growth are population growth and lifestyle resulting to more residential surface per person (Aguilera and Bonin, ESCo, 2017, sections 5). However, the SLEUTH simulations are based on the historical data and the model does not considers the altering rate of demographic data and construction types. Thus, the urban fabric determinants such as population growth rate or building types are not considered explicitly in the model. This make it difficult to use the results in order to make reasonable decision for sustainable urban planning and management (see section 2.4).

In the method proposed in this thesis, two more data (building types and population) are added and different scenarios, called urban fabric scenarios, are defined to have various images of the city of tomorrow, respecting the several land priorities and limitations. In order to integrate the demography and life style, the buildings are classified to six different residential categories

considering their height and configuration in order to study the Human Settlement Capacity (HSC). This classification is based on the classification of different building types of a city provided by department of planning and environment of NSW (New South Wales) government of Australia (NSW Government, Australia, 2017). The historical demographic data and artificial geographical features, e.g. human settlement, are used and a relation between the building types and the capacity is defined. Then, the new simulated urban patches are classified according to the defined building classes, and a land use pattern is generated (see section 2.4.1). Next, the intermediate population for the study area is estimated (see section 2.4.2). According to the expected population growth and the building types, some fictive urban fabric scenarios called primary urban fabric scenarios are assumed and compared in order to better understand how this land could be used and how many inhabitants could live in these new areas. Based on the results the new urban fabric scenarios called final urban fabric scenarios are defined to enrich the simulations (see section 2.5). Figure 2.1, illustrates the proposed method procedure.

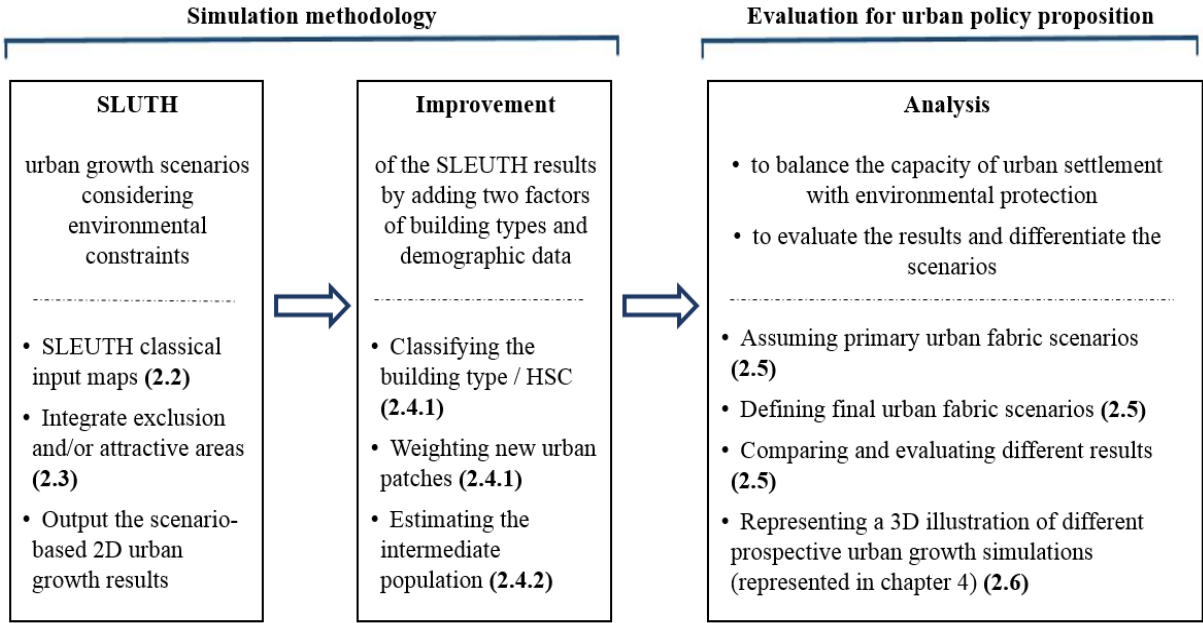


Figure 2. 1. The proposed method procedure

In fact, in order to improve the SLEUTH simulation results, first we estimate the population per area to estimate the quantity of population per type of building (per unit). Afterwards, knowing the population rate at different dates, we forecast the approximate rate of the population for the desired future date. Finally, by analyzing the urban fabric scenarios, we can evaluate the quantity of population per type of building for n simulation cycles. We can also evaluate the required number of growth cycles (so the urban sprawl extension) to locate a certain quantity of population per type of buildings.

For each urban fabric scenario, a 3D representation is provided in order to facilitates the interpretation of the SLEUTH simulation and differentiate the scenarios (see section 2.6 and Chapter 4). In 3D illustrations, we rely on the existing data (e.g. positioning of the current buildings). In the process of making 3D models of prospective urban fabric scenarios, in order

to go from pixels to buildings shapes, some constraints are considered such as the distances from the roads, rivers, excluded areas and the current buildings as well as the distances between the new simulated buildings. Having the number of the new building and their height (that gives the number of floors), the population capacity of the scenarios are recalculate and the result are analyzed (see chapter 4).

2.2. SLEUTH Urban Growth Model Structure

SLEUTH is developed in order to simulate the spatial expansion of urban spaces. SLEUTH is available on the Gigalopolis project website as an open access program ([project Gigalopolis, 2018](#)). As illustrated in figure 2.2 the SLEUTH model is a popular urban growth and land use change model ([Chaudhuri et al., 2013](#)). Figure 2.2 shows the worldwide application of SLEUTH model extracted from the published applications of SLEUTH until 2012. After 2012, this model has been widely used by many researchers in many study area in different countries, also in France ([Doukari et al. 2016; Da Silva et al., 2016; Aguejdad et al. 2016; Da Silva et al., 2018](#)). Looking at the publication page of the Gigalopolis website, we can find other applications of the model after 2012.

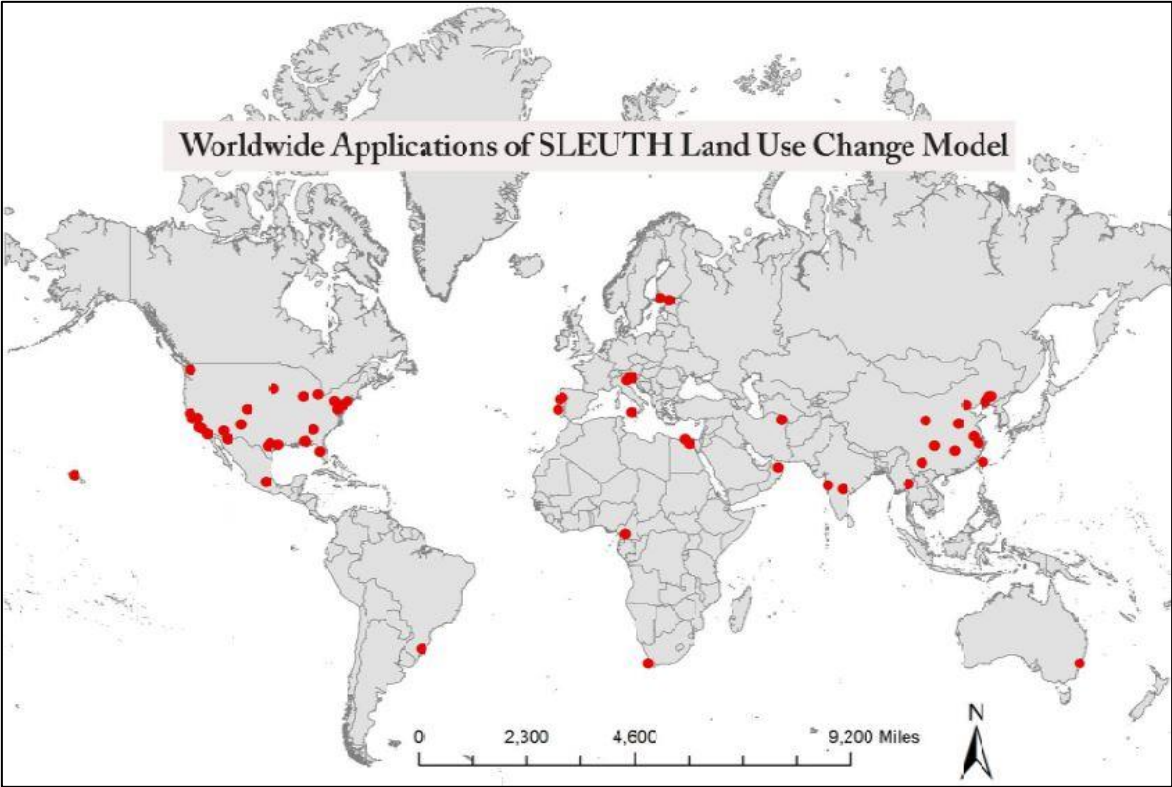


Figure 2. 2. Worldwide Application of SLEUTH Land Use Change Model extracted from the published applications of SLEUTH until 2012 ([Chaudhuri et al., 2013](#))

The SLEUTH is coded in C and runs on UNIX. As mentioned in the last chapter, the acronym for SLEUTH is derived from its input data included Slope, Land use, Exclusion areas from urbanization, Urban areas, Transportation network and Hillshade. SLEUTH has two sub-models within deltatron land use model and urban growth model. The requirement of land use

input map for modeling the urban growth is optional. In SLEUTH, a scenario file controls the variables during a model execution including coefficient, random number seed, the number of Monte Carlo iteration, data output and color table settings. SLEUTH urban growth model process flow and one of the used scenario files is represented in detail in Annex B. The SLEUTH structure is illustrated in figure 2.3 (Chaudhuri et al., 2013).

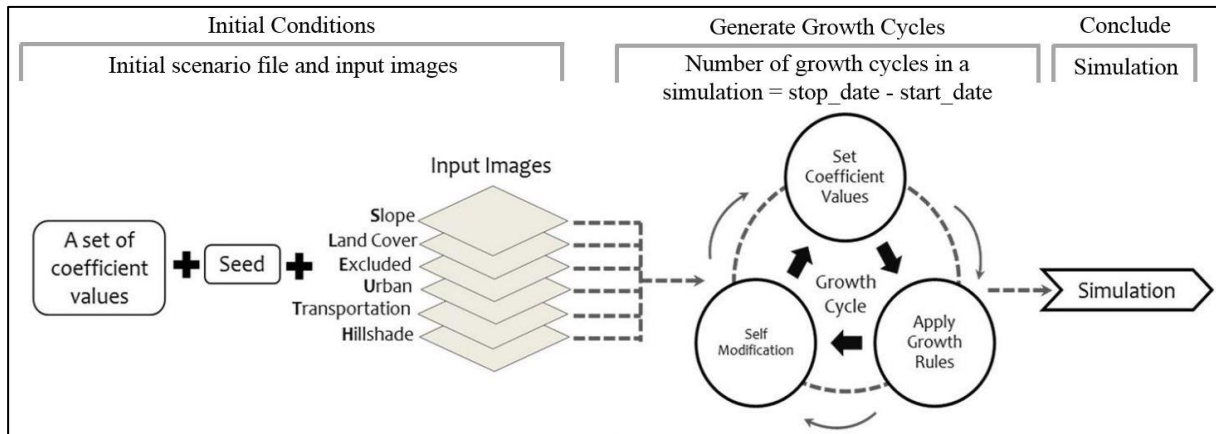


Figure 2.3. Structure of the SLEUTH model (Chaudhuri et al., 2013)

SLEUTH belongs to a model based on an empirical and spatially explicit approach. It contains three different process flow modes where each mode has variations on how simulations are executed. The SLEUTH modes are as follow:

- Testing process flow for test mode,
- Calibration process flow that is needed to customize the model for area of study. The calibration requires a historical dataset to replicate past urban development trends (Clarke et al., 1997, Candau, 2002, Jantz and Goetz, 2005, Caglioni et al., 2006),
- Prediction process flow for prediction mode.

2.2.1. Growth Cycle

A cycle of simulation called growth cycle is the basic unit of SLEUTH execution. The growth cycle starts by giving a unique value to each of the coefficients and then each of the growth rules are applied. Afterwards, the growth rate is evaluated. If the growth rate exceeds or falls below a specific critical threshold, the value of these prediction coefficients may increase or decrease by self-modification to simulate accelerated or depressed growth (see figure 2.4).

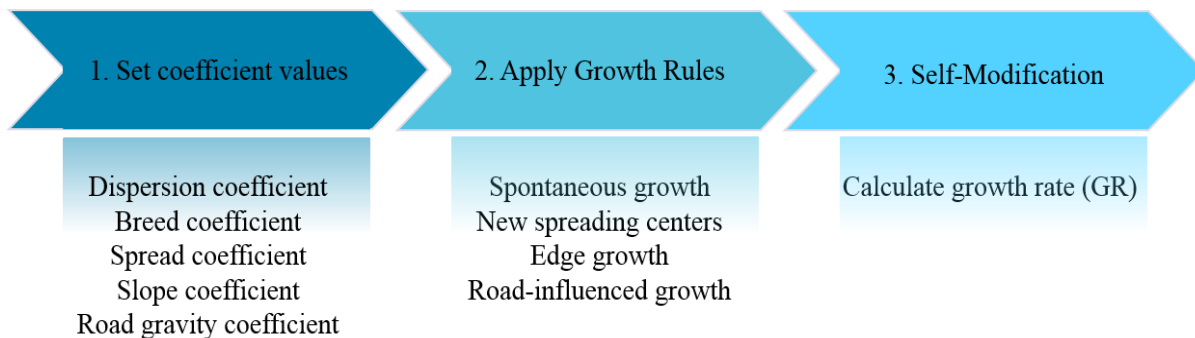


Figure 2. 4. SLEUTH growth cycle

2.2.2. Growth Coefficients

Five coefficients are used to control how the simulation rules are applied. The values of these coefficients are between 0 and 100 and they are defined in calibration process by comparing simulated land cover change to the historical data of the study area (project Gigapolis, 2018).

- Dispersion coefficient determines the number of cells created by spontaneous growth and controls the number of times a pixel randomly selected for possible urbanization. It is also applied to road_influenced growth to control how many pixels, make up a random walk along the transportation network on a road trip.
- Breed coefficient corresponds to the probability that a spontaneous growth cell becomes a new spreading center. In the similar process, it is applied to road_influenced growth too.
- Spread coefficient is the probability of continuous growth created by edge growth that specifies the probability that any pixel of a spreading center will generate an additional urban pixel in its neighborhood.
- Slope coefficient determines the suitability of urbanization and affects all growth rules. The resistance of the slopes makes it possible to take into account the influence of slopes on urbanization.
- Road gravity coefficient specifies the maximum distance to the road where the urbanization can take place.

2.2.3. Growth Rules

SLEUTH is a cellular automaton model that functions based on a probabilistic and self-adaptive process (Clarke et al., 1997). It is based on a Boolean logic since each cell of the image corresponds only two possible states, the urban state or non-urban state. The state of these cells is determined and updated according to four spatial rules of urban expansion performed sequentially including the spontaneous growth, creation of new centers, continuity of the existing urban and along roads (Candau, 2002).

2.2.3.1. Spontaneous Growth

Spontaneous growth assigns the probability of randomly changing the state of a cell from non-urbanized become urbanize in any time step. Dispersion coefficient determines the spontaneous and the slope coefficient determines the weighted probability of the local slope (see figure 2.5). The spontaneous growth can be defined by (project Gigapolis, 2018):

$$U(i,j,t+1) = f1[dispersion_coefficient , slope_coefficient , U(i,j,t), random], \tag{2-1}$$

where, $U(i,j,t+1)$ describe a new urbanized cell at time $t+1$ and $U(i,j,t)$ is a given cell at coordinate (i,j) at time t .

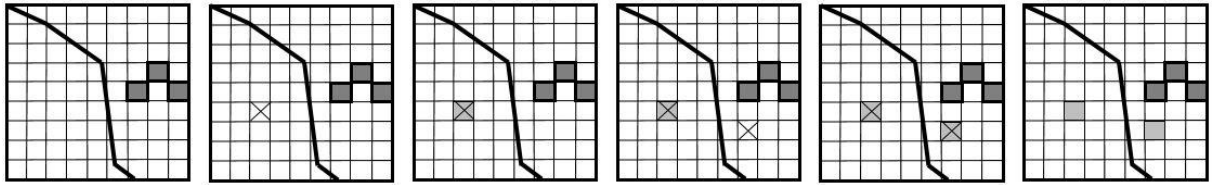


Figure 2. 5. Spontaneous growth example (Project Gigapolis, 2018)

2.2.3.2. New Spreading Center Growth

An urban spreading center is defined as a location with three or more adjacent urbanized pixels. New spreading centers determines whether any of the new spontaneously urbanized cells will become new urban spreading centers. The breed coefficient, for each new urbanized cell investigate if the neighbors of the new spreading center cell can be transform to urban pixel. The slope coefficient also control the cell state transition availability by checking the local slope of the cell (see figure 2.6). This growth rule can be expressed by (project Gigapolis, 2018):

$$U'(i,j,t+1) = f2[breed-coefficient, U(i,j,t+1), random], \tag{2-2}$$

where, $U'(i,j,t+1)$ is a new spreading center, (k,l) are nearest neighbors to (i,j) and $U(i,j,t+1)$ is a new spontaneous urbanized cell.

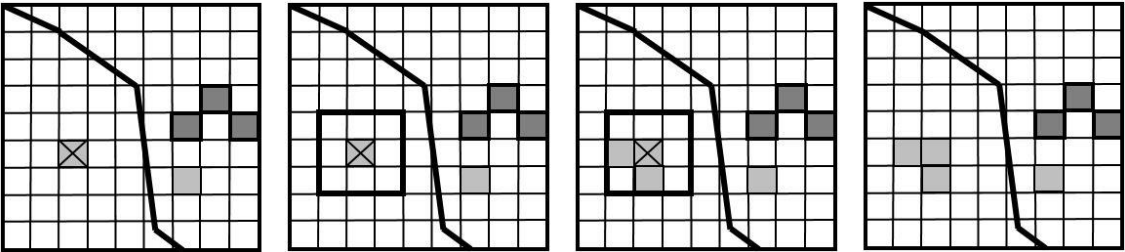


Figure 2. 6. New spreading center growth example (Project Gigapolis, 2018)

2.2.3.3. Edge Growth

Edge-growth dynamics define the probability for a non-urban cell that has at least three urbanized neighboring cells, to become urbanized affected by the spread coefficient, given it is possible to build on the cell considering slope coefficient (see figure 2.7). The edge growth can be represented by (project Gigapolis, 2018):

$$U(i,j,t+1) = f3[spread_coefficient, slope_coefficient, U(i,j,t), U(k,l), random], \quad (2-3)$$

where, $U(i,j,t+1)$ describe a new urbanized cell at time $t+1$, $U(i,j,t)$ is a given cell at coordinate (i,j) at time t and (k,l) are nearest neighbors to (i,j) .

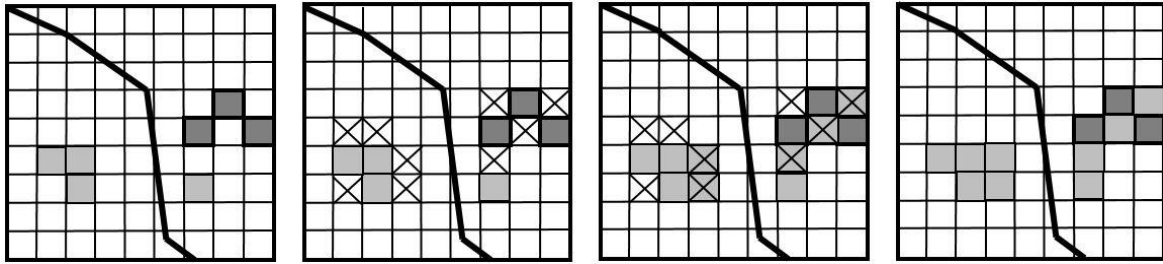


Figure 2. 7. Edge growth example (Project Gigapolis, 2018)

2.2.3.4. Road Influenced Growth

The road-influenced growth is related to the existing transportation network and the new urban pixels obtained from previous steps. First, new urban cells are selected and the model verify the existence of a road in their given maximal radius and place a temporary urban cell at the closest point to the selected cell on the road. Afterwards, the temporary urban cell conducts a random walk along the road and its final spot considered as a new urban spreading center. The number of steps is specified by dispersion coefficient. Then, the model checked the feasibility of changing the state of the neighbors of the temporary urbanized cell. Later, if two adjacent cells to this newly urbanized cell that are randomly chosen are also available for urbanization, the model will change their states (see figure 2.8). The road influenced growth can be expressed by (project Gigapolis, 2018):

$$U'(k,l,t+1) = f4.1[U(i,j,t+1), road_gravity_coefficient, R(m,n), random], \quad (2-4-1)$$

where, $U'(k,l,t+1)$ defines the temporary urbanized cell on the road, $i, j, k, l, m,$ and n are cell coordinates, and $R(m,n)$ defines a road cell.

$$U''(i,j,t+1) = f4.2[U'(k,l,t+1), dispersion_coefficient, R(m,n), random], \quad (2-4-2)$$

where, $U''(i,j,t+1)$ defines the random walk on the road, (i,j) are road cells neighboring (k,l) .

$$U'''(i,j,t+1) = f4.3[U''(p,q,t+1), R(m,n), slope_coefficient, random], \quad (2-4-3)$$

where, $U'''(i,j,t+1)$ defines the new adjacent urban spreading center and (p,q) determines the location of the temporary urbanized cell at the end of the random walk.

$$U''''(i,j,t+1) = f_{4.4}[U'''(p,q,t+1), slope_coefficient, random], \quad (2-4-4)$$

where, $U''''(i,j,t+1)$ define the two additional adjacent urbanized cells and (i,j) and (k,l) belong to the nearest neighborhood of (p,q) .

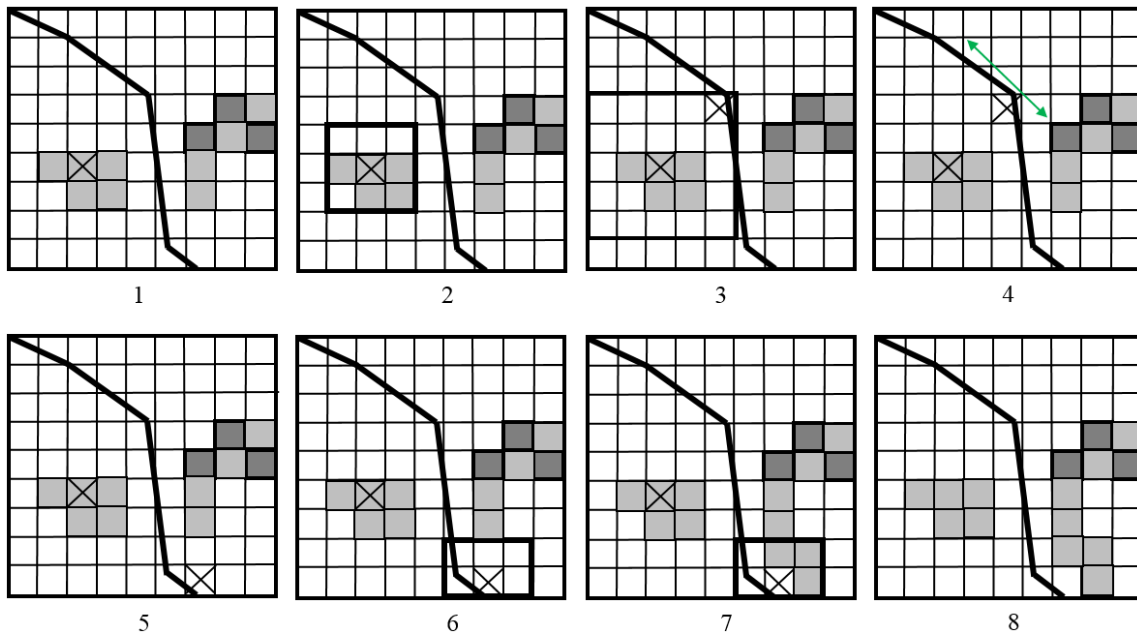


Figure 2. 8. Road influenced example (Project Gigalopolis, 2018)

2.2.4. Self-Modification

The self-modifying function enables SLEUTH model to adjust the values of coefficients at each cycle of the simulation, which is usually one year. Otherwise, SLEUTH would reproduce the same number of urbanized cells at a linear growth rate. Depending on the rate of change that may exceed or fall below a specific critical threshold, the value of these prediction coefficients may increase or decrease to simulate accelerated or depressed growth (Jantz and Goetz, 2005).

The self-modification limits are defined in scenario file of the SLEUTH (see Annex B). These limits, which are specified by two `critical_low` and `critical_high` constants, affect the growth coefficients (see figure 2.9).

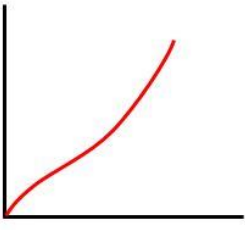
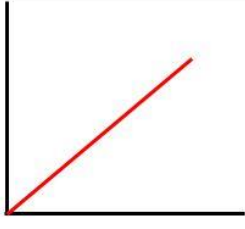

	<p>Rapid Growth: greater than critical number of hectares per year</p> <ul style="list-style-type: none"> • Dispersion is multiplies by a constant > 1.0 • Spread is multiplies by a constant > 1.0 • Breed is multiplies by a constant > 1.0
	<p>Normal Growth: between rapid growth and little or no growth</p> <ul style="list-style-type: none"> • If average Slope $> 10\%$, increase Spread • Road_gravity increases by percent of road network • Slope résistance increase by $0.2 \times$ percent of urban land available
	<p>Little or No Growth: annual growth rate is less than critical value</p> <ul style="list-style-type: none"> • Dispersion is multiplies by a constant < 1.0 • Spread is multiplies by a constant < 1.0 • Breed is multiplies by a constant < 1.0

Figure 2. 9. Self-modification (Project Gigalopolis, 2018)

2.3. Urban Growth Modeling Considering Environmental Constraints Scenarios

As discussed in chapter one, urbanization impacts on the physical, chemical and biological properties of soils and in general on the environment. In this research, different environmental urban growth scenarios are provided in order to investigate the impacts of environmental rules on urban sprawl. For simulation modeling the version of SLEUTH-3r is used according to the available data and the case studies. In this section, first, the modifications of this version to SLEUTH basic version are represented. Next, the procedure of urban growth scenarios considering environmental constraints including the calibration, forecasting and the environmental scenarios generation is explained.

2.3.1. SLEUTH-3r Modifications to the SLEUTH

As discussed before, the basic version of the SLEUTH has some constraints. The SLEUTH-3r provided by Jantz et al. (2010), made effort to overcome some of these limitations. In this version four restrictions are improved including:

- (1) SLEUTH tends towards edge growth, so it could not generate an appropriate level of dispersed growth.
- (2) Most of the fit statistics used for calibration are least squares regression scores (r^2) that measure the relation between a simulated area and observed urbanization area. Therefore, four input map for calibration is needed to cover four points in time for regression equation including a map to initialize the model and three additional for the control points. Moreover,

using the r^2 statistic without additional information such as the y-intercept of the linear regression equation, model may appear to work well but with over- or under-estimating growth rates or patterns.

- (3) SLEUTH utilizes computer memory inefficiently.
- (4) In SLEUTH, usually the excluded area are defined but the attractive area are missed in its simulation.

In SLEUTH original code, the number of spontaneous urbanization attempts that comes from the dispersion value (D_V) depends on the calibrated value for the dispersion coefficient (D_C), a constant number as dispersion coefficient multiplier (D_M), and the number of pixels in the image diagonal. While in SLEUTH-3r, D_M is no longer a constant, which allows the user to modify this multiplier value interactively.

$$D_V = D_C \times D_M \times \sqrt{R^2 + C^2} \quad (2-5)$$

D_V is the dispersion value, D_C is the dispersion coefficient, D_M is the dispersion coefficient multiplier (in the original version of SLEUTH the D_M is a constant number equal to 0.005), R is the number of rows and C is the number of columns. To find the appropriate value of D_M the growth coefficients have to be set to produce the maximum level of spontaneous new growth. The dispersion set to one hundred and other coefficients set to zero and the model perform in the calibration mode. Different value for D_M are tested to find the appropriate value. This desired value can be obtained when the model capture or even over-estimate, the number of urban clusters which is represented by the cluster fractional difference metric.

The fit statistics are improved by a new metric table files created in SLEUTH-3r. This table includes the difference and ratio measures that directly compare the modeled variable to the observed variable for all control dates. The added metrics contains the algebraic, ratio and fractional changes in the modeled value relative to the observed value can be used in calibration, when fewer than three control points are available.

The road search algorithm is improved in this version. Contrary to the previous version, this version creates a data structure containing only the coordinates of the road network points that are road cells. In addition, it makes a new data structures for multiple grids that list nonzero cell coordinates and modify the procedures that treat these grids so that they do not need to check for zero-valued cells and only treat non-zero cells (see figure 2.10). In the new version the memory usage model is also modified.

All these modifications and improvements, make this model more and more suitable to be used in this thesis.

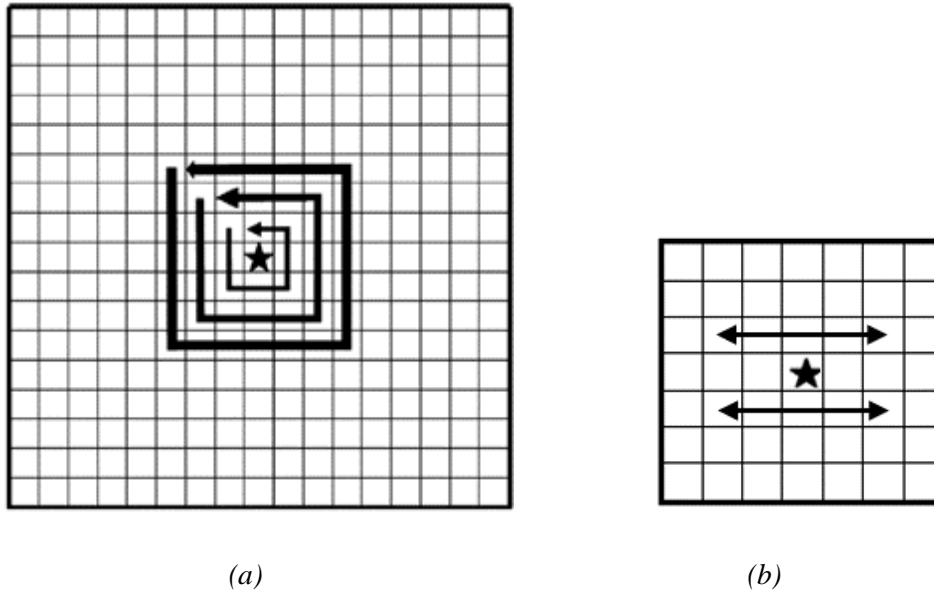


Figure 2. 10. a: Illustration of the search algorithm in the original SLEUTH (Jantz et al., 2010);
 b: Illustration of the search algorithm in the original SLEUTH-3r

2.3.2. Calibration of the SLEUTH-3r Model and Determining the Goodness of Fit

The calibration process is executed by running a calibration scenario file. During the calibration process, the model tries to find a set of values for the five parameters including dispersion, breed, spread, road growth and slope. These values make the model be able to accurately simulate land-cover changes within the study area (see figure 2.11).

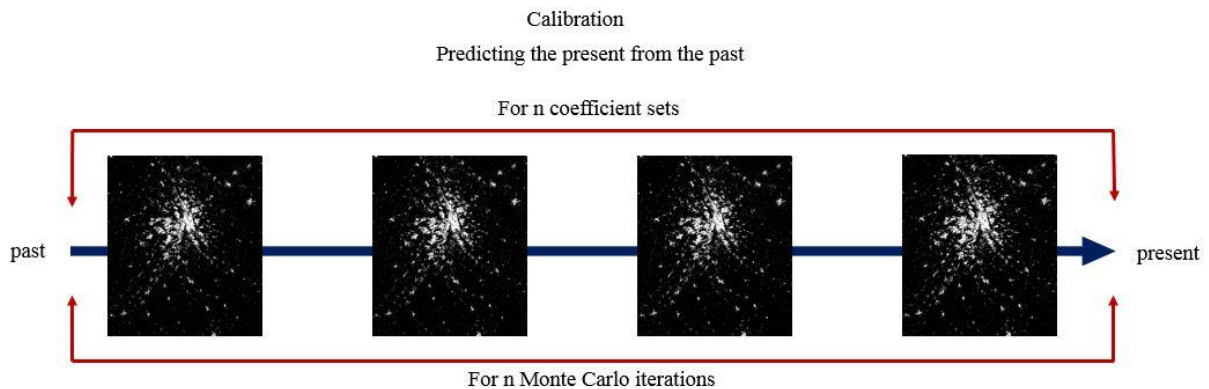


Figure 2. 11. Calibration, concept and procedure

The best-fit coefficients are obtained from the fit statistics provide in a new metric table file (ratio_pe_0.log) during calibration process. An appropriate goodness of fit of the coefficients values can precise and optimize the model significantly. Before executing the calibration process it is needed to calculate the dispersion coefficient multiplier. The dispersion coefficient multiplier is calculated for each environmental scenario separately.

The SLEUTH has three calibration steps contains coarse, fine and final and after it is possible to derive forecasting coefficients. In SLEUTH-3r the calibration could be done in one step as a coarse calibration. Our model performs using four historical urban extent maps, four historical transport maps, slope and hillshade maps, and the excluded maps for each environmental scenario. In calibration process, first an initial value for each coefficient is defined. The values for each parameter ranged from 1 to 100 by increments of 25 (i.e. 1, 25, 50, 75, and 100). Running SLEUTH in calibrate mode will perform brute force Monte Carlo runs through the historical data and the combinations of the 3125 unique parameter are tested. The calibration provide a list of metrics.

In basic SLEUTH model, thirteen parameters are often provided to determine the goodness of fit for each outcome (see table 2.1). In this model, first the coarse calibration is performs and the results are examined in order to find the goodness of fit for each of the parameter sets (Dietzel and Clarke, 2007). Then, the metrics evaluations, specify the parameter sets for the fine step that usually give narrower range of parameters. The same process continue for the final and derive forecasting coefficients steps. The best-fit of the parameters from the third calibration are used in forecasting urban growth. For choosing the best matric from the provided parameters, there is no clear consensus as to which metrics are the appropriate ones to use during the calibration process (Dietzel and Clarke, 2007). Lee-Sallee metric is one of the metrics that is widely used (Lee and Sallee, 1970). This metric is the ratio of the intersection and the union of the simulated and actual urban areas. Silva and Clarke (2002) used only the Lee-Sallee metric in their modeling. Other metrics are also used in order to determine the sets of parameter that describe the replication of the historical datasets. These metrics often use the compare statistic and population statistics e.g. Yang and Lo (2003) used a weighted sum of all the metrics in the calibration process, while Jantz et al. (2004) examined and applied the compare, population, and Lee-Sallee statistics metrics during their modeling (Dietzel and Clarke, 2007).

Table 2. 1. Metrics that can be used to evaluate the goodness of fit of the basic SLEUTH model (Dietzel and Clarke, 2007)

Metric Name	Description
Product	All other scores multiplied together
Compare	Modeled population for final year/actual population for final year, or IF Pmodeled > Pactual {1 – (modeled population for final year/actual population for final year)}.
Pop	Least squares regression score for modeled urbanization compared to actual urbanization for the control years
Edges	Least squares regression score for modeled urban edge count compared to actual urban edge count for the control years
Clusters	Least squares regression score for modeled urban clustering compared to known urban clustering for the control years
Cluster Size	Least squares regression score for modeled average urban cluster size compared to known average urban cluster size for the control years
Lee-Salle	A shape index, a measurement of spatial fit between the model’s growth and the known urban extent for the control years
Slope	Least squares regression of average slope for modeled urbanized cells compared to average slope of known urban cells for the control years
% Urban	Least squares regression of percent of available pixels urbanized compared to the urbanized pixels for the control years
X-Mean	Least squares regression of average x_values for modeled urbanized cells compared to average x_values of known urban cells for the control years
Y-Mean	Least squares regression of average y_values for modeled urbanized cells compared to average y_values of known urban cells for the control years
Rad	Least squares regression of standard radius of the urban distribution, i.e. normalized standard deviation in x and y
F-Match	A proportion of goodness of fit across landuse classes. {#_modeled_LU correct/(#_modeled_LU correct + #_modeled_LU wrong)}

SLEUTH-3r creates new metric table that could be find in ‘ratio_pe_0.log’ file generated in the calibration process (see table 2.2). This table includes difference and ratio metrics that directly compare the modeled variable with the observed variable for all control dates (Jantz et al., 2010). In the calibration process the SLEUTH-3r calculates three value for each metric parameter for each run and for each control year including the algebraic difference between the observed value and modeled value, the ratio of the modeled value to the observed value, and the fractional change in the modeled value relative to the observed value (Jantz et al., 2010). The metrics of the table 2.1 can be used when at least four control points are available. However, the new fit metrics made by SLEUTH-3r model, can be used in calibration process even when at fewer than three control points are available (Jantz et al., 2010).

Table 2. 2. New fit metrics available in SLEUTH-3r (Jantz et al., 2010)

Fit statistic	Definition
Pixels	Modeled urban pixels compared to actual urban pixels for each control year. Referred to as “population” and as “area” in SLEUTH’s output files
Edges	Modeled urban edge pixels compared to actual urban edge pixels for each control year
Clusters	Modeled number of urban clusters compared to actual urban clusters for each control year. Urban clusters are areas of contiguous urban land. In cell space, clusters can consist of a single pixel or multiple, contiguous urban pixels. Contiguity is determined using the eight-neighbor rule
Cluster size (mn_cl_sz)	Modeled average cluster size compared to actual average urban cluster size for each control year. This is not an area-weighted mean
Slope (avg_slope)	The average slope for modeled urban pixels compared to actual average slope for urban pixels for each control year
% Urban	The percent of available pixels urbanized during simulation compared to the actual urbanized pixels for each control year
X-mean	Average x-axis values for modeled urban pixels compared to actual average x-axis values for each control year
Y-mean	Average y-axis values for modeled urban pixels compared to actual average y-axis values for each control year
Radius	Average radius of the circle that encloses the simulated urban pixels compared to the actual urban pixels for each control year

In calibration procedure of this thesis, two metrics of the pixel fractional difference (PFD) and the clusters fractional difference (CFD), that are proposed by Jantz et al., (2010), are used. PFD makes direct comparisons between the numbers of urban pixels in the control maps and the corresponding simulated maps. Obtaining an accurate fit for this metric ensured that the overall amount of development would be matched. The CFD focuses on the frequency of clusters in the urban system and compares the number of urban clusters. The accurate metrics indicate that the model could create the urban form and could avoid the dispersed settlement patterns (Jantz et al., 2010).

In this research, the set of parameters are selected that could achieve the best goodness of the fit in both PFD and CFD with less ratio of differences (see Annex C). For the initial run 25 Monte Carlo trial is used. After obtaining the range of the desired value, another execution by setting 100 Monte Carlo trial is done. Since the input excluded maps of the environmental scenarios are different, for each environmental scenario the calibration process is run in order to achieve its best fit coefficient for the forecasting process.

Annex C, represents the process of computing the dispersion coefficient multiplier and five best fit growth coefficients. A portion of the table of the "ratio_pe_0.log" file is shown as an example in this Annex.

2.3.3. Defining our Environmental-based Scenarios

SLEUTH model has the possibility of generating different scenarios of land use changes by setting the composition of SLEUTH input layers. For this thesis, five different environmental-based scenarios are defined with different level of environmental protection. Four of them are scenarios level 0 to level 3, where the upper scenarios preserve more the environment (e.g. green lands and the forests), and last scenario is defined as an attraction-based scenario that, in addition to excluded areas, also integrates areas of attraction into the simulation algorithm. Therefore, the last scenario can simultaneously consider both the exclusion and attraction areas of growth. These scenarios are created by changing the excluded areas and defining attractive areas. This leads to the production of new excluded and/or attractive maps.

The excluded/attractive maps have the pixel value range from 0 to 100. In excluded/attractive maps provided for these scenarios, the value of 50 indicates theoretically open areas for development in the calibration process. This value of 50 indicates a neutral weight for development. This makes it possible to define the more desirable areas for urbanization in excluded and attractive maps by giving the value more or less than 50 respectively. Therefore, in these maps, the areas that have the value more than 50 are less likely to be developed and the lands more likely to be developed have the value less than 50. This makes to improve the overall performance of the model by allowing the inclusion of growth attractors (e.g. areas expected for population growth). The value 100 indicates the protected areas that are 100% excluded from the possible urban growth or any changes.

International Union for the Conservation of Nature (*Union Internationale pour la conservation de la nature - UICN*) has defined six categories of areas protection including strict nature reserves or wilderness areas, national parks, monuments or natural elements, habitat or species management area, protected landscapes or seascapes, protected areas for the sustainable use of natural resources (Martinez, C., 2007).

All the data used for exclusion area in environmental-based scenarios are extracted from database of the French National Geographic Institute (*Institut Géographique National - IGN*) IGN data base. In BD TOPO database provided by IGN, vegetation coverage data contains the parks, closed forests including wood land, closed coniferous forest, closed deciduous forest, mixed closed forest and tree area, and open forest, hedge, woody heath, peupleraie, orchard and vine. In creating the environmental scenarios, vegetation coverage are divided to three different areas (1) national parks, (2) closed forests areas (wood land, closed coniferous forest, closed deciduous forest, mixed closed forest and tree area), and (3) open forest, hedge, woody heath, peupleraie, orchard, vine. In the scenarios provided in this thesis, the first areas are 100% protected from urbanization, in all scenarios. The second areas are more resistant to urbanization and the last area is less resistant. This means in urbanization process it is more probable to change the third area than the second one. Following, we present five different environmental-based scenarios.

2.3.3.1. Scenario Protection Level 0 (Nearly No Environmental Protection - NEP)

In the Nearly No Environmental Protection (NEP) scenario, the excluded areas are fully protected from urban growth. They are excluded 100% of the possible urban growth. They take the value of 100 and the others take the value of 50 for the entry of SLEUTH into NEP during the calibration and forecasting process. The value of 50 means they are neutral from the exclusion or attraction (see table 2.3). In this scenarios, there is nearly no protection for the environmental zone except for the following areas:

- Remarkable buildings, cemeteries, airfields and sport grounds
- Railways stations, triage areas
- Activity areas (administrative, culture and leisure, education, water management, industrial or commercial, health, sports and transport)
- Water surfaces
- National parks

2.3.3.2. Scenario Protection Level 1 (Limited Environmental Protection - LEP)

In Limited Environmental Protection (LEP) scenario, excluded areas are totally protected from urban growth, considered 100% excluded from the possible urban growth, and have got the value 100 for SLEUTH input. Closed forests and some woodlands that have been extracted from the database of the IGN are added to exclude areas. Non-exclusion zones with a value of 50 indicate a neutral weight for development (see table 2.3). The excluded areas in this scenario are as follow:

- Remarkable buildings, cemeteries, airfields and sport grounds
- Railways stations, triage areas
- Activity areas (administrative, culture and leisure, education, water management, industrial or commercial, health, sports and transport)
- Water surfaces
- National parks
- Closed forests areas (wood land, closed coniferous forest, closed deciduous forest, mixed closed forest and tree area)

2.3.3.3. Scenario Protection Level 2 (Moderate Environmental Protection - MEP)

In this scenario, the open forests and green areas derived from the IGN database are generated as a separate layer with a value of 75 and represent the 50% probability of exclusion from urban growth. The other excluded areas that are fully protected from urban growth, took the value of 100 for the input of SLEUTH in Moderate Environmental Protection (MEP) scenario. Non-exclusion zones with a value of 50 indicate a neutral weight for development (see table 2.3). The excluded areas are described below:

- Remarkable buildings, cemeteries, airfields and sport grounds
- Railways stations, triage areas

- Activity areas (administrative, culture and leisure, education, water management, industrial or commercial, health, sports and transport)
- Water surfaces
- National parks
- Closed forests areas (wood land, closed coniferous forest, closed deciduous forest, mixed closed forest and tree area)
- Open forest, hedge, woody heath, peupleraie, orchard and vine

2.3.3.4. Scenario Protection Level 3 (Extreme Environmental Protection - EEP)

In the Extreme Environmental Protection (EEP) scenario, the exclusion layer of open forests and green areas has a value of 100, demonstrating extreme protection of sensitive environmental terrains with a 100% probability of exclusion from urban growth, and other cells have taken the value of 50 in the simulation algorithm (see table 2.3). The excluded areas considered in this scenario are including:

- Remarkable buildings, cemeteries, airfields and sport grounds
- Railways stations, triage areas
- Activity areas (administrative, culture and leisure, education, water management, industrial or commercial, health, sports and transport)
- Water surfaces
- National parks
- Closed forests areas (wood land, closed coniferous forest, closed deciduous forest, mixed closed forest and tree area)
- Open forest, hedge, woody heath, peupleraie, orchard and vine

2.3.3.5. Attraction-based Scenario Protection Level 1 (Attraction-based Limited Environmental Protection - ALEP)

The excluded areas of Attraction-based Limited Environmental Protection (ALEP) scenario are similar to the LEP scenario and are 100% protected from the urbanization (see table 2.3). The excluded areas in this scenario are as follow:

- Remarkable buildings, cemeteries, airfields and sport grounds
- Railways stations, triage areas
- Activity areas (administrative, culture and leisure, education, water management, industrial or commercial, health, sports and transport)
- Water surfaces
- National parks
- Closed forests areas (wood land, closed coniferous forest, closed deciduous forest, mixed closed forest and tree area)

In addition to the excluded layer, three other layers are also created to define the attraction zones in this scenario as follow:

- 1) The first layer contains concentric zones of attraction. This layer is combination of several concentric attraction zones with different radius. The number of concentric zones and their radius can be considered according to the demands of the user and specifications and characteristics of a case study such as scale, area, the population and the density of the buildings. The corresponding values of the concentric attraction zones are given the different values less than 50.
- 2) Another attraction layer specifies the urbanization attraction along the water surfaces such as rivers and the lakes. This layer is given the values less than 50.
- 3) The last layer determines the attraction areas around railway stations which take the values less than 50.

It should be noted that the values of the areas located in the intersection of the last two layers and the concentric attraction zones, should be considered as more attraction areas. This means if an area locates in concentric attraction zones and near to a river or to the railway station, this area has a cumulative attraction for urbanization. The values assigned to the attraction zones are different. These values and the way to determine the attraction zones are described in detail per study area in the chapter 3.

Table 2. 3. The percentage of the environment protection for excluded areas and the attractive areas considered in the environmental protection scenarios

	National parks (%)	Remarkable building & areas (%)	Railways stations, triage areas (%)	Activity areas (%)	Water surfaces (%)	Closed forests (%)	Open forests & green areas (%)	Attraction areas
Scenario Protection Level 0 (NEP)	100	100	100	100	100	0	0	-
Scenario Protection Level 1 (LEP)	100	100	100	100	100	100	0	-
Scenario Protection Level 2 (MEP)	100	100	100	100	100	100	50	-
Scenario Protection Level 3 (EEP)	100	100	100	100	100	100	100	-
Attraction-based Scenario Protection Level 1 (ALEP)	100	100	100	100	100	100	0	✓

2.3.4. Model Forecasting

The prediction scenario file control the forecasting process of the SLEUTH. The model is initialized with the growth coefficient best fit values that were derived during calibration. In the scenario file, forecasting start and the target dates are defined. The difference of these two dates gives the number of the growth cycle. The model in this mode generate an urban growth map for each growth cycle. The prediction mode is performed 100 Monte Carlo runs. The slope sensitivity and the critical low and high values of the self-modifications are set and different execution of the model is done in order to simulate the different environmental scenarios. SLEUTH outputs consist of the statistics, logs, images, uncertainty maps and the animations, where each of them can help the user to analyse and evaluate the obtained results.

2.3.5. Model Evaluation and Investigation the Impacts of Urbanization Determinants on Model

The results of SLEUTH model provide a series of simulated urban growth cycles. All these results are made according to the historical data of the study area which are learned by the model during the calibration process. The model uses four historical urban maps consisting of 2000, 2008, 2012 and 2017 urban maps. To evaluate the accuracy of the model, it is first run with the input urban map of 2000 and run the model to forecast the prospective urban map for 2017. A brute-force search is used to systematically enumerate all urban pixels to check the goodness-of-fit of urban growth projections. The algorithm compares between the observed and the simulated pixels. The overall accuracy (OA) is calculated to measure the overall proportion of the pixels that change correctly to the total number of cells. After evaluating the results the model is run with the input urban map of 2017 to forecast the urban growth for 2050.

The SLEUTH results are limited to raster data that are difficult to interpret for decision makers. The results are some pixels on which urbanization is supposed to occur, which do not make sense from urbanism point of view.

In addition, SLEUTH model uses the historical data and the impacts of population growth and urban tissue are implicitly considered during the calibration phase on the historical urban maps. However, the changes in population growth rate or in building types cannot be included in its simulations.

2.4. Integrate the Type of Buildings and Demography on Urban Sprawl Simulation

In order to improve the SLEUTH results, different 2D urban growth simulation scenarios have been defined based on the SLEUTH model by adding buildings type and the estimation of the population growth as urban fabric factors. Each simulation corresponds to policies that are more or less restrictive of spaces considering what these territories can accommodate as a type of building and as a global population. In addition, the simulations can help the user to protect the desired lands such as the environmental spaces from urbanization. These scenarios show the simulation capabilities of the model and make it possible to improve our understanding of an urban sprawl simulation (see figure 2.12).

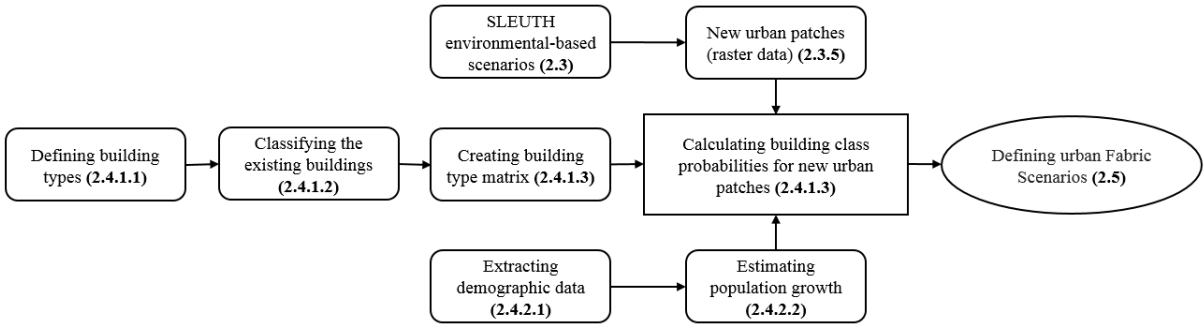


Figure 2. 12. Process of creating the urban fabric scenarios

2.4.1. Determinants and Impacts of Building Types on Urban Sprawl

In this section, the building type classification, extraction of the numbers and height of existing buildings for each class and making an active land use pattern are discussed. Considering the land use patterns, the building classification, will give weight to the urban patches. The weight is defined as the value of the average height of the buildings that are located in the same zone in land use pattern. The current buildings could give us the prospective view for the futures building. The building classification are considered in generating the urban fabric simulation scenarios.

2.4.1.1. Building Type Classification

Department of planning and environment of NSW Government of Australia, is defined and classified clearly the different building types of a city (NSW Government, Australia, 2017). These building types are used as elements classifications of the study area to create the land use patterns.

The single dwellings are often the buildings with 1 to 2 floors in height (i.e. $h = 3\text{m} \sim 5\text{m}$) that contain single detached dwellings and dual occupancies (see figure 2.13).

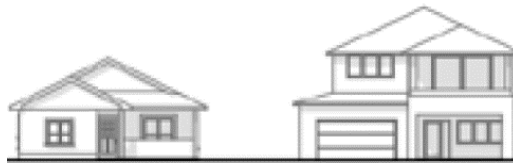


Figure 2. 13. Single dwellings (NSW Government, Australia, 2017)

Low-rise housing contain townhouse and terrace housing and small-scale residential apartment buildings with 2 to 4 floors and the height of 6m to 12m (see figure 2.14).

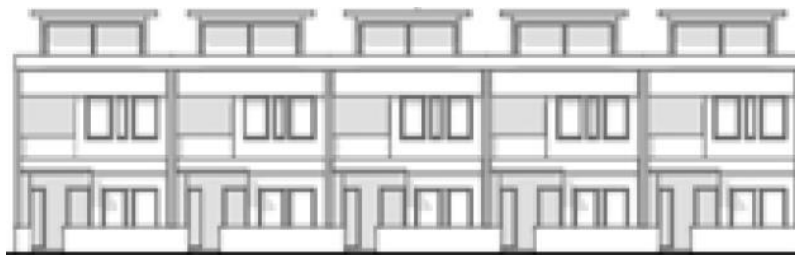


Figure 2. 14. Low-rise housing (NSW Government, Australia, 2017)

As illustrates in the figure 2.15, the shop top housing are generally the buildings with 3 to 5 floors in height (i.e. $h = 14\text{m} \sim 17\text{m}$). In these buildings, the ground floor consists of shops and retail stores and the residential apartments are located above them. Some areas with heights up to eight floors can also be considered in this class (e.g. corner sites and deep blocks).

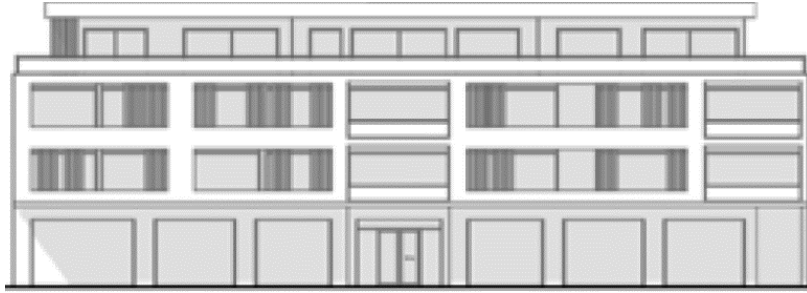


Figure 2. 15. Shop top housing (NSW Government, Australia, 2017)

The medium-rise housing and medium/high-rise housing are two next classes that both are residential apartment buildings. The medium rise housing are the buildings with 5 to 7 floors with height of 18m~25m and the medium/high rise housing contains the buildings with 8 to 9 floors with height of 26m~29m (see figure 2.16).



Figure 2. 16. Medium-rise housing and medium/high-rise housing (NSW Government, Australia, 2017)

The high-rise housing are contains of three categories, the 9 to 12 floors, 13 to 18 floors and 19 to 25 floors. In general, the heights of these types of buildings are 30m~59m. The residential towers generally have a low-rise podium at street level that may include a mix of retail, residential and commercial uses (see figure 2.17).



Figure 2. 17. High-rise housing (NSW Government, Australia, 2017)

2.4.1.2. Classifying the Existing Buildings

Due to the building type classification, the structure elements of the study areas should be classified. To do that, the information of the two layers of undifferentiated and industrial buildings are taken into account. These two layers contains the significant factors that impact urban sprawl. This information is derived from BD TOPO of IGN database. As mentioned in section 2.3.3, other structure elements of the city such as remarkable buildings and activity areas are considered in excluded area. For both undifferentiated and industrial buildings, buildings over 3m height and over 50m² are intended. From our territory experimental, the buildings that have the height less than 3m are ignored because they could not be considered neither as a residential buildings nor industrial. Figure 2.18 illustrates the meaning of the height attribute of the buildings. The building height corresponding to the difference between the highest z of the building perimeter and a point at the foot of the building. The height is rounded to the meter (Content description of BD TOPO version 2.1, IGN).

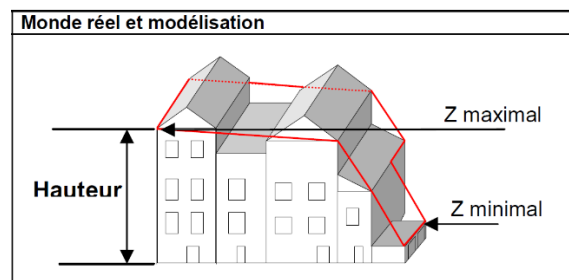


Figure 2. 18. Meaning of height attribute, content description (Content description of BD TOPO version 2.1, IGN)

In undifferentiated buildings, for each type of building class, the numbers and the height of the buildings are extracted and an average height for each type is calculated. Estimating the buildings height for the new urban area is needed in order to detect three-dimensional changes and to estimate urban densification. The industrial buildings are classified to commercial buildings, industrial buildings, agricultural buildings, greenhouses and silos. For each class an average value of height is calculated. Since the green houses and silos are often located out of the urban zones they are ignored from industrial fields. The results of this process is presented in chapter three for each study area separately.

2.4.1.3. Creating Building Type Matrix (Active Land Use Model)

In this section, we create a building type matrix that aims to compute the probability that each new pixel will belong to the building classes. This building type matrix can be used as an active land use pattern to classify the new urban patches according to existing buildings.

As discussed before, the predefined land use models have to be created manually for each study area. Therefore, these patterns are rough for the forecasting urban growth. Unlike the predefined land use models, the proposed active model can be applied for different study areas. Having the current urban area and the simulated growth area, the model can create an accurate pattern.

To create the active land use pattern the building classification discussed before is used. We collect, different urban maps that are classified by buildings height and create a 3D matrix of building types. In building type matrix, of each map corresponds to one type of building with specific height. Figure 2.19 illustrates the building type matrix of active Land use pattern. The figure corresponds to Toulouse study area. For Toulouse case study, the building type matrix consists of 9 layers of 1658*1422 pixels.

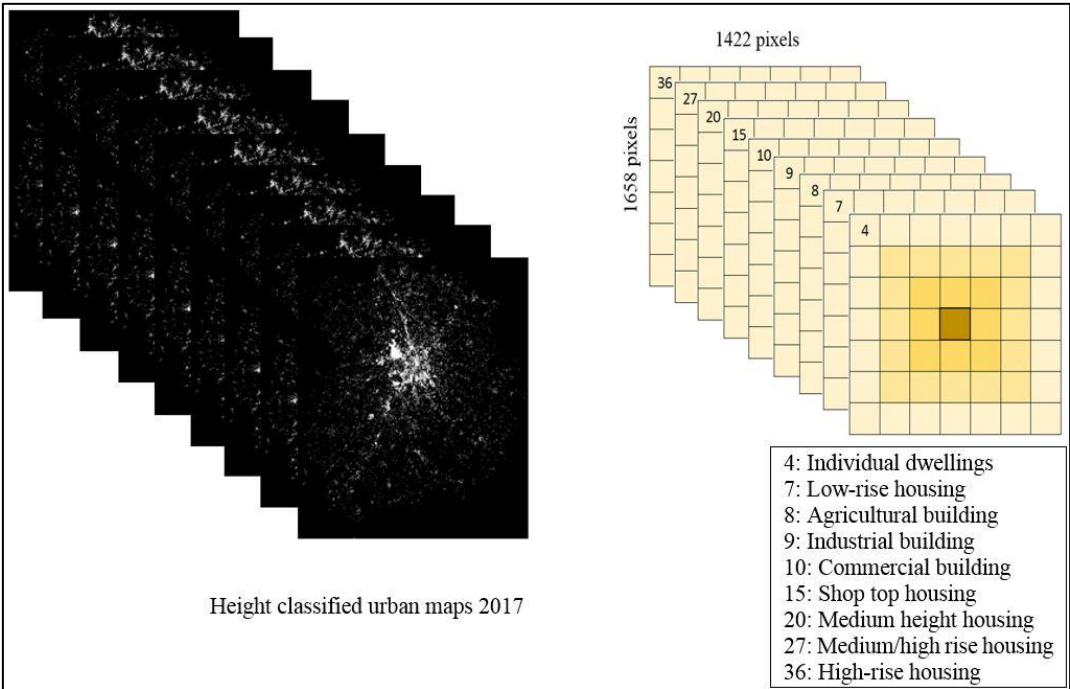


Figure 2. 19. Building type matrix that is used in active land use pattern. The 3D matrix includes 9 maps. Each map corresponds to one type of building with specific height. The value of each layer is the average heights of the buildings with regards to the building type classification.

The next step is to generate a map of the growth area. The difference of the simulated urban map and the current urban map gives the forecasted growth area. Figure 2.20 shows an example of this process for Toulouse study area. The current urban map is for 2017 and the prospective urban map is for 2050.

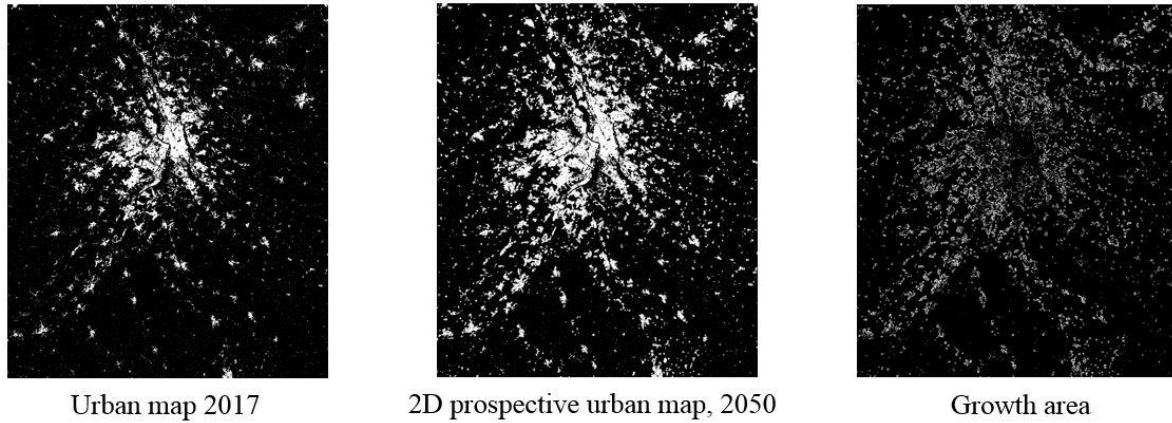


Figure 2. 20. Urban map of 2017, prospective urban growth map of 2050 and the simulated growth area during the 33 years growth cycle for Toulouse.

The urban patches in the growth area map represent the new pixels created during the simulation process. These pixels do not contain a value of the height and they have to be classified. To classify the new urban pixels, it is necessary to calculate the likelihood of each value for each pixel, considering the neighbors values. The first step to calculate the likelihood is to check the first loop of neighbors around the new urban pixels in the 3D matrix. If in the first loop of neighbors, all the pixels were null, the process will continue and the second and third loops of neighbors will be checked. Figure 2.21 illustrates a sample of this step. It indicates how the maps that have the pixels with the value of the height in the neighbors are chosen.

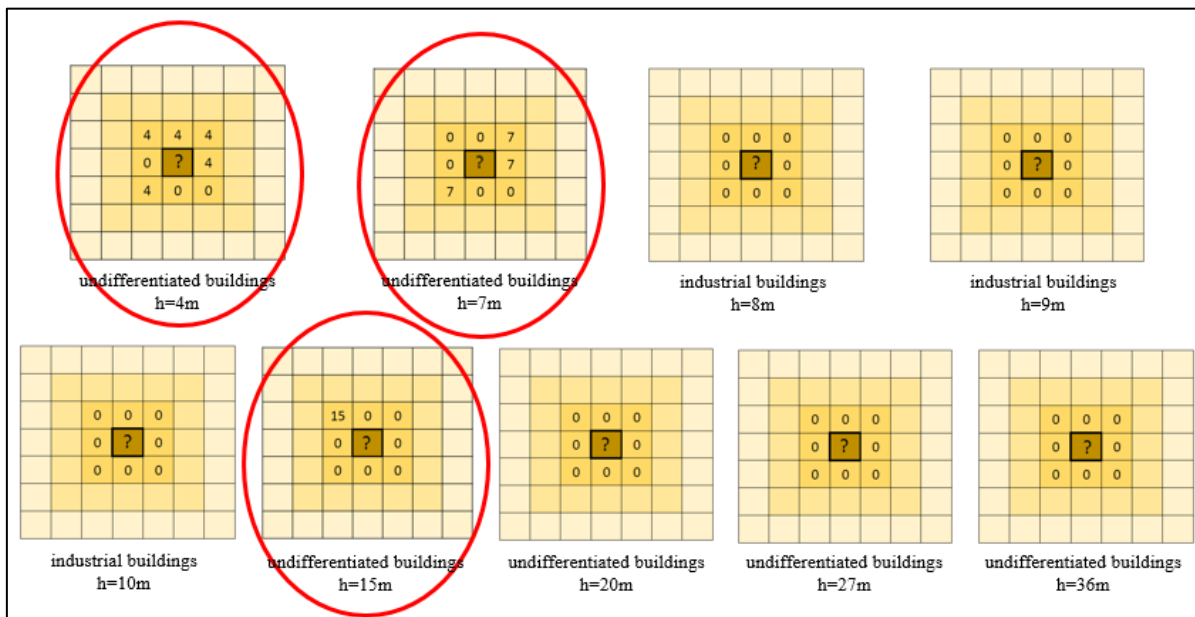


Figure 2. 21. Checking the first loop of neighbors around the new urban pixels in building type matrix

After choosing the required map in 3D matrix, it is the time to calculate the likelihood of each value for each pixel as follow:

$$P(n) = \left(\frac{\sum_{i=1}^8 V}{8N} + \frac{\sum_{j=1}^{16} V}{16N} + \frac{\sum_{k=1}^{24} V}{24N} \right), \text{ for } n=1, \dots, 9 ; \quad \hat{P} = \frac{P(n)}{\sum_{n=1}^9 P(n)} \quad (2-6)$$

In equation 2-6, \hat{P} is the likelihood for height value to be given to new urbanized pixel, P is a local value of the percentage, V is the number of pixels that have height value more than zero in each map, N is the number of chosen maps, and i, j and k are the number of first, second and third neighbors loop respectively.

As determined in the equation, in this step after choosing the required map in building type matrix, all three loops of neighbors have to be taken in to account. Figure 2.22 illustrates a sample of calculating the likelihood of each value for each pixel.

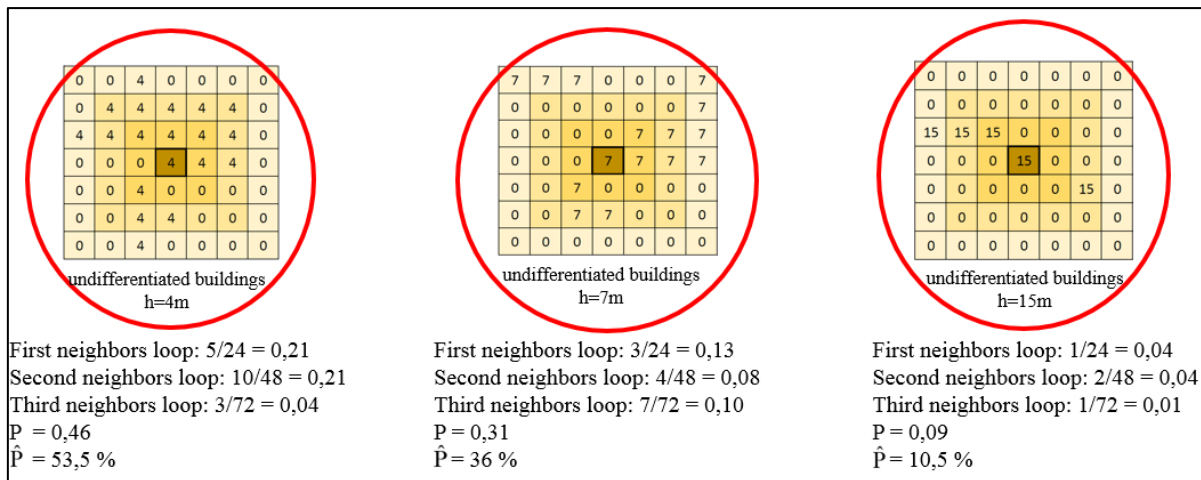


Figure 2. 22. Calculating the likelihood of each value for each pixel in the building type matrix

In sample above, three height values are calculated for the new urban pixel including 4m, 7m and 15m heights with the likelihood 53.5%, 36% and 10.5% respectively. Therefore, it exists 53.5% probability of constructing individual dwellings, 36% to create low-rise housing and 15.5% to make shop top housing in this new urbanized pixel.

2.4.2. Determinants and Impacts of Population Growth on Urban Sprawl

As mentioned before the SLEUTH model does not consider explicitly population in its simulation. In order to simulate different land priorities and constraints, we proposed to integrate the demography and life style to achieve distinguished residential categories and study the Human Settlement Capacity (HSC).

2.4.2.1. Demographic Data

The used data to obtain the demographic information is derived from the INSEE database which gives the population information per area. This base includes 18 variables on the age structure of individuals, household characteristics e.g. tenant, owner, and income for December 31, 2010.

The documentation of the INSEE data including the source, the generating information and the list and description of variables are described in the Annex E. For each study areas a population map is created from the INSEE database with regards to the total number of individuals per pixel. Using the population map that gives the ratio of individuals per pixel and the total population of study area, the number of inhabitants per building classes are calculated. This is done by integrating the number of individuals per pixel (derived from the generated INSEE maps), the building classes and the number and kinds of the existing buildings (derived from the IGN - BD TOPO). The population maps and the calculation of the number of inhabitants for each building classes per study area are provided in chapter 3.

2.4.2.2. Population Growth Estimation

After calculating the number of inhabitants for each building type, now it is the time to estimate the population growth in order to calculate the quantity of required buildings and therefore, define the urban fabric scenarios.

The SLEUTH simulation results are definitely needed to be evaluate by the population density. To estimate the population growth, first the value of the compound annual population is calculated as follow (Jantz et al., 2010):

$$G_{t_y, t_{y'}} = \left(\frac{P_{t_{y'}}}{P_{t_y}} \right)^{\left(\frac{1}{t_{y'} - t_y} \right)} - 1 \quad (2-7)$$

where, G is compound annual population growth rate and P is successive population for the years of t_y and $t_{y'}$.

After the calculation of the compound annual population growth rate for a study area during the desired number of the growth cycles. The annual and total percentage of the increased population is estimated, considering the actual population. Having the population and compound annual population rate, the average population for the coming years is estimated as follow:

$$P'_{t_x} = P_{t_y} \times \left(1 + G_{t_y, t_{y'}} \right)^{(t_x - t_y)} \quad (2-8)$$

In equation 2-8 the P' is the average estimate of population. P indicates successive population values, t_y & $t_{y'}$ are the year intervals, t_x is the desired year and G is compound annual population growth rate.

2.5. Urban Fabric Scenarios and Urban Configuration

Having the building classes, the simulated urban growth and the estimated mean population, in this section, the suitable growth cycle is rated to achieve the desired urban fabrics. The proposed urban model aims to compare the determinants of the urbanization and its measurement in

different scenarios of urban sprawl. In order to achieve this purpose different primary urban fabric scenarios are defined. These scenarios are fictive and they do not correspond to reality but they help to better understand how this land could be used and how many inhabitants could live in these new areas. These scenarios are defined based on building classification and the observation of the existing building. They help to have a basic perspective on defining the final scenarios. For example, for Toulouse study area, we have initially consider the urban fabric scenarios with one or combination of single dwellings and medium rise housing and four scenarios are defined as follow:

- 1) Sprawl urban: The first scenario considered that all new urban patches filled with single dwellings.
- 2) Medium dense urban: In second scenario, it is assumed that in 50% of the new simulated urban areas, single dwellings will be built and in the other 50% the medium rise housing.
- 3) Medium/High dense urban: The third scenario presumed the 30% of single dwellings and other 70% medium rise housing
- 4) High dense urban: The forth scenario defined to accommodate just medium rise housing.

Table 2.4 illustrates primary urban fabric scenarios that are defined for Toulouse study area, as well as the rate of the combination of each building type in each scenario.

Table 2. 4. Primary urban fabric scenarios for Toulouse study area.

Primary urban fabric scenarios	Single dwelling (%)	Medium rise housing (%)
Sprawl urban scenario	100	0
Low dense urban scenario	50	50
Medium dense urban scenario	30	70
Medium/high dense urban scenario	0	100

For each scenario, the simulated urban growth results from SLEUTH are tested considering the specific population increased. After, the amount of the accommodation of the people is calculated for each scenario. It is clear that the sprawl urban scenario can accommodate less number of population while in the high dense scenario, many more people can be placed and therefore the city will be less spread. The primary urban fabric scenarios consist of different densities from sprawl to high dense urban. Considering the amount of population that could be accommodate for each scenario and the estimated population for the target date, the final urban fabric scenarios are defined. In the final scenarios it is necessary to test the SLEUTH results for different growth cycle to find out which growth cycle would match better the desired urban fabric. These procedure is done for all the environmental scenarios. The results show that changing urban fabric scenarios has a strong impact on the limitation of urban sprawl, thus saving agricultural and natural landscapes. They also help us to understand how different urban fabrics impact the urban sprawl. The urban fabric scenarios of three study areas are produced and the results are represented and analyzed in chapter 3.

2.6. 3D Representation of Prospective Urban Growth Simulations

A 3D representation for each prospective urban growth simulations is provided in order to facilitates the interpretation of the SLEUTH simulation and differentiate the scenarios. The findings allow having different images of the city of tomorrow for applying to urban policies. In 3D modeling process, the land use achieved from 2D modeling will be rectified with regards to the location of the existing buildings and the geographic features of the study area. Finally, another growth analyses will be done considering these modifications. The 3D representation of the model, its process and results are discussed in chapter 4.

2.7. Chapter Conclusion

Nowadays, urban sprawl phenomena is a big challenge for the authorities and urban planners. This chapter presents a methodology to evaluate the SLEUTH results and to investigate the effects of environmental constraints and constructions on urban sprawl. In this chapter, the process of the SLEUTH-3r model execution is explained.

In order to give more flexibility in urban sprawl simulation, the environmental-based scenarios are defined, and by adding the building type factor and demographic factor, different urban fabric scenarios are generated. Therefore, in this research two type of scenarios are provided as follow:

1. Environmental-based scenarios: to represent the impacts of environmental constraints on urban sprawl.
2. Urban fabric scenarios (consists the primary and final urban fabric scenarios): to represent the impacts of population and constructions on urban sprawl as well as environmental constraints.

The SLEUTH model is executed with regards to the environmental constraints that are integrated by environmental-based scenarios in the model. Although, we defined environmental-based scenarios in our simulation and the results respect some environmental constraints, but the SLEUTH results are limited to some raster data that is difficult to interpret for decision makers. They are some pixels on which urbanization is supposed to occur. Moreover, SLEUTH model uses the historical data, and the impacts of population growth and urban tissue are implicitly considered during the calibration phase on the historical urban maps. However, the changes in population growth rate or in building types cannot be included in its simulations.

To overcome these problems, a building classification is defined and existing buildings are classified according to their height. The new urban pixels are also classified according to probabilities that are calculated from the nearest neighbor height. This is done in order to study the Human Settlement Capacity (HSC). The population growth is estimated for the target date. Integrating the population growth and the building classification of the new urban pixels with the SLEUTH results, different urban fabric scenarios are generated. A set of different simulations that related to different land priorities and constraints are proposed. We have

defined the primary urban fabric scenarios with different urban densities from sprawl to high dense. The final urban fabric scenarios are defined based on the results that are obtained from primary scenarios and by taking in account the amount of population that could be accommodate for each scenario, and the population growth estimation for the simulation date. These final scenarios can give good view of the urban growth with deferent level of sprawl. Proposing different simulation of urban sprawl is fundamental because it shows the possible impact of urban sprawl but also the capacity of urban settlement according to different scenario. The implementations of the model on three different study area with different scales and their results are presented and discussed in Chapter 3. The results help us to understand how different urban fabrics impact the urban sprawl.

Chapter 3 : Application of the Model to Diversify the Simulations of Urban Sprawl

Contents

- 3.1. General presentation of study area
 - 3.2. Developing Different Simulation Scenarios to Illustrate the Impacts of Environmental Constraints, Construction and Population on the Growth of a Metropolis - Toulouse Metropolis
 - 3.2.1. Data and Materials
 - 3.2.2. Environmental Constraints Scenarios
 - 3.2.3. 2D Urban Growth Simulations
 - 3.2.4. Urban Fabric Scenarios
 - 3.3. Developing Different Simulation Scenarios to Illustrate the Impacts of Environmental Constraints, Construction and Population on the Growth of a Town - Saint Sulpice la Pointe
 - 3.3.1. Data and Materials
 - 3.3.2. Environmental Constraints Scenarios
 - 3.3.3. 2D Urban Growth Simulations
 - 3.3.4. Urban Fabric Scenarios
 - 3.4. Developing Different Simulation Scenarios to Illustrate the Impacts of Environmental Constraints, Construction and Population on the Growth of a small community - Rieucros
 - 3.4.1. Data and Materials
 - 3.4.2. Environmental Constraints Scenarios
 - 3.4.3. 2D Urban Growth Simulations
 - 3.4.4. Urban Fabric Scenarios
 - 3.5. The Impacts of Pixel Size and Calibration on Sustainability of Model
 - 3.6. Chapter conclusion
-

SLEUTH is an urban growth model that uses cellular automata, terrain mapping and land cover deltatron modeling to address urban growth. This chapter presents the applications of the model to simulating urban growth. Furthermore, the Impacts of environmental constraints, construction and population on urban sprawl in three different areas contain urban metropolis, peri-urban and rural area are discussed and evaluated. For each study area, different scenarios are simulated that show the capabilities of the model and make it possible to improve our understanding of an urban sprawl simulation. The simulation results of three different study areas with various sizes and populations provide a good view of the scalability of the proposed method and the findings allow having different images of the city of tomorrow to choose and reflect on urban policies.

In this chapter, general presentation of the study areas, the reasons for their selections, and their scales and resolutions are represented in section 3.1. The implementation of the model on Three study areas including Toulouse metropolitan, Saint Sulpice la Pointe (a town around Toulouse), and Rieucros (a small community in a rural area) are represented in the section 3.1 to 3.3 respectively. A comparison and discussion of the model is provided on section 3.4. The chapter is concluded in section 3.5.

3.1. General Presentation of Study Areas

The model is applied on three study areas including Toulouse metropolitan, Saint Sulpice la Pointe and Rieucros, in order to evaluate the scalability of the model. In selection of the case studies the historical urban growth rate, population growth and the size of them are considered as well as availability of the data. These areas have grown faster than many of the surrounding areas in recent years. They have different scales in terms of density, type of building, population and urban features.

Toulouse study area is the fourth largest and populous city in France. Toulouse had highest increasing of the urbanization area and highest population growth rate between 2006 and 2011 of any French metropolitan area with more than 300,000 inhabitants. As discussed in Chapter 2, the undifferentiated buildings (provided as shape file in BD-TOPO of IGN) are used to create the urban maps for SLEUTH input. The SLEUTH input maps are the raster files, so the vector data is converted to the raster data and the map of 1658×1422 pixels with the pixel size of 52m×52m (~2700 m²) are extracted (study area ~ 637515 ha). The pixel size is obtained by experiments. We take the pixel size so that it can cover the whole study area with full pixel size while taking into account the computational complexity and performance. We noted that the SLEUTH calibration process is long and requires a lot of space in RAM for numerous internal cell arrays. The calibration time depends to the size of maps and the number of required iterations which can be from some minutes to some hours. Therefore, the smaller size of pixel for Toulouse is not desirable in the data processing process. Larger size for pixels can make the process of creating the 3D buildings difficult. As we will see in Chapter 4, different urban constraints (e.g. distances from current buildings and distances from the roads and rivers) are considered in process of creating the 3D scenarios and the larger pixels can make problem facing to constraints. In addition the coarse size of the pixels reduce the accuracy of the model.

Saint Sulpice la Pointe is the second study area that is a town around Toulouse. Saint Sulpice la Pointe is exist as a part of the first study area (i.e. Toulouse) that could help to verify the scalability of the model. The extent of the study area is 3600 ha and the input maps have the size of 200×200 pixels that feature a cell size of 30m×30m (900 m²). In Saint Sulpice la Pointe, the average area of existing buildings is smaller than Toulouse study area. Furthermore, the extent of the study area is much less than Toulouse. Therefore, we have chosen smaller size for the pixels without much affecting the model complexity. Since Saint Sulpice la Pointe is also exist in the Toulouse study area, the effect of different pixel sizes on the simulations can be compared.

The last case study is Rieucros, which is a small community in a rural area. Choosing the study area in extent of Rieucros can give different view of urban growth modeling. The extent of this study area is 400 ha and the input maps have the size of 100×100 pixels with the cell size of 20m×20m (400 m²). The same way as before is used to choose the pixel size.

3.2. Developing Different Simulation Scenarios to Illustrate the Impacts of Environmental Constraints, Construction and Population on the Growth of a Metropolis - Toulouse Metropolis

In 1950, around 45% of the people in France lived in rural place and 55% lived in cities. The urban population in France is increased to more than 75% in 2014 and it is anticipated to growth to more than 85% for 2050 (see figure 3.1) ([United Nations, 2018](#)).

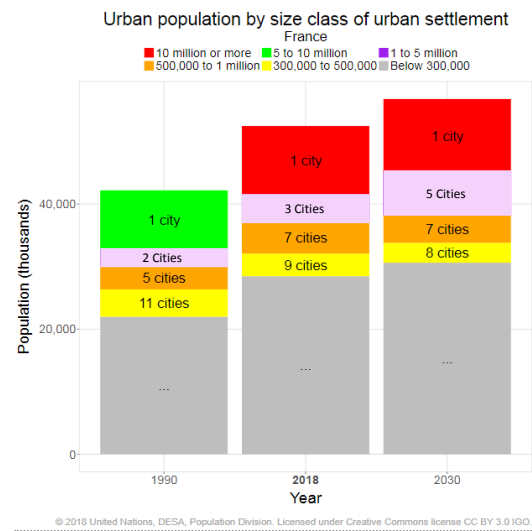
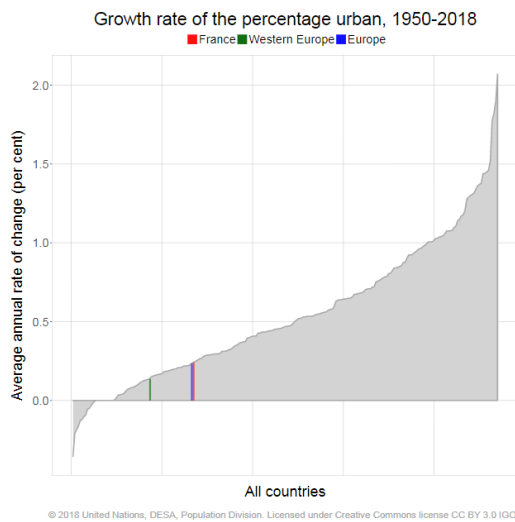
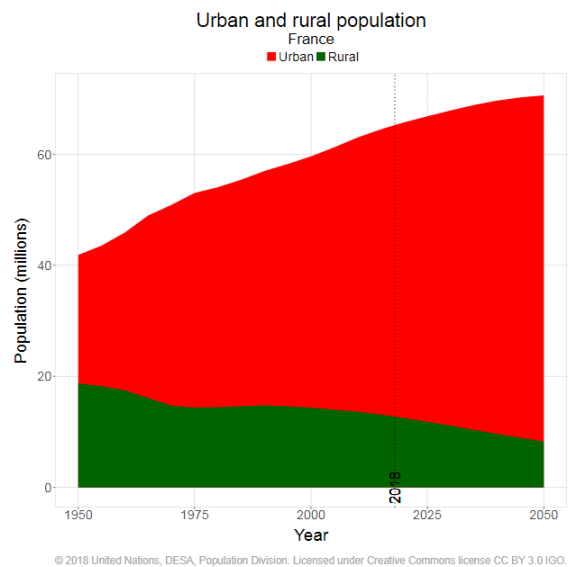
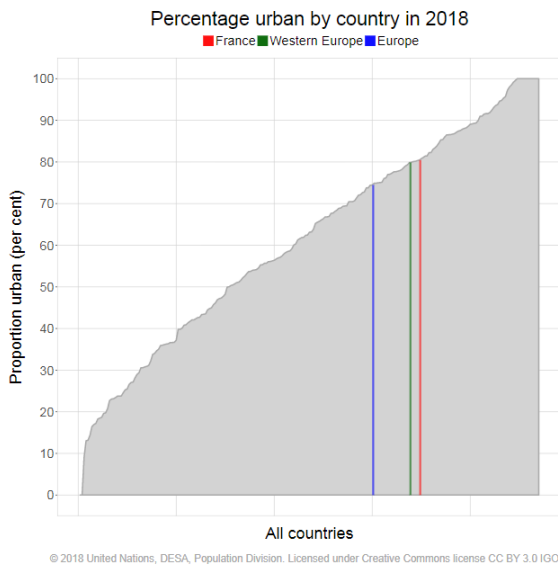
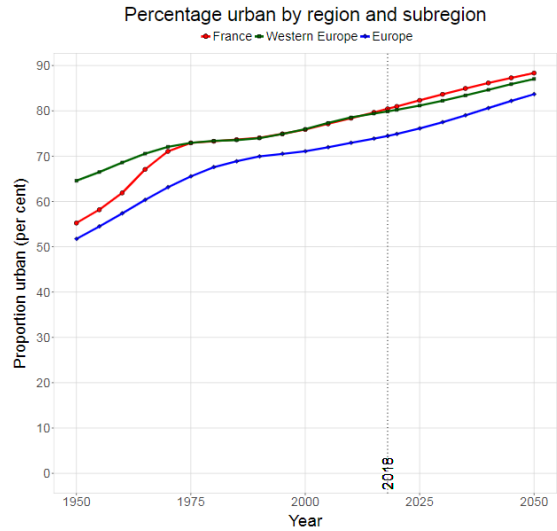
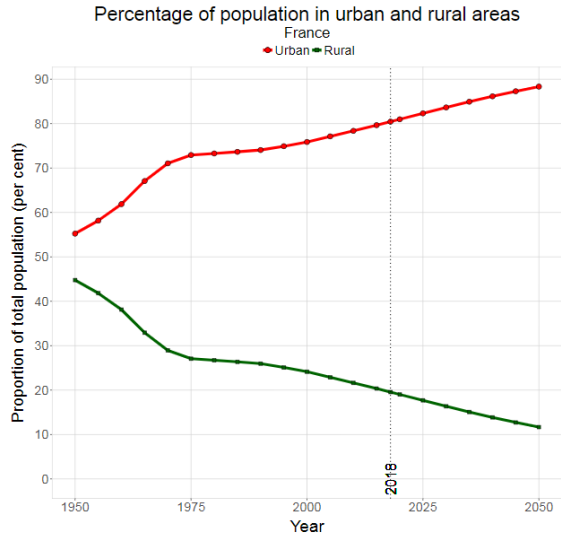


Figure 3. 1. France population profile, 1950 - 2050 (United Nations, 2018)

The study area of this section is Toulouse, the fourth most populous commune in France, which is the capital of the French department of Haute-Garonne and the region of Occitanie, located in south-west of France (43°36'16" North, 1°26'38" East). The extent of Toulouse study area is 637515 ha and it is bigger than the city of Toulouse including some parts of five other departments around Toulouse i.e. departments Gers (32), Tarn-et-Garonne (82), Tarn (81), Aude (11) and Ariège (9) (see figure 3.2).

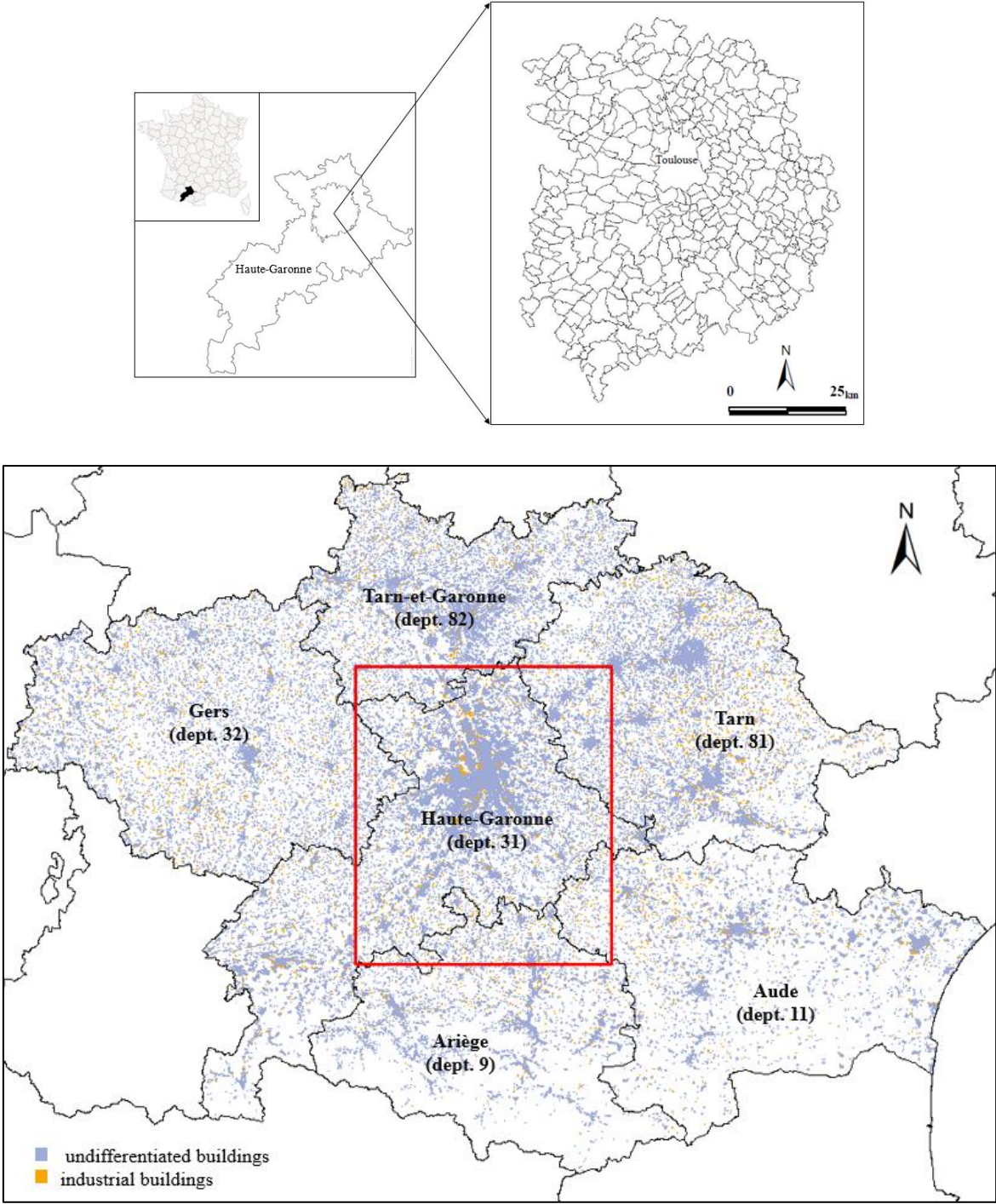


Figure 3. 2. Location and extent of the urban area of Toulouse

Toulouse contains of 342 municipalities. From 1990 to 2006 the population has been grown, due to 14 000 newcomers per year. This demographic growth led to increase of urbanization area around 1 300 ha per year over the same period. The population growth rate between 2006 and 2011 was +1.34% per year. This growth rate is the highest growth rate of any French metropolitan area with 300,000 inhabitants or more; however, it is slightly lower than the growth rate registered between the 1999 and 2006 censuses (United Nations, 2018). In 2018, the population of the metropolitan area was more than 1.33 million inhabitants. Table 3.1 shows the percentage of the urban population residing in Toulouse urban agglomeration with 300,000 inhabitants or more derived by united nation in 2018.

Table 3. 1. Percentage of the urban population residing in Toulouse, (United Nations, 2018)

Location	1950	1960	1970	1980	1990	2000	2010	2020	2030
Toulouse urban population residing (%)	0.6	0.8	0.9	1.1	1.1	1.3	1.4	1.6	1.6

3.2.1. Data and Materials - Toulouse

As mentioned in Chapter 2, we use SLEUTH-3r as an urban growth model that uses the input data including slope, land use, exclusion, urban, transportation and hillshade that we call hereafter ‘map’. These maps are indeed matrices of parameter values. Geospatial database and geographic information systems are used to create initial spatial data and used during the simulation. All these input maps have the size of 1658×1422 pixels that feature a cell size of 52m×52m (~2700 m²). The desirable number of each type of maps depends on the needed calibration accuracy for the prospective model and it will be discussed in the next chapter.

The Geospatial database that is used as input topographic data is composed of the maps of 2000, 2008, 2012 and 2017 from IGN BD TOPO. Slope and hillshade maps are derived from Digital Elevation Model (DEM) of RGE ALTI with a spatial resolution of 5m, provided by IGN. Urban areas, excluded areas and transportation maps are generated automatically from BD TOPO and BD ORTHO from IGN. Urban map is classified into two classes of urban and nonurban. Population and census on district zone are taken from INSEE database of 2011. Figure 3.3 illustrates the population map created from INSEE. In this figure, each pixel has the resolution of 200×200 meters which corresponds to the number of individual living there. We use this map and the total amount of population in Toulouse study area (which both derived from INSEE) to calculate the distribution of the population in study area and calculate the number of inhabitants per pixel and finally per building (considering the building class). The number of inhabitants for each type of building represented in table 3.9 (section 3.2.4.3).

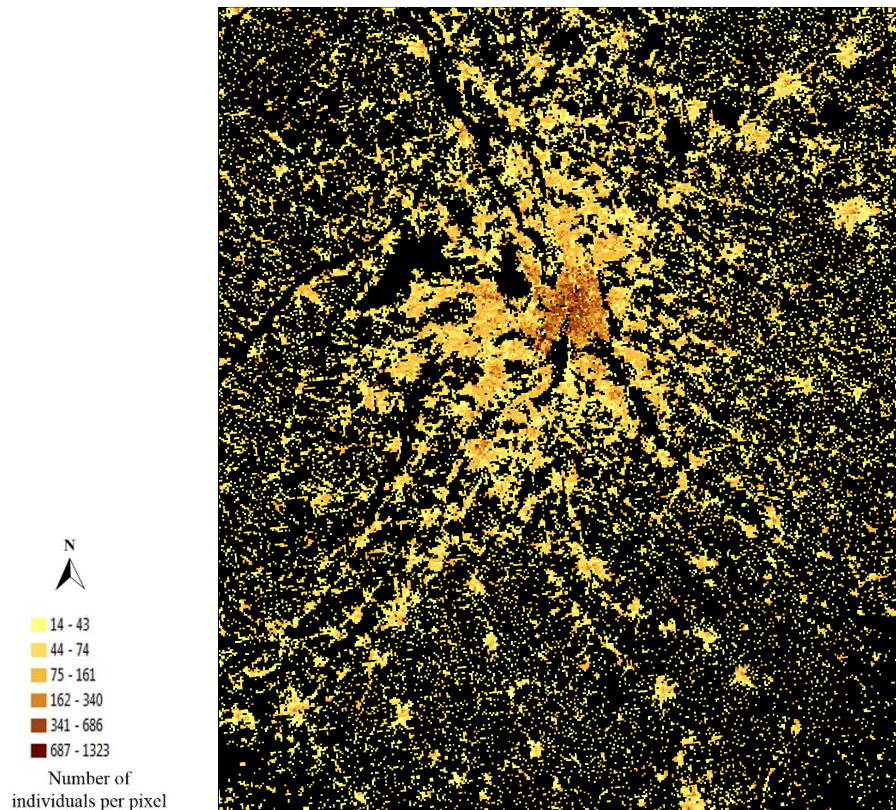


Figure 3. 3. Population map (INSEE, 2011)

In this chapter, different 2D urban growth prospective scenarios are defined. Each scenario needs its specific layer input maps. Therefore, the different types of each input maps are presented and it will be explain how the scenario input maps are generated.

To create the urban map, two building classes of IGN data are used which contains Bati_indifferencie, Bati_industriel. For undifferentiated and industrial, the only buildings with more than 3m height and more than 50m² surface are considered. As discussed in the chapter 2, this is done due to the height classification of the constructions. The buildings that have the height less than 3m and the area less than 50m² are ignored (see chapter 2). In the created map, only the buildings are considered but there are always some surfaces around the buildings (e.g. yards, corridors and protected spaces between the buildings), where new buildings could not be built there. To avoid these, different erodes for dilation-erosion are applied. According to the experimental results, an appropriate value of dilation-erosion that can fill the space between the adjacent buildings, and surround them is a value close to the SLEUTH input pixel size. Therefore, dilation-erosion at 50m is applied on each historical urban data (i.e. 2000, 2008, 2012, and 2017) and a raster file (.gif) is extracted to be used as input urban map of SLEUTH model. Figure 3.4 illustrates the urban map of 2017.

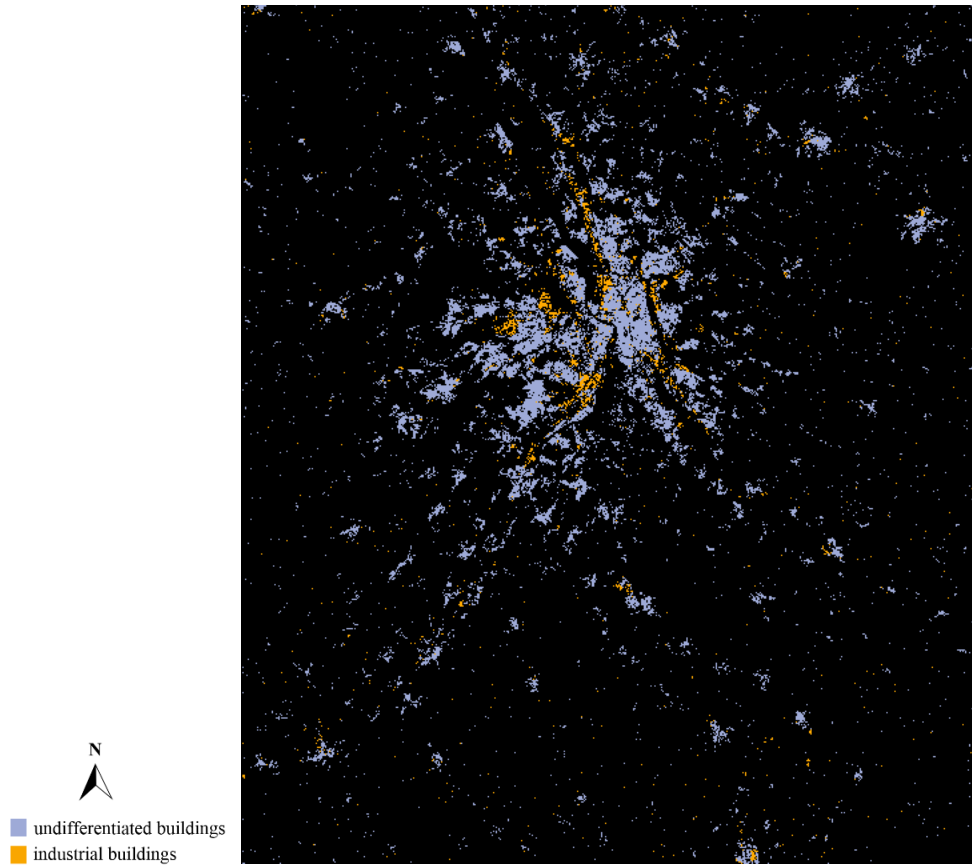


Figure 3. 4. Toulouse urban map contains the undifferentiated and industrial buildings, 2017, IGN

The slope, hillshade, urban, transportation and excluded maps are illustrated in figure 3.5. We used SLEUTH as an environmental scenario dependent model to simulate the urban growth with respect to environmental constraints. The constraints are considered in the model by altering the excluded maps. The excluded maps have some exclusion areas with the pixel value range from 51 to 100, which make them less likely to be developed. In next section the environmental constraints scenarios and the ways to create the excluded and attraction maps are represented.

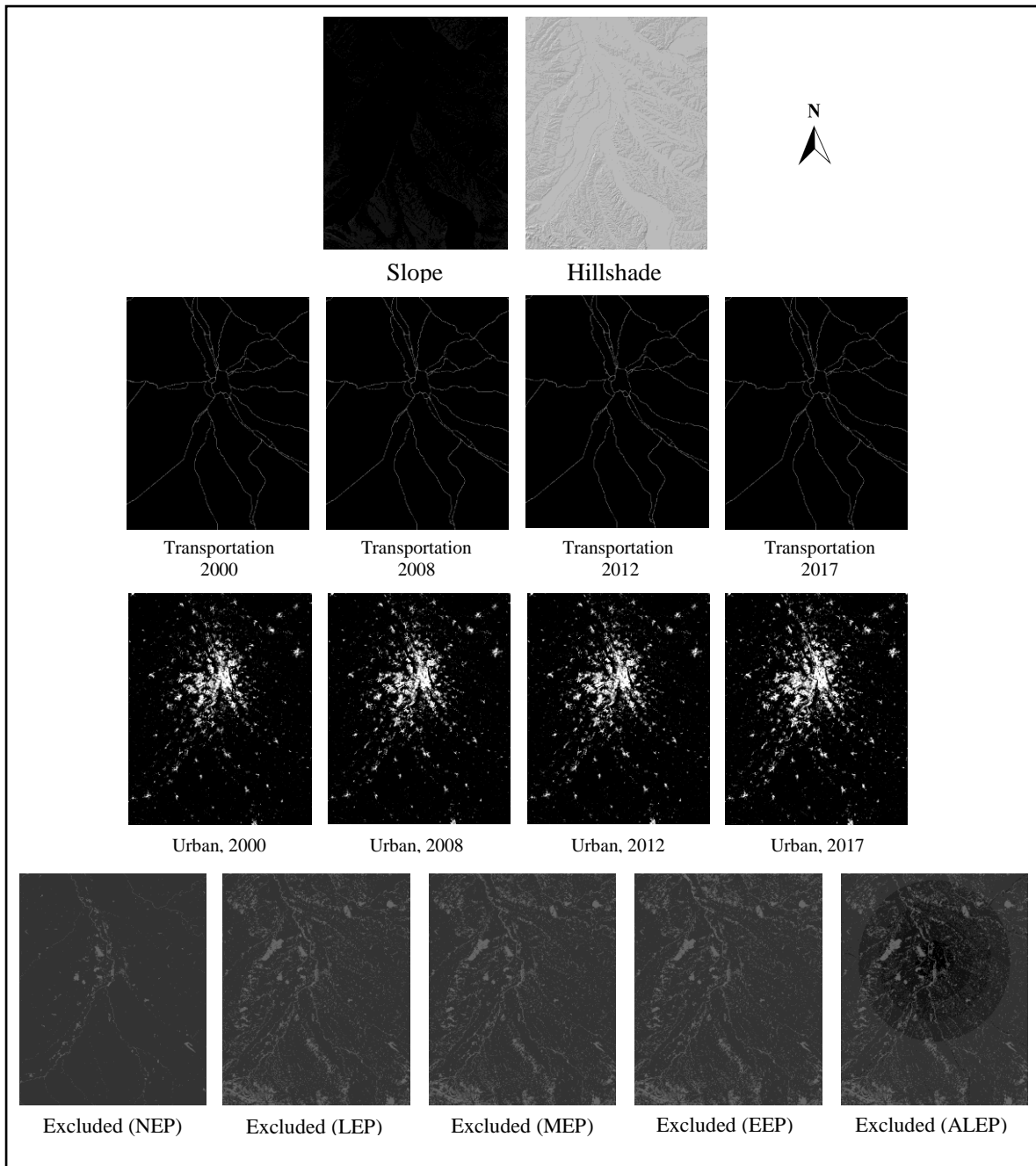


Figure 3. 5. Slope, hillshade, transportation, urban and exclusion maps of Toulouse

3.2.2. Environmental Constraints Scenarios - Toulouse

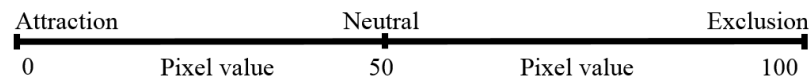
In our research, different scenarios are defined in order to challenge the environmental protection and to improve the urban sprawl simulation results. Each scenario corresponds to different explicit priorities. None of the results will ever occur in the real world but they shape the possibilities and are useful for decision-making.

SLEUTH model has the possibility of generating different scenarios of urban growth by changing the composition of SLEUTH input layers. In a SLEUTH model, the maps of exclusion and attraction are essential. The excluded maps define the places where the city does not have

the right to extend such as parks and the maps of attraction describe the places or objects that attract urbanization e.g. along the roads. The exclusion and attractive maps are generated by using topographic data. These maps give the opportunity to determine five different environmental protection scenarios as follow:

- Scenario Protection Level 0 (Nearly No Environmental Protection - NEP)
- Scenario Protection Level 1 (Limited Environmental Protection - LEP)
- Scenario Protection Level 2 (Moderate Environmental Protection - MEP)
- Scenario Protection Level 3 (Extreme Environmental Protection - EEP)
- Attraction-based Scenario Protection Level 1 (Attraction-based Limited Environmental Protection - ALEP)

The excluded areas in SLEUTH identify with their pixel values. Here, we define the pixel values from 0 to 100 where 100 means that those pixels are protected 100% from the possible urban growth and the value of zero represents free zones to build. The value of 50 indicates a neutral weight for development. Between 100 and 50 is a relative exclusion whereas under 50 means that there is an attraction (see table 2.3).



The changes of land use occupation for the years 2006 and 2014 in Midi-Pyrénées region derived from Teruti-Lucas source is represented in table 3.2. This table offers a view on the land occupation, the amount of the urbanization and artificialization (e.g. forested lands, artificialized area, and water surfaces) in the region of the study area between 2006 and 2014, which demonstrates the need of environmental protecting in future urban development.

Table 3. 2. Changes in physical occupation between 2006 and 2014 in Midi-Pyrénées region (309080 points), Teruti-Lucas

Type of occupation in 2014	Surfaces	Type of occupation in 2006								
		Built surfaces	Coated or stabilized surfaces	Other artificial lands	Agricultural lands	Forested lands	Landes	Natural bare lands	Water surfaces	Prohibited areas
Built surfaces	Surface (ha)	42 258	2 699	3 777	7 189	1 259	3 606	179	-	-
	Half confidence interval	6 262	1 380	1 641	2 307	959	1 691	362	-	-
Coated or stabilized surfaces	Surface (ha)	1 439	119 414	6 655	10 453	6 124	2 706	180	-	-
	Half confidence interval	1 025	10 138	2 249	2 820	2 075	1 404	363	-	-
Other artificial lands	Surface (ha)	2 879	4 326	95 646	17 503	4 509	6 486	1 261	-	1 806
	Half confidence interval	1 681	1 822	10 235	3 832	1 875	2 234	959	-	3 624
Agricultural lands	Surface (ha)	542	7 926	10 843	2 280 471	28 844	28 990	1 437	1 262	-
	Half confidence interval	628	3 634	2 831	42 516	4 679	5 275	1 009	959	-
Forested lands	Surface (ha)	536	3 058	2 882	17 663	1 382 713	24 354	721	539	536
	Half confidence interval	811	1 548	1 483	3 955	40 800	4 466	869	628	942
Landes	Surface (ha)	538	1 442	2 878	42 911	23 433	191 450	1 260	360	-
	Half confidence interval	513	1 146	1 427	7 512	4 588	16 192	1 580	513	-
Natural bare lands	Surface (ha)	-	181	544	1 618	1 437	538	104 207	182	-
	Half confidence interval	-	363	628	1 057	1 132	601	13 463	363	-
Wetlands	Surface (ha)	-	542	895	2 353	1 623	544	179	40 378	-
	Half confidence interval	-	628	959	1 392	1 294	628	181	7 358	-
Prohibited areas	Surface (ha)	-	-	-	359	909	730	-	-	2 728
	Half confidence interval	-	-	-	513	1 494	1 450	-	-	4 052

3.2.2.1. Scenario Protection Level 0 (Nearly No Environmental Protection - NEP)

In Nearly No Environmental Protection (NEP) scenario, the excluded areas are fully protected from urban growth. They are excluded 100% of the possible urban growth. They take the value of 100 and the others take the value of 50 for the entry of SLEUTH into NEP during the calibration and forecasting process. The excluded areas considered in this scenario are illustrated in figure 3.6. These areas include the remarkable buildings, cemeteries, airfields, sport grounds; railways stations, triage areas; activity areas (administrative, culture and leisure, education, water management, industrial or commercial, health, sports and transport) and national parks; that are shown in red and the water surfaces represented in blue in the figure. The national parks are protected 100% in all scenarios.

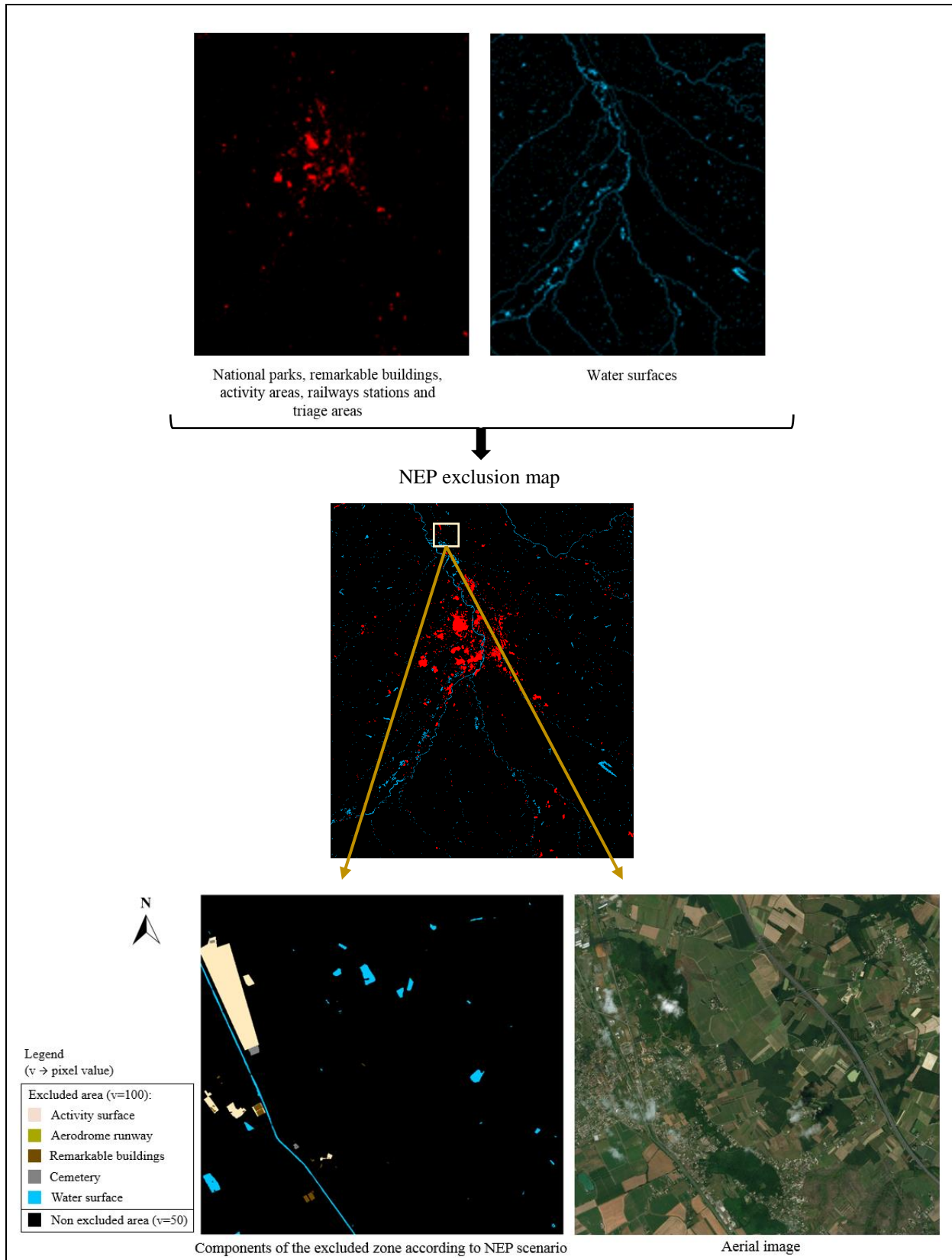


Figure 3. 6. NEP exclusion map generated for Toulouse, 2017. In all excluded maps, the common areas between urbanized and excluded areas are considered as urbanized areas.

3.2.2.2. Scenario Protection Level 1 (Limited Environmental Protection - LEP)

For Limited Environmental Protection – (LEP) scenario, the excluded areas are fully protected from urban growth, considered as 100% exclusion from possible urban growth and have given the value of 100 and non-exclusion zones with a value of 50 indicate a neutral weight for development (see figure 3.7). As mentioned in chapter 2, in this scenario, the excluded map includes all parks, protected areas and water bodies have made from the database of the IGN for 2017 including the remarkable buildings, cemeteries, airfields, sport grounds; railways stations, triage areas; activity areas (administrative, culture and leisure, education, water management, industrial or commercial, health, sports and transport) and national parks that are shown in red, the water surfaces represented in blue and the closed forests areas (wood land, closed coniferous forest, closed deciduous forest, mixed closed forest and tree area) in dark green in the figure3.7.

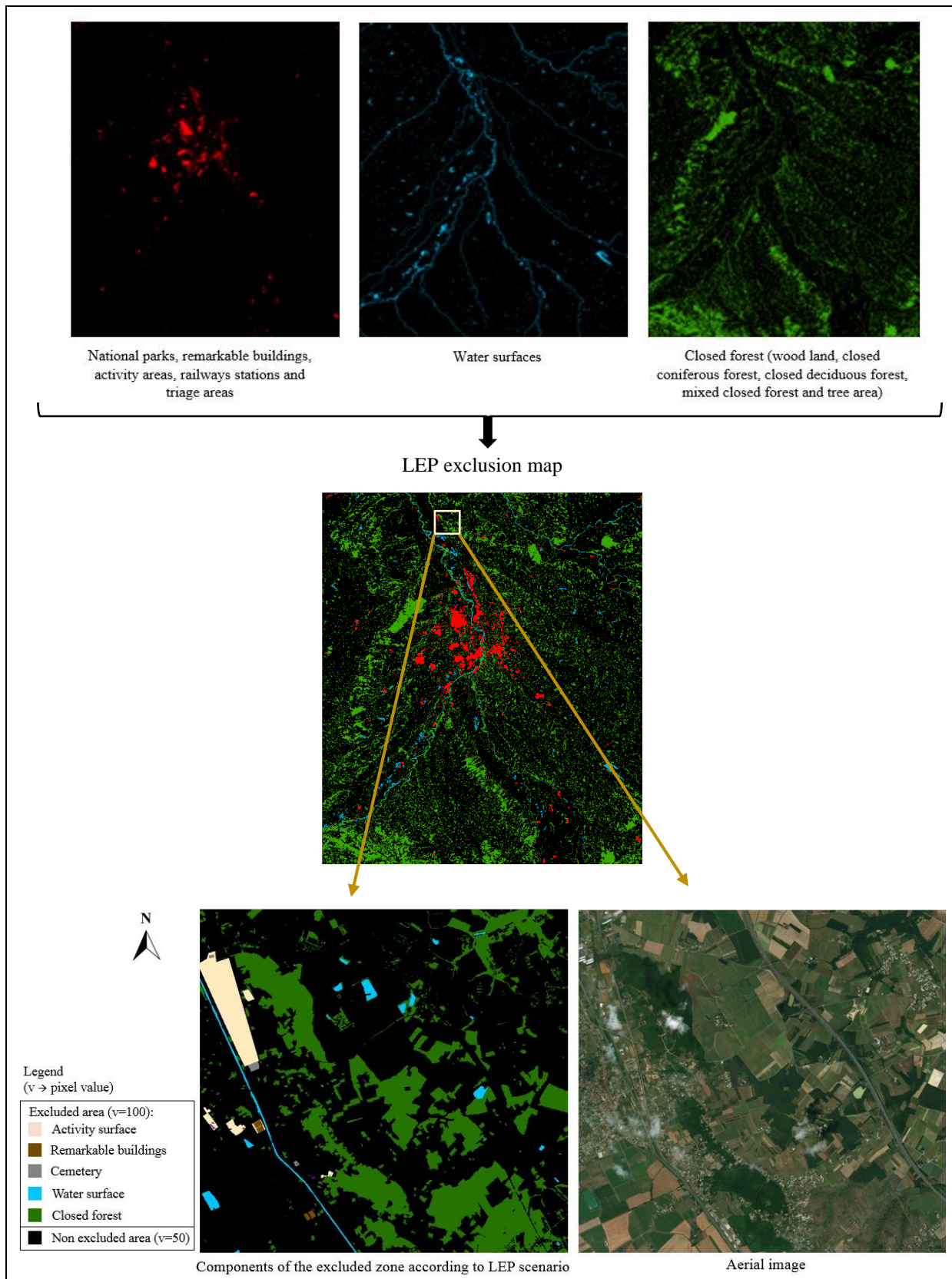


Figure 3. 7. LEP exclusion map generated for Toulouse, 2017. In all excluded maps, the common areas between urbanized and excluded areas are considered as urbanized areas.

3.2.2.3. Scenario Protection Level 2 (Moderate Environmental Protection - MEP)

In the Moderate Environmental Protection (MEP) scenario, open forests and green areas derived from the IGN database are generated as a separate layer with a value of 75 and represent the 50% probability of exclusion from urban growth. The areas that are fully protected from urban growth, took the value of 100 and the non-exclusion zones have gotten a value of 50 similar to the previous scenario (see figure 3.8). The excluded map contains all parks, protected areas and water bodies have made from the database of the IGN for 2017 including the remarkable buildings, cemeteries, airfields, sport grounds; railways stations, triage areas; activity areas (administrative, culture and leisure, education, water management, industrial or commercial, health, sports and transport) and national parks that are shown in red, the water surfaces represented in blue, the close forest areas (wood land, closed coniferous forest, closed deciduous forest, mixed closed forest and tree area) in dark green and the open forest, hedge, woody heath, peupleraie, orchard, vine in light green in the figure.

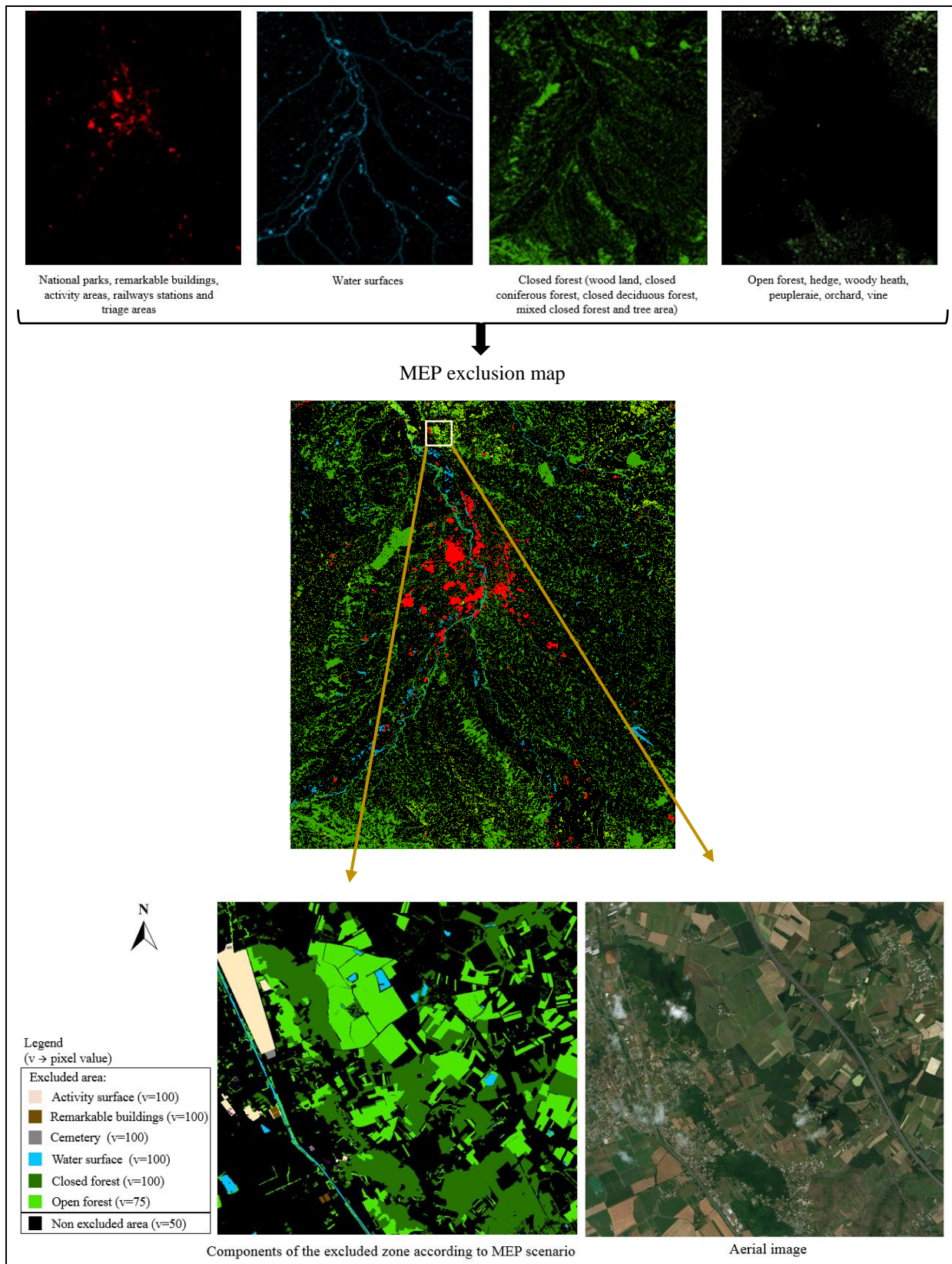


Figure 3. 8. MEP exclusion map generated for Toulouse, 2017. In all excluded maps, the common areas between urbanized and excluded areas are considered as urbanized areas.

3.2.2.4. Scenario Protection Level 3 (Extreme Environmental Protection - EEP)

The Extreme Environmental Protection (EEP) scenario, is similar to the MEP scenario, but the exclusion layer of open forests and green areas has a value of 100, demonstrating extreme protection of sensitive environmental terrains with a 100% probability of exclusion from urban growth, and other cells have taken the value of 50 in the simulation algorithm. Figure 3.9, illustrates the EEP exclusion map generating procedure. The excluded areas are also similar to the MEP scenario includes all parks, protected areas and water bodies have made from the database of the IGN for 2017 including the remarkable buildings, cemeteries, airfields, sport grounds; railways stations, triage areas; activity areas (administrative, culture and leisure, education, water management, industrial or commercial, health, sports and transport) and national parks that are shown in red, the water surfaces represented in blue, the close forests areas (wood land, closed coniferous forest, closed deciduous forest, mixed closed forest and tree area) in dark green and the open forest, hedge, woody heath, peupleraie, orchard, vine in light green in the figure.

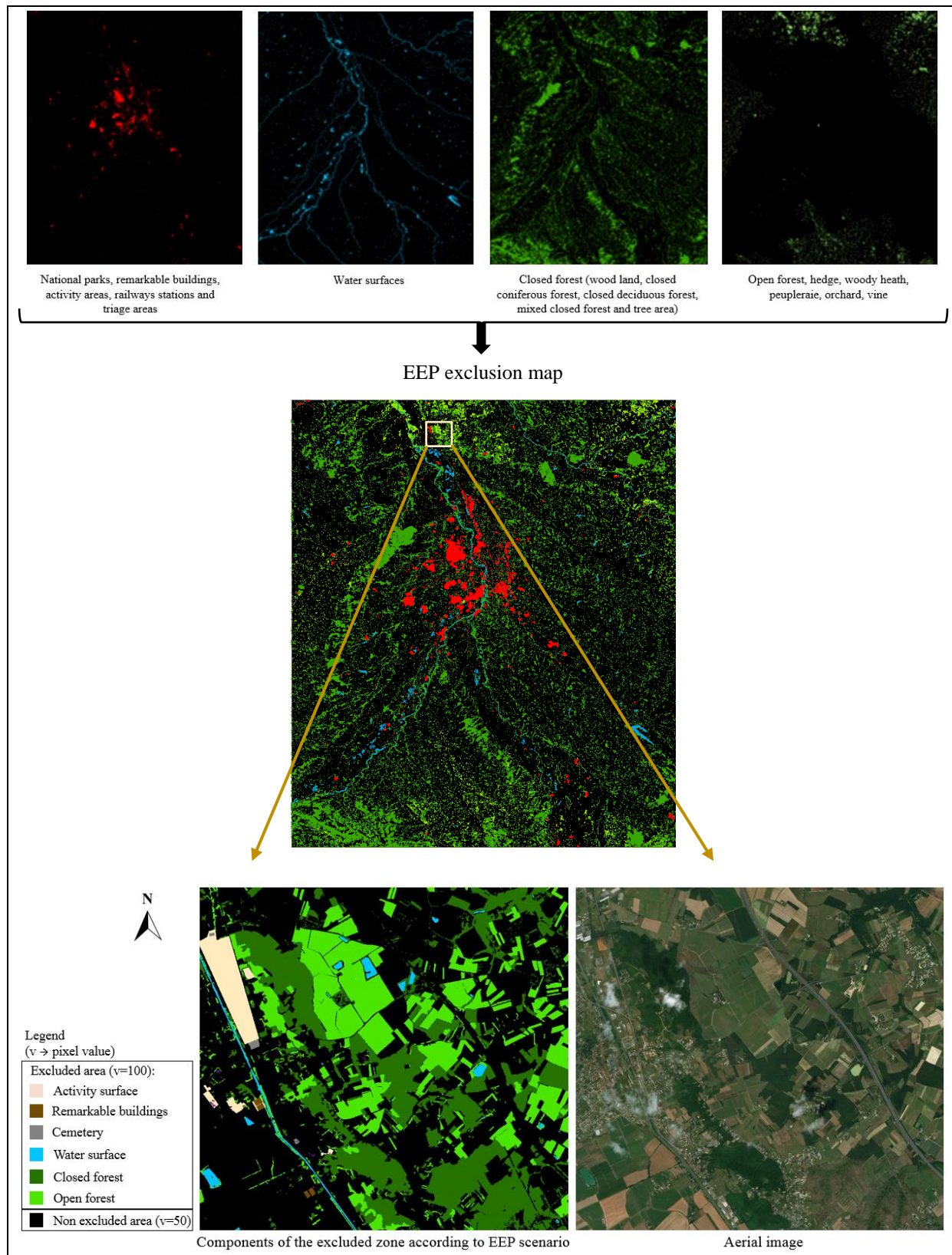


Figure 3. 9. EEP exclusion map generated for Toulouse, 2017. In all excluded maps, the common areas between urbanized and excluded areas are considered as urbanized areas.

3.2.2.5. Attraction-based Scenario Protection Level 1 (Attraction-based Limited Environmental Protection - ALEP)

The Attraction-based Limited Environmental Protection (ALEP) scenario can automatically consider a tendency for the growth area to be occurred in the desired places. In this scenario, we imagine that a city center is more attractive for the inhabitants. We defined four concentric zones with different attraction rates, which make more attraction to the center of the city and less in periphery. The water surfaces and railway stations are also considered as attraction areas for dwelling. As previously mentioned, in the excluded/attraction maps, the pixels with the values less than 50 could make the attraction. The excluded input map of this scenario, is combination of four different layers:

1. The layer of concentric zones of attraction has four zones of attraction with radius of 7.5, 15, 22.5 and 30 km from the center of the city. The corresponding values of the zones are 10, 20, 30 and 40 from the center of the city and the others are 50. The first radius is defined in such a way that it can cover the dense part of the city from the center. The radiuses are defined based on the observation of the density and the agglomeration of the buildings and being homogeneous. The concentric zones of attraction are created from global view of the study area, however we can make them locally for each small agglomeration around the center as well.
2. [Zhuang and Zhao \(2014\)](#), have done a research on effects of land and building usage on population, land price and passengers in station areas. They have made their research on the annual data on land and buildings usage within a radius of 0 to 400 meters for railway stations and 400m to 800m for subway stations. In general, the areas that are located in these distances have priority development.
In this research, we have considered the distance less than 400m (i.e. ~364 meters) for the attraction area according to the resolution of the maps and the urban situation. The areas with the attraction of the railway stations have the values 5, 15, 25, 35, 45 with respect to the concentric zones of attraction. They are areas with distances of seven pixels (~ 364m) around railways stations, which is about 7 to 10 minutes of walking from a railway station.
3. The areas with the attraction of the water surface have the values 5, 15, 25, 35, 45 with respect to the concentric zones of attraction. They are areas with distances of seven pixels (~ 364m) around water surfaces, which is about 7 to 10 minutes of walking from water surfaces.
4. The last layer is the exclusion zone, that here the excluded map LEP is used.

The EEP exclusion map generating procedure is illustrated in figure 3.10. In this figure, "v" represents the pixel value and "r" the radius of a concentric zone.

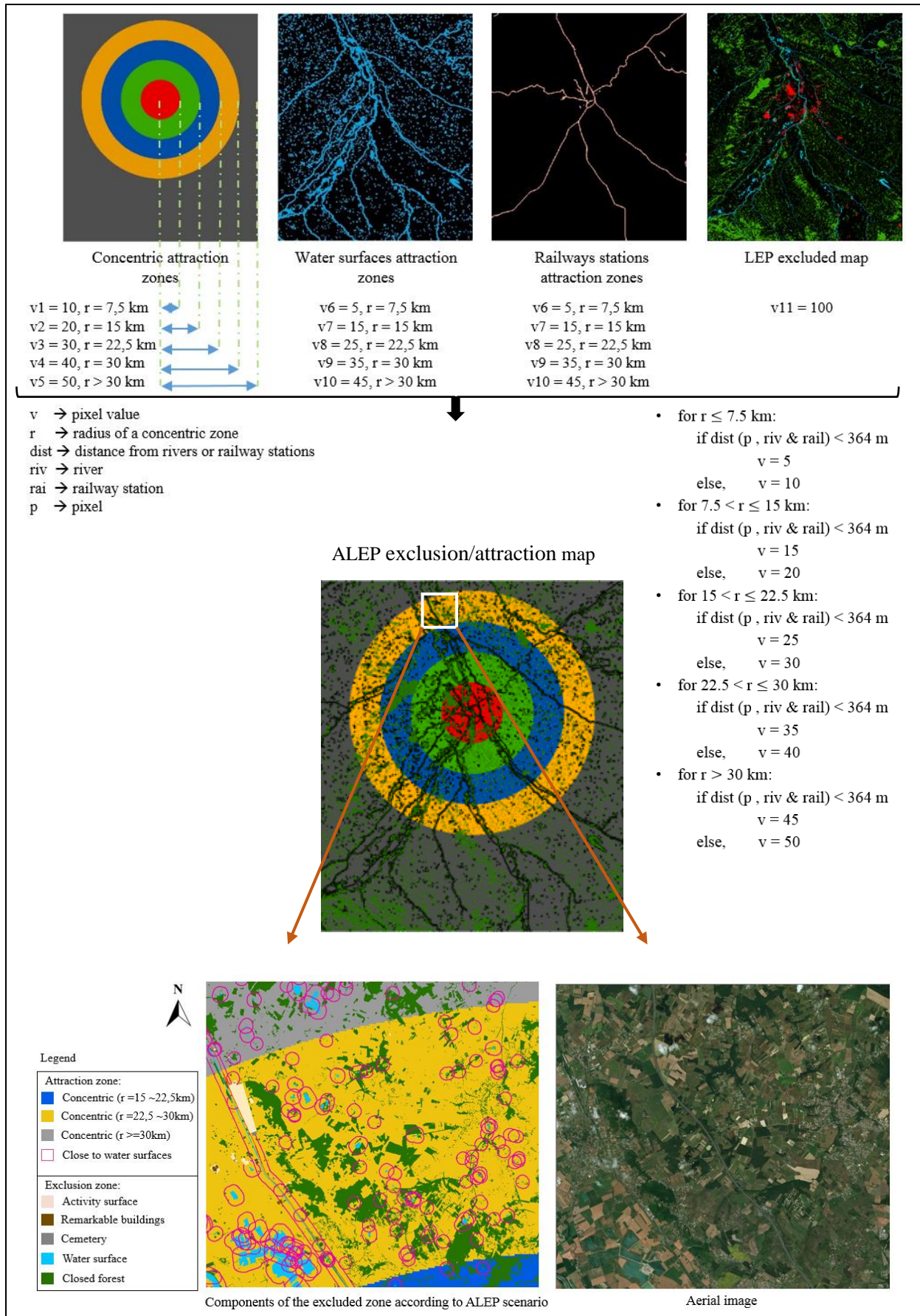


Figure 3. 10. ALEP exclusion/attraction map generated for Toulouse, 2017. In all excluded maps, the common areas between urbanized and excluded areas are considered as urbanized areas.

3.2.3. 2D Urban Growth Simulations - Toulouse

The simulation is based on the growth rules i.e. spontaneous growth, new spreading centers, edge growth and road-influenced growth. In SLEUTH model, five coefficients of dispersion, breed, spread, slope and road gravity, are affected on how the growth rules are applied. These coefficients are calculated by calibration process on historical maps. Each scenario is calibrated independently with its own excluded/attraction input map. The objective in calibration process is to calibrate each scenario from the past in order to obtain the new urban zone such as present.

As mentioned in chapter two, in SLEUTH-3r, the dispersion coefficient multiplier is no longer a constant, which allows the user to modify this multiplier value interactively. Table 3.3 illustrates the dispersion coefficient multiplier obtained for Toulouse study area. The dispersion coefficient multiplier is calculated for each environmental scenario separately using the historical urban and transportation maps of 2000, 2008, 2012 and 2017 as the input maps of the SLEUTH model in coarse calibration mode. Section 1 of Annex C, represents the process of finding the dispersion coefficient multiplier.

Table 3. 3. Dispersion coefficient (D_M) multiplier per environmental protection scenario, Toulouse.

Scenarios	Dm_multi
Scenario protection level 0 (NEP)	0,003
Scenario protection level 1 (LEP)	0,004
Scenario protection level 2 (MEP)	0,004
Scenario protection level 3 (EEP)	0,004
Attraction-based scenario protection level 1 (ALEP)	0,0035

The SLEUTH model includes three processes of calibration, forecasting and self-modification. In calibration process, the user initializes a value for each coefficient. To find the best-fit coefficient values, the process of SLEUTH coarse calibrations performs Monte Carlo number of times through the historical data using the brute force method. The urban and transportation maps that are used in calibration mode consist the maps of 2000, 2008, 2012 and 2017. Different Monte Carlo iteration was tested in this search. However, twenty five Monte Carlo iteration is found sufficient to quantify the spatial variability resulting from random processes.

The historical maps that are used in coarse calibration have the resolution of the data is 1/4 of their full size. In the initial coarse calibration step, the whole range from 1 to 100 for all five coefficients is explored using large increments of 25. These values for each coefficient are 1, 25, 50, 75 and 100. Therefore, the combinations of the 3125 unique parameter are tested. The coarse calibration provides a list of metrics that is sufficient for finding the best-fit coefficients. As discussed in chapter 2, two metrics of the pixel fractional difference (PFD) and the clusters fractional difference (CFD) are used to find the best-fit coefficients. In fact, the accurate fit for these metric ensured that the model could create the urban form and the overall amount of development would be matched (Jantz et al., 2010). Table 3.4 represents the calibration accuracy results which provide the best-fit coefficients for each environmental scenario of

Toulouse study area. The process of computing the best-fit coefficients during the calibration is represented in section 2 of Annex C. The best-fit coefficients values are then used in forecasting process of simulation.

Table 3. 4. Best-fit coefficient values driven from calibration process of SLEUTH-3r, Toulouse

Coefficient values					
Scenarios	Dispersion	Breed	Spread	Slope	Road gravity
Scenario protection level 0 (NEP)	100	25	25	75	100
Scenario protection level 1 (LEP)	100	1	25	25	50
Scenario protection level 2 (MEP)	100	1	25	25	100
Scenario protection level 3 (EEP)	100	1	25	25	1
Attraction-based scenario protection level 1 (ALEP)	100	1	25	100	1

In forecasting process, the model is first run with the input urban map of 2000 to obtain the prospective urban map for 2017. In this case, it is possible to evaluate the accuracy of the model with different scenarios comparing to real urban map of 2017. The critical slope threshold in SLEUTH is often considered between 15% and 21%. In this research, we take the construction slope threshold of 15% to find the more desirable area for urban developing. The simulated urban maps for 2017 are illustrated in figure 3.11, figure 3.12 and figure 3.13.

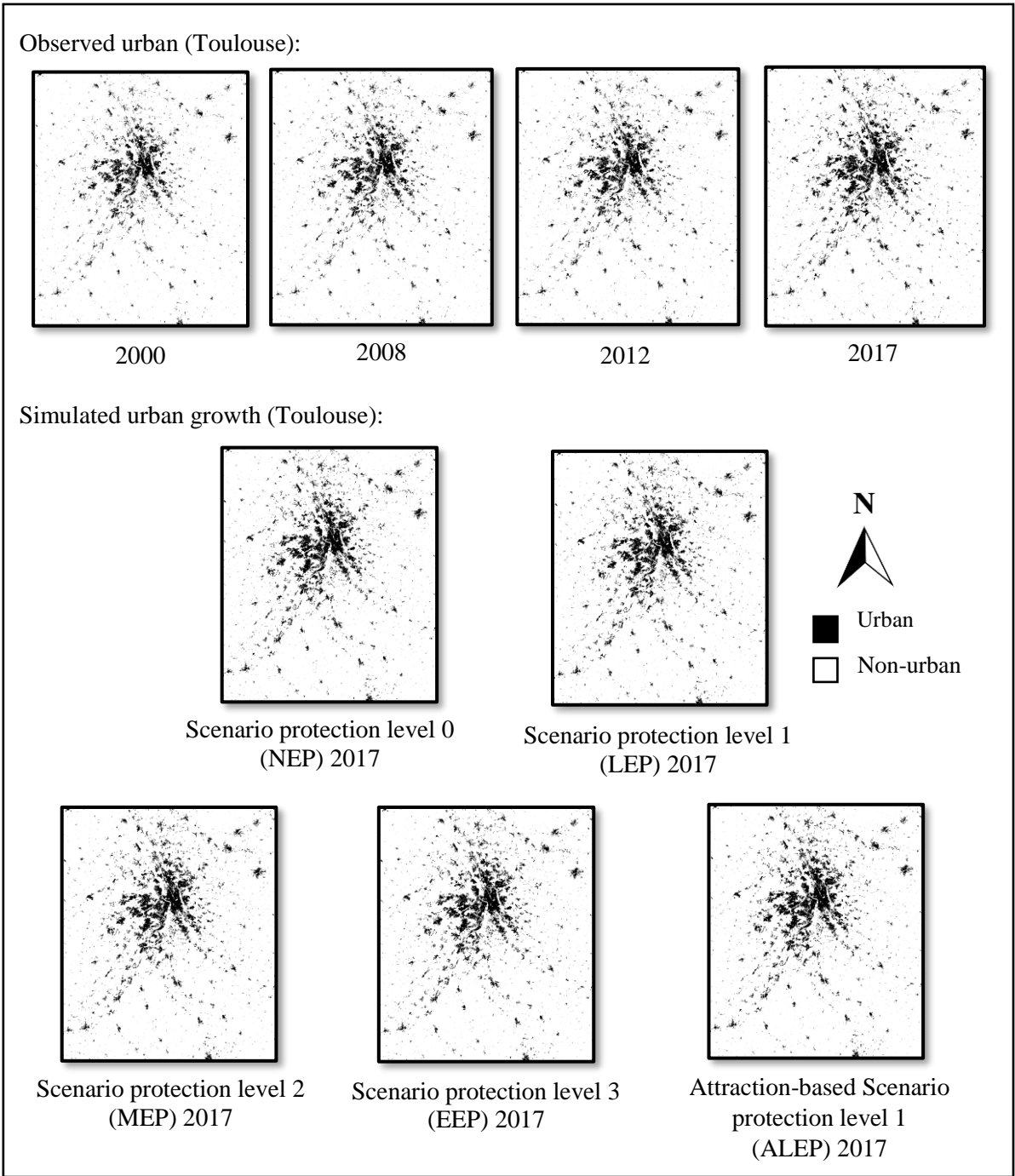


Figure 3. 11. Historical urban maps of 2000 and 2017 and prospective urban maps that are simulated by different environmental protection scenarios for 2017, Toulouse

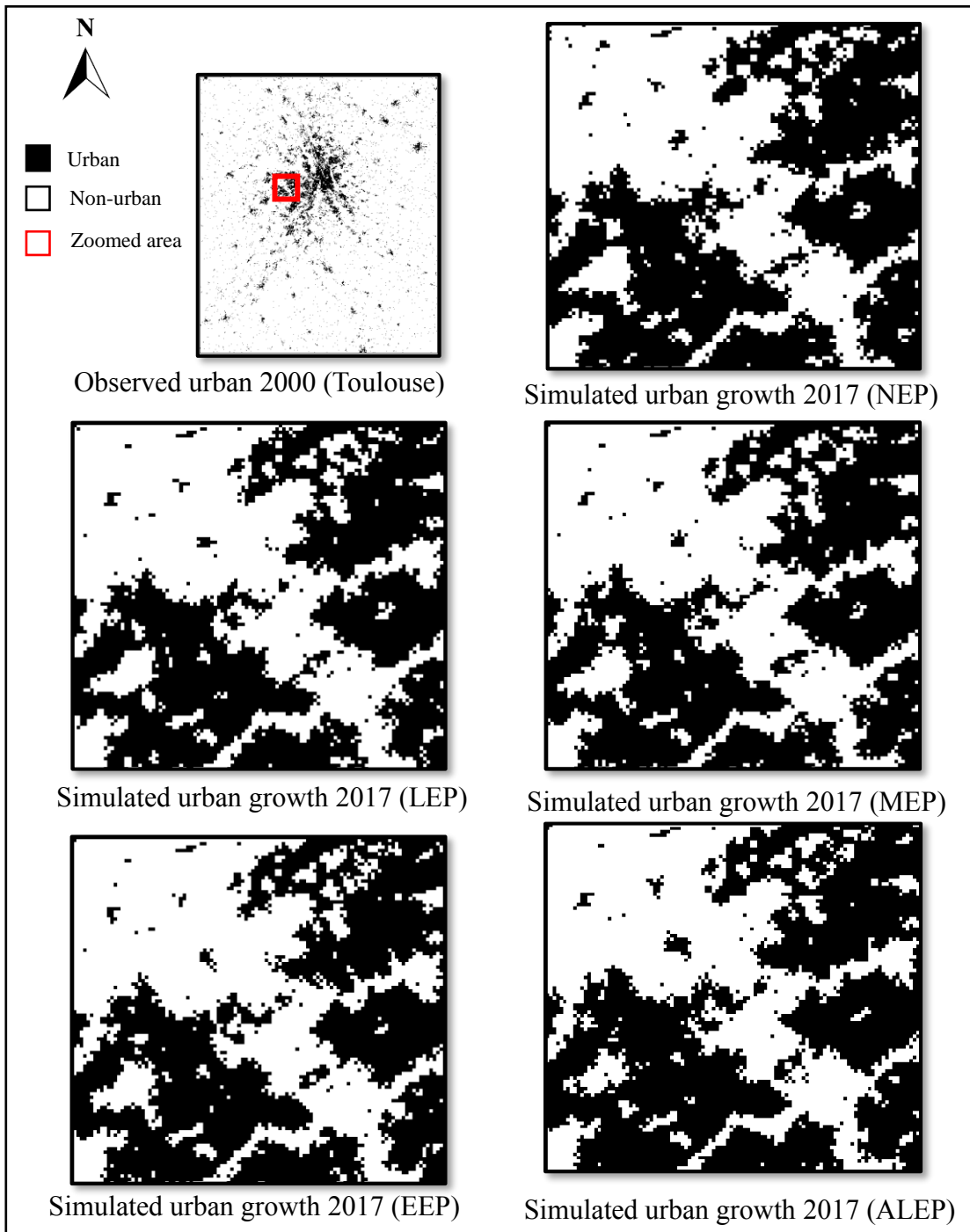


Figure 3. 12. Comparison of urban patches simulated by different environmental protection scenarios, 2017, Toulouse

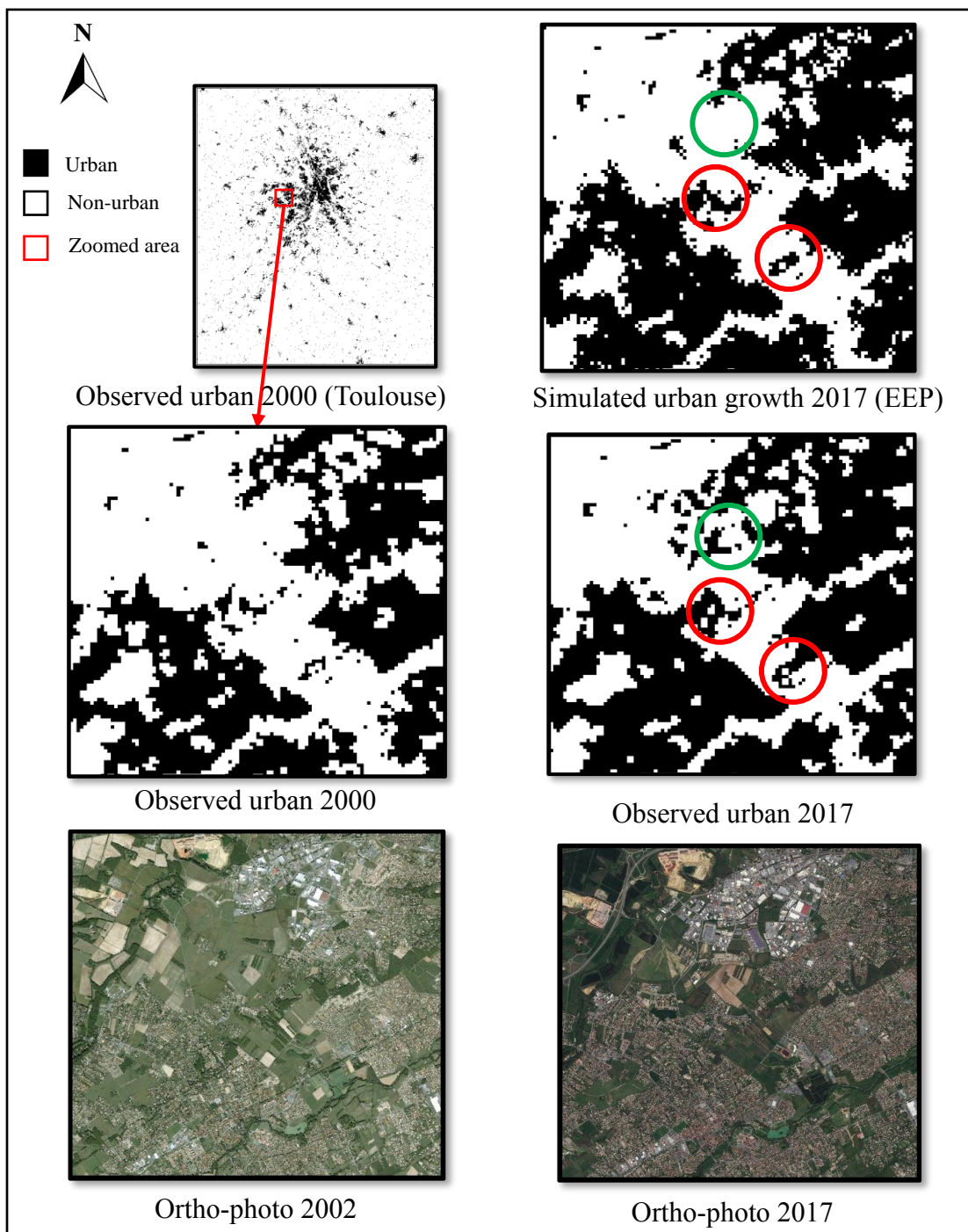


Figure 3. 13. Comparison of the historical urban patch and corresponding prospective patch that is simulated by SLEUTH-3r through environmental protection scenario level 3 (EEP), Toulouse

As illustrated in figure 3.13, a visual comparison of the results shows that SLEUTH could simulate urban growth in some area successfully (Red circles), however in some area the simulation is not well done (green circle). Therefore, we calculate the goodness-of-fit of the simulated maps in order to evaluate the model accuracy.

A brute-force search is used to systematically enumerate all urban pixels to check the goodness-of-fit of urban growth projections. The algorithm compares between the observed, the simulated

change and persistence. The overall accuracy (OA) is calculated to measure the overall proportion of the pixels that change correctly to the total number of cells. Table 3.5, illustrates the results of simulated urban maps for 2017 and compare them to the real urban map of 2000 and 2017.

Table 3. 5. Urban growth simulated results obtained from different environmental protection scenarios and the comparison of the results to the observed map of 2017, Toulouse.

Results - 2017						
Scenarios	Observed urban area in 2000 (pixels)	Increased urban area (pixels)	Urban growth rate (%)	Urban area increased (ha)	Total urban area (ha)	Growth goodness-of-fit (%)
Scenario protection level 0 (NEP)	127881	43918	25,56	11858	46386	81,48
Scenario protection level 1 (LEP)	127881	43689	25,46	11796	46324	82,19
Scenario protection level 2 (MEP)	127881	43521	25,39	11751	46279	82,28
Scenario protection level 3 (EEP)	127881	43179	25,24	11658	46186	82,3
Attraction-based scenario protection level 1 (ALEP)	127881	47940	27,27	12944	47472	83,3
Observed urban area in 2017	171432	43551	25,40	11759	46287	100

As shown, five different results are obtained due to the different scenarios. Comparison of the simulation results of all scenarios shows that the simulated urban areas will be reduced if the environment is more protected. The evaluations demonstrate that the attraction-based scenario protection level 1, has the most rate of goodness-of-fit with the highest growth rate, while the scenario level 2 obtains more precise growth rate comparing to the real urban 2017. Although the growth rate of the scenario level 3 is lower than the actual rate, it is the most accurate of all the scenarios given the growth rate. However, the attraction-based scenario protection level 1, has the possibility of directing the urban sprawl towards the desired attractive areas.

Afterwards, we have prepared the scenario files to produce the forecasting urban growth simulation for 2050. The model is run with the input urban map of 2017 (the real one, not the simulated) to obtain the prospective urban map for 2050 by different scenarios. The simulation results of 2050 are illustrated in figure 3.14 and figure 3.15. Table 3.6 represents the simulated prospective urban growth results for 2050.

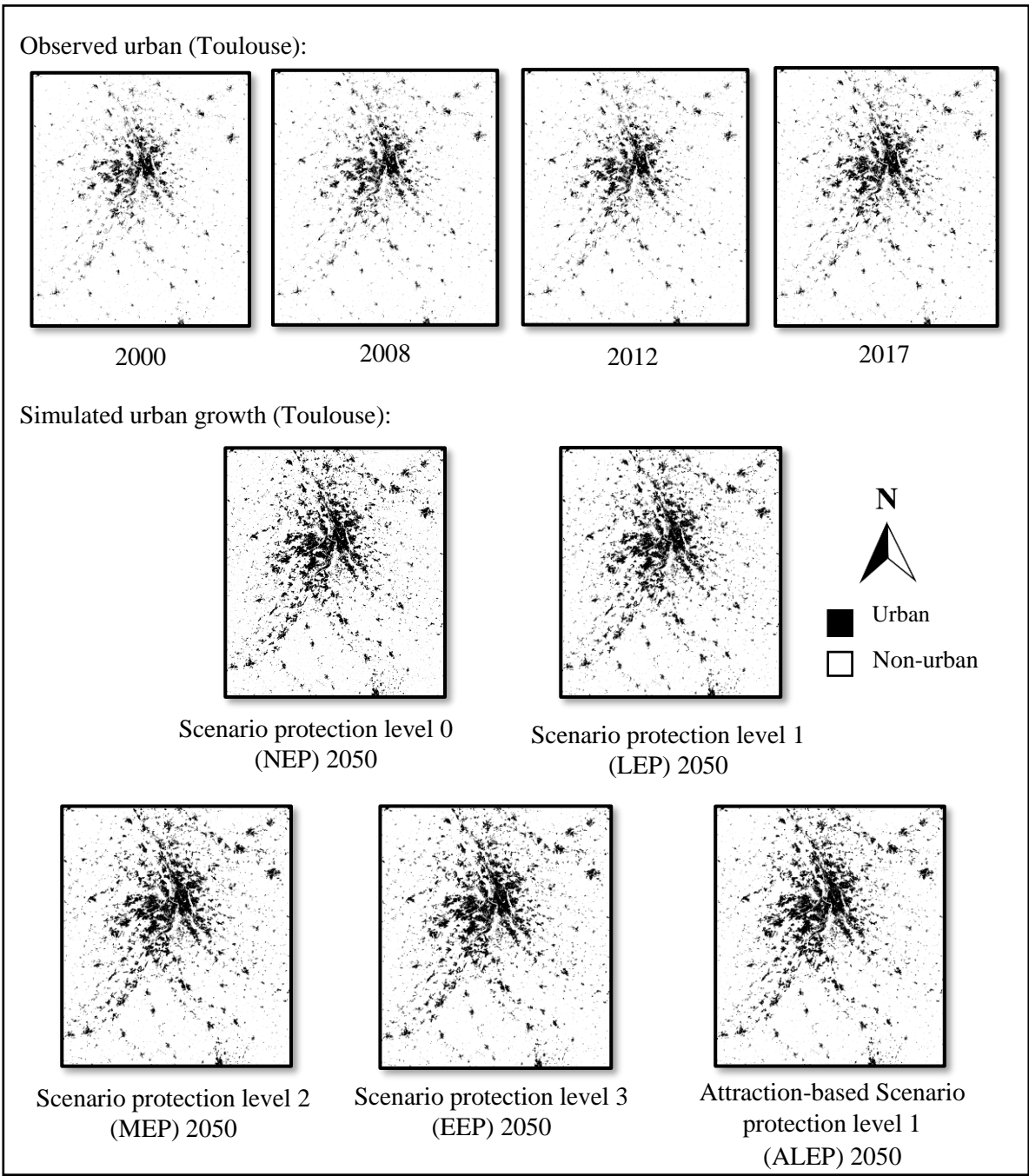


Figure 3. 14. Urban map of 2050 and prospective urban maps for 2050, Toulouse

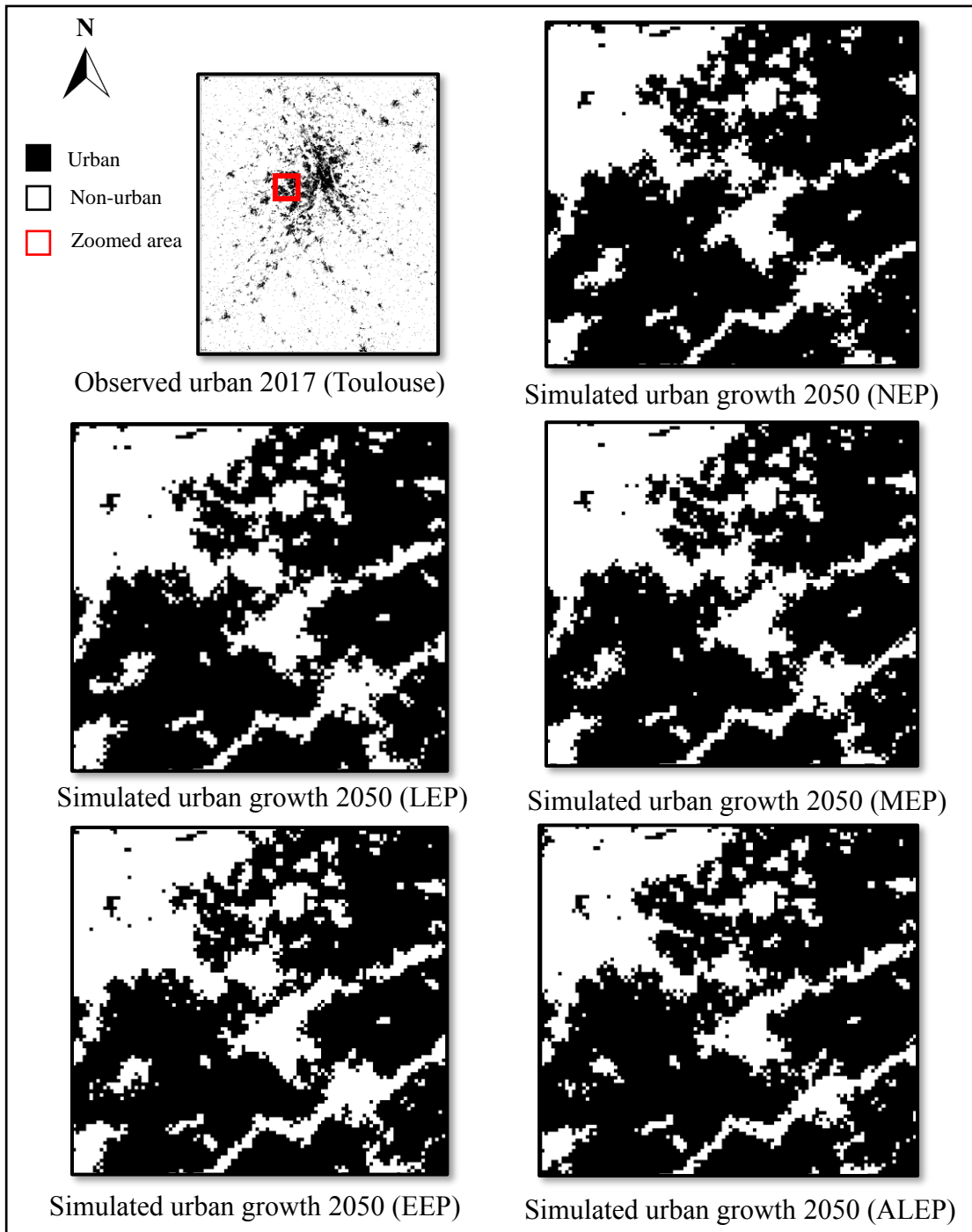


Figure 3. 15. Comparison of urban patches simulated by different environmental protection scenarios, 2050, Toulouse

Table 3. 6. Urban growth simulated results obtained from different environmental protection scenarios for 2050, Toulouse.

Results - 2050				
Scenarios	Existing Urban Area in 2017 (pixels)	Urban growth rate (%)	Urban area increased (ha)	Total urban area (ha)
Scenario protection level 0 (NEP)	171432	37,89	28238	74525
Scenario protection level 1 (LEP)	171432	36,97	27150	73436
Scenario protection level 2 (MEP)	171432	36,49	26600	72886
Scenario protection level 3 (EEP)	171432	36,35	26432	72719
Attraction-based scenario protection level 1 (ALEP)	171432	37,04	27236	73523

The table 3.6 demonstrates that in urban growth simulation for 2050, the simulated urban areas are reduced in the scenarios that are more environmental protected. Although, in Table 3.5 (urban growth simulation for 2017), the urban growth rate of the attraction-based scenario protection level 1 is higher than the other scenarios, this growth rate for the simulation of 2050 is slightly decreased and it comes lower than scenario Level 0 (but it's still more than other scenarios). This indicates that for growth cycles from 2000 to 2017, there are more free areas to convert from non-urban pixels to urban pixels, thus, the attraction-based scenario produces more urban pixels. However, in the 2050 simulation, with less urban pixels being produced in attractive areas, less attractive areas remain. In addition, it should be considered that the protected spaces in attraction-based scenario protection level 1 are more than scenario Level 0, which affects the amount of urban pixels produced.

Despite the simulation results illustrated in table 3.5, the future growth will definitely be different due to the population growth, urban planning, land prices and other factors; and might be closer to the other scenarios. As discussed before, the SLEUTH simulation results are some pixels that are difficult to interpret. Even though these simulations are interesting, they are under-defined and stay abstract because there are plenty of ways to fill the new urban areas produced by the simulation model. In order to be able to understand and to use these simulations, we propose to try to see what could mean these new urban areas in terms of building types, what would be its capacity of human settlement and how does it fit with demographic forecasting. Hence, in the next section we propose to use population growth and building type to try to improve the results.

3.2.4. Urban Fabric Scenarios - Toulouse

The form and the configuration of a city is related to its geography and natural environment. The urban expansion is the consequence of the life style and increased population via newborn generation, migration and succession. Urban sprawl could be constrained by the authorities in order to protect the environment and prevent the risk through urban planning. In the following, we try to see the kind of buildings (called the urban fabric) that could fill the simulated urban areas and for each scenario to see the quantity of population could include. However, this is a simplification of reality because not all population increasing are located in this new urban area, but it allows comparing the scenarios.

The SLEUTH model is based on calibrating from the historical data. Therefore, in its forecasting simulation, it simulates the same type of building that are observed today. Accordingly, it is interesting to integrate some effective factors such as demography and building types to the model. In order to improve the SLEUTH results, different urban fabric scenarios are defined by adding buildings type and the estimation of the population growth as urban fabric factors. Each simulation corresponds to policies that are more or less restrictive of spaces considering what these territories can accommodate as a type of building and as a global population. These scenarios lead to different simulations that are related to different land priorities and constraints and make it possible to improve our understanding of an urban sprawl simulation. In order to integrate the demography and building types, the buildings are classified to different residential categories considering their height and configuration to study the Human Settlement Capacity (HSC).

As mentioned in chapter 2, in our research, new method of land use planning is presented. This urban land use pattern can be applied for different study area. Having the existence urban area and the growth area, we propose to create new building patterns in the growth area. To create these patterns, we first need to use a building type classification.

3.2.4.1. Building Type Classification

The building classification of Toulouse is done considering the land use planning and the urban fabrics of the city and according to the classification that is defined in chapter 2 (section 2.4.1).

To classify the structural elements of our study area, the information of two kinds of buildings are considered, including undifferentiated and industrial buildings. This information derived from BD TOPO of IGN database. In undifferentiated buildings, for each types of urban objects, the numbers and the height of the buildings are extracted and an average height for each type is calculated. The industrial buildings are classified to commercial buildings, industrial buildings, agricultural buildings, greenhouses and silos. For each class an average value of height is calculated. The green houses and silos are ignored from industrial fields of classification because of their low effects on urban planning. Table 3.7 and table 3.8 represent the classification of the current situation of the Toulouse industrial and undifferentiated buildings, respectively. We can see single dwellings and low-rise housings are occupied a large

area of Toulouse. All other types of building are around 5% of total build areas (see figure 3.16).

Table 3. 7. Number, area and height of undifferentiated buildings according to our building classification, Toulouse

Building class	Number of buildings	Total Area		Average height (m)
		m ²	%	
Single dwellings	225 969	34 628 683	47,80%	4
Low-rise housing	183 221	33 844 432	46,71%	8
Shop top housing	5 352	2 432 630	3,36%	15
Medium-rise housing	2 223	1 195 725	1,65%	20
Medium/high-rise housing	208	148 571	0,21%	27
High-rise housing	307	201 323	0,28%	36

Table 3. 8. Number, area and height of industrial buildings, Toulouse

Building class	Number of buildings	Total Area		Average height (m)
		m ²	%	
Industrial	23 061	15497619	80,19%	9
Commercial	970	1 916 498	9,92%	8
Agricultural	1 486	828 934	4,29%	7
Greenhouse	1 197	985 696	5,10%	5
Silo	378	96 859	0,50%	14

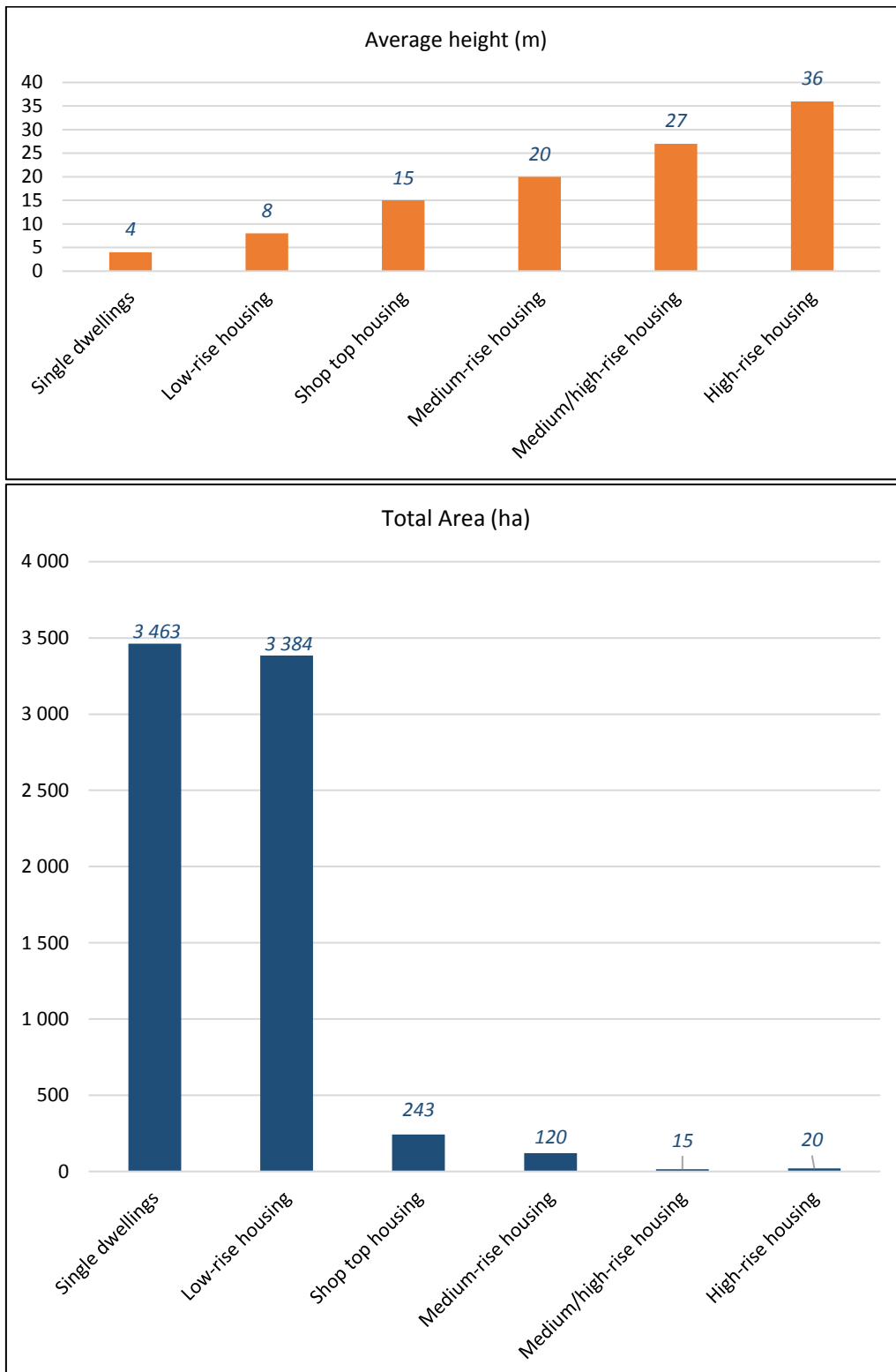


Figure 3. 16. Illustration of the average heights and the average surfaces of undifferentiated buildings classified according to building types, Toulouse

3.2.4.2. Creating Building Type Matrix and Urban Weighting the Patches

After classifying the current building according to building type classification, we calculate the probability that each new pixel will belong to the building classes. Therefore, we use the building type matrix for this study area. The different urban classes of 2017 classified by buildings types and height are collected and a multi-layer matrix consists of different class is created in which, each layer corresponds to one type of building with specific height.

The difference of the simulated urban growth and real urban map of 2017 (results obtained in section 3.2.3) give the forecasted grown area, during the desired growth cycle. The urban patches in the grown area represent the new pixels created during the simulation process. Therefore, these pixels have no information of urban fabric configuration and should be classified. To classify the new urban pixels, first we have to find out what is the likely type of building in each new pixel. In the proposed pattern, the probability of building type for each pixel is calculated considering the likeness to the neighbors. The algorithm is not based on neighborhood likeness, but we use this probability in creating the combination of the buildings in the urban fabric scenarios. The first step to calculate the likelihood is to check the first loop of neighbors around a new urban pixel in the created matrix. If all the pixels were null in the first loop of neighbors, the survey will go to the second and third loops of neighbors. Afterwards, it is the time to calculate the likelihood of each class for each pixel. The used equation and procedure is explained in Chapter 2 (section 2.4.1.3). Later, having the demography the number of people in correspond pixels will calculated.

3.2.4.3. Demography and Population Management

As discussed before, the SLEUTH simulation results are definitely needed to be evaluate by the population density. In this section, we rate the suitable growth cycle to achieve the desired urban fabrics according to the building classes, the simulated urban growth and the mean population.

To interpolate population, first we estimate the compound annual population rate as explained in chapter 2 (section 2.4.2.2). The average population growth rate estimated during 1999 and 2011 is around 1.34% per year. This growth rate is used to estimate the forecasting population growth.

Afterwards, having the population count and compound annual population rate, we estimate the intermediate population for the coming years. The compound annual growth rate of the population is calculated for simulated urban growth of 2050 means in 33 growth cycles starting in 2017. This estimated rate, gives 55% of the population increased, given the number of the actual population of 1.35 million inhabitants in 2017.

To create urban fabric scenarios, you need to know how many buildings are needed to accommodate the projected population. Therefore, we calculate the number of inhabitant for each type of buildings in 2011 (the available data from INSEE, see section 3.2.1), and the used

space of each inhabitant. We assume the similar rate of residential space per person for forecasting date, according to building types.

Our study area is not limited to the city of Toulouse and it covers some small towns and surrounding counties. Thus, we use the data squared from INSEE (see annex E). These data can be used to create a population map for the entire study area. It gives a population map with the squares of 200×200 meters in which, the range of population amount is provided (figure 3.3). We extract this data with the resolution of the other maps (i.e. 52 × 52m) and compare it with the urban maps. For homogeneity between the urban map and the population map, only the population areas that cover the urban map are considered. In other hand, we have the information of the number and type of buildings as well as the estimation of total number of inhabitant. These information help to estimate the number of inhabitants per building. This statistical estimation is not accurate, however, it can give the general information about the link between the numbers of inhabitants and buildings. It is noted that among undifferentiated buildings there are some buildings such as secondary houses, haunted buildings and touristic buildings that no one lives there permanently. These buildings affect the amount of estimated average number of inhabitants. Table 3.9 illustrates the estimation of the number of inhabitant per building type for undifferentiated buildings in Toulouse study area.

Table 3. 9. Estimation of the average number of inhabitant for each type of buildings, Toulouse

Building class	Estimated average number of inhabitants
Single dwellings	3
Low-rise housing	5
Shop top housing	10
Medium-rise housing	21
Medium/high-rise housing	43
High-rise housing	83

3.2.4.4. Implementation, Results and Discussion

Next, we define four different urban fabric scenarios. These primary scenarios are fictive and they do not correspond to reality but they help to better understand how this land could be used and how many inhabitants could live in these new areas. The four scenarios are as follow:

- 1) Sprawl urban: The first scenario considered that all new urban patches filled with single dwellings.
- 2) Medium dense urban: Second scenario, assumed that single dwellings placed in 50% of the new simulated urban areas and others 50% filled by medium rise housing.
- 3) Medium/High dense urban: The third scenario presumed the 30% of single dwellings and other 70% medium rise housing
- 4) High dense urban: The fourth scenario defined to accommodate just medium rise housing.

For each scenario, we assay the simulated urban growth results from SLEUTH having the specific population increased. For each pixel, the number of inhabitants is estimated from the building classification of urban land use pattern and the population map driven from INSEE. Table 3.10, illustrates the comparison of all these scenarios. As it shows, we cannot accommodate enough people in the sprawl urban scenario during the 33 growth cycles, while in the high dense scenario, many more people can be placed and therefore less spread. However, we have produced different scenarios with different densities from sprawl to high dense urban but none of those gives the estimated population growth rate of 55% for 33 simulated growth cycles.

Table 3. 10. Comparing the population growth of four different primary urban fabric scenarios, Toulouse

Increased population per urban fabric scenarios in 2050	Sprawl urban fabric scenario		Medium dense urban fabric scenario		Medium/high dense urban fabric scenario		High dense urban fabric scenario	
	100% single dwelling		50% single dwelling & 50% medium rise housing		30% single dwelling & 70% medium rise housing		100% medium rise housing	
Scenario protection level 0 (NEP)	296 328	22%	1 185 312	88%	1 540 906	114%	2 074 296	154%
Scenario protection level 1 (LEP)	279 036	21%	1 116 144	83%	1 450 987	107%	1 953 252	145%
Scenario protection level 2 (MEP)	273 351	20%	1 093 404	81%	1 421 425	105%	1 913 457	142%
Scenario protection level 3 (EEP)	269 130	20%	1 076 520	80%	1 399 476	104%	1 883 910	140%
Attraction-based scenario protection level 1 (ALEP)	288 423	21%	1 153 692	85%	1 499 800	111%	2 018 961	150%

Therefore, we tried to find out which growth cycle would match better the desired urban fabric, and thus we applied other growth cycles. These new scenarios called final urban fabric scenarios. As represented in table 3.11, the 13th, 18th and 23rd growth cycles give the best results for the medium dense, medium/high dense and high dense urban fabric scenarios respectively with the population growth of around 55%. In order to find the urban fabric similar to today's expansion tendency, we define another urban fabric scenario called low dense urban for the 33rd growth cycle. In this scenario, 35% of new simulated urban areas are considered as single dwellings, 40% as low-rise housing and the remaining 25% as medium rise housing. These building class percentages are closer to the existing urban fabric of Toulouse metropolitan. In all scenarios represented in table 3.11, the urban growth environmental

protection level 2 and level 3 taking the best goodness-of-fit and in attraction-based scenario protection level 1 the urban sprawl is more directed to the attractive areas. The SLEUTH results of different urban fabric scenarios (different growth cycles) for NEP (scenario protection level 0) are shown in figure 3.17, as an example to illustrates the visual difference of the urban sprawl.

Table 3. 11. Urban fabric scenarios comparison according to the growth cycle to have similar rate of increased population. The gray column represents the population increasing of low dense urban fabric scenario during 33-growth cycle that is closer to the existing urban fabric, Toulouse

Increased population per urban fabric scenarios in 2050	Sprawl urban fabric scenario		Low dense urban fabric scenario		Medium dense urban fabric scenario		Medium/high dense urban fabric scenario		High dense urban fabric scenario	
	100% single dwelling		35% single dwelling & 40% low-rise & 25% medium rise housing		50% single dwelling & 50% medium rise housing		30% single dwelling & 70% medium rise housing		100% medium rise housing	
	33th growth cycle		33th growth cycle		23th growth cycle		18th growth cycle		13th growth cycle	
Scenario protection level 0 (NEP)	296 328	22%	819 841	61%	804 480	60%	804 648	60%	768 831	57%
Scenario protection level 1 (LEP)	279 036	21%	772 000	57%	769 140	57%	775 429	57%	743 190	55%
Scenario protection level 2 (MEP)	273 351	20%	756 271	56%	752 748	56%	761 389	56%	735 210	54%
Scenario protection level 3 (EEP)	269 130	20%	744 593	55%	744 660	55%	754 042	56%	724 731	54%
Attraction-based scenario protection level 1 (ALEP)	288 423	21%	797 970	59%	804 252	60%	815 786	60%	795 690	59%

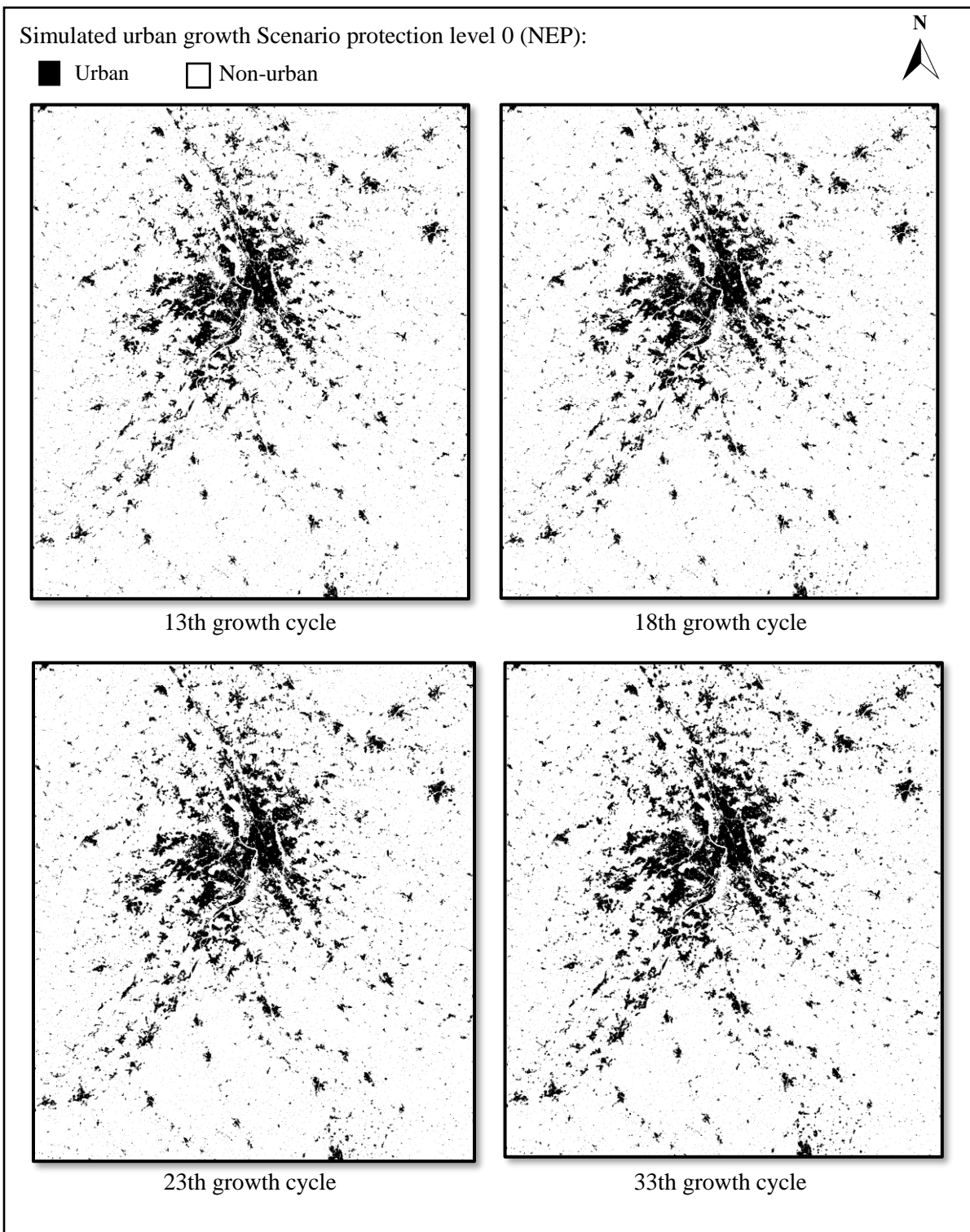


Figure 3. 17. Simulated urban growth that are used in urban fabric scenarios, Toulouse

Figure 3.18, illustrates the urban land use simulated per growth cycle for each prospective urban growth scenarios. In this figure, the grown amounts from the dense city to sprawl city for the same population growth rate is obvious. We kept the 55 % population growth where the land occupations vary from around 100 km² to 280 km² where the differences of them represents the loss of the natural and environmental resources. It shows that changing the urban fabric scenarios has a very strong impact on the limitation of urban sprawl, thus saving agricultural and natural landscapes.

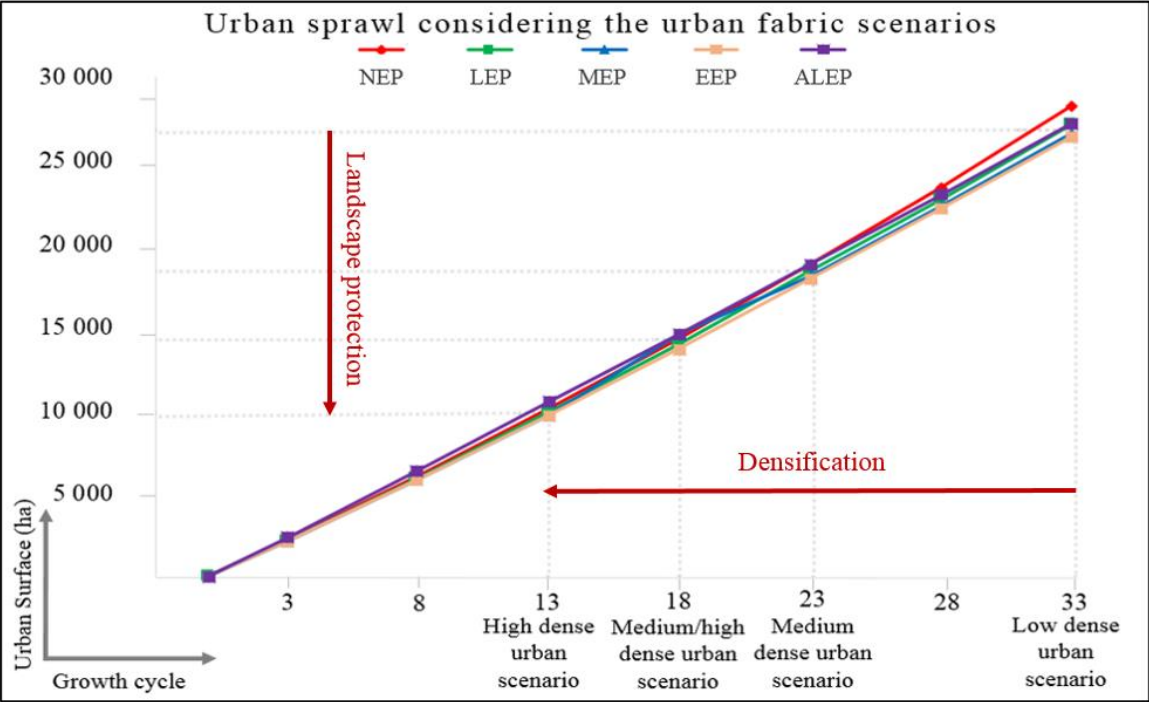


Figure 3. 18. Urban sprawl via the urban fabric scenarios to locate 55% urban population growth, Toulouse

3.3. Developing Different Simulation Scenarios to Illustrate the Impacts of Environmental Constraints, Construction and Population on the Growth of a town - Saint Sulpice la Pointe peri-urban

The second study area is Saint Sulpice la Pointe, a peri-urban that is located in the department of Tarn, in east of Toulouse ($43^{\circ}46'30''$ North, $1^{\circ}41'14''$ East) (see figure 3.19). The extent of the study area is 3600 ha. Saint Sulpice la Pointe had 8934 inhabitants in 2016 and its average population growth rate between 2009 and 2016 was +1.73% per year (Legal populations, INSEE, 2016).

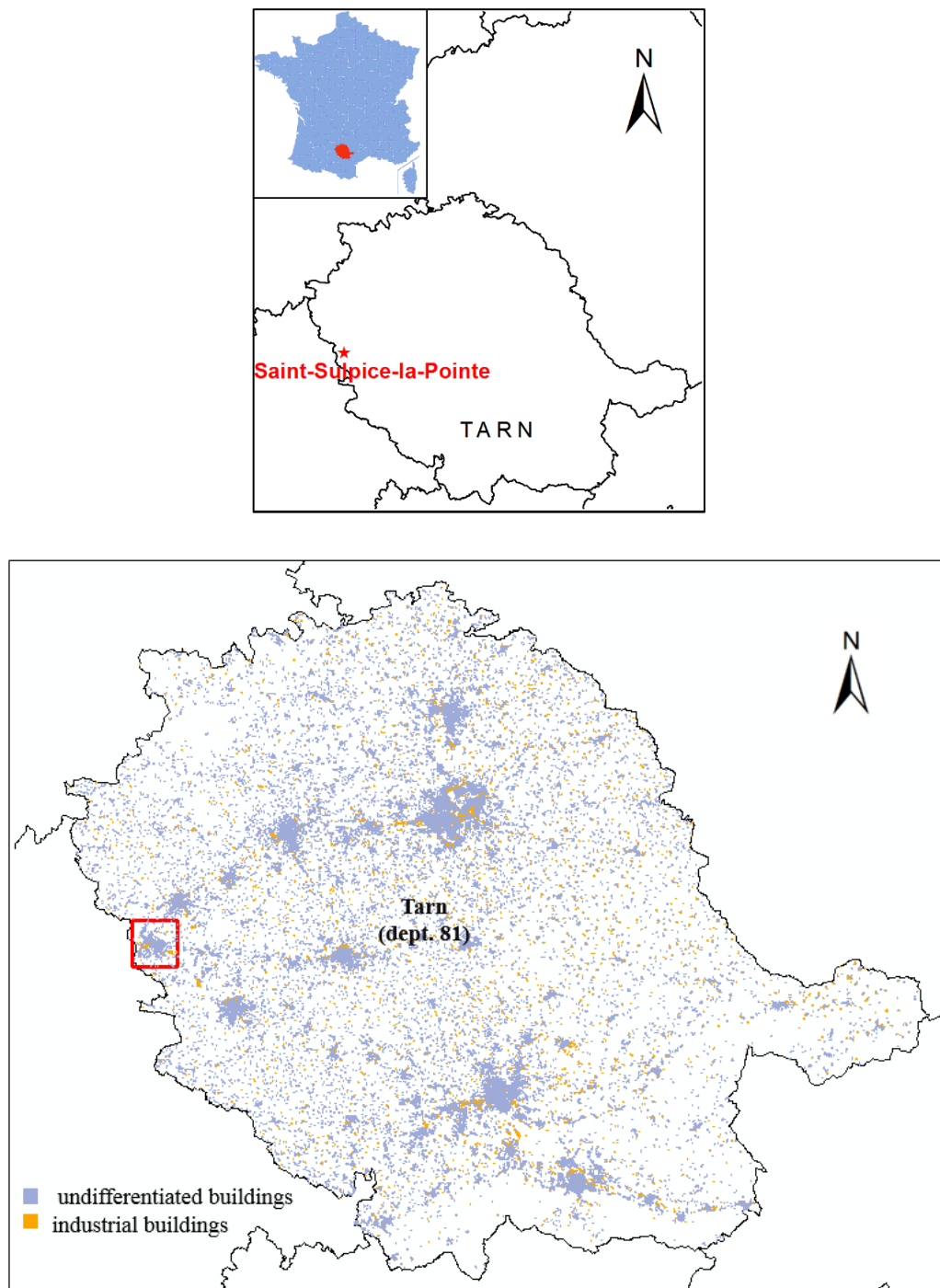


Figure 3. 19. Location and extent of the urban area of Saint Sulpice la Pointe study area

3.3.1. Data and Materials - Saint Sulpice la Pointe

We use SLEUTH for the simulations of this study area like the Toulouse. Geospatial database and geographic information systems are applied to create the input maps. All the input maps have the size of 200×200 pixels that feature a cell size of 30m×30m (~900 m²). Similar to Toulouse, the Geospatial database that is used as input data consists the maps of 2000, 2008, 2012 and 2017 as follow:

- Slope and hillshade maps are derived from Digital Elevation Model (DEM) of RGE ALTI with a spatial resolution of 5m, provided by IGN.
- Urban areas, excluded areas and transportation maps are generated automatically from BD TOPO and BD ORTHO from IGN. Urban map is classified into two classes of urban and nonurban.
- Population and census on district zone are taken from INSEE database of 2011.

Different 2D urban growth prospective scenarios are defined as well and each scenario needs its specific input maps. Two layers of undifferentiated and industrial buildings with more than 3m height and more than 50m² surface from BD TOPO (IGN data base) are used to create the urban maps (see chapter 2). Similar to previous study area, a dilation-erosion (30m) according to the pixel size is applied to fill the spaces between adjacent buildings. The input maps are illustrated in figure 3.20. Different environmental dependent scenarios are defined by altering the excluded maps according to the environmental constraints.

3.3.2. Environmental Constraints Scenarios - Saint Sulpice la Pointe

As discussed before, five different environmental protection scenarios are defined by altering the excluded map including (see sections 2.3.3 chapter 2 and 3.2.2 chapter 3):

- Scenario Protection Level 0 (Nearly No Environmental Protection - NEP) (see figure 3.21)
- Scenario Protection Level 1 (Limited Environmental Protection - LEP) (see figure 3.22)
- Scenario Protection Level 2 (Moderate Environmental Protection - MEP) (see figure 3.23)
- Scenario Protection Level 3 (Extreme Environmental Protection - EEP) (see figure 3.24)
- Attraction-based Scenario Protection Level 1 (Attraction-based Limited Environmental Protection - ALEP) (see figure 3.25)

Each pixel of the excluded maps have a value. In environmental protection scenarios, we generate the pixel values from 0 to 100. Value 100 indicates a pixel that is 100% protected from the possible urban growth and the value of zero shows free zones to build. The value of 50 represents a neutral weight for development. Between 100 and 50 is a relative exclusion whereas under 50 means that there is an attraction (see table 2.3).

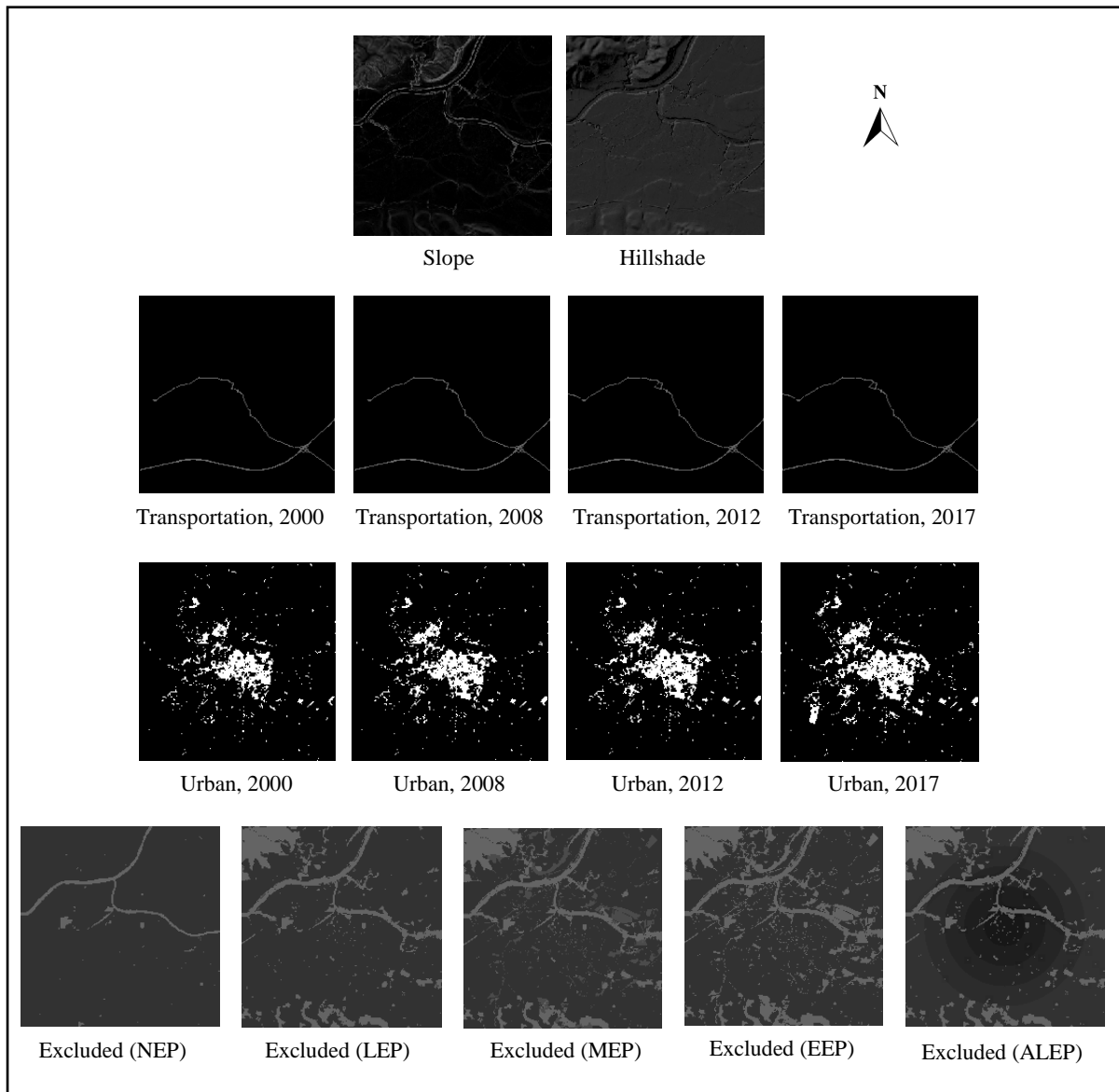


Figure 3. 20. Slope, hillshade, transportation, urban and exclusion maps of Saint Sulpice la Pointe

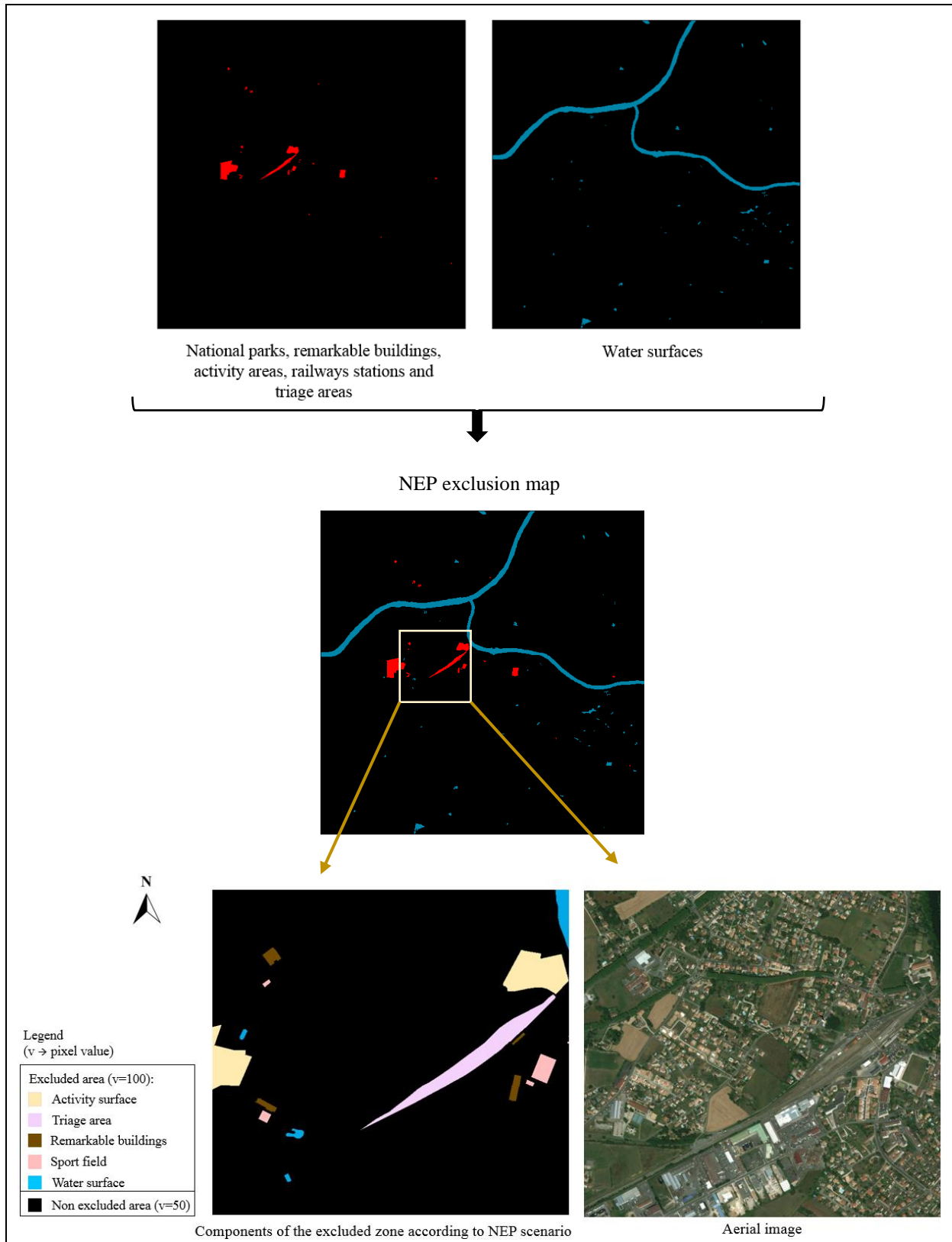


Figure 3. 21. NEP exclusion map generated for Saint Sulpice la Pointe, 2017. The excluded areas include the remarkable buildings, cemeteries, airfields, sport grounds; railways stations, triage areas; activity areas (administrative, culture and leisure, education, water management, industrial or commercial, health, sports and transport) and national parks; that are shown in red and the water surfaces that are represented in blue. They take the value of 100 and the others take the value of 50.

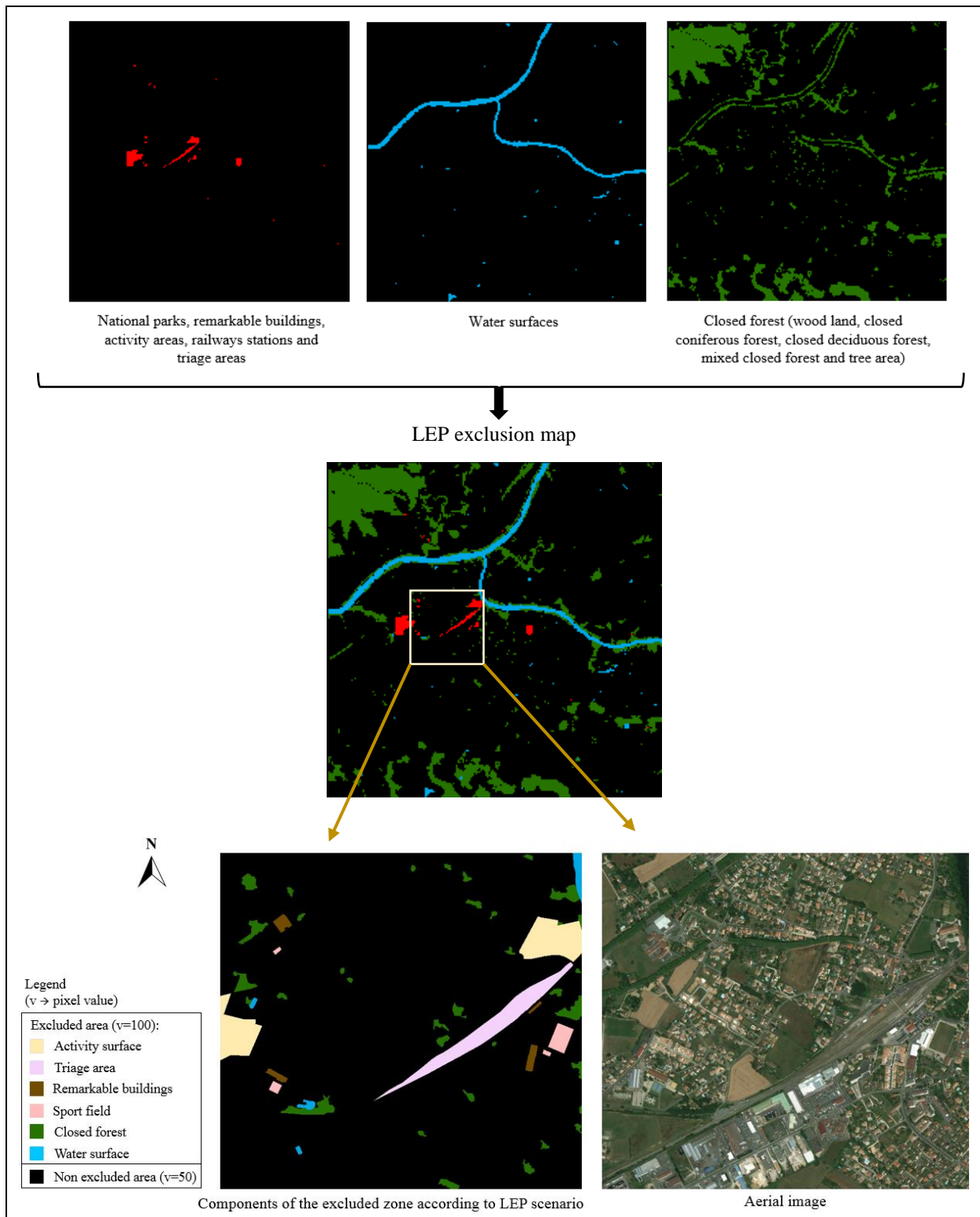


Figure 3. 22. LEP exclusion map generated for Saint Sulpice la Pointe, 2017. The excluded areas indicate the remarkable buildings, cemeteries, airfields, sport grounds; railways stations, triage areas; activity areas (administrative, culture and leisure, education, water management, industrial or commercial, health, sports and transport) and national parks that are shown in red, the water surfaces represented in blue and the closed forests areas (wood land, closed coniferous forest, closed deciduous forest, mixed closed forest and tree area) in dark green. They take the value of 100 and the others take the value of 50.

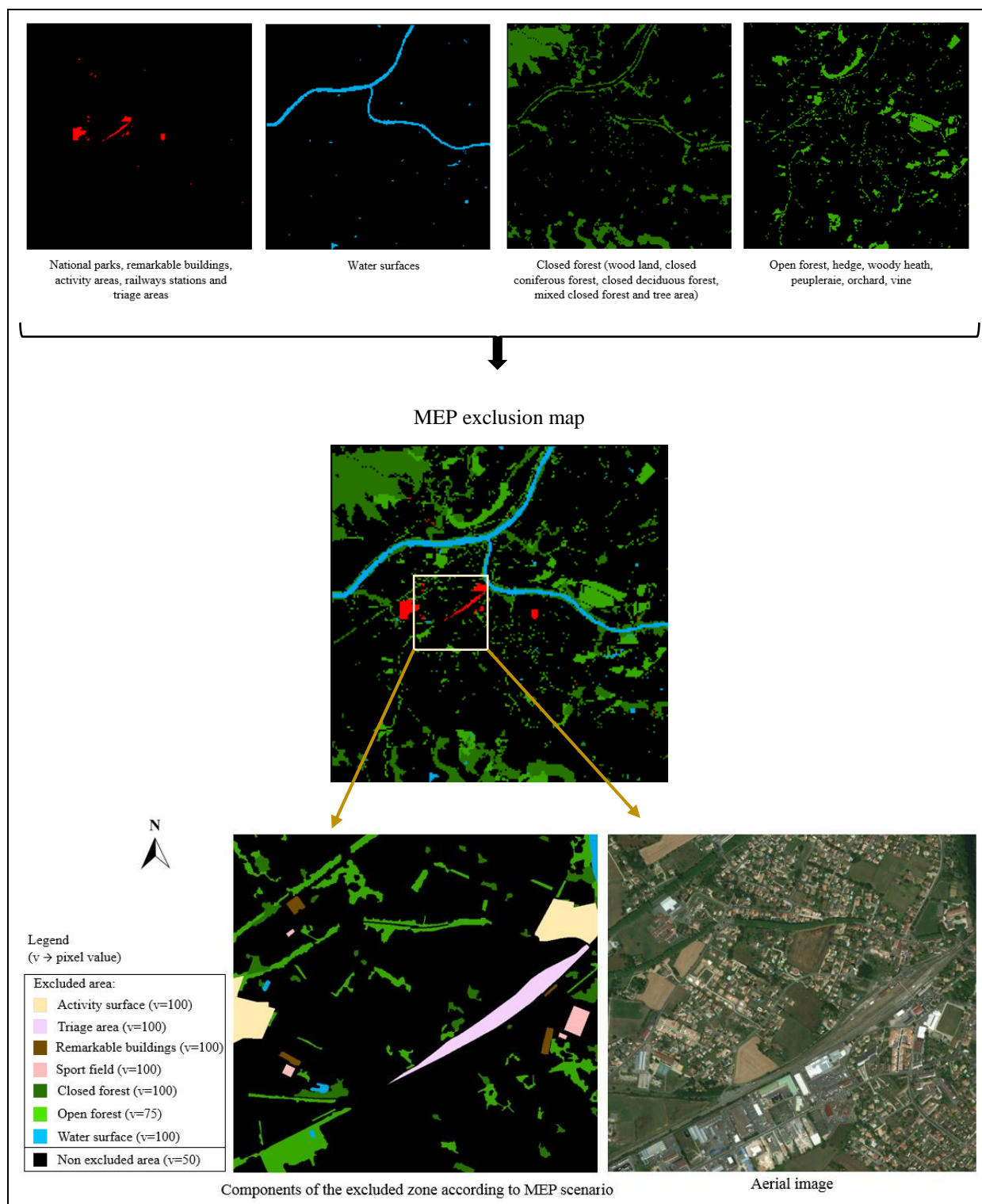


Figure 3. 23. MEP exclusion map generated for Saint Sulpice la Pointe, 2017. The excluded map contains all parks, protected areas and water bodies have made from the database of the IGN for 2017 including the remarkable buildings, cemeteries, airfields, sport grounds; railways stations, triage areas; activity areas (administrative, culture and leisure, education, water management, industrial or commercial, health, sports and transport) and national parks that are shown in red, the water surfaces represented in blue, the close forest areas (wood land, closed coniferous forest, closed deciduous forest, mixed closed forest and tree area) in dark green (value 100) and the open forest, hedge, woody heath, peupleraie, orchard, vine in light green (value 75).

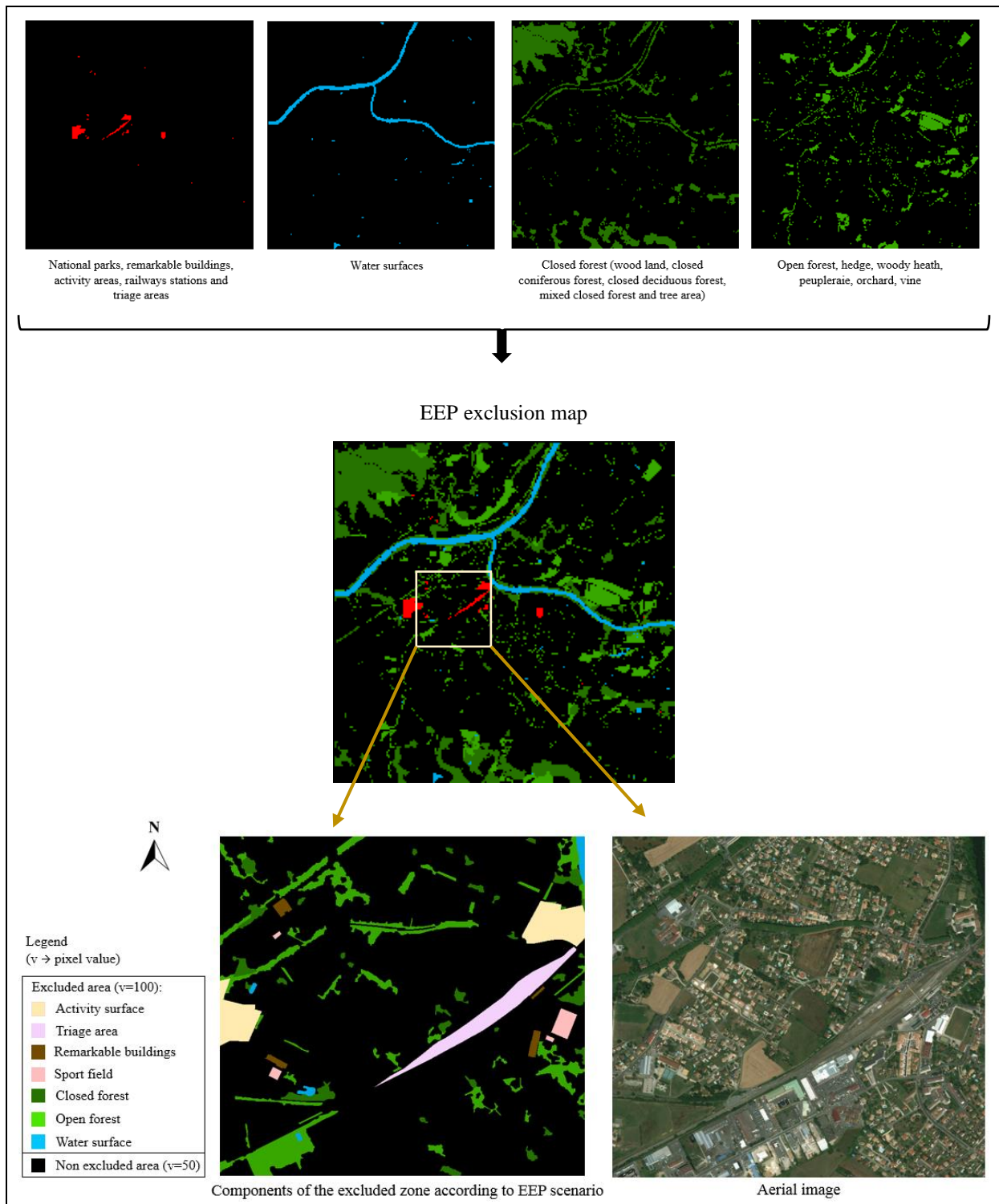


Figure 3. 24. EEP exclusion map generated for Saint Sulpice la Pointe, 2017. The excluded map contains the remarkable buildings, cemeteries, airfields, sport grounds; railways stations, triage areas; activity areas (administrative, culture and leisure, education, water management, industrial or commercial, health, sports and transport) and national parks that are shown in red, the water surfaces represented in blue, the close forest areas (wood land, closed coniferous forest, closed deciduous forest, mixed closed forest and tree area) in dark green and the open forest, hedge, woody heath, peupleraie, orchard, vine in light green. All excluded areas take the value of 100 and the others take the value of 50.

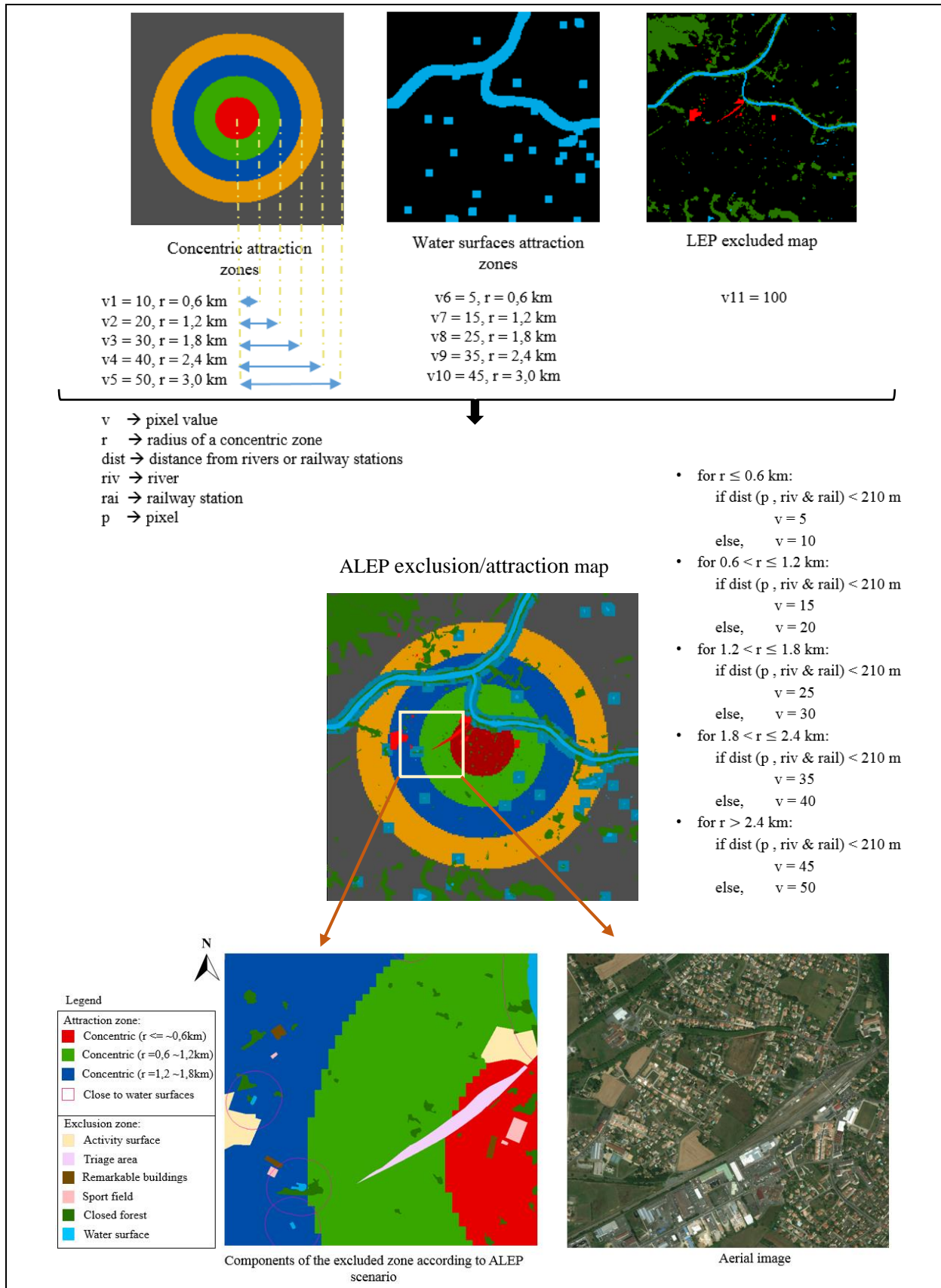


Figure 3. 25. ALEP exclusion/attraction map generated for Saint Sulpice la Pointe, 2017. Four concentric zones with different attraction rates, make attraction force to the center. The areas in distances of seven pixels (~ 210m) around water surfaces are considered as attraction areas for dwelling as well. The LEP exclusion map is used for the excluded areas.

3.3.3. 2D Urban Growth Simulations - Saint Sulpice la Pointe

Table 3.12 represents the dispersion coefficients and table 3.13 illustrates the best-fit coefficients that are obtained for Saint Sulpice la Pointe. Annex C, represents the process of computing the dispersion coefficient multiplier and the calibration.

Table 3. 12. Dispersion coefficient (D_M) multiplier per environmental protection scenario, Saint Sulpice la Pointe

Scenarios	Dm_multi
Scenario protection level 0 (NEP)	0,0006
Scenario protection level 1 (LEP)	0,0006
Scenario protection level 2 (MEP)	0,0006
Scenario protection level 3 (EEP)	0,0006
Attraction-based scenario protection level 1 (ALEP)	0,0005

Table 3. 13. Best-fit coefficient values driven from calibration process of SLEUTH-3r, Saint Sulpice la Pointe

Coefficient values					
Scenarios	Dispersion	Breed	Spread	Slope	Road gravity
Scenario protection level 0 (NEP)	100	1	25	75	100
Scenario protection level 1 (LEP)	100	25	25	100	100
Scenario protection level 2 (MEP)	100	1	25	75	1
Scenario protection level 3 (EEP)	100	25	25	100	1
Attraction-based scenario protection level 1 (ALEP)	100	1	25	100	1

In forecasting process, the model is first run with the input urban map of 2000 to obtain the prospective urban map for 2017 in order to evaluate the accuracy of the model with different scenarios comparing to real urban map of 2017. The construction slope threshold of 15% is considered as critical slope (see section 3.2.3).

These scenarios lead to obtain five different results. The simulated urban maps for 2017 are illustrated in figures 3.26. The comparison of the results and evaluation to the observed map are presented in table 3.14 (see also figure 3.27).

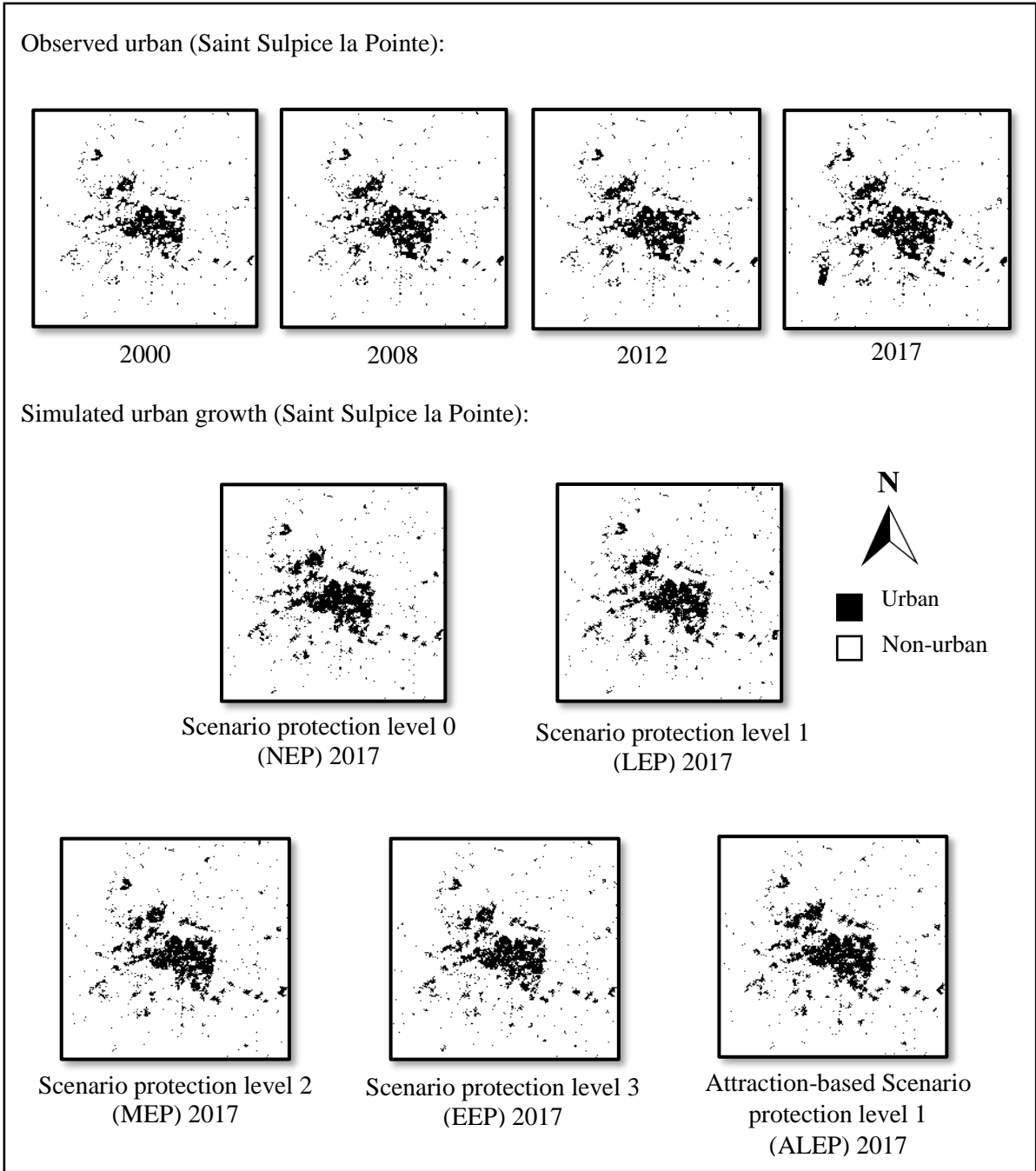


Figure 3. 26. Historical urban maps of 2000 and 2017 and prospective urban maps that are simulated by different environmental protection scenarios for 2017, Saint Sulpice la Pointe

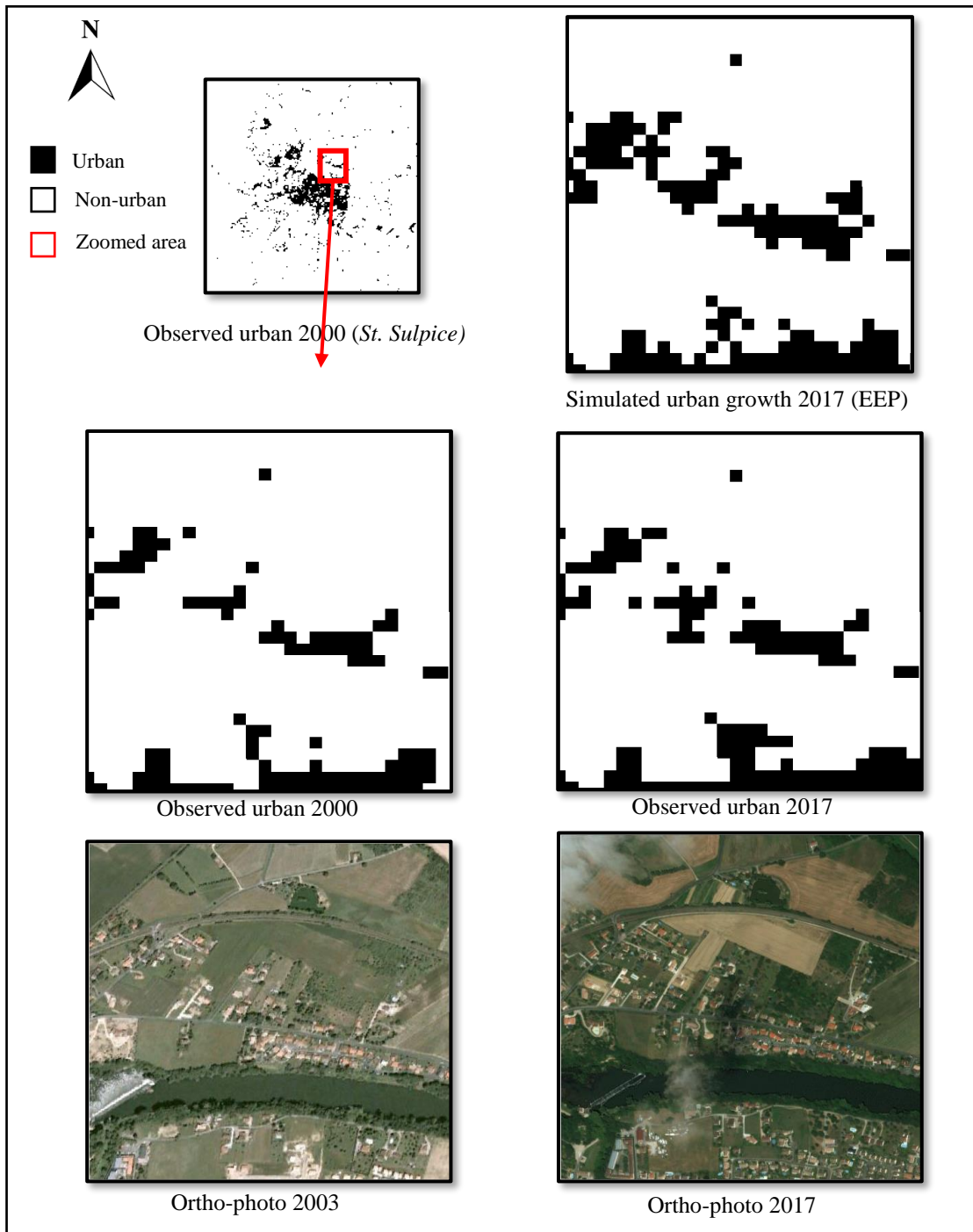


Figure 3. 27. Comparison of the historical urban patch and corresponding prospective patch that is simulated by SLEUTH-3r through environmental protection scenario level 3 (EEP), Saint Sulpice la Pointe

Table 3. 14. Urban growth simulated results obtained from different environmental protection scenarios and the comparison of the results to the observed map of 2017, Saint Sulpice la Pointe

Results - 2017						
Scenarios	Observed urban area in 2000 (pixels)	Increased urban area (pixels)	Urban growth rate (%)	Urban area increased (ha)	Total urban area (ha)	Growth goodness-of-fit (%)
Scenario protection level 0 (NEP)	2304	984	29,93	89	296	75,67
Scenario protection level 1 (LEP)	2304	908	28,27	82	289	77,77
Scenario protection level 2 (MEP)	2304	879	27,62	79	286	78,35
Scenario protection level 3 (EEP)	2304	767	24,98	69	276	80,27
Attraction-based scenario protection level 1 (ALEP)	2304	1147	33,24	103	311	73,98
Observed urban area in 2017	3395	1091	32,14	98	306	100

The results show that by increasing the amount of protected area, the rate of growth is decrease. By comparing the goodness of the fit we can find that the attraction-based scenario produced more urban area and closer to the observed urban area of 2017. The best fit is achieved by scenario protection level 3. This scenario produced less growth rate (24.98%) but with the best goodness-of-fit (80.27%). Therefore, comparing the results are used both to examine the impact of environmental rules in forecasting growth and to obtain more accurate goodness of the fit.

Next, we give the maps apply the model with the input urban map of 2017 (the observed maps) to obtain the prospective maps of 2050. The results of the simulation for 2050 are illustrated in figure 3.28 and the table 3.15 illustrates the simulated prospective urban growth results for 2050.

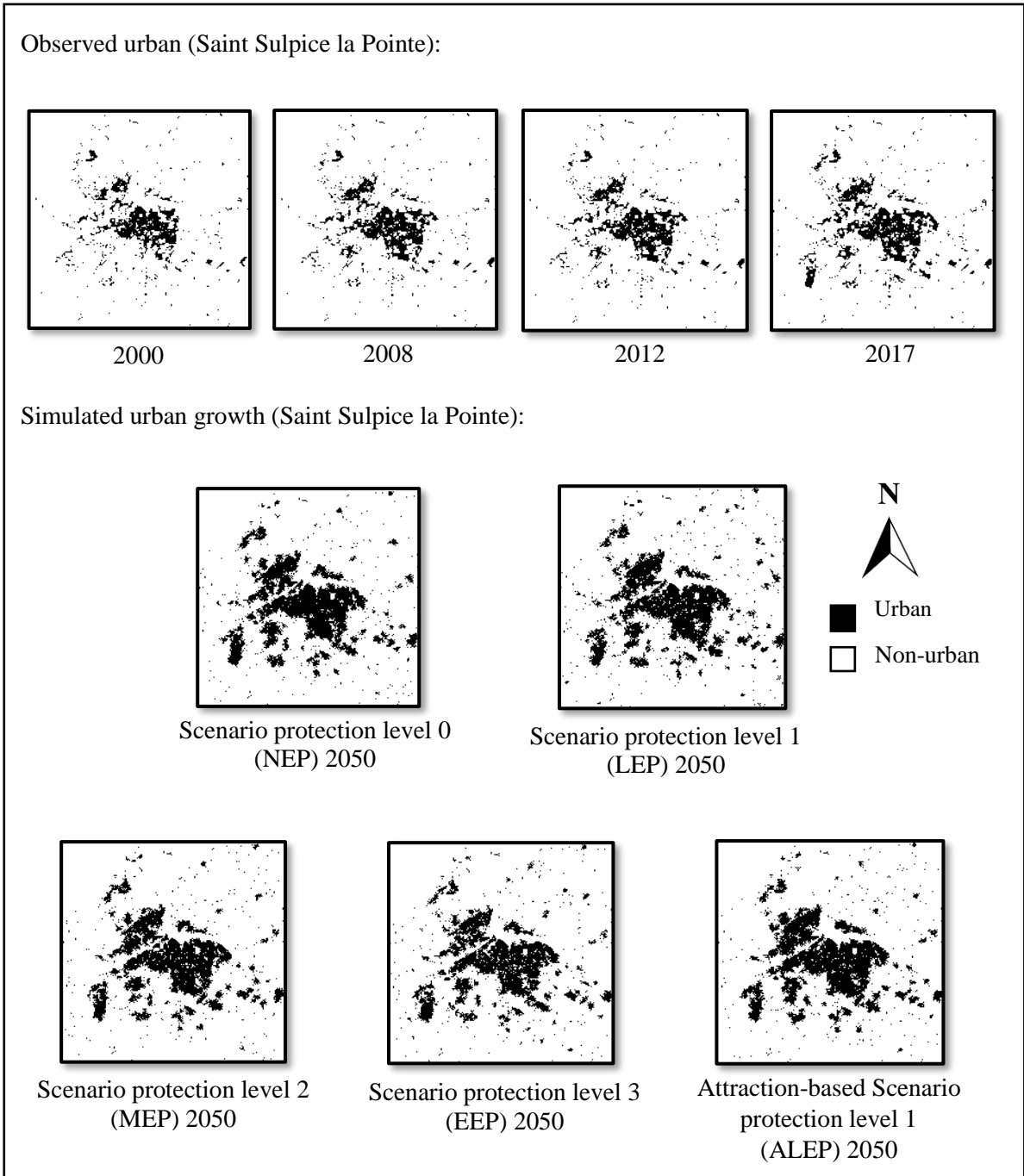


Figure 3. 28. Urban map of 2050 and prospective urban maps for 2050, Saint Sulpice la Pointe

Table 3. 15. Urban growth simulated results obtained from different environmental protection scenarios for 2050, Saint Sulpice la Pointe.

Results - 2050				
Scenarios	Existing Urban Area in 2017 (pixels)	Urban growth rate (%)	Urban area increased (ha)	Total urban area (ha)
Scenario protection level 0 (NEP)	3395	44,05	241	546
Scenario protection level 1 (LEP)	3395	43,41	234	540
Scenario protection level 2 (MEP)	3395	40,82	211	516
Scenario protection level 3 (EEP)	3395	38,34	190	496
Attraction-based scenario protection level 1 (ALEP)	3395	45,23	252	558

Similar to the simulation results of 2017, the simulated urban areas are reduced in the scenarios that are more environmentally protected in 2050. There are always less open nonurban spaces to be developed in 2050 comparing to 2017, thus the growth rate for the simulation of 2050 is slightly decreased in attraction-based scenario. After achieving the results for 2050, it is needed to see what could mean these new urban areas in terms of urban fabric. Therefore, in next section we define the urban fabric scenarios in order to interpret the meaning of the new pixels in term of building types and the capacity of human settlement in these scenarios.

3.3.4. Urban Fabric Scenarios - Saint Sulpice la Pointe

In this section we first classify the current buildings according to defined building types (Chapter 2, section 2.4.1). We use undifferentiated buildings that are derived from BD TOPO of IGN database. Table 3.16 illustrates the number and occupied surfaces of the existing buildings of the Saint Sulpice la Pointe with regard to building type classification. It shows that near to the 69.80% of the current buildings are single dwellings and the low-rise buildings are 29.76%, while the shop top buildings are only 0.44 %. After classifying the current buildings, we create the building type matrix contains the information corresponds to the types of building.

Table 3. 16. Number, area and height of undifferentiated buildings according to our building classification, Saint Sulpice la Pointe.

Building class	Number of buildings	Total Area		Average height (m)
		m ²	%	
Single dwellings	2 782	420 239	69,80%	4
Low-rise housing	1 189	179 156	29,76%	8
Shop top housing	6	2 674	0,44%	15

In 2016, according to INSEE data, 8934 inhabitants were living in Saint Sulpice la Pointe ([Legal populations, INSEE, 2016](#)). The population growth rate that is calculated for this study area is

equal 1.73% per year. Based on this rate the average population growth rate of the population for 2050 shows the increasing of 79% (see Chapter 2, section 2.4.2.2).

Similar to the first study area we estimate the number of inhabitant per building. Table 3.17 illustrates the estimation of the number of inhabitants per building type for undifferentiated buildings in Saint Sulpice la Pointe (see section 3.2.4.3). The estimated averages are based on the total population and the number of existing buildings. This estimation aims to give an idea about the number of individuals per buildings and help to define the link between building types and the population. However, Saint Sulpice la Pointe is also present in the study area, we re-estimate the average number of inhabitant. The estimated average number of inhabitants per building are different to previous study area. The difference is because here we are in local level and the average can be closer to reality.

Table 3. 17. Estimation of the average number of inhabitants for each type of buildings, Saint Sulpice la Pointe.

Building class	Estimated average number of inhabitants
Single dwellings	2
Low-rise housing	3
Shop top housing	6

The process of creating the urban fabric scenarios is similar to Toulouse study area. These scenarios are defined based on the combinations of single dwelling and shop top housing. Table 3.18 represents the comparison of all these scenarios for the primary urban fabric scenarios.

Table 3. 18. Comparing the population growth of four different primary urban fabric scenarios, Saint Sulpice la Pointe.

Increased population per urban fabric scenarios in 2050	Sprawl urban fabric scenario		Medium dense urban fabric scenario		Medium/high dense urban fabric scenario		High dense urban fabric scenario	
	100% single dwelling		50% single dwelling & 50% shop top housing		30% single dwelling & 70% shop top housing		100% shop top housing	
Scenario protection level 0 (NEP)	5 346	60%	10 692	120%	12 830	144%	16 038	180%
Scenario protection level 1 (LEP)	5 208	58%	10 416	117%	12 499	140%	15 624	175%
Scenario protection level 2 (MEP)	4 684	52%	9 368	105%	11 242	126%	14 052	157%
Scenario protection level 3 (EEP)	4 222	47%	8 444	95%	10 133	113%	12 666	142%
Attraction-based scenario protection level 1 (ALEP)	5 608	63%	11 216	126%	13 459	151%	16 824	188%

As it is illustrated in table 3.18, among primary urban fabric scenarios, sprawl urban fabric scenario could not provide desired amount of the population increasing rate and all environmental-based scenarios make less than 79%. Other urban fabric scenarios also passed this rate. Therefore, we define final urban fabric scenarios considering other results of SLEUTH in different growth cycles (table 3.19). In final scenarios, the SLEUTH results of 18, 23 and 28 growth cycles, provide the desirable rate of population. The combination of the buildings in both medium dense urban fabric scenario and medium/high dense urban fabric scenario are 50% single dwelling and 50 % shop top housing while they are produced with different growth cycles. We also create another urban fabric scenario with 33 growth cycle and the combination of 45% single dwelling, 45% low-rise and 10% shop top housing which gives the population rate around 79%.

Table 3. 19. Urban fabric scenarios comparison according to the growth cycle to have similar rate of increased population. The gray column represents the population increasing of low dense urban fabric scenario during 33-growth cycle that is closer to the existing urban fabric, Saint Sulpice la Pointe.

Increased population per urban fabric scenarios in 2050	Low dense urban fabric scenario		Medium dense urban fabric scenario		Medium/high dense urban fabric scenario		High dense urban fabric scenario	
	45% single dwelling & 45% low-rise & 10% shop top housing		50% single dwelling & 50% shop top housing		30% single dwelling & 70% shop top housing		100% shop top housing	
	33th growth cycle		28th growth cycle		23th growth cycle		18th growth cycle	
Scenario protection level 0 (NEP)	7 618	85%	8 892	100%	7 236	81%	8 460	95%
Scenario protection level 1 (LEP)	7 421	83%	8 664	97%	7 052	79%	8 100	91%
Scenario protection level 2 (MEP)	6 675	75%	7 924	89%	6 456	72%	7 470	84%
Scenario protection level 3 (EEP)	6 016	67%	7 100	79%	5 728	64%	6 522	73%
Attraction-based scenario protection level 1 (ALEP)	7 991	89%	9 424	105%	7 724	86%	8 946	100%

As shown in table 3.19, low dense urban fabric scenario accommodate (nearly) the number of inhabitants through environmental scenario protection level 2 (75%). The rate of 79% for medium dense urban fabric scenario is obtained through scenario protection level 3 and for medium/high dense urban fabric scenario via scenario protection level 1. High dense urban fabric scenario could accommodate more population while less sprawl.

3.4. Developing Different Simulation Scenarios to Illustrate the Impacts of Environmental Constraints, Construction and Population on the Growth of a small community - Rieucros rural area

The last study area is Rieucros, a small community in a rural area that is located in the department of Ariège in south of Toulouse (43°05'07" North, 1°46'04" East) (see figure 3.29). The extent of the study area is 400 ha with 686 inhabitants (Legal populations, INSEE, 2016).

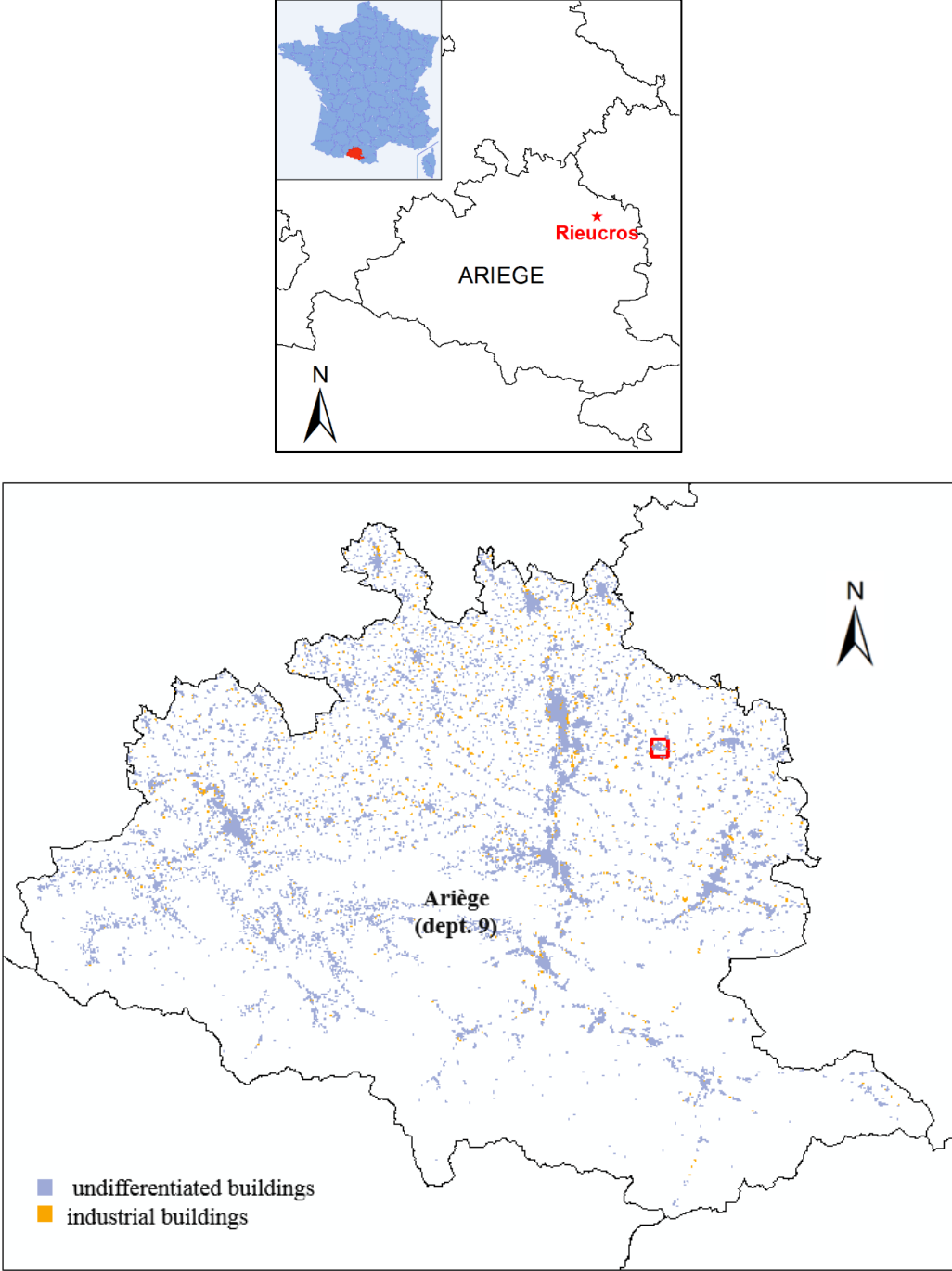


Figure 3. 29. Location and extent of the urban area of Rieucros study area

3.4.1. Data and Materials - Rieucros

Geospatial database and geographic information systems are applied to create the input maps. All the input maps have the size of 100×100 pixels that feature a cell size of 20m×20m (~400m²). Similar to Toulouse, the Geospatial database that is used as input data consists the maps of 2000, 2008, 2012 and 2017 as follow:

- Slope and hillshade maps are derived from Digital Elevation Model (DEM) of RGE ALTI with a spatial resolution of 5m, provided by IGN.
- Urban areas, excluded areas and transportation maps are generated automatically from BD TOPO and BD ORTHO from IGN. Urban map is classified into two classes of urban and nonurban.
- Population and census on district zone are taken from INSEE database of 2011.

Using SLEUTH, different 2D urban growth prospective scenarios are defined. The undifferentiated buildings with more than 3m height and more than 50m² surface from BD TOPO (IGN data base) are used and a dilation-erosion (20m) according to the pixel size is applied to create the urban maps (see chapter 2). Figure 3.30 illustrates the SLEUTH input data for Rieucros study area. The databases and the procedures are as previous study areas.

3.4.2. Environmental Constraints Scenarios - Rieucros

Similar to previous study area, five different environmental protection scenarios are defined by altering the excluded map including (see sections 2.3.3 chapter 2):

- Scenario Protection Level 0 (Nearly No Environmental Protection - NEP) (see figure 3.31)
- Scenario Protection Level 1 (Limited Environmental Protection - LEP) (see figure 3.32)
- Scenario Protection Level 2 (Moderate Environmental Protection - MEP) (see figure 3.33)
- Scenario Protection Level 3 (Extreme Environmental Protection - EEP) (see figure 3.34)
- Attraction-based Scenario Protection Level 1 (Attraction-based Limited Environmental Protection - ALEP) (see figure 3.35)

Each pixel of the excluded maps have a value between 0 and 100 where, value 100 indicates 100% protection from the possible urban growth and the value of zero shows free zones to build. The value of 50 represents a neutral weight for development. Between 100 and 50 is a relative exclusion whereas under 50 means that there is an attraction (see table 2.3).

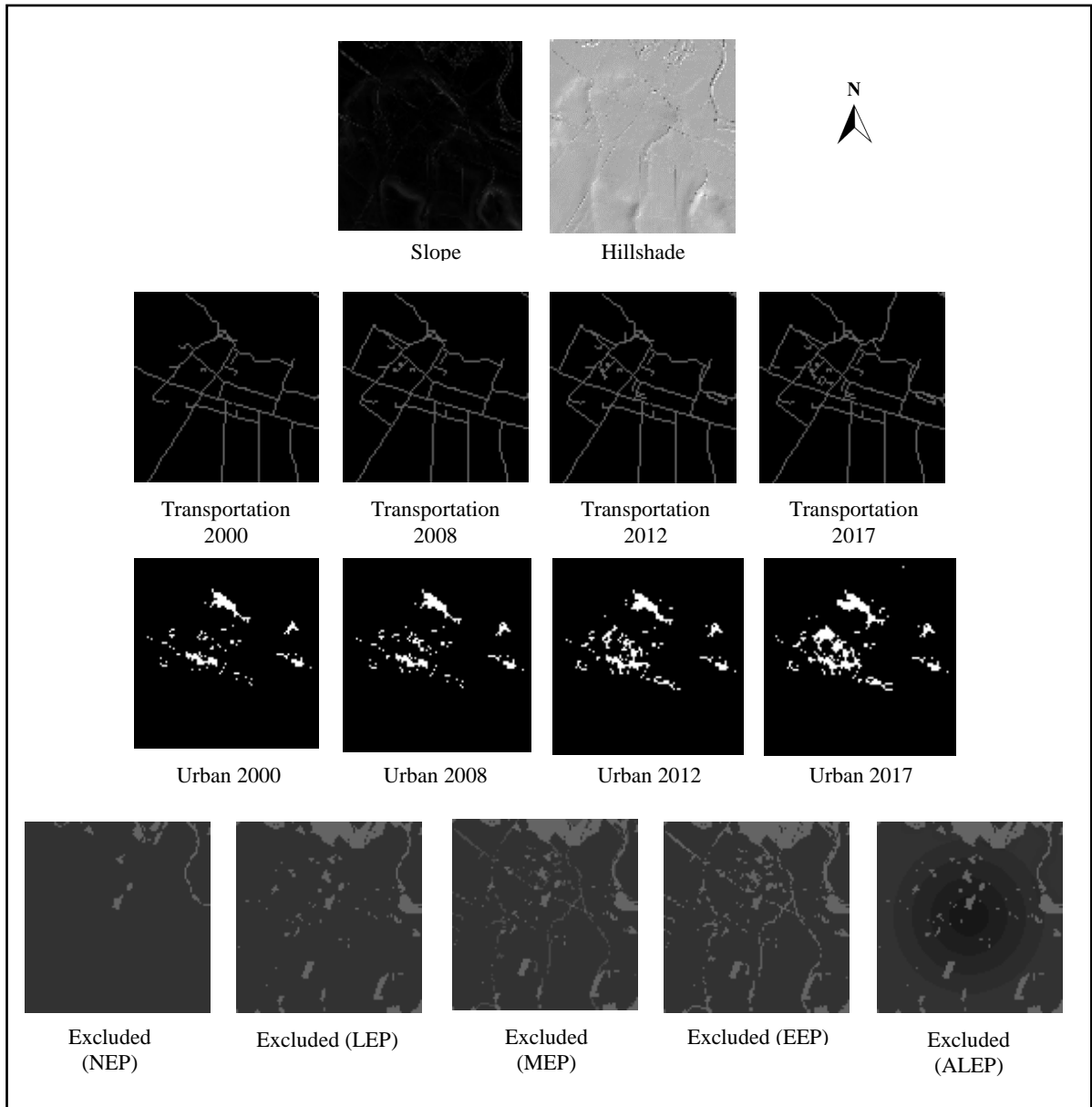


Figure 3. 30. Slope, hillshade, transportation, urban and exclusion maps of Rieucros

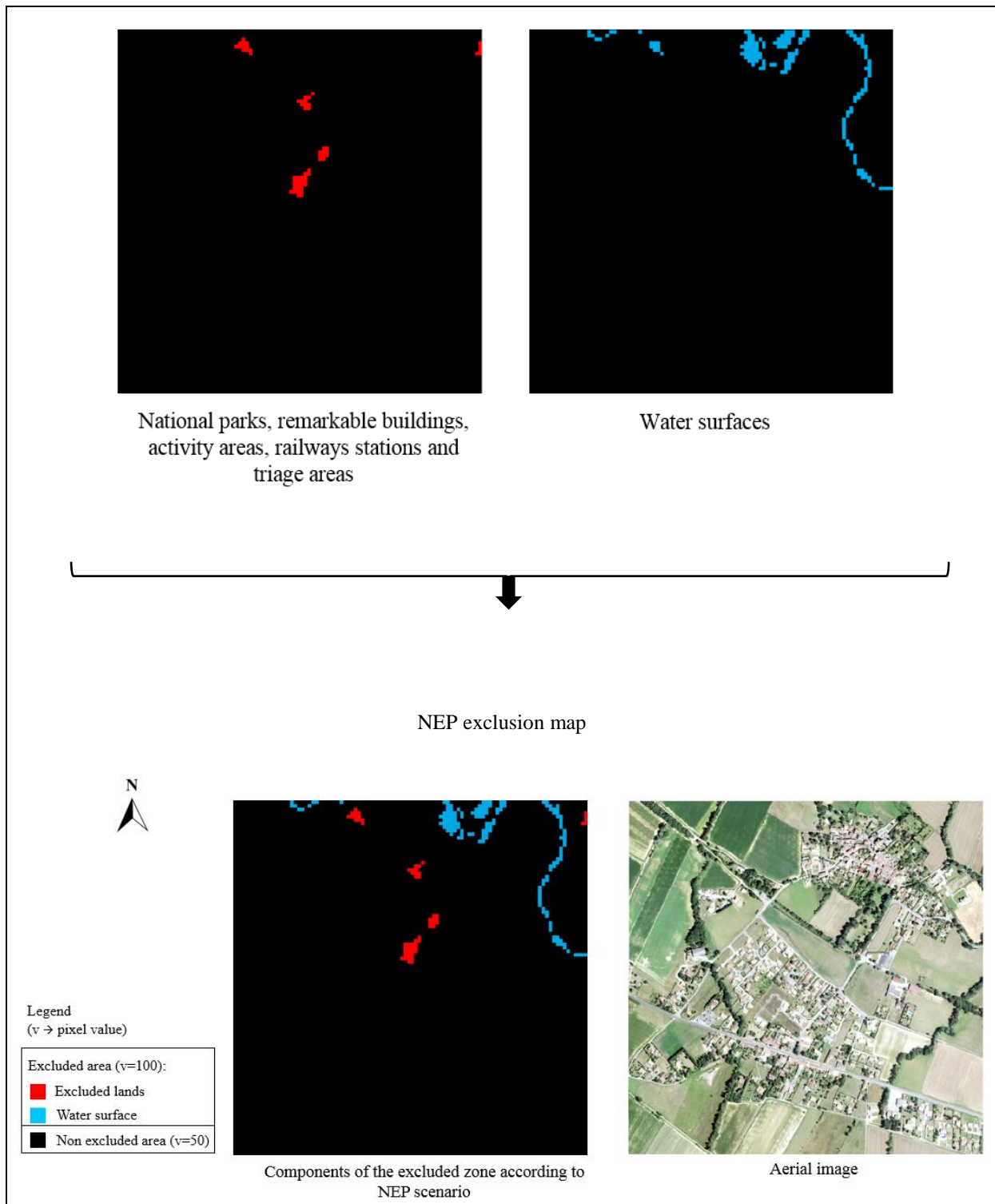


Figure 3. 31. NEP exclusion map generated for Rieucros, 2017. The excluded areas include the remarkable buildings, cemeteries, airfields, sport grounds; activity areas (administrative, culture and leisure, education, water management, industrial or commercial, health, sports and transport) and national parks; that are shown in red and the water surfaces that are represented in blue. They take the value of 100 and the others take the value of 50.

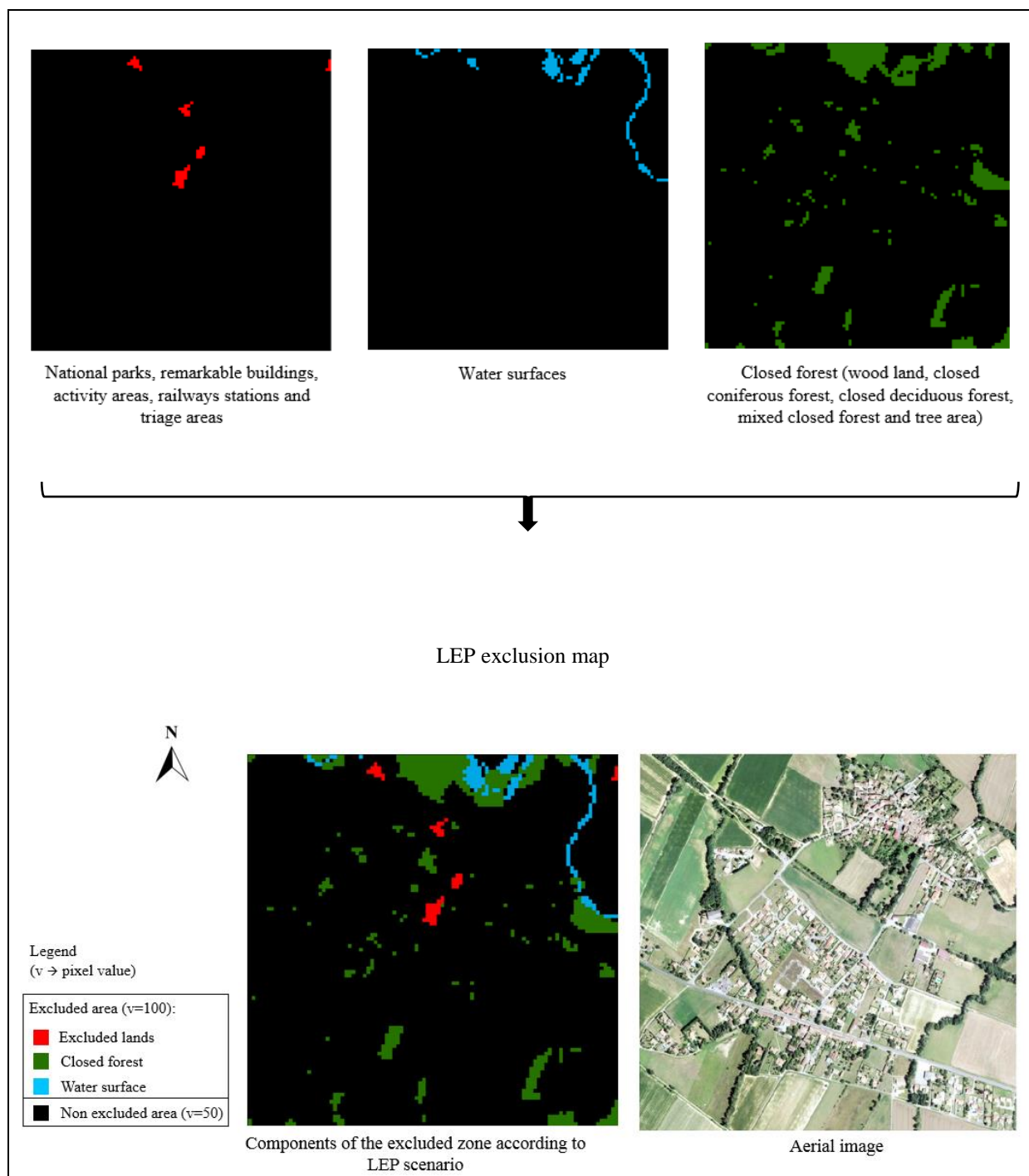


Figure 3. 32. LEP exclusion map generated for Rieucros, 2017. The excluded areas indicate the remarkable buildings, cemeteries, airfields, sport grounds; activity areas (administrative, culture and leisure, education, water management, industrial or commercial, health, sports and transport) and national parks that are shown in red, the water surfaces represented in blue and the closed forests areas (wood land, closed coniferous forest, closed deciduous forest, mixed closed forest and tree area) in dark green. They take the value of 100 and the others take the value of 50.

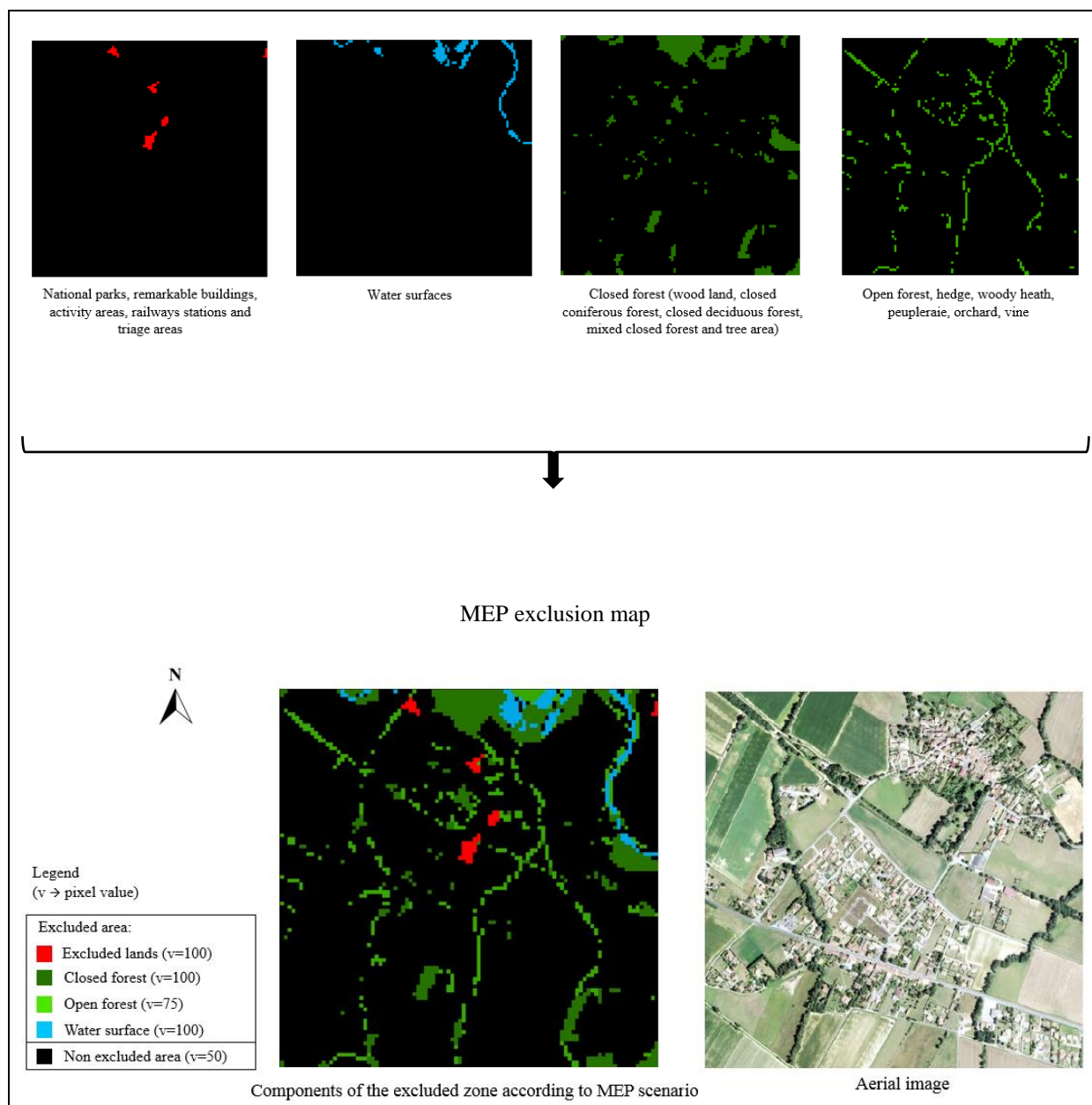


Figure 3. 33. MEP exclusion map generated for Rieucros, 2017. The excluded map contains all parks, protected areas and water bodies have made from the database of the IGN for 2017 including the remarkable buildings, cemeteries, airfields, sport grounds; activity areas (administrative, culture and leisure, education, water management, industrial or commercial, health, sports and transport) and national parks that are shown in red, the water surfaces represented in blue, the close forest areas (wood land, closed coniferous forest, closed deciduous forest, mixed closed forest and tree area) in dark green (value 100) and the open forest, hedge, woody heath, peupleraie, orchard, vine in light green (value 75).

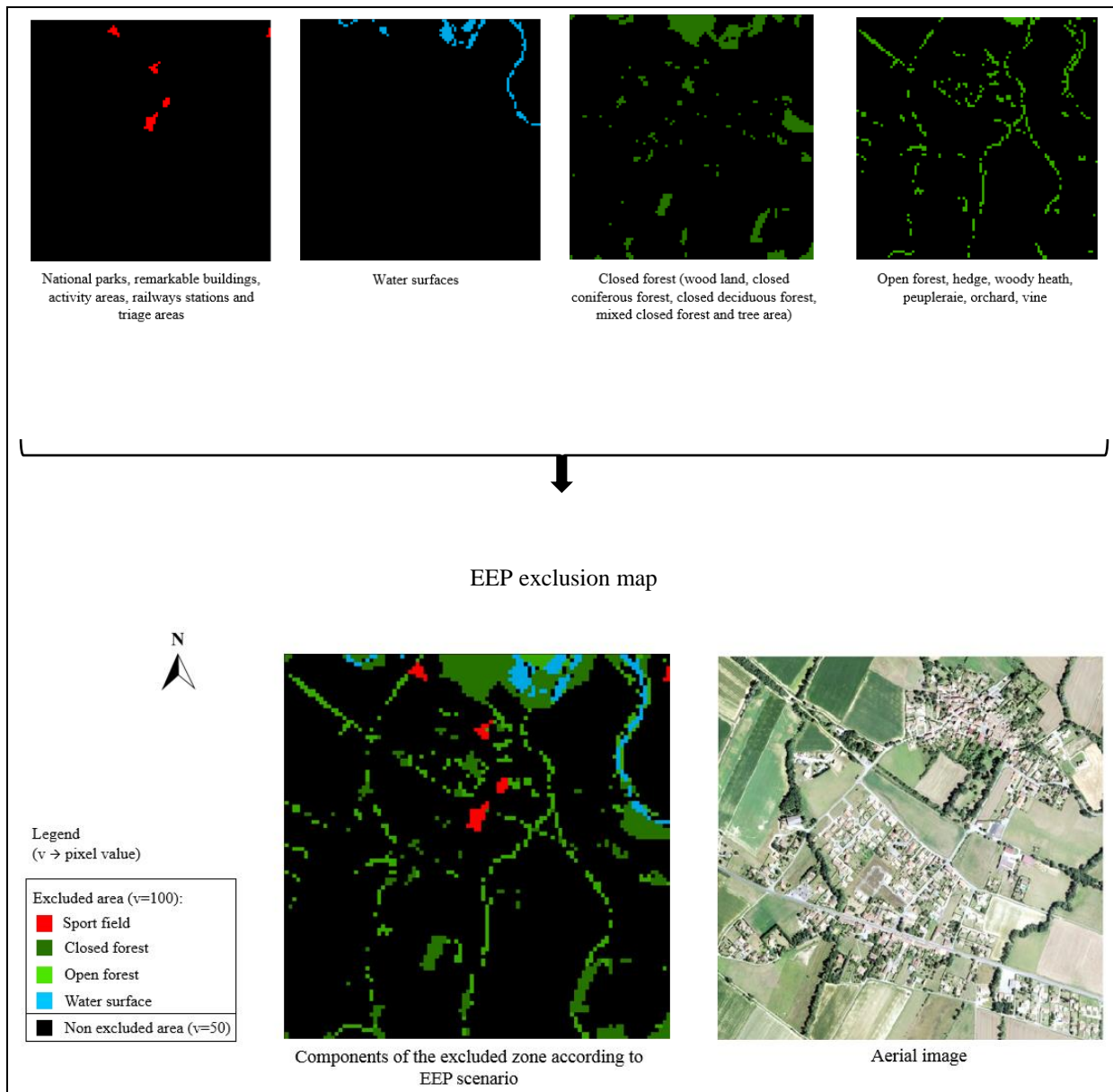


Figure 3. 34. EEP exclusion map generated for Rieucros, 2017. The excluded map contains the remarkable buildings, cemeteries, airfields, sport grounds; activity areas (administrative, culture and leisure, education, water management, industrial or commercial, health, sports and transport) and national parks that are shown in red, the water surfaces represented in blue, the close forest areas (wood land, closed coniferous forest, closed deciduous forest, mixed closed forest and tree area) in dark green and the open forest, hedge, woody heath, peupleraie, orchard, vine in light green. All excluded areas take the value of 100 and the others take the value of 50.

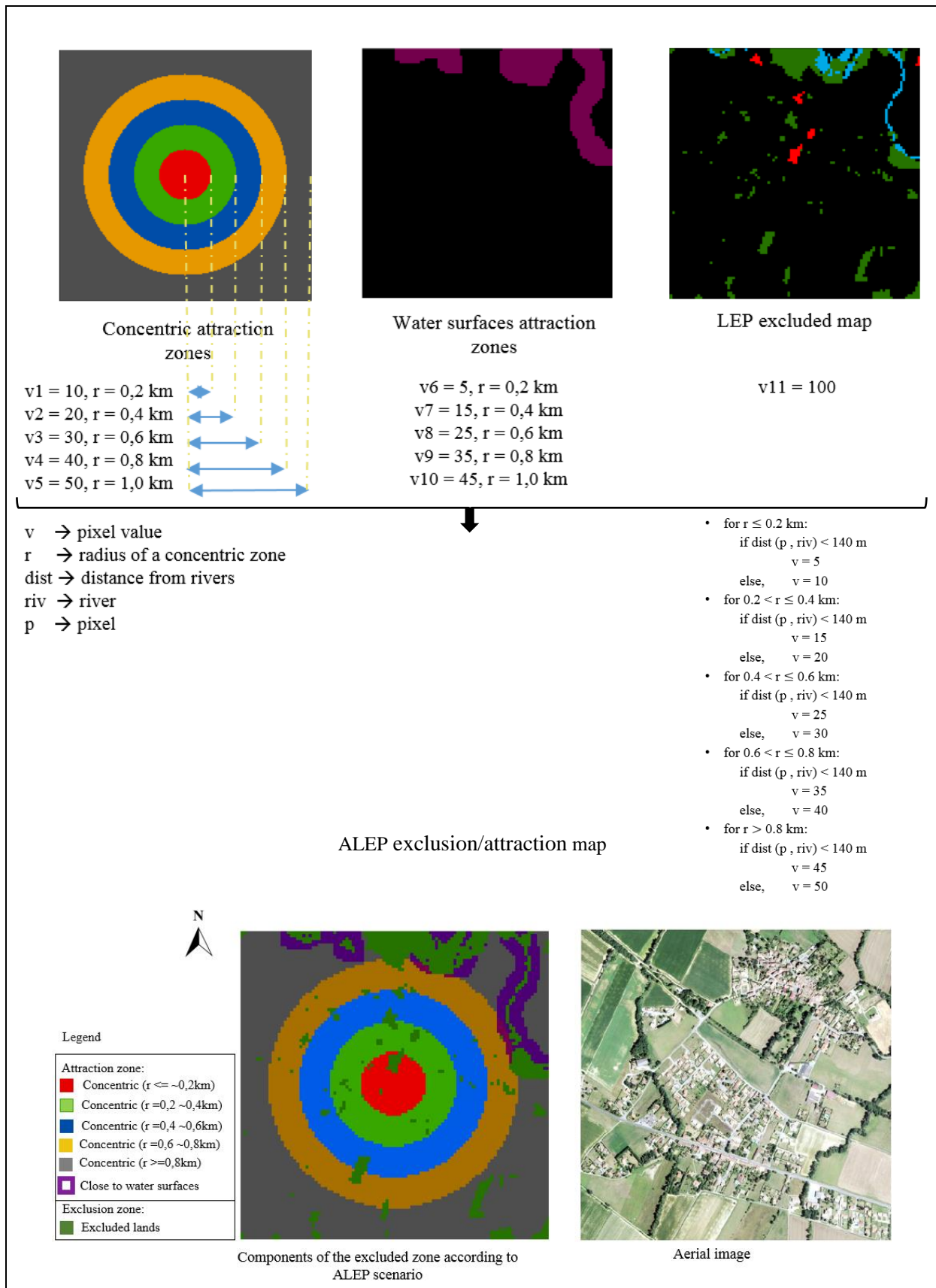


Figure 3. 35. ALEP exclusion/attraction map generated for Rieucros, 2017. Four concentric zones with different attraction rates, make attraction force to the center. The areas in distances of seven pixels (~140m) around water surfaces are considered as attraction areas for dwelling as well. The LEP exclusion map is used for the excluded areas.

3.4.3. 2D Urban Growth Simulations - Rieucros

The dispersion coefficients multiplier and the best-fit coefficients that are calculated for this study area are represented in table 3.20 and table 3.21 respectively. The process of obtaining the coefficients are presented in Annex C.

Table 3. 20. Dispersion coefficient (D_M) multiplier per environmental protection scenario, Rieucros

Scenarios	Dm_multi
Scenario protection level 0 (NEP)	0,0002
Scenario protection level 1 (LEP)	0,0002
Scenario protection level 2 (MEP)	0,0002
Scenario protection level 3 (EEP)	0,0002
Attraction-based scenario protection level 1 (ALEP)	0,0002

Table 3. 21. Best-fit coefficient values driven from calibration process of SLEUTH-3r, Rieucros

Coefficient values					
Scenarios	Dispersion	Breed	Spread	Slope	Road gravity
Scenario protection level 0 (NEP)	100	1	25	100	1
Scenario protection level 1 (LEP)	75	25	25	100	100
Scenario protection level 2 (MEP)	75	1	25	100	1
Scenario protection level 3 (EEP)	100	25	25	100	100
Attraction-based scenario protection level 1 (ALEP)	75	50	25	100	1

To test and evaluate the model, we first run the model with the input maps of 2000 to simulate the growth for 2017, for all five scenarios of environmental protection. The simulated urban maps for 2017 are illustrated in figure 3.36. Figure 3.37 illustrates the simulated urban map of 2017, observed urban maps of 2000 and 2017 as well as their Ortho-photos. The comparison of the results is provided in table 3.22.

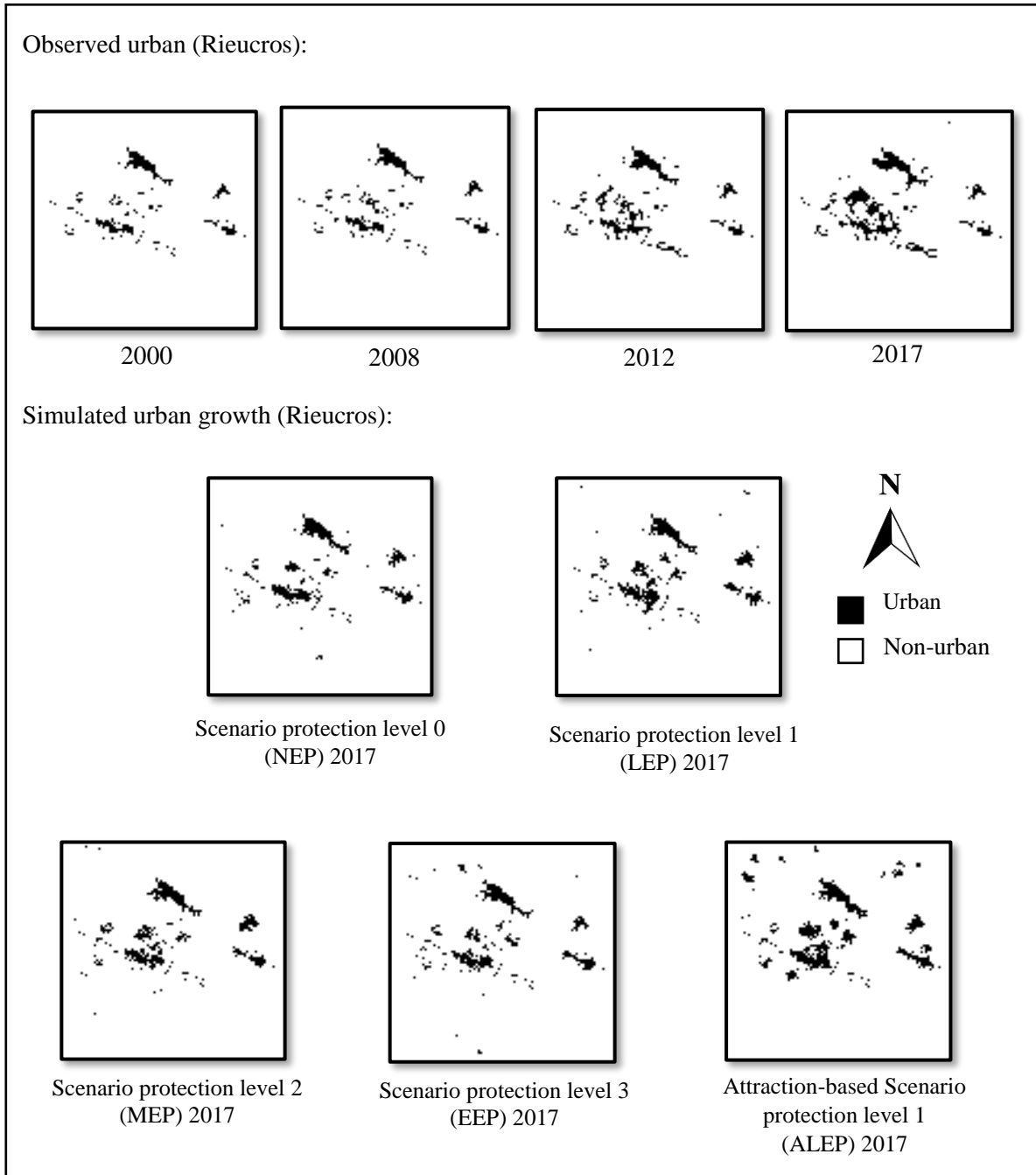


Figure 3. 36. Historical urban maps of 2000 and 2017 and prospective urban maps that are simulated by different environmental protection scenarios for 2017, Rieucros

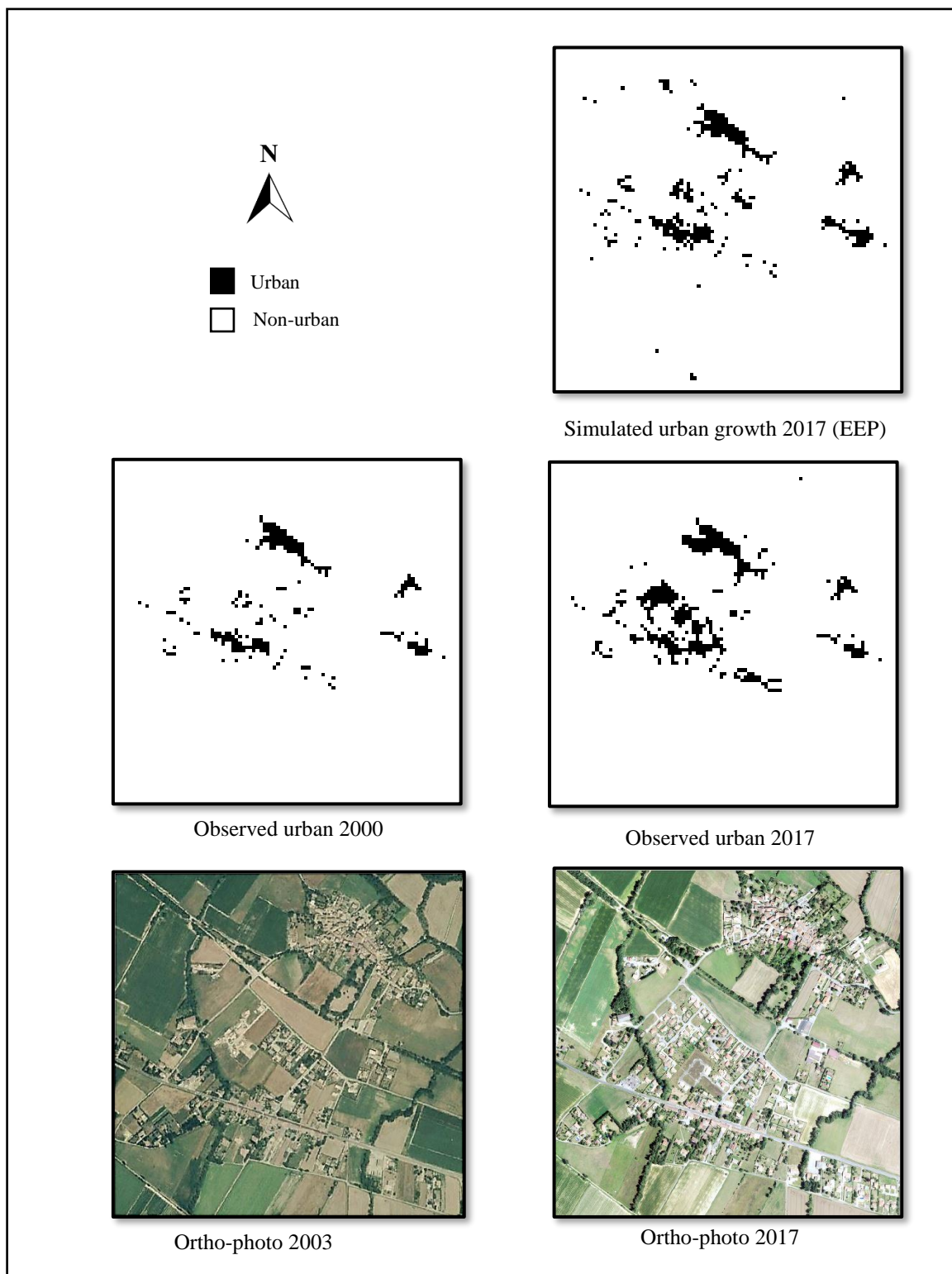


Figure 3. 37. Comparison of the historical urban patch and corresponding prospective patch that is simulated by SLEUTH-3r through environmental protection scenario level 3 (EEP), Rieucros

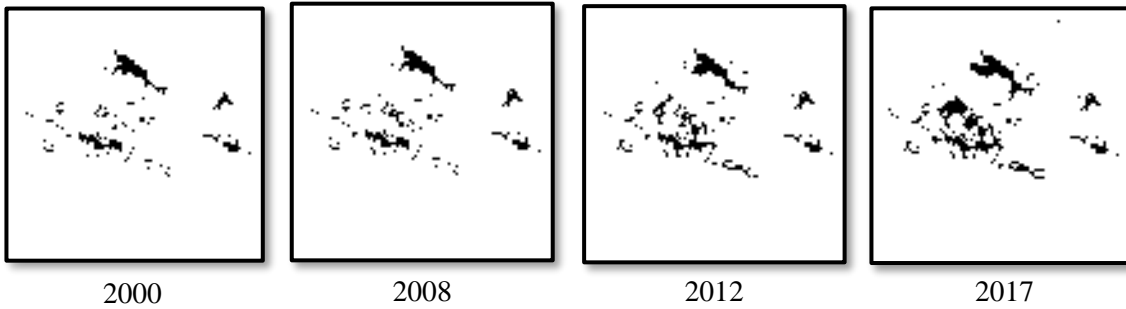
Table 3. 22. Urban growth simulated results obtained from different environmental protection scenarios and the comparison of the results to the observed map of 2017, Rieucros

Results - 2017						
Scenarios	Observed urban area in 2000 (pixels)	Increased urban area (pixels)	Urban growth rate (%)	Urban area increased (ha)	Total urban area (ha)	Growth goodness-of-fit (%)
Scenario protection level 0 (NEP)	255	109	29,95	4	15	74,18
Scenario protection level 1 (LEP)	255	163	39,00	7	17	67,70
Scenario protection level 2 (MEP)	255	141	35,61	6	16	70,96
Scenario protection level 3 (EEP)	255	118	31,64	5	15	73,73
Attraction-based scenario protection level 1 (ALEP)	255	296	53,72	12	22	53,36
Observed urban area in 2017	458	203	44,32	18	41	100

Normally, as environmental protection increases, the growth rate of the growth areas should be reduced, but this value is increased at level 1 compared to level 0. This is because the scenarios are calibrated independently. In this calibration process different coefficients are extracted, however the process of calibration is similar. In this process we search for the coefficients that could give values for two metrics of the pixel fractional difference (PFD) and the clusters fractional difference (CFD) that cover the growth amount. Comparing the goodness of the fit show that scenario protection level 1 has produced the closer amount to observed map of 2017. The scenario protection level 0 simulate less urban growth rate (29.95%), but its simulation areas are closer to observed map with goodness-of-fit of 74.18% (comparing amount and accuracy).

Afterwards, we have generate the prediction scenario files to produce the forecasting urban growth simulation for 2050. We run the model with the input urban map of 2017 (observed) to obtain the prospective urban map for 2050 for different scenarios. The simulation results of 2050 are illustrated in figure 3.38 and table 3.23 represents the simulated prospective urban growth results for 2050.

Observed urban (Rieucros):



Simulated urban growth (Rieucros):

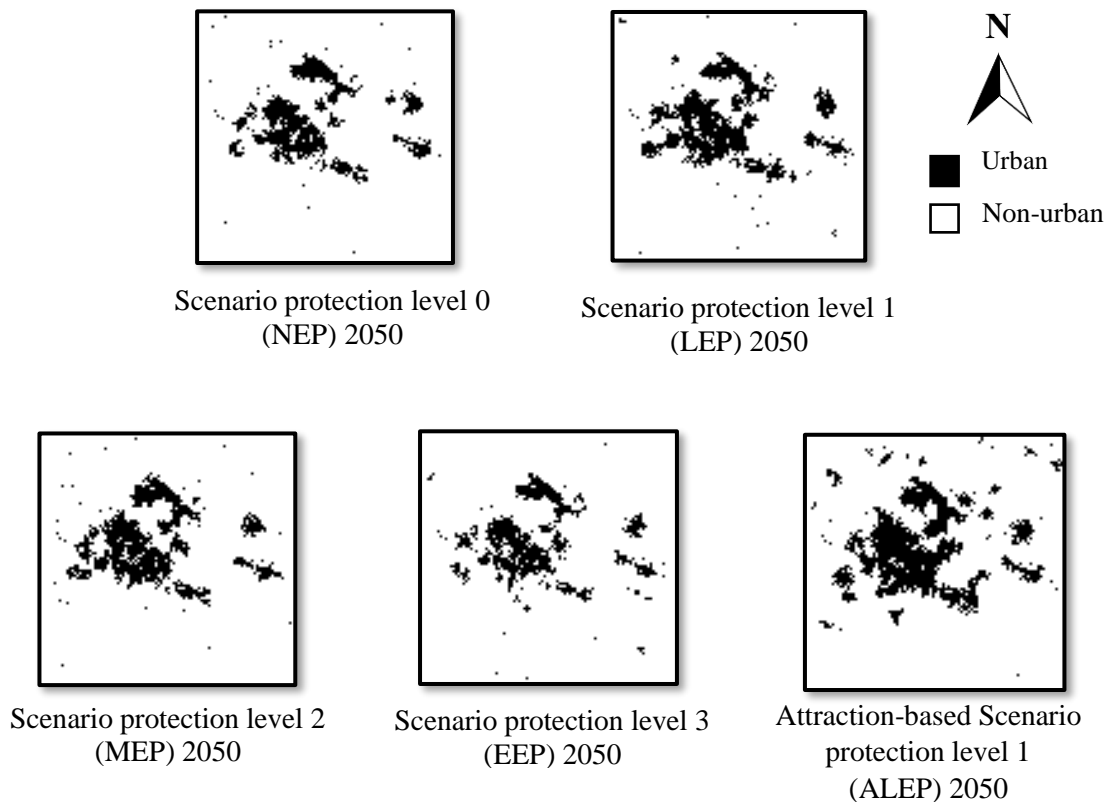


Figure 3. 38. Urban map of 2050 and prospective urban maps for 2050, Rieucros

Table 3. 23. Urban growth simulated results obtained from different environmental protection scenarios for 2050, Rieucros.

Results - 2050				
Scenarios	Existing Urban Area in 2017 (pixels)	Urban growth rate (%)	Urban area increased (ha)	Total urban area (ha)
Scenario protection level 0 (NEP)	458	47,48	17	35
Scenario protection level 1 (LEP)	458	58,51	26	44
Scenario protection level 2 (MEP)	458	55,79	23	41
Scenario protection level 3 (EEP)	458	45,67	15	34
Attraction-based scenario protection level 1 (ALEP)	458	67,90	39	57

After obtaining the simulated results for 2050, we should create the urban fabric scenarios to see what could mean these new urban areas in terms of building types and the capacity of human settlement.

3.4.4. Urban Fabric Scenarios - Rieucros

The process of creating the urban fabric scenarios is similar to previous study area. We classify the current buildings (undifferentiated data of IGN, BDTPO) according to defined building types (Chapter 2, section 2.4.1) and extract the number and occupied surfaces of the existing buildings (see table 3.24). This study area consists of two type of building including single dwellings (42.1%) and low-rise buildings (57.9%). Later, the building type matrix is created according to these two building types.

Table 3. 24. Number, area and height of undifferentiated buildings according to our building classification, Rieucros.

Building class	Number of buildings	Total Area		Average height (m)
		m ²	%	
Single dwellings	187	28 205	42,10%	4
Low-rise housing	134	38 798	57,90%	8

The population of Rieucros is 686 inhabitants ([Legal populations, INSEE, 2016](#)), the annual growth rate is 1.70% and the average population growth rate for 2050 shows the increasing of 77% of growth. For this amount the estimated average of inhabitants per building type is illustrated in table 3.25.

Table 3. 25. Estimation of the average number of inhabitant for each type of buildings, Rieucros.

Building class	Estimated average number of inhabitants
Single dwellings	2
Low-rise housing	3

Next, we define the urban fabric scenarios based on the combinations of single dwelling and low-rise housing. Table 3.26 shows the population growth that is obtained from five different primary urban fabric scenarios from sprawl to high dense.

Table 3. 26. Comparing the population growth of five different primary urban fabric scenarios, Rieucros.

Increased population per urban fabric scenarios in 2050	Sprawl urban fabric scenario		Medium dense urban fabric scenario		Medium/high dense urban fabric scenario		High dense urban fabric scenario		Too high dense urban fabric scenario	
	100% single dwelling		80% single dwelling & 20% low-rise housing		50% single dwelling & 50% low-rise housing		30% single dwelling & 70% low-rise housing		100% low-rise housing	
Scenario protection level 0 (NEP)	1 022	149%	1 124	164%	1 278	186%	1 380	201%	1 533	223%
Scenario protection level 1 (LEP)	1 292	188%	1 421	207%	1 615	235%	1 744	254%	1 938	283%
Scenario protection level 2 (MEP)	1 156	169%	1 272	185%	1 445	211%	1 561	227%	1 734	253%
Scenario protection level 3 (EEP)	770	112%	847	123%	963	140%	1 040	152%	1 155	168%
Attraction-based scenario protection level 1 (ALEP)	1 938	283%	2 132	311%	2 423	353%	2 616	381%	2 907	424%

The primary urban fabric scenarios are created from SLEUTH simulated map of 33 growth cycles. As illustrated in table 3.26, all primary scenarios passed the desired amount of the population increasing estimated for 2050 (77%). The primary scenarios gives an idea for defining the final urban fabric scenarios. Therefore, we tried to find out which growth cycle would match better the desired urban fabric. The final scenarios, are defined as low dense, medium dense and medium/high dense urban fabrics that obtained from the 23th, 18th and 13th growth cycles of the SLEUTH simulations table (3.27).

Table 3. 27. Urban fabric scenarios comparison according to the growth cycle to have similar rate of increased population. The gray column represents the population increasing of low dense urban fabric scenario during 33-growth cycle that is closer to the existing urban fabric, Rieucros.

Increased population per urban fabric scenarios in 2050	Low dense urban fabric scenario		Medium dense urban fabric scenario		Medium/high dense urban fabric scenario	
	100% single dwelling		80% single dwelling & 20% low-rise housing		50% single dwelling & 50% low-rise housing	
	23th growth cycle		18th growth cycle		13th growth cycle	
Scenario protection level 0 (NEP)	570	83%	471	69%	380	55%
Scenario protection level 1 (LEP)	812	118%	667	97%	528	77%
Scenario protection level 2 (MEP)	748	109%	612	89%	470	69%
Scenario protection level 3 (EEP)	478	70%	409	60%	328	48%
Attraction-based scenario protection level 1 (ALEP)	1 200	175%	1 012	148%	758	110%

As illustrated in table 3.27, the medium/high dense urban fabric can accommodate 77% of population growth through scenario protection level 1. The two other urban fabric scenarios are more sprawl, however they can accommodate the desired number of inhabitants with more environmental protection level.

3.5. The Impacts of Pixel Size and Calibration on Sustainability of Model

Choosing the best pixel size is a challenge in CA urban modeling. The pixel size can affect the densification of the simulated area. In this research, we have applied the forecasting urban growth (SLEUTH) on three study areas with different scales. The input maps of SLEUTH are the raster data with the pixel size of 52m×52m for Toulouse, 30m×30m for Saint Sulpice la Pointe and 20m×20m for Rieucros. As discussed before, the urban maps are generated from undifferentiated buildings of BD-TOPO IGN with the surfaces more than 50m², which are the shape files (vector data) that are extracted to raster data for using in SLEUTH. The pixel sizes of these raster files, can impress the simulation efficiency.

- In some districts, only one or some individual buildings that have much less area than the pixel size makes it an urban pixel. For example, in Toulouse study area a building with an area well below the pixel surface make an urban pixel with 2700 m². Therefore, these pixels are considered as urban area (as an input map of SLEUTH) and the densification cannot occur there, which causing the city to be sprawl. It should be noted that we cannot ignore the small buildings because they exist as a reality that can affect the urbanization.

- Choosing a small pixel size, especially for a large study area such as Toulouse, can cause other problems. The smaller pixel size cannot cover large buildings that often exist in big cities. In addition, due to the size of the study area the model computation time and required memory will greatly increase especially in calibration process.
- The impact of pixel size in transportation maps is also noteworthy. The roads affect the urbanization, which is properly considered in SLEUTH, however the model considers the pixel width as the width of the roads.

Therefore, we have applied different study areas in different scale to see the impacts of the pixel size as well. Although, Saint Sulpice la Pointe exist in Toulouse study area, we simulate the urban growth for this area separately. Figure 3.39 illustrates Saint Sulpice la Pointe in both simulation with pixel size of 52m*52m (according to Toulouse study area) and 30m*30m (according to Saint Sulpice la Pointe study area), which shows the impacts of pixel size and scalability as well.

The process of choosing the best fit coefficients in calibration is not definite and there is no clear consensus to choose the appropriate ones to use during the calibration process. In calibration, we calculate some metrics in order to find the best coefficients of growth. These metrics are evaluated to find the best goodness of the fit in one or some metrics with less ratio of differences. This process is done separately for each environmental-based scenario, which make to find different coefficients and the model gives various results. In addition, we have defined different environmental protection scenarios. In these scenarios, except the exclusion map, we use same input maps in SLEUTH simulations. We cannot directly compare the results that are obtained, according to different exclusion maps, from different scenarios, however the impact of the environmental rules on urban growth simulation in different scenarios can be compared and evaluated. Therefore, we do not have control on simulation results, thus we propose to verify the impacts of the population growth and building types on the simulation results.

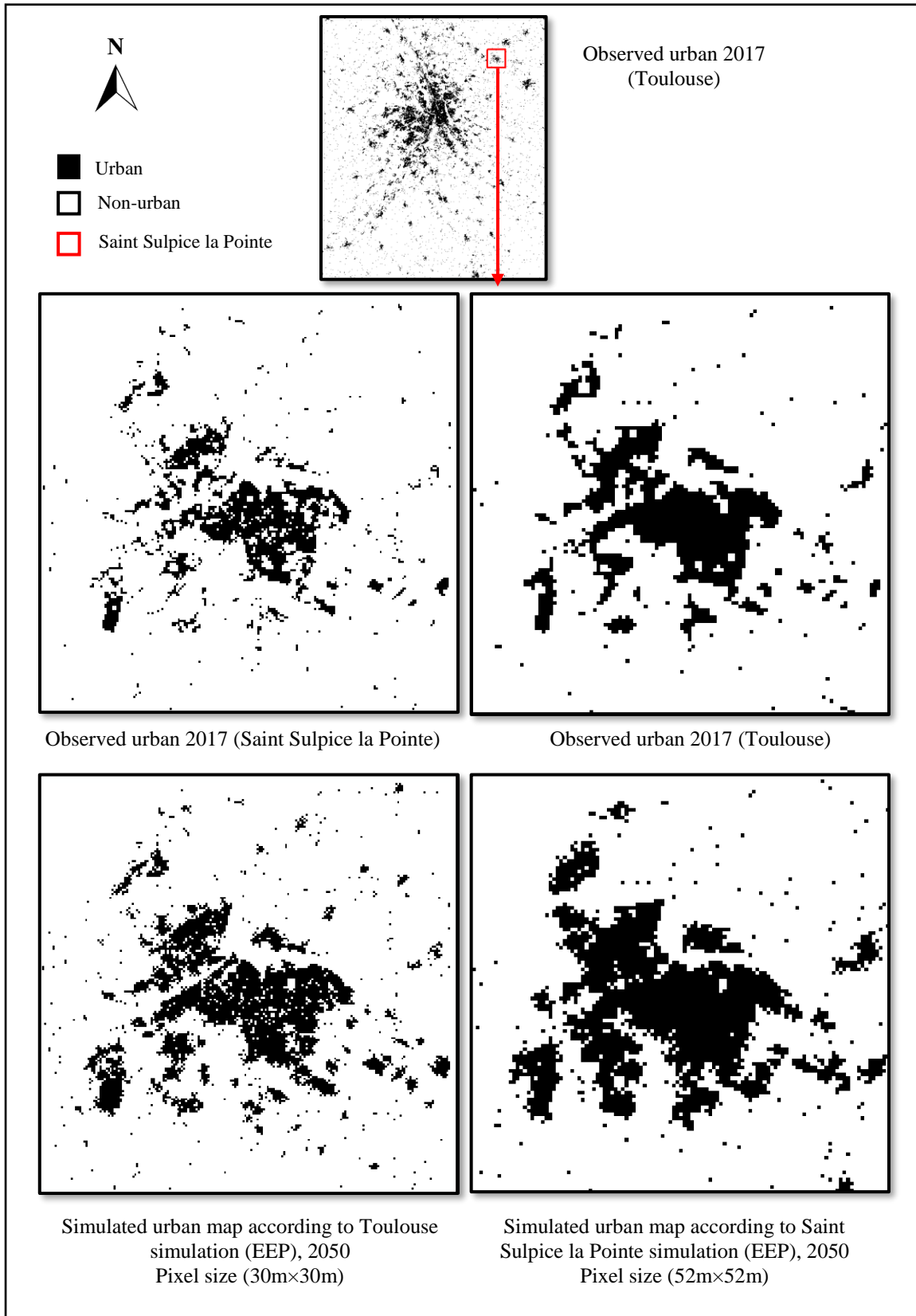


Figure 3. 39. Urban growth simulation of Saint Sulpice la Pointe study area according to two different pixels size

3.6. Chapter Conclusion

In this chapter, we have applied the SLEUTH model on in three different areas contain urban metropolis (Toulouse), peri-urban (Saint Sulpice la Pointe) and (Rieucros) rural area in order to verify the impacts of environmental constraints, construction and population on urban sprawl. We use three different pixel sizes (for three study areas) to verify the impacts of pixel size in SLEUTH simulation results. The results show that the size of the pixel has great influence on simulation of the urban sprawl.

We have integrated the prospective spatial data, urban fabrics and demography to improve the forecasted urban sprawl and to obtain more reliable urban growth simulation results for the desired target date. Two types of scenarios for each study area including the environmental protection scenarios and urban fabric scenarios are defined and set of different simulations that are related to different land priorities and constraints have proposed.

Different forms of dense city and sprawl city are generated during the prospective urban growth simulation and compared while keeping the same population growth rate. We have improved the realism of each simulation and their adequacy with the real world by using common data such as topographic data, buildings and demography. We have showed the urban growth is widely dependent to building type and demography as the urban fabric factors, and different growth cycles might give the similar results by altering the scenarios. The urban fabric scenarios demonstrate the capacity of urban settlement according to different scenario.

In next chapter we create the fictive 3D buildings according to our building classification and the urban fabric scenarios. Next, the 3D representation of the urban fabric scenarios are provided in order to visualize the scenarios and better understand the SLEUTH simulations.

Chapter 4 : Creation of Fictive 3D Buildings to Facilitate the Interpretation of Simulation Results and Differentiate Scenarios

Contents

- 4.1. 3D City Generating Applications and Procedure
 - 4.2. From Pixel to 3D Building Representation
 - 4.3. 3D Visualization of the City of Tomorrow
 - 4.4. Chapter Conclusion
-

In previous chapters, the objective was to simulate different urban fabric scenarios for our urban growth forecasting model by explicitly integrating two variables of building classes and population density into the model. In this chapter, we generate the fictive 3D buildings and provide the 3D representation of the urban fabric scenarios, in order to visualize the scenarios and better understand the SLEUTH simulations.

As discussed earlier, the SLEUTH results are limited to some pixels on which urbanization is supposed to occur. These pixels have to be transformed into 3D building representations, while respecting the building classification as well as urban fabric scenarios. Therefore, the pixels have to first create the footprints of the buildings, and next, take the value of the heights.

To create a building from a pixel, we transform the pixel from raster data to building footprints. In the process of transformation of a pixel to building footprints, different considerations and constraints are taken into account such as the direction of the footprints and the distances to urban objects and geographic features. Thereafter, appropriate heights are added to these footprints. The height depends on building classification and probability of the height of adjacent buildings considering the urban fabric scenarios. Finally, a 3D representation is carried out.

Although the provided 3D model is a primary and simple model, the 3D representations of scenarios allow having different images of the city of tomorrow for supporting the scientists and authorities in charge of urban planner and management.

In this chapter, 3D city modeling procedures and some 3D modeling tools and applications are reviewed briefly in section 4.1. The procedure of transforming a pixel to a 3D representation of a building is describe in section 4.2. The 3D visualization of the urban fabric scenarios are provided in section 4.3. The chapter is concluded in section 4.4.

4.1. 3D Urban Generating Applications and Procedure

In previous chapters, we have used a CA model and simulated the forecasting urban growth for our study areas. We have integrated urban fabric factors (i.e. building types and demography data) to improve the simulation. In this chapter, we aim to create the 3D building representations from the pixels and next, illustrate the 3D view of the urban fabric scenarios in order to differentiate the scenarios and understand the urban sprawl simulated by each scenario.

The distance from the constraints and the neighborhoods of geographical objects are not explicitly considered in CA model. Therefore, we use the topographic objects such as buildings, rivers, excluded areas and the current buildings and make a set of constraints. Considering these constraints we create the footprints of the buildings and then we give them the value of the height according to the urban fabric scenarios.

In recent years, governments, municipalities and companies have shown great interest in building virtual models of cities in 3D, for different purposes such as communication, management of urban heritage, the urban planning projects and simulation modeling in terms of noise, solar, pollution, climate change, flooding and urban sprawl (Servières and Gesquière, MAGIS, 2019). A 3D city models are used to represent the urban surfaces and the important objects attached to them including the buildings and the environment (Zhu et al., 2009; Billen et al., 2012; Billen et al., 2014; Pedrinis and Gesquière, 2017). They are used for a variety of different situations, including 3D reconstruction and semantic models (Julin et al., 2018).

Although the main uses of 3D GIS is geo-visualization, they are also used for many other applications (Shiode, 2000; Kolbe and Gröger, 2003; Biljecki et al., 2015; Servières and Gesquière, MAGIS, 2019). In practical applications, different projects have different requirements for various reasons. For example, some projects have a small scope, require accurate models, and pay less attention to time and efficiency, while other projects, involving large areas, focus on creating effective and large-scale models in a limited time.

In order to select the most appropriate technique for 3D modeling, some factors should be considered such as data availability, the performance accuracy, efficiency, speed and human capital and costs. There are many different techniques to generate a 3D city model such as 3D building creation from urban footprints (Ledoux and Meijers, 2011; Pedrinis and Gesquière, 2017) and 3D reconstruction and data integration that are used in merging photogrammetry or laser scanning with GIS data (Haala and Kada, 2010; Kapoor et al. 2010; Hervy et al., 2012; Billen et al., 2012; EL Meouche et al. 2013; Tomljenovic et al. 2015). Photogrammetry and remote sensing have always focused on how to create fast, accurate and realistic 3D models of ground terrain and various features through the captured 2D image data (Kobayashi, 2006). In 3D modeling, photographic measurement method can obtain geometric information of many features of the digital city model framework, like spatial location, terrain fluctuations, size and

height of features. In addition, a large amount of available texture information can be obtained from image data by manual or automatic processing.

Interoperability of a 3D city model and integration with other models is defined according to some standard exchange formats in 3D GIS, such as IFC and CityGML.

IFC is a neutral and open data format of an international standard (ISO 19739) developed by buildingSMART in order to facilitate interoperability exchange in the fields of architecture, engineering and construction (AEC) industry. IFC is an object-based file format with a data model that is commonly used in BIM based projects to facilitate the software interoperability (BuildingSMART, 2019). IFC works well in building modeling, though it has some lacks in building sectors such as incomplete implementation (e.g. extrusion, Boolean operations) or uses that are not really oriented towards the field of infrastructure (e.g. pre-stressing) (Benning, 2017).

CityGML is an Open Geospatial Consortium (OGC) standard based on the Geography Markup Language, which represents the geometrical, semantical, topological, and visual aspects of a 3D city model (Cox et al., 2004; Gröger et al., 2012; Billen et al., 2012; Pedrinis and Gesquière, 2017; Biljecki et al., 2017; Biljecki, 2017; Servières and Gesquière, MAGIS, 2019). It covers all relevant features within urban areas including buildings and infrastructures. The features are organized into modules such as building, transportation, water bodies, tunnel and bridge. In CityGML the features are represented in five discrete Levels of Detail (LoD) from zero to four (see figure 4.1). The geometric and semantic details increased in each level and reflects specific application requirements. The LoDs facilitate data visualization and analysis of GIS data. Although, each feature can be displayed simultaneously in different LoDs, while these features are in the same in a LoD, data integration and interoperability are facilitated (Biljecki, 2017). The LoD1 are often used for visualisation, however they are also used in many applications, such as solar potential estimation, flood simulation, satellite visibility prediction and shadow estimation (Biljecki et al., 2015; Biljecki et al., 2017).

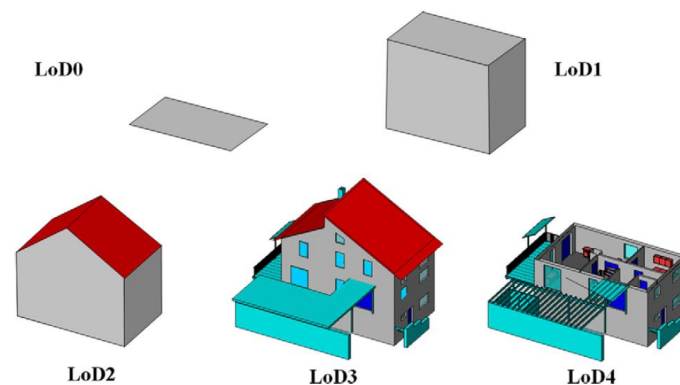


Figure 4. 1. The five LoDs of the OGC CityGML (Gröger et al., 2012)

Isikdag and Zlatanova (2009) indicated that the IFC models contain all necessary information to generate CityGML models in different LoDs. They have defined some rules to make a transformation framework between CityGML and IFC models for geometric transformation and semantic matching. Hijatzi et al. (2011) made a web based tool that integrated IFC data

into a 3D GIS environment. It could support the navigation and visualization functionalities and some analysis operations such as routing and network analyses. Even though, IFC and CityGML are two data exchange standards that are used in 3D modeling domain, they have some semantic and geometrical differences as follow (Gröger and Plümer, 2012):

- CityGML can be used in all relevant urban elements such as the buildings and infrastructures, while IFC is still more used for modeling the buildings.
- In CityGML, the building elements are defined as what are observed, like the walls for each single room. IFC defines the construction elements such as walls identified for a whole building.
- As spatial properties definition, CityGML uses boundary representation and focuses on buildings usage and observation. IFC additionally applies the Constructive Solid Geometries (CSG) and sweep geometries.
- In IFC, the objects are defined with one LoD. In CityGML they are represented in different LoDs.
- IFC is used to build a building model whereas CityGML to represent a whole city.

It should be mentioned that in this research the 3D buildings are created as the simple shape files and we would like to develop this model based on a data exchange standard in subsequent work.

Nowadays, many tools exist in order to produce a 3D model in different field such as industrial, mechanical, electronic, architectural, film, television and games. In this section, some more common 3D tools are compared and their advantages and disadvantages are discussed including Maya, 3ds Max, Auto CAD, Sketch Up, Unity, City Engine and ArcGIS. Although there are some other BIM 3D modeling tools (such as Revit, Rhino, Archicad), they are rarely used in the study areas of a city scale because they are mainly used for modeling the new buildings.

- **Maya** is a well-known 3D computer animation platform software with powerful modeling, strong rendering effects, outstanding performance, and focus on the details of the model. It is used in high-demand, professional-level film and television advertisements, game character animation, and movie 3D effects. As the software does not focus on polygon modeling and it is relatively difficult to use, it is rarely used in digital city modeling (Tang, 2014).
- **3ds Max** is a classic computer-aided design set that integrates 3D modeling, animation and rendering. It has a wide range of applications, including film and television effects, character animation, game development and multimedia production as well as industrial, mechanical, architectural design. 3ds max has a complete set of modeling tools including ability to effectively modify the plane or surface object model, provides 2D and 3D texture programs for fast and personalized texture processing. It supports a variety of flexible and efficient rendering processing techniques. It has a scalability, compatibility, and numerous plugins, which facilitate the practical application of various fields. In 3ds Max the terrain overlay is not supported (Neng Chen et al. 2014).
- **AutoCAD** is currently one of the most widely used two-dimensional design tools. Its graphic drawing and editing capabilities are powerful. In the version of AutoCAD R10, 3D

modeling ability is added to enable the design, rendering and editing of 3D models. The main advantages of AutoCAD 3D include easy to use, high accuracy of graphic position, data exchange interface such as SCR, DXF, and development environment such as AutoLisp and ARX and its ability for the users to customize the environment and functions according to their own needs (Autodesk, 2019). However, its processing tools are relatively weak. Therefore, in practical applications, it is still based on two-dimensional graphics.

- **SketchUp** is a 3D design software that is especially suitable for 3D building design. It consists of a set of design tools that directly face the design process rather than the performance. SketchUp can easily and quickly create and modify 3D models and share models under certain conditions. Other advantages of SketchUp include the ability to create large-scale 3D scenes and high efficiency in modeling (SketchUp, 2019). This tool is not powerful in rendering the features and the model fineness is not high.
- **Unity 3D** is a multi-platform integrated game development tool that can easily create interactive content such as 3D video games, landscape visualization and real-time 3D animation. It integrates scene editing, graphics rendering, terrain and vegetation creation, physical effects, audio and video, lighting, shades. The unity 3D script is compatible with a variety of development languages and it has GUI class library resources. It also supports multiple platforms and has a dazzling 3D rendering effect. One of the biggest features of the Unity 3D game engine is the powerful script editor MonoDevelop. This provides a good development environment for later implementation of the visualization system (Zhao et al. 2013).
- **City Engine** can quickly create 3D scenes with 2D GIS data. The software is compatible with a variety of 3D data formats, and can achieve perfect support for ArcGIS, enabling many existing basic GIS data to quickly realize 3D modeling without conversion. City Engine can be used in digital cities, urban planning, rail transit, power, pipelines, construction, defense, simulation, game development and film production (Singh et al. 2013).

In this research, the term of 3D city model refers to virtual city model. In this chapter, the 3D buildings are created by giving the third dimension to 2D footprints of the buildings. The third dimension indicates the height of a building that is obtained from the urban fabric scenarios according to the building class and population density. The buildings are illustrated in block models with flat roof structure similar to LoD1 of CityGML to illustrate the differences between the scenarios. We use ArcGIS 10.6 for our 3D modeling process. GIS based applications let us creating the 3D buildings and analyzing geographic information. The objective here is not to create a 3D city model, but to illustrate the 3D representation of the urban fabric scenarios while respecting a set of constraints.

4.2. From Pixel to 3D Building Representation

As discussed before, the SLEUTH results are limited to some raster data that is difficult to interpret for decision makers. The results are some pixels on which urbanization is supposed to occur, which do not make much sense from urbanism point of view. Therefore, we propose to transform the pixels into 3D building representations, while respecting the building

classification and urban fabric scenarios and to place different types of building in all of the available spaces and according to the chosen urban fabric scenarios.

In order to visualize the scenarios in three-dimensional space, first, the pixels need to be transformed from raster data to building footprints. The number of the buildings that can be located in each pixel depends to pixel size and the surface of the buildings. An average surface for each building type are calculated based on the average surface of current buildings in each study area. Afterwards, appropriate heights are added to these footprints. The height is based on the urban fabric scenarios. In the process of transformation of the pixel to a building footprints, different considerations and constraints are taken into account such as the direction of the footprints and the distances to urban objects and geographic features. The distance of the new building to the urban objects and geographic features (e.g. current buildings, roads, railways, rivers, vegetation, cemeteries, airfields, activity areas) are obtained from the average distances of the existing buildings to them.

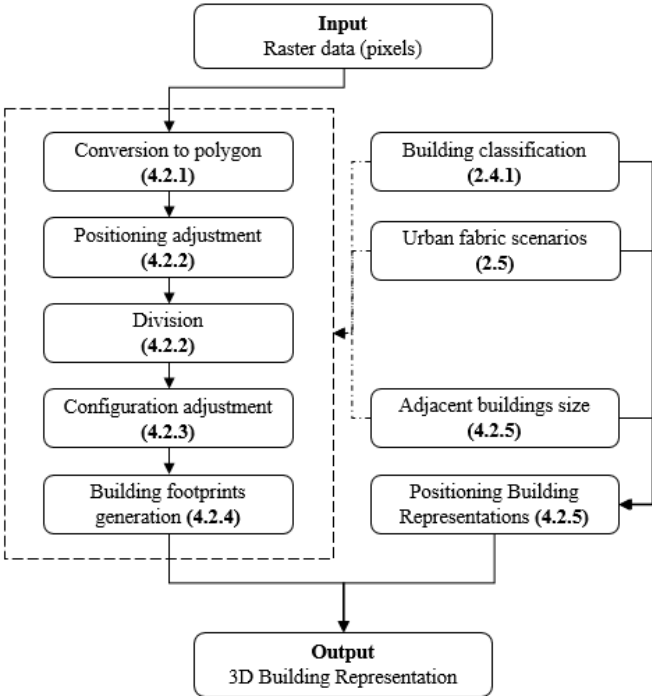


Figure 4. 2. The 3D building representation procedure

As it is illustrated in figure 4.2, in order to create the 3D building model, the pixels have to first change to polygons that indicate the buildings footprints, and take the value of heights. To transform a pixel to a polygon, first the SLEUTH output maps (the raster data that are derived from SLEUTH simulation for each urban fabric scenario) should be georeferenced and converted to vector data. This provides the polygons instead of each pixel, which simplify the processing (see section 4.2.1).

In the next step, each polygon is oriented along its nearest road section. Afterwards, the polygons are divided to smaller squares depending to their sizes. Each polygon is divided to four squares for Rieucros and Saint Sulpice la Pointe and sixteen squares for Toulouse. This is because in our algorithm the position of the building respects certain distances from urban objects and geographic features. If these distances are not observed, the polygon will be

removed. Therefore, by dividing a polygon into smaller squares, we decrease the risk of losing the whole polygon. Furthermore, these small squares will be used in creating more than one 3D building in a big polygon. For example, in case of Toulouse a polygon has the area of 2700m², while the buildings footprints are much less according to the building classification and the scenarios (see section 4.2.2).

The urban objects and the geographic features define some constraints for a polygon. These constraints cause the configuration of the polygons to be adjusted. We have defined two type of constraints including linear constraints (e.g. roads, rivers and railways) and discrete constraints (e.g. cemeteries, airport, and existing buildings). The difference of these two constraints are on the calculation of the average distance of the current buildings to them that will define later in section 4.2.3. As discussed before, the pixels were turned along their nearest road sections. This overlaps the polygons that are adjacent each other. Therefore, in this step the overlaps and the parts of the polygons that are close to the constraints will remove.

In next step, the small squares that are identified a polygon are assembled considering the urban fabric scenario and building class. As defined in previous chapter, each urban fabric scenario consists one or more type of building. Different surfaces for each building class are defined according to the average area of the current buildings in that class. Therefore, the surface of the building with regards to scenarios should be considered in the process of assembling the small squares. Finally, the surfaces are set according to the scenarios by making an erosion to achieve the desired footprints for each building (see section 4.2.4).

The process of calculation the building heights is also done, in parallel to footprints generation. According to each scenarios this process is different. For scenarios that consist of one type of building class (e.g. single dwellings only), we only need to give the height of that building class to the building footprints. But for complex scenarios, the process is different. In this cases, we first calculate the surface of each building footprint. In the cases that the surfaces are too small that cannot be in the upper building class, we give the height according to their surfaces. Others footprints take the height of the nearest neighbors, until the rate of the building classes that are defined in each scenario will be filled. The process of giving height to the building foot prints will be explained in detail in section 4.2.5.

4.2.1. From Pixel to Polygon

The SLEUTH outputs include the non-geo-referenced raster that contains three types of pixels representing the current urban area, new urban area and null pixels. The purpose of this step is to geo-reference this raster data with respect to BD-TOPO vector data. Since SLEUTH generates the new buildings, they are not part of the BD-TOPO data. This process is based on a polynomial transformation that uses a first-order polynomial built on the control points and a least-squares adjustment algorithm. It renders the Root Mean Square deviations (RMS) as a control index, which in general, must be below the size of a pixel. For example, in Saint Sulpice la Pointe the pixels size are 30m×30m and RMS is acceptable (see figure 4.3).

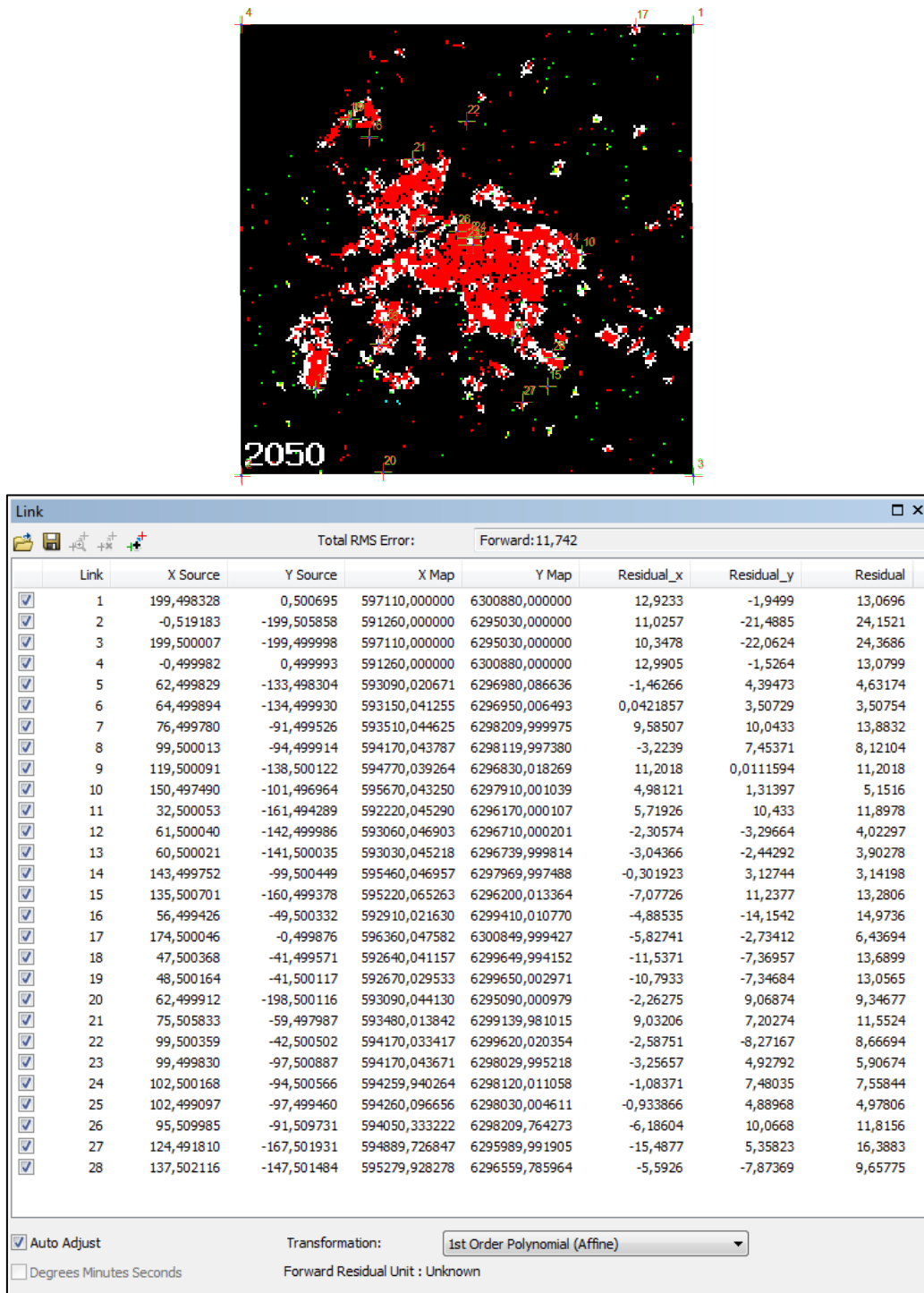


Figure 4. 3. An example of geo-referencing the SLEUTH output map Saint Sulpice la Pointe (EEP simulation scenario, 2050)

Later, the raster data is converted to vector data to facilitate the processing. In fact, we extract raster data from shape files (vector data) for creating the input maps of SLEUTH and now we do the inverse function. Before that, it is necessary to carry out a filter, which eliminates the null pixels. Otherwise, the model will consider the centers of all the pixels of the grid. To do this, we used the tool Set Null in the toolbox (Conditional Spatial Analyst tools) (see figure 4.4).

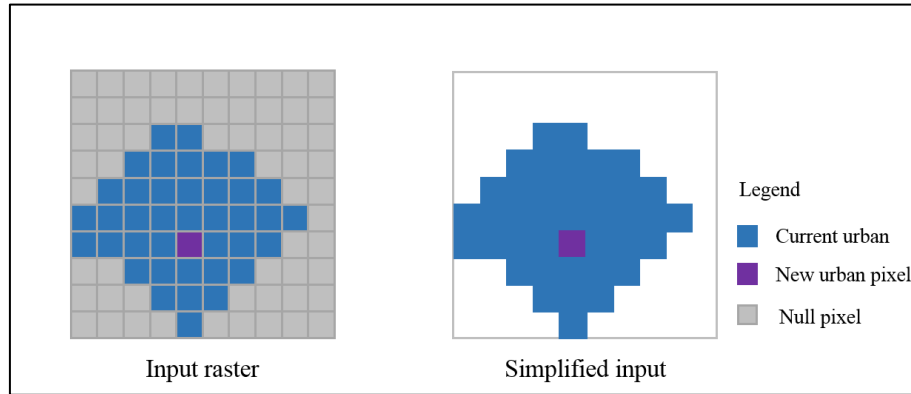


Figure 4. 4. A schema of eliminating the null pixels

4.2.2. Positioning the Building footprints

After preparing the output of the SLEUTH model for 3D procedure, in this section, the generated polygons, should be rotated along the closest road section (Perret et al. 2010; Curie et al., 2011). The orientation is done based on the size of a polygon and the coordinates of its center (X_c, Y_c). The orientation is made with respect to the nearest road section. In fact, the roads are divided into small sections, then their directing coefficient (C_d) is calculated with equation bellow:

$$C_d = \frac{Y_e - Y_s}{X_e - X_s} \quad (4-1)$$

where (X_s, Y_s) and (X_e, Y_e) are the start and the end coordinates of the section, respectively. Then the angle of orientation of the road section is calculated according to the horizontal axis in two cases:

Case 1, if $X_e - X_s = 0$ (section parallel to vertical axis):

$$\Theta = \pi/2 \quad (4-2)$$

Case 2, if not:

$$\Theta = \arctan (C_d) \quad (4-3)$$

Finally, the squares are oriented using this angle by associating each oriented polygon to a local coordinate system and considering the coordinates of the corners of the polygons in the overall reference. Therefore, the solution becomes a simple change of reference in the plane (only 1 rotation + 2 translations). The rotation according to Z is as follows:

$$R_z = \begin{bmatrix} \cos \Theta & -\sin \Theta & 0 \\ \sin \Theta & \cos \Theta & 0 \\ 0 & 0 & 1 \end{bmatrix} \quad (4-4)$$

As illustrated in figure 4.5, the two translations of the center are X_c according to X and Y_c according to Y.

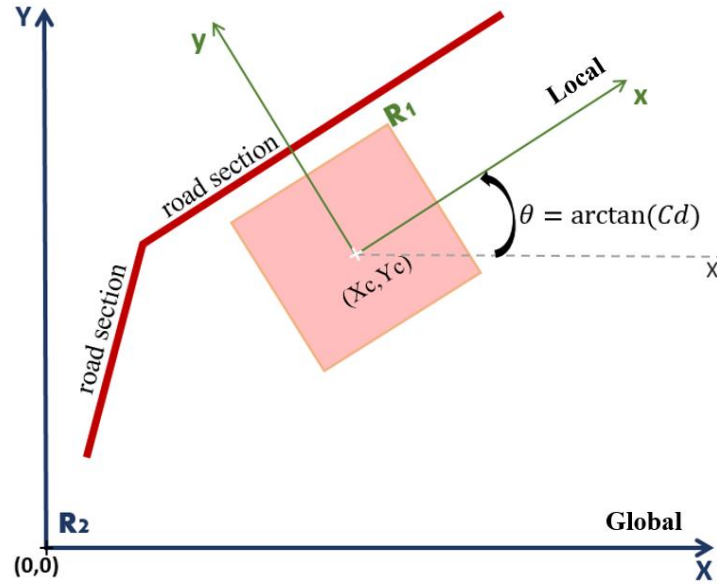


Figure 4. 5. Orientation of a polygon, R_1 and R_2 are the local and overall references respectively

The change is made according to the following equation. The angle calculated in the counterclockwise direction.

$$\begin{cases} X = Xc + x \cos \theta - y \sin \theta \\ Y = Yc + x \sin \theta + y \cos \theta \end{cases} \quad (4-5)$$

Where (x, y) are the coordinates of the corners expressed in local coordinate system and (X, Y) their associates in global coordinate system.

$$\begin{cases} X = Xc + \left(\frac{R}{2}\right) (\cos \theta - \sin \theta) \\ Y = Yc + \left(\frac{R}{2}\right) (\sin \theta + \cos \theta) \end{cases} \quad (4-6)$$

Afterwards, we change the sign of the cosine and sine for the coordinates of four corners.

Corner 1:

$$\begin{cases} x = \frac{R}{2} \\ y = \frac{R}{2} \end{cases} \Rightarrow \begin{cases} X1 = Xc + \left(\frac{R}{2}\right) (\cos \theta - \sin \theta) \\ Y1 = Yc + \left(\frac{R}{2}\right) (\sin \theta + \cos \theta) \end{cases} \quad (4-7)$$

Corner 2:

$$\begin{cases} x = \frac{R}{2} \\ y = -\frac{R}{2} \end{cases} \Rightarrow \begin{cases} X2 = Xc + \left(\frac{R}{2}\right) (\cos \theta + \sin \theta) \\ Y2 = Yc + \left(\frac{R}{2}\right) (\sin \theta - \cos \theta) \end{cases} \quad (4-8)$$

Corner 3:

$$\begin{cases} x = -\frac{R}{2} \\ y = -\frac{R}{2} \end{cases} \rightarrow \begin{cases} X3 = Xc + \left(\frac{R}{2}\right) (-\cos \theta + \sin \theta) \\ Y3 = Yc + \left(\frac{R}{2}\right) (-\sin \theta - \cos \theta) \end{cases} \quad (4-9)$$

Corner 4:

$$\begin{cases} x = -\frac{R}{2} \\ y = \frac{R}{2} \end{cases} \rightarrow \begin{cases} X4 = Xc + \left(\frac{R}{2}\right) (-\cos \theta - \sin \theta) \\ Y4 = Yc + \left(\frac{R}{2}\right) (-\sin \theta + \cos \theta) \end{cases} \quad (4-10)$$

Pixel orientation process is automated using Python code using the Arcpy package (see figure 4.6).

```
import arcpy
import os
def getParameterInfo(self):
    ...
R=arcpy.GetParameter(2)
...
def orient(Xc,Yc,Xs,Ys,Xe,Ye):
    if Xe-Xs==0:
        t=double(math.pi/2)
    else:
        t=math.atan((Ye-Ys)/(Xe-Xs))
    X1=Xc+(R/2)*(math.cos(t)-math.sin(t))
    Y1=Yc+(R/2)*(math.sin(t)+math.cos(t))
    X2=Xc+(R/2)*(math.cos(t)+math.sin(t))
    Y2=Yc+(R/2)*(math.sin(t)-math.cos(t))
    X3=Xc+(R/2)*(-math.cos(t)+math.sin(t))
    Y3=Yc+(R/2)*(-math.sin(t)-math.cos(t))
    X4=Xc+(R/2)*(-math.cos(t)-math.sin(t))
    Y4=Yc+(R/2)*(-math.sin(t)+math.cos(t))
    return [(X1,Y1),(X2,Y2),(X3,Y3),(X4,Y4)]
```

Figure 4. 6. Python code used for orientation

For our study areas, we used three different resolution of 20m×20m (Rieucros), 30m×30m (Saint Sulpice la Pointe) and 52m×52m (Toulouse). Whereas, based on the building classification, the defined area of the buildings are smaller than the area of the polygons (see table 4.1.).

Table 4. 1. Number and the area of the current buildings classified based on the building types

Building classes	Rieucros		Saint-Sulpice-la-Pointe		Toulouse	
	Number of buildings	Average Area (m ²)	Number of buildings	Average Area (m ²)	Number of buildings	Average Area (m ²)
Single dwelling	187	151	2 782	151	225 969	153
Low-rise housing	134	290	1 189	151	183 221	185
shop top housing	-	-	6	446	5 352	455
Medium-rise housing	-	-	-	-	2 223	538
medium/high-rise housing	-	-	-	-	208	714
High-rise housing	-	-	-	-	307	656

In order to both, considering the constraints and preserving the surfaces of the polygons as much as possible, the polygons are divided into the smaller squares. Therefore, if constraints drive the model to delete a polygon, the algorithm will delete a small square, which meet the restrictions, instead of whole polygon. To facilitate the process of dividing the polygon to the smaller squares, we follow divide and conquer strategy. For the case studies of Rieucros and Saint Sulpice la Pointe, the polygons are divided to 4 squares and for the Toulouse study area, the polygons are divided to 16 squares by double division out of 4 squares. Subdivision is done by frequently using the dichotomy of each side of the square. The process of division is done by the following method that is illustrated in figure 4.7. The python code has been made to automate this process as well (see figure 4.8).

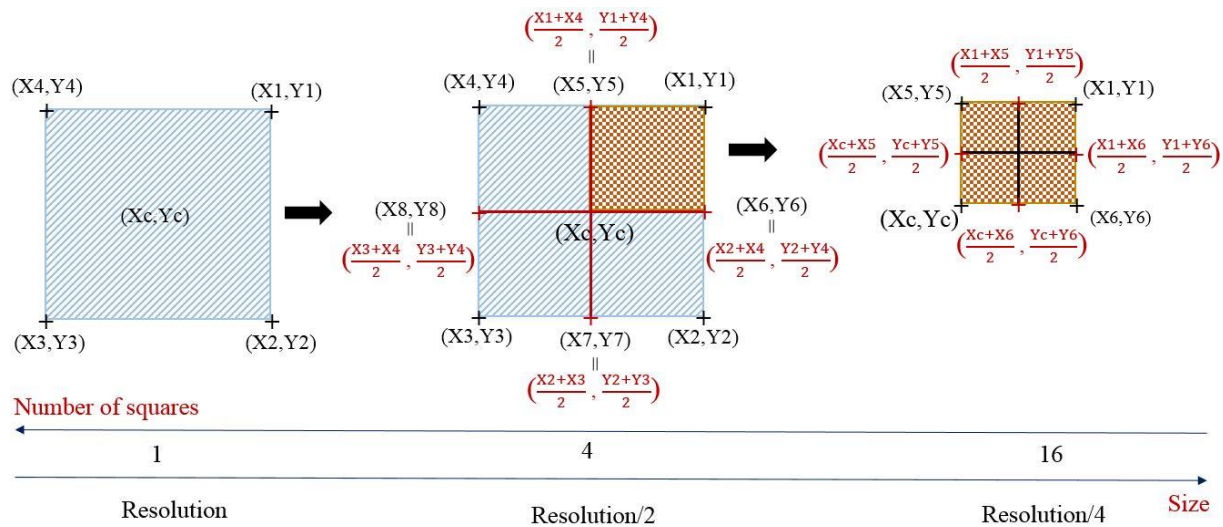


Figure 4. 7. An example of subdividing a polygon to smaller squares

```
def pix1(Xc, Yc, Xs, Ys, Xe, Ye) :
    T=orient(Xc, Yc, Xs, Ys, Xe, Ye)
    pix1X1=T[3][0]
    pix1Y1=T[3][1]
    pix1X2=(T[3][0]+T[0][0])/2
    pix1Y2=(T[3][1]+T[0][1])/2
    pix1X3=Xc
    pix1Y3=Yc
    pix1X4=(T[3][0]+T[2][0])/2
    pix1Y4=(T[3][1]+T[2][1])/2
    return [(pix1X1,pix1Y1), (pix1X2,pix1Y2), (pix1X3,pix1Y3), (pix1X4,pix1Y4)]
```

Figure 4. 8. Python code used for subdividing a polygon

4.2.3. Configuration the Building footprints

After orienting a polygon, some overlap between them to other layers of land occupation occur. In addition, it is necessary to define a distance between a polygon (which will define the new buildings representation) and different land occupation entities. The adjustment and positioning of new buildings follow the layout of the old buildings. Therefore, we apply the situation of existing buildings on the polygons in order to create new buildings that would respect the distance between buildings, distance to the river, and railways.

Two types of constraints are taken into account.

- The constraints that have a linear distribution in space including vegetation, water, roads and railways.
- The discrete constraints that can be modeled by points or small areas including remarkable buildings, cemeteries, airfields and sport grounds, activity areas, industrial or commercial areas and existing buildings.

The logic that is considered for these two types of constraints bases on finding the nearest neighbor and respecting the distances similar to it. The only difference is the definition of the notion 'nearest' between linear and discrete constraints.

To explain the method of defining linear constraints, we use the following example of the river. This method is essentially based on a double geo-processing buffer as follow:

- First, we measure the distance from the nearest existing building to the river (D_r) then we make a buffer of ten times of this distance ($10 \times D_r$). We assume all the buildings close to the sections of the river are at this distance (second buffer), which means the buildings that are at the edge of the river.
- The average distance of these buildings from the river is then calculated (the average distance of the buildings located in the second buffer). This average is considered as a minimum distance for new buildings off the river bank.

For other linear constraints, the similar procedure is done. In these cases the distance of the nearest building to each road section is measured and it is considered as an average distance for new buildings. Figure 4.9 illustrates the sample of the linear constraints definition.

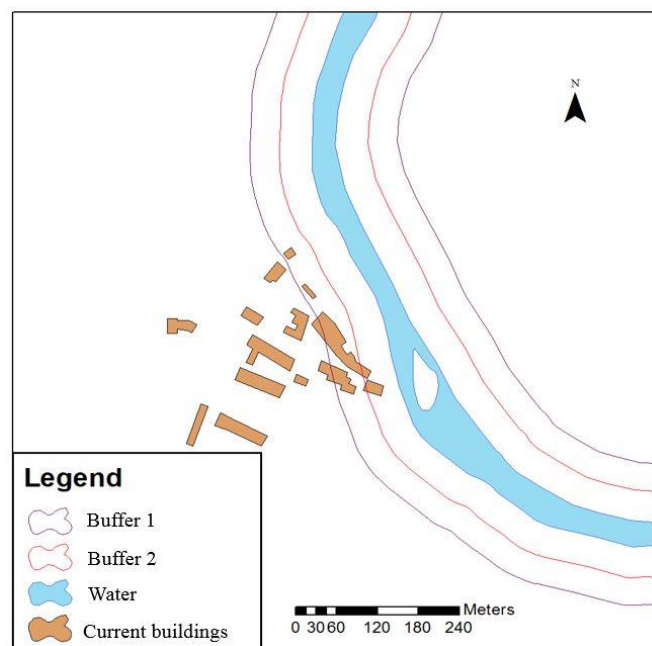


Figure 4. 9. Definition of river proximity constraint

To apply linear constraints to the polygon, the algorithm makes a second buffer with a distance equal to the average distance and remove the intersection of this buffer with the polygon. As mentioned earlier, one of the advantages of dividing polygons into smaller squares is that when we want to remove the intersection of polygons with a buffer, only the small squares that are within a buffer constraint are eliminated. When only a part of a polygon intersects with the buffer, this subdividing can help the model not to lose the polygon completely. In addition, a threshold for the intersection of a square to a buffer is defined. This threshold is equal to 30% of a square area that intersects with the buffer. This means, if a buffer overlaps more than 70% with a square, that square is deleted.

The discrete constraints are defined by the undifferentiated buildings, industrial buildings and some special spaces (i.e. excluded area, remarkable buildings, cemeteries, airfields, activity areas). In order to taking into account the distance of a polygon from the discrete constraints, it is needed to measure the distance of the current buildings from each other and from other discrete constraints. After obtaining the average distance for the current buildings, this distance is applied to the nearest discrete constraints for each polygon. Therefore, a buffer of the average distance is generated that defines the constraint of the existence of a building or special place. Afterwards, the same argument for eliminating intersections as for linear constraints applies to discrete constraints.

As discussed, in orientation each polygon rotates parallel to the closest road section. In the cases that are located two polygons next together, if the road orientation change, one polygon overlaps with part of the other. Therefore, this part of the overlap should be deleted from one of the polygons. The amount of overlap is depend on the angle of change of road direction from one section to another. The higher the road turning, the greater the overlap. In this step, the division of pixels plays an important role and the small square from one polygon, which overlap with another is removed. Therefore, we have created distances between the polygons while avoiding the problem of the superposition (see figure 4.10).

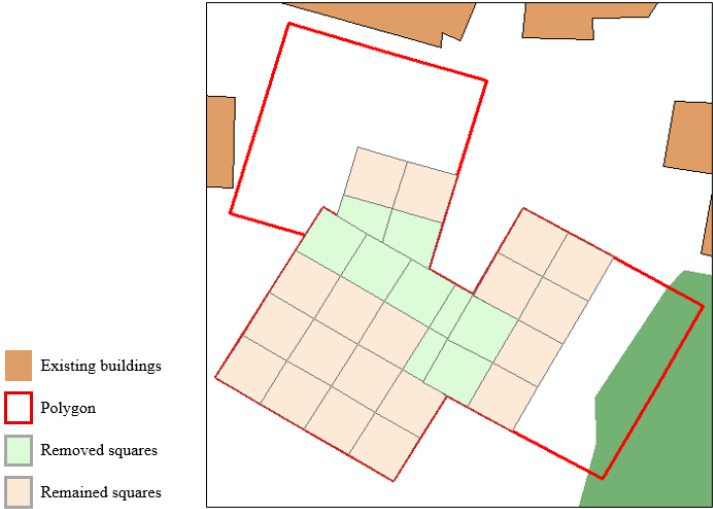


Figure 4. 10. Removed overlap areas of the polygons

4.2.4. Building Footprints Generation

After considering the required distance from the constraints, in this section we create the building footprints. In previous section the polygons were divided to small squares. Here, in order to generate the footprints these squares are assembled according to the building type classification and the urban fabric scenarios.

As illustrated in table 4.2, we make identifiers for the polygons and the small squares, while dividing them that identify the polygons (N°2), the big squares (N°3) and the small squares (N°4). Therefore, each polygon is divided to four squares (for Rieucros and Saint Sulpice la Pointe study area) and sixteen squares (for Toulouse study area). These identifiers can help us to reconstruct the polygon. In addition, they make it possible to identify the position of the squares of the same level of division (N°1) and are used to create buildings footprints (see figure 4.11).

Table 4. 2. Pixel identifiers description

N°	Label	Description
1	name	L : left R :right D :down U :up
2	polygon	identifier of a polygon (Toulouse, Saint Sulpice la Pointe and Rieucros)
3	big square	identifier of a big square (Toulouse and Saint Sulpice la Pointe)
4	small square	identifier of the squares of subdivision (Toulouse)

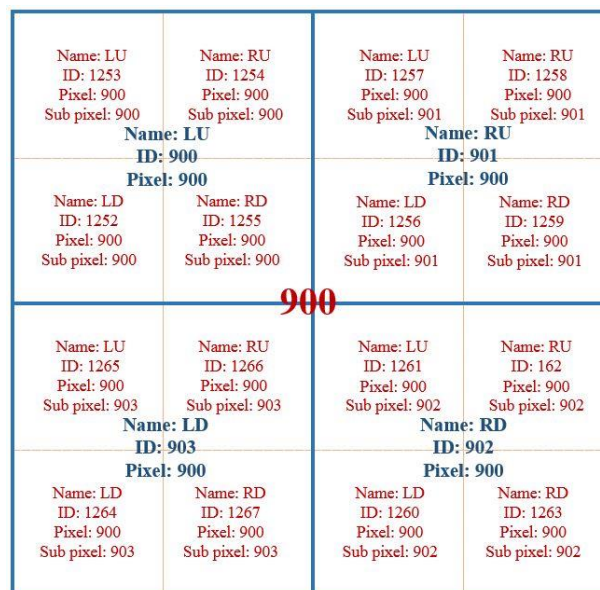


Figure 4. 11. An example of the polygons and the squares identifiers, case study of Toulouse

The idea is to build buildings footprints with the surfaces remains among the small squares. We have defined maximum of different areas (Smax) for the new building footprints with regards to the building classification, the urban fabric scenarios and the size of the polygons (see table 4.3).

Table 4. 3. Area of the new building foot prints buildings classified based on the building types

Study area	Smax (m2)			
	Single dwelling	Low-rise housing	shop top housing	Medium-rise housing
Rieucros	144	224	-	-
Saint Sulpice la Pointe	121	250	400	-
Toulouse	196	272	-	441

The squares are assembled according to Smax of each study area. This Smax classification is also used in the urban fabric scenario with mixed building classes. For make the footprints of buildings we should first assemble small squares (with same IDs), while checking if the total area exceeds the maximum defined area relative to each scenario (Smax). If the area of the assembled squares be less than Smax, the whole polygon will represent one building. Then, we build a layer that contains only the polygons whose surfaces exceed Smax. For these polygons, we return to the state of the decomposition using a simple function "clip" of ArcGIS. We gathers the two small squares which belong to the same subpixel (the square of the first division) but which are both to the left or to the right of the set of small squares of the sub-pixel, i.e. LU (Left/Up) with LD (Left/Down) and RU (Right/Up) with RD (Right/ Down).

This combination is chosen because in our algorithm we assume the width of a building locates on the side of the road. Since the polygons are oriented towards the road, the sub-squares facing the road are chosen in such a way that they carry the 'U' (Up). In the case that we assemble the two squares that bring 'U' together and the two others bring 'D' together, we will have a house facing the road and one behind the other (see figure 4.12). Therefore, the both buildings will have access to nearest road.

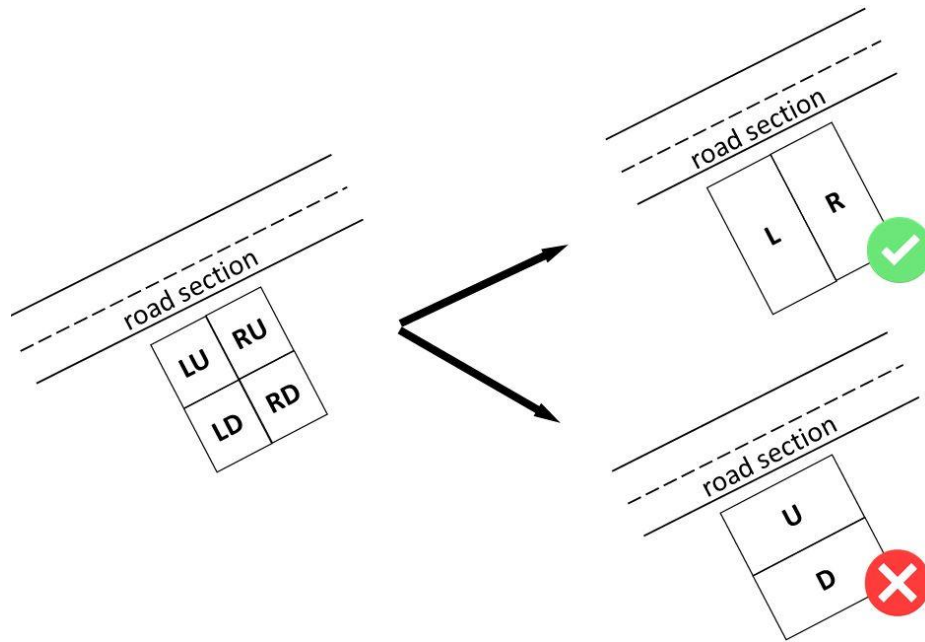


Figure 4. 12. Assembling sub pixels respecting the roads

Afterwards, we make the union of three sectors:

- Left part: which contains the left part of the polygons that have the area larger than S_{max}
- Right part: which contains the right side of the polygons that have the area larger than S_{max}
- Inf S_{max} : which contains polygons that have a surface less than S_{max}

4.2.5. Positioning Building Representations according to Urban Fabric Scenarios

The urban fabric scenarios are based on one or the combination of the building types considering the density of population. After assembling the squares, we define different possible types of footprints considering an erosion to each polygon according to their surfaces and the urban fabric scenarios (see figure 4.13, figure 4.14 and figure 4.15). Therefore, we obtain the desired surface for the building footprints as well as respecting the S_{max} and the distances between the new buildings. Defining different footprints is used in next step to create the 3D representation of the scenarios.

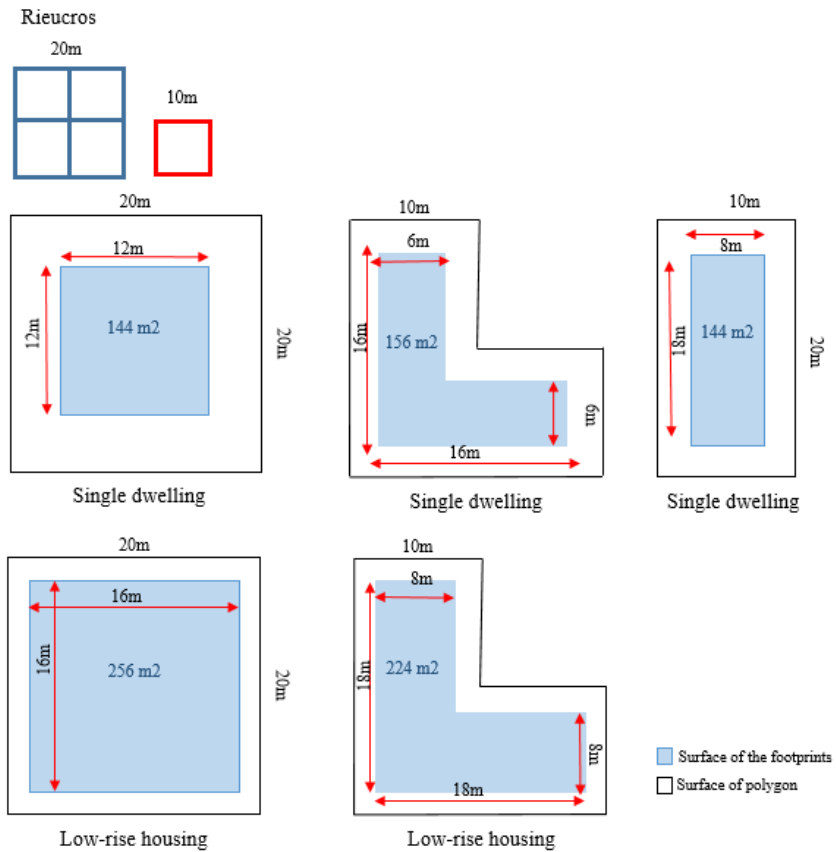


Figure 4. 13. Create the building footprints by making different erosion to each polygon according to the scenarios, Rieucros

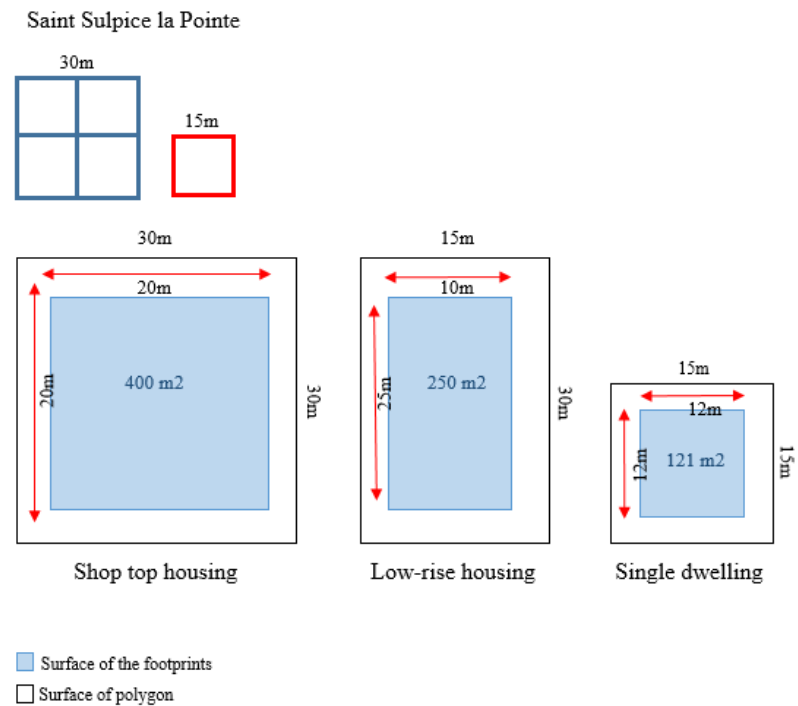


Figure 4. 14. Create the building footprints by making different erosion to each polygon according to the scenarios, Saint Sulpice la Pointe

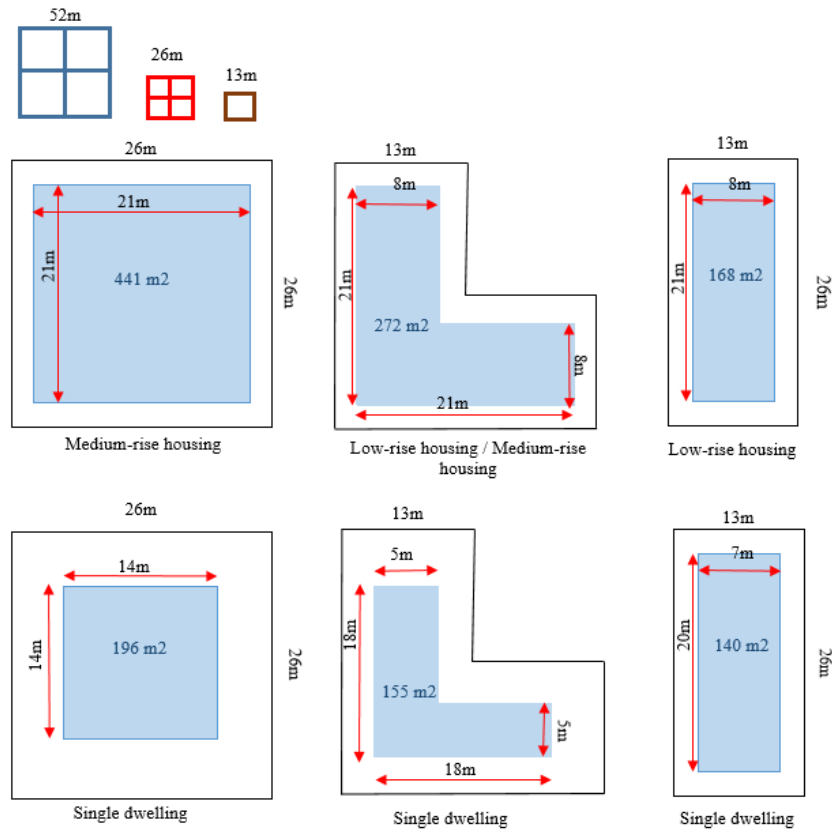


Figure 4. 15. Create the building footprints by making different erosion to each polygon according to the scenarios, Toulouse

There is often a relation between the height of the buildings, their number of floors and their footprints area as well as population density (Biljecki, 2017). In this section, we calculate different probabilities for each polygon according to its neighborhood building class. These give the information of the possible height for the new buildings. The process of finding height for a new building respects different scenarios. For uniform scenarios, we add an extrusion value to our model. Given the scenarios where it is necessary to have mixed height values according to predefined percentages associated with each height (the percentages of different building types that are defined by urban fabric scenarios), we use an algorithm that combines the random aspect and a statistical interpolation (see figure 4.17).

According to urban fabric scenarios, we have maximum three types of buildings that have three different heights (two types in Rieucros and three types in Toulouse and Saint Sulpice la Pointe). In our algorithm, we ordered the buildings in ascending order of their surfaces ($SB1 < SB2 < SB3$). For each building type of B1, B2 and B3, their percentages of combination in the scenarios are defined by Prs1, Prs2 and Prs3, respectively. P1, P2 and P3 indicate the average height probabilities for each building. The average height probability for each building is calculated from the nearest current building height to it. To do this, it is needed to classify the new building according to the distance to the neighbor as follows (see figure 4.16):

- Class1: New buildings that have at least one neighbor that is part of the current buildings on a circle (r_1)
- Class2: New buildings that have at least one neighbor that is part of the current buildings on a limited ring between the small circle (r_1) and the large circle (r_2)
- Class3: New buildings that have no neighbors that are part of the current buildings on a circle (r_2)

The values r_1 and r_2 are the radius that are calculated from the distance nearest neighbor of each existing building and apply the quintile classification. We calculate the distance between the new building and the current buildings, which is in the spaces that is defined by the class (DIS), then the inverse distance (IDIS) and the sum of the inverse distance (SIDIS). Then, we calculate the influence weight of the type of each building on the type of the new building (building with height equal H_i). Finally, we deduce the total probability for each type associated with this building and we obtain a new P_i which give the probability of the building with height H_i .

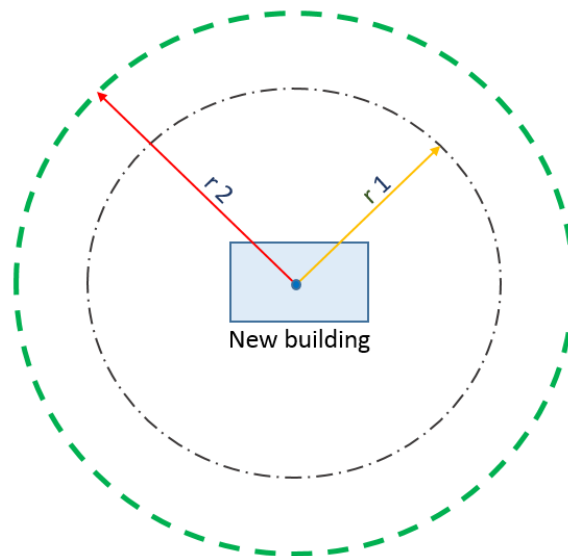


Figure 4. 16. Searching for the nearest neighbor

In next step, we divide the buildings in three class according to their types associated with a scenario. We calculate the initial percentage (P_{ri}) of each type for the variable percentage (P_r):

- The buildings that have the surface SB1 associated with the height, H_1 ($P_r = P_{ri1}, P_{rs1}$)
- The buildings that have the SB2 surface associated with the height, H_2 ($P_r = P_{ri2}, P_{rs2}$)
- The buildings that have the surface SB3 associated with the Height H_3 ($P_r = P_{ri3}, P_{rs3}$)

Therefore, three different percentages for each type of building are calculated including:

- Initial percentage: fixed

- Variable percentage: variable
- Desired percentage: goal

Then, we try to adjust the current percentage so that it is very close to the percentages entered by the user of the model according to the following diagram (see figure 4.17):

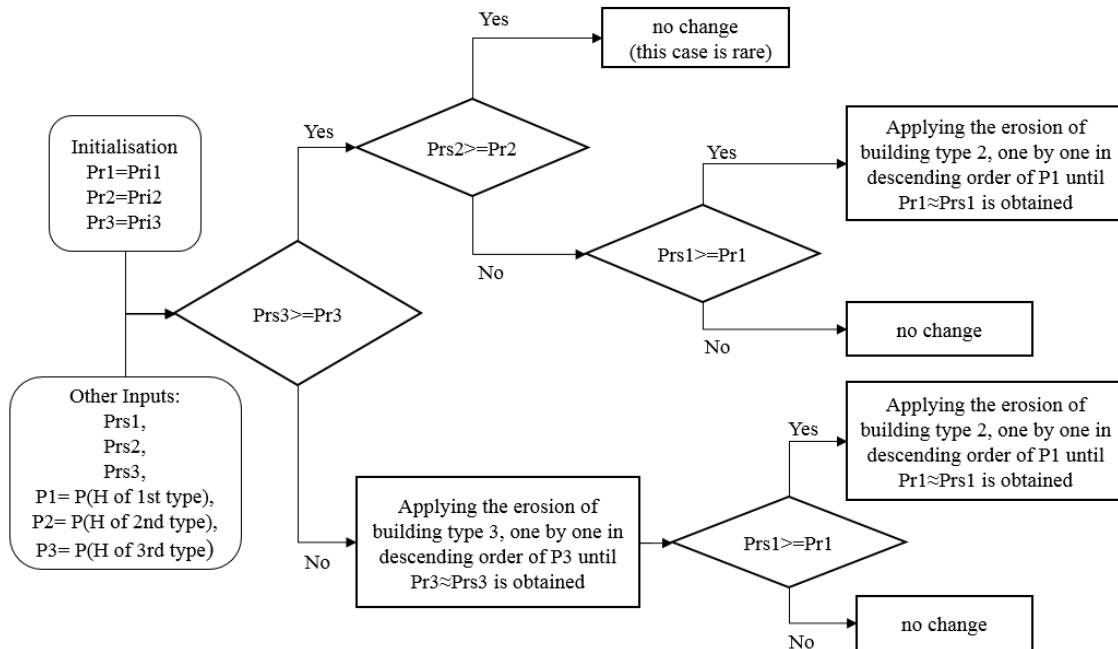
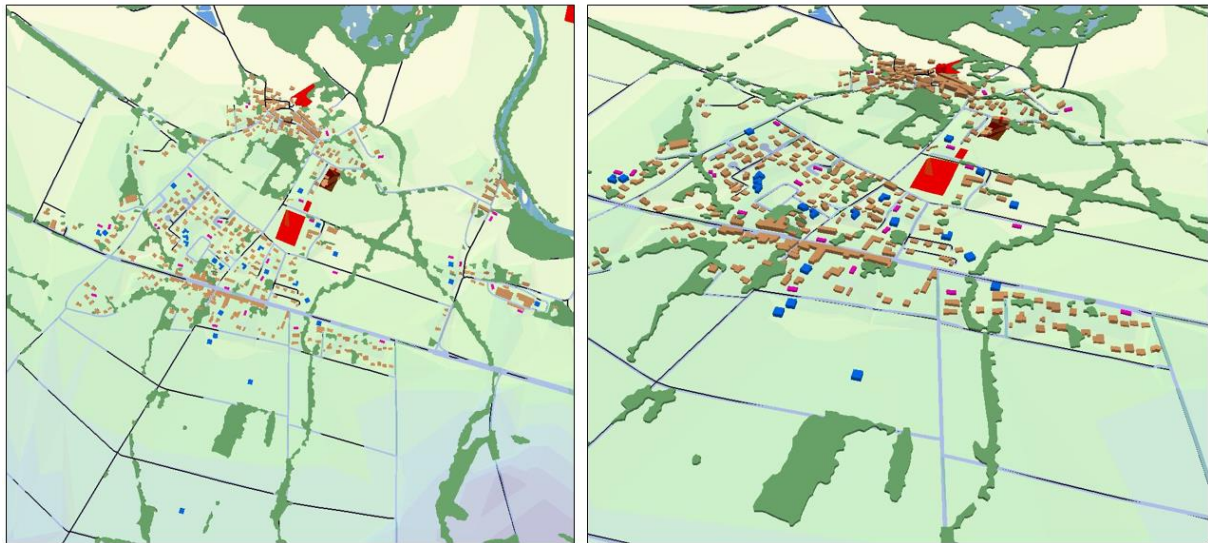


Figure 4. 17. The algorithm of calculating the probability of the height for each building according to the building types and urban fabric scenario

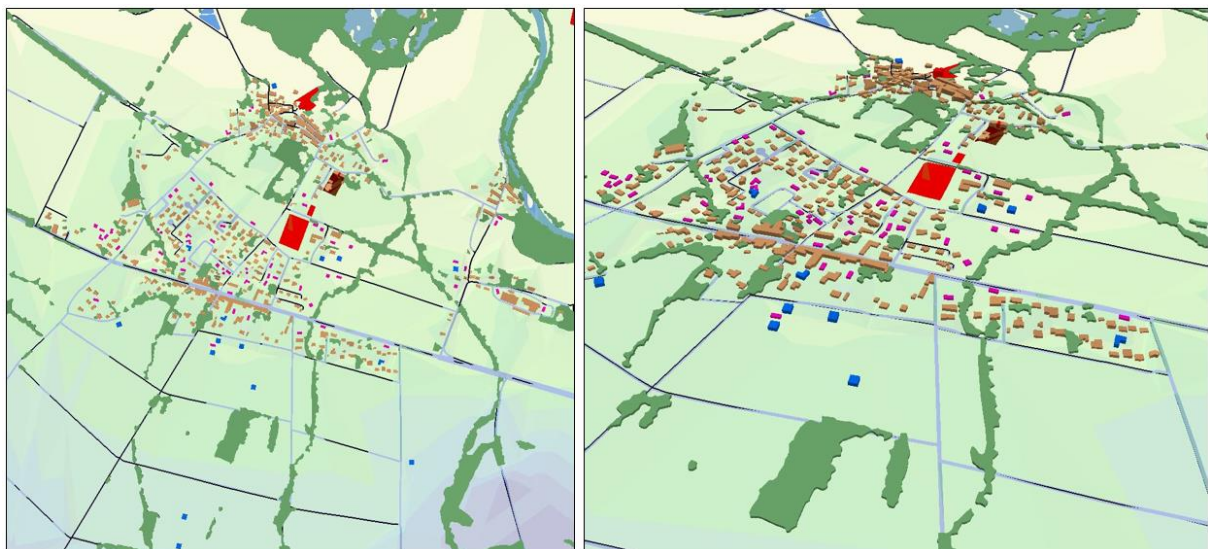
4.3. 3D Visualization of the City of Tomorrow

After, generating the footprints and estimating their related height, in this section we illustrate the 3D representation of the model for each scenario. In order to visualize the 3D model of the city, we first create the Digital Elevation Model (DEM) using BD Topo data altitudes (IGN). We use a standard process of rasterization and 3D interpolation with Arcgis and obtained a DEM in IGN69 altimetry system. Afterwards, we use the "InterpolateShape" tool in the surface feature section (3D analysis on Arcgis) to associate third dimension with new buildings. The results are displayed in ArcScene by making an extrusion of the various layers including new buildings using the height calculated in the previous section. Figures 4.18, 4.19 and 4.20 illustrate the 3D representations of the urban fabric scenarios of Rieucros study area for the environmental protection scenario level 3 (EEP). These figures show the different urban sprawl obtained for the urban fabric scenarios.



- Existing buildings
- Low-rise housing
- Single dwelling

Figure 4. 18. 2D and 3D views, medium/high dense fabric scenario (13 growth cycle), Rieucros



- Existing buildings
- Low-rise housing
- Single dwelling

Figure 4. 19. 2D and 3D views, medium dense urban fabric scenario (18 growth cycle), Rieucros



Figure 4.20. 2D and 3D views, low dense urban fabric scenario (23 growth cycle), Rieucros

4.4. Chapter Conclusion

In this chapter, the SLEUTH results (pixels) are transformed into 3D building representations with regards to the urban fabric scenarios. We have transformed the pixel from raster data to building footprints. In this process we have consider different constraints such as the direction of the footprints and the distances to urban objects and geographic features. Afterward the probability of the appropriate heights depending to building classifications are calculated according to the urban fabric scenarios and added to these footprints and the results are displayed in ArcScene.

Although the provided 3D model is a primary and simple model, 3D representations of scenarios allow having different images of the city of tomorrow for applying it to urban policies and supporting the scientists and authorities in charge of urban planner and management

Chapter 5 : Conclusion and Perspectives

In final chapter, we review the research contributions of the thesis and discuss possible perspective work directions. This research proposes some urbanization scenarios by applying SLEUTH model improvement that integrates more topographic data, urban fabric and demographic data. SLEUTH's acronym is derived from its data input requirements including Slope, Land use, Exclusion, Urban, Transportation and Hillshade. The proposed method investigates the impacts of building types and environmental rules on urban sprawl, in order to help the public policies decision making.

The main objectives of this work include:

1. Representing the impacts of constructions and environmental constraints on urban sprawl.
2. Generating diverse urbanization scenarios, which lead:
 - to show the possible impact of urban sprawl.
 - to study the Human Settlement Capacity (HSC).
 - to improve our understanding of an urban sprawl simulation.
 - to give different images of the city of tomorrow to choose and reflect on urban policies.
 - to improve public policies decision making.
3. Challenging the results of the classical urban growth methods that are often independent from the factors of building types and population, and give an improvement to provide a more reliable method.
4. Providing a way to simulate urban growth, with less semantic information loss, and to show the differences of sprawl and dense growth.

With these objectives, this Ph.D. attempts to response of the following questions about the evolutionary trajectory of urbanization as well as densification:

- *What are the urbanization and densification?*

The balance between housing and land protection is one of the environmental and social concerns of the public authorities. Public policies are based on providing housing according to the demands while considering the effects of urbanization and densification. Urban growth modeling attempts to represent different scenarios of the urban expansions in terms of space consumption, the urban sprawl configuration,

density and demography, and the socio-economic and environmental effects of urbanization. A prospective simulation is interesting to explain the determinants of urbanization or to study the effects of new policies on artificialization.

- *Why doing urban sprawl simulation, while we know that all simulations are fictions and they are based on some assumptions?*

Urban growth simulations can be used to see what can happen in the future, and how will be the housing, population growth and land cover changes and where can occur. These simulations can help us find and protect some areas against urbanization. Moreover, they can be used to think about future urbanization and make choices on urban politics.

Thesis Contributions

The main contributions of this thesis are as follows:

1. SLEUTH model has the possibility of generating different scenarios of land use changes by setting the composition of SLEUTH input layers. As discussed before, five different environmental-based scenarios are defined with different level of environmental protection. Four of them are scenarios level 0 to level 3, where the upper scenarios preserve more the environment (e.g. green lands and forests), and last scenario is defined as an attraction-based scenario that, in addition to excluded areas, also integrates areas of attraction into the simulation algorithm. The proposed environmental scenarios lead to simulate the forecasting urban growth while respecting geographical features and the environmental constraints.
2. A building type classification is defined. The numbers and height of existing buildings are extracted and the current buildings are classified according to building type classification. The current buildings give us the prospective view for the futures building. The new urban pixels are also classified according to probabilities that are calculated with regard to their nearest neighbor (current buildings).
3. SLEUTH model does not consider explicitly population in its simulation. For the current buildings the number of inhabitants are estimated and for the prospective urban growth the average estimate of population is calculated.
4. Based on estimated population growth and building type classification, the primary urban fabric scenarios consist of different densities from sprawl to high dense urban are defined.
5. Considering the amount of population that could be accommodate for each scenario and the estimated population for the target date the final urban fabric scenarios are specified.
6. Fictive 3D buildings are generated and 3D representation of the urban fabric scenarios are provided, in order to facilitate the interpretation of simulation results, differentiate the scenarios and better understand the SLEUTH simulations.

Urban sprawl phenomena is a big challenge for the authorities and urban planners. Urban simulation techniques are willing to solve the various problems of urban growth modeling. Among all dynamic models the Cellular Automata (CA) models are more common for their applications in urban areas and they can be easily integrated with RS data and GIS. SLEUTH as a CA model offers great potential for simulating the dynamic nature of urban expansion and can be compatible with urban environment modeling. SLEUTH uses the historical data in order to calibrate the model. In this model, the impacts of population growth and urban tissue are implicitly considered during the calibration phase, however, the changes in population growth rate or in building types cannot be included in its simulations. In addition, the results of SLEUTH model are limited to some raster data that is difficult to interpret for decision makers. The results are some pixels on which urbanization is supposed to occur. These results do not make much sense from urbanism point of view. This Ph.D. provides a method to evaluate the SLEUTH results and to investigate the effects of environmental constraints and constructions on urban sprawl. In our research, the version SLEUTH-3r is used and different types of scenarios are defined according to urban policies.

The Geospatial database that is used as input topographic data is composed of the maps of 2000, 2008, 2012 and 2017. Slope and hillshade maps are derived from Digital Elevation Model (DEM) of RGE ALTI with a spatial resolution of 5m, provided by IGN. Urban areas, excluded areas and transportation maps are generated automatically from BD TOPO and BD ORTHO from IGN. Population and census on district zone are taken from INSEE database of 2011.

In this research, the SLEUTH model is applied on three study areas including Toulouse metropolitan, Saint Sulpice la Pointe and Rieucros, in order to evaluate the scalability of the model. We use three different pixel sizes (for three study areas) to verify the impacts of pixel size in SLEUTH simulation results. The results show that the size of the pixel has great influence on simulation of the urban sprawl.

In calibration process of SLEUTH, the growth coefficients are calculated in order to simulate the prospective urban growth with the same tendency as today. The metrics that are used for choosing the best-fit coefficients are calculated separately in calibration process for each scenario according its input maps. The process of choosing the best fit coefficients in calibration is not definite. There are different ways to find the appropriate coefficients that do not necessarily lead to a single answer. Therefore, several results can obtain from different scenarios that is difficult to control them.

The environmental-based scenarios are created by altering exclusion maps of the input data of SLEUTH. Afterwards, by adding the building type and demographic factors, different urban fabric scenarios are generated in order to give more flexibility in urban sprawl simulation. Integrating the additional data leads hopefully to better parameterization of the model. Given that we know that prediction of urban growth is an indeterminate proposition, several prospective scenarios based on the new model parametrizations are defined related to different urban area (the Toulouse metropolitan, Saint Sulpice la Pointe that is a town around Toulouse, and Rieucros as a small community in a rural area), in order to query the simulation ability in

different scale. These scenarios show the simulation capabilities of the model and make it possible to improve our understanding of an urban sprawl simulation. The simulation results of the three different case studies with various sizes and populations provide a good view of the scalability of the proposed method. A 3D representation for each prospective urban growth simulations is provided to facilitate the interpretation of the SLEUTH simulation, to better understand the SLEUTH simulation results and to differentiate the scenarios, in order to support the scientists and authorities in charge of urban planner and management. The findings allow having different images of the city of tomorrow to choose and reflect on urban policies.

Considering the specific population increased, the urban fabric scenarios provide four different type of urban growth including sprawl urban, medium dense urban, medium/high dense urban and high dense urban. The results show that changing the urban fabric scenarios has a strong impact on the limitation of urban sprawl, thus saving agricultural and natural landscapes. They also help us to understand how different urban fabrics impact the urban sprawl.

In this research, different urban sprawl scenarios for different kind of environmental protection rules while taking into account the population demand or at least population growth estimation are defined. Some new effective factors including estimated population, building types and more topographic data are integrated to our model in order to improve the number and location of simulated pixels per growth cycle. Classification of the building types and the estimation of the population growth try to provide required amount of urban growth, and the protection rules attempt to regulate the location of growth areas. We have demonstrated that the urban growth is widely dependent to those factors and different growth cycles might give the similar results by altering the scenarios. Proposing different simulation of urban sprawl shows the possible impact of urban sprawl and the capacity of urban settlement according to different scenario as well. To conclude, we can say that the proposed method in this research can remarkably improve our understanding of an urban sprawl simulation.

Perspective

In the course of this Ph.D., we have faced to some challenges and questions. These queries lead us to further improvement and future works.

Zoning: In this research, the SLEUTH model is used to simulate different study areas including a metropole, a town and a small commune in a rural area. In large cities, the building types and density of downtown and their suburbs are different. In general, the density decreases from the city centers towards the edges of the cities. In addition, there are few lands that are available to build in the centers. Zoning of the study area in the calibration phases of SLEUTH model could improve the results of the simulation and increase the accuracy of the model. Although, in this research, zoning is used in attraction-based environmental protection scenario for all the study areas, it can be considered in calibration mode, as well.

Effects of road networks: As discussed in this research, the road network affects the SLEUTH results through the road gravity coefficient and road influenced growth rule. This means that

simulated urban expansion is influenced by the road network. The SLEUTH model, initially simulates the urban pixels for the first growth cycle and iteratively continues the process (considering the simulated urban map of the previous growth cycle) until achieving the target date. Although, the SLEUTH updates the urban map for each growth cycle in order to simulate the urban growth for the next step, the role of the new roads in this process has been overlooked.

For this purpose, we have designed an algorithm, which aims to update automatically the transportation map to connect the simulated urban patches to the existing roads network. The shortest way is considered to connect the urban area to the road network, while avoiding to pass through protected or urbanized areas. When it is faced with protected or urbanized areas, it launches again at the end of the detour to finish the path. The algorithm runs frequently and the roads update in each period. This algorithm is a combination of two interactive process: the houses that are constructed influenced by roads gravity (roads creates houses) and the roads that are constructed to connect the new houses (houses creates roads). The results are presented in the EDUBIM (Da Silva et al., 2018), however, the algorithm is still in infancy.

Therefore, updating the road network for each growth cycle during the modeling could influence the amount of the urban pixels and simulated urban expansion. Moreover, it can improve the process of building creation (chapter 4). In the 3D modeling of this research, when we want to adjust the polygons to a road section (in orientation step), the new roads can help to orient the polygons to the forecasting road networks that are closer to them. The can affect also in dividing the pixels and positioning the buildings.

Modeling the non-residential 3D buildings: The 3D buildings that are created in this research are the undifferentiated buildings. The accuracy of the model can be improved by calculating the average estimate of employments and therefore obtaining the required amount of commercial and industrial buildings. Moreover, by estimating the population growth separately for different ages, we can define the scenarios that simulate the educational buildings and the sport activity areas, as well.

Pixel resolution: By the pixel resolution of this research (52*52m, 30*30m and 20*20m), each pixel, often in largest pixels, represents more than one building. This means that in one pixel might be many buildings from different building class. For the future work, it could be considered the SLEUTH input maps with smaller pixel size (in case of availability of the data). In this case each building can be represented by one pixel or more. Later, the pixels that are belong to a building can be joined together, to represent the whole building (similar to section 4.2.4, chapter 4). Therefore, the scalability of the model and accuracy of the simulation can be increased. Moreover, when the model is faced to constraints, the small pixels can be eliminated which affects the amount and precision of the simulated urban areas.

As discussed in the report, in our model the pixels are divided to small squares size (for the study areas of Toulouse and Saint Sulpice la Pointe) in order to create buildings from the pixels. The pixel division is done also to limit deletion of urban pixels in places that overlap with restrictions or to observe the distance between pixels to restrictions or other urban objects. The maps with larger resolution can be used as in SLEUTH modeling, however, they greatly increase the running time of the algorithm.

Creating 3D buildings with more details: The 3D buildings represented in this research are the block models with flat roof structure (equivalent to LoD1 of CityGML). In the future works, buildings could be developed in more LoDs. Considering the new polygons achieved in chapter 4, the 3D buildings with more LoDs can be created based on CityGML standards and construct the 3D building representations according to the footprints of the polygons (Pedrinis and Gesquière, 2017). Developing a 3D model based on CityGML can facilitate the data exchanges as well (Billen et al., 2012; Chaturvedi et al., 2017).

Creation of the 3D buildings with respecting urban regulations: Local Urban Planning schemes (LUPs) aim to regulate the development of a city. Therefore, the urban plans are designed according to the scale of a city or a building as well as their displacement, orientations or other subjects while respecting LUP. The city issues have complex relations, which make it difficult to respect different aspects of the city in modeling (He et al., 2014; Brasebin et al., 2016).

He et al. (2014) have proposed to generate 3D building layouts that comply with LUP rules, while optimizing urban indicators. Their model respects some of the urban planning articles as well as considering the distance to parcel borders, distance between buildings, parcel coverage ratio, floor area ratio, angle to parcel borders and building height.

In creation of the buildings (in chapter 4), the adjustment and positioning of new buildings follow the layout of the existing buildings. In addition, the average distance from new buildings to existing buildings and to other urban objects is calculated and considered in the creation of new buildings. In the future works, we can develop a model that respect to some of the articles that are provided by the urban planning code in France (similar to works of He et al. (2014) and Brasebin et al. (2016)), although, they have worked on a small study area.

Applications of urban fabric scenarios: Except the effect of different urban fabric scenarios on environment and the impacts of constructions and environmental constraints on urban sprawl, the urban fabric scenarios that are presented in this research can be used in other applications. As an example, the amount of the energy consumption can be estimated according to dense and sprawl urban growth. The estimation of consuming energy can be achieved with regards to building classes, residential surfaces and the population growth in different scenarios, which can be used by decision makers for the future urban development. As another example, the traffic rate can be estimated according to the population and urban fabric scenarios, as well. This can help to calculate the pollution that can be produced according to different scenarios of dense and sprawl development.

Annex A: Classified List of Researches and Applications of Simulating Urban Growth and Land Use / Land Cover Change

As mentioned in Chapter one, some distinct applications used as land use and urban simulation techniques have been identified. The more used urban growth and LUCC modeling techniques could be divided into four categories including fractal modeling, artificial neural network modeling, agent-based modeling and cellular automata modeling. Here, based on the categories defined before, a list of different simulation techniques as well as their required data, their constraints, their interoperability to other data and systems (e.g. RS data, GIS) are presented. The list of documented applications is illustrated in table A1. The classified list could be useful for the urban planners and researchers to choose the best method for their use case and could provide an appropriate view for urban planners in the field of urban planning development.

Table A. 1. Examples of the applications of urban growth and LUCC models, divided into four groups including fractal modeling, artificial neural network modeling, agent-based modeling and cellular automata modeling.

Research title	Application
<i>Fractal modeling: The fractals are the dynamic objects that their self-similarity and scale dependency can define the complexity of spatial objects (section 1.2.2.1)</i>	
1 The Use of Remote Sensing and Landscape Metrics to Describe Structures and Changes in Urban Land Uses (Herold et al., 2002)	In order to detect urban land use changes, the landscape metrics contain the fractal dimension are used.
2 Urban Growth Prediction Modeling Using Fractals and Theory of Chaos (Triantakonstantis, 2012)	The fractals urban growth and theory of Chaos are used for prediction modeling in the touristic village of Pogonia Etoloakarnanias, western Greece.
<i>Artificial neural network modeling: ANN models use a machine learning approach to quantify and to model complex behavior of urban development (section 1.2.2.2)</i>	
3 Artificial Neural Networks: Forecasting Time Series (Vemuri and Rogers, 1994)	In this research, the time series and the forecasting problem contains forecasting the behavior of multivariate time series using neural networks have been explored.
4 Modeling urban dynamics with artificial neural networks and GIS (Weisner and Cowen, 1997)	The GIS and ANN as spatial analytic tools are integrated in order to model the urban growth in sub-regions of a metropolitan area. Comparing to a linear regression model, ANN performs more accurate as a non-linear model of dynamic urban systems.

Table A.1. (Continued)

Research title	Application
5 Using neural networks and GIS to forecast land use changes: a land transformation model (Pijanowski et al., 2002)	The Land Transformation Model (LTM), GIS and ANN have been used in order to forecast land use changes of Michigan's Grand Traverse Bay Watershed; and the impact of some factors such as roads, highways, residential streets, rivers, Great Lakes coastlines, recreational facilities, inland lakes and agricultural density have been reviewed on urbanization patterns.
6 Urban Expansion Simulation Using Geospatial Information System and Artificial Neural Networks (Tayyebi et al., 2009)	The GIS, ANN, Remote Sensing (RS), socio-economic and environmental variables have been used to simulate an urban expansion model which parameterized for Tehran Metropolitan Area; and the impacts of some factors such as road, building area, service center, green space, elevation, aspect and slope on urbanization have been reviewed.
7 An urban growth boundary model using neural network parameterization: An application to Tehran (Tayyebi et al., 2011)	An urban growth boundary model (UGBM) is presented that has used ANN, GIS and RS to simulate the complex geometry of the urban boundary of Tehran, Iran. Seven predictor variables of urban boundary geometry of the study area including the roads, green spaces, slope, aspect, elevation, service stations, and built-area were used in this model.
8 Urban growth modeling using an artificial neural network, a case study of Sanandaj city, Iran (Mohammady et al., 2014)	The ANN, GIS and RS data set are used in this research in order to model the urban growth in Sanandaj metropolitan, Iran. The data set that has been used contains the distance to principle roads, distance to residential areas, elevation, slope, distance to green spaces and distance to region centers.
<i>Agent-based modeling: Agent-based models are used to simulate the effects of the non-linear behavior of individuals on land change and the complex urban systems (section 1.2.2.3)</i>	
9 Agent-based modeling and genetic programming for modeling land change in the Southern Yucatán Peninsular Region of Mexico (Manson, 2005)	The use of genetic programming as a computational intelligence technique is shown in order to model a decision making considering the social and environmental drivers of land change in simulation modeling in the Southern Yucatán Peninsular Region of Mexico.

Table A.1. (Continued)

Research title	Application
10 Key challenges in agent-based modeling for geospatial simulation (Crooks et al., 2008)	The Agent-based modeling (ABM) and its challenges have been described. The challenges are included the purpose for which the model is built; the extent to which the model is rooted in independent theory; the extent to which the model can be replicated; the ways the model might be verified, calibrated and validated; the way model dynamics are represented in terms of agent interactions; the extent to which the model is operational; and the way the model can be communicated and shared with others. These challenges are investigated with a pedestrian model for emergency evacuation, a hypothetical model of residential segregation model and an agent-based residential location model on London.
11 Modeling the impacts of land system dynamics on human well-being: Using an agent-based approach to cope with data limitations in Koper, Slovenia (Robinson et al., 2012)	In this research, the utility theory, logistic regression, and cellular automaton-like rules are integrated to represent the decision-making strategies of different agents. The purpose of this study is to evaluate the impact of land-use and land-cover changes on human well-being in the Municipality of Koper, Slovenia, by investigation on the provision of highly productive agricultural soil, the extent of noise pollution, and quality-of-life measurements.
12 Spatiotemporal simulation of urban growth patterns using agent-based modeling (Arsanjani et al., 2013)	They have integrated socioeconomic data, RS and GIS in order to provide a geo-simulation approach that couples agent-based modeling with multi criteria analysis and simulate spatiotemporal patterns of urban growth in Tehran, Iran.
<i>Cellular automata modeling: CA models are bottom-up and discrete dynamic spatial models that could be used in urban sprawl mechanisms, urban planning theories and urbanization effects (section 1.2.2.4)</i>	
13 Cellular automata and fractal urban form: a cellular modeling approach to the evolution of urban land use patterns (White and Engelen, 1993)	In this paper, a CA model is developed in order to simulate the spatial structure of urban land use over time. The model produced fractal land-use structures for the urbanized area and for each individual land-use type.
14 From cells to cities (Batty and Xie, 1994)	A general class of CA models is proposed for urban simulation. The model is used to simulate the historical ‘cell’ city of Savannah, Georgia.

Table A.1. (Continued)

	Research title	Application
15	Methods and techniques for rigorous calibration of a cellular automation model of urban growth (Clarke et al., 1996)	In this research, the different calibration methods that used in CA simulation of the spatial extent of urban growth are explored.
16	Cellular automata and geographic information systems (Wagner, 1997)	The GIS and CA are integrated and the advantages of this integration are discussed.
17	Loose-coupling of a cellular automaton model and GIS: Long-term growth prediction for the San Francisco and Washington/ Baltimore (Clarke and Gaydos, 1998)	The calibration and prediction results of two rapidly growing study areas (San Francisco Bay region in California and Washington/Baltimore corridor in the Eastern United States) are presented and compared and the role of GIS in the model is discussed.
18	Modeling urban dynamics through GIS-based cellular automata (Batty et al., 1999)	The generic problem of modeling within GIS is introduced and a range of hypothetical urban simulations that illustrate the diversity of model types is presented.
19	Calibration of cellular automata by using neural networks for the simulation of complex urban systems (Li and Yeh, 2001)	In this research, a CA model is used to simulate the complex urban systems. They have used ANN, in both calibration and simulation process.
20	Geographic Information Systems and Environmental Modeling (Clarke et al., 2001)	The modeling frameworks, paradigms and approaches of GIS, spatial data processing and environmental modeling are reviewed.
21	Neural-network based cellular automata for simulating multiple land use changes using GIS (Li and Yeh, 2002)	A new method of simulating the evolution of multiple land uses based is presented. In this method, the CA is integrated to neural networks in order to calculate conversion probabilities for competing multiple land uses. GIS is used to obtain site attributes and training data, and to provide spatial functions for constructing the neural network.
22	Modeling Dynamic Spatial Processes: Simulation of Urban Future Scenarios through Cellular Automata (Barredo et al., 2003)	In this research, the land use factors are integrated to CA in order to simulate the urban land use scenarios for the city of Dublin.
23	Urban growth pattern modeling: a case study of Wuhan city, PR China (Cheng and Masser, 2003)	In this research, a spatial data analysis method including exploratory data analysis and spatial logistic regression technique is presented to model the major factors of urban growth, which can visually explore the spatial impacts of variables and can provide a systematic confirmatory approach for comparing them.

Table A.1. (Continued)

	Research title	Application
24	Cellular automata for simulating land use changes based on support vector machines (Yang et al., 2008)	In order to achieve higher accuracy and overcome some constraint of CA models, a Support Vector Machine-Cellular Automata (SVM-CA) model has been developed for the Shenzhen City, China.
25	A decade of Cellular Urban Modeling with SLEUTH: Unresolved Issues and Problems (Clarke, 2008)	The SLEUTH cellular automaton urban model is introduced, the applications are reviewed and some model improvements and sensitivity tests are mentioned.
26	Fuzzy inference guided cellular automata urban growth modeling using multi-temporal satellite images (Alkheder et al., 2008)	In this research, a fuzzy inference guided CA approach is developed to model the growth of the city of Indianapolis.
27	Modeling dynamic urban expansion processes incorporating a potential model with cellular automata (He et al., 2008)	An urban expansion dynamic model is developed that incorporates a potential model into a CA model for Beijing, China.
28	Using neural networks and cellular automata for modeling intra-urban land-use dynamics (Almeida et al., 2008)	The CA simulation model and a supervised back-propagation neural network are used in order to simulate intra-urban land-use change model.
29	Application of an integrated system dynamics and cellular automata model for urban growth assessment: A case study of Shanghai, China (Han et al., 2009)	An integrated system dynamics and CA model in socio-economic driving forces analysis and in urban spatial pattern evaluation for Shanghai city in China is presented.
30	Urban ecological security assessment and forecasting, based on a cellular automata model: a case study of Guangzhou China (Gong et al., 2009)	In this paper, a forecasting model for ecological security based on CA has been developed by using preliminary spatial data from an ecological security assessment of Guangzhou in China.
31	Cellular Automata Models for the Simulation of Real-world Urban Processes: A Review and Analysis (Santé et al., 2010)	Some urban CA models that applied to real-world cases are reviewed and compared in this research.
32	Designing and implementing a regional urban modeling system using the SLEUTH cellular urban model (Jantz et al., 2010)	In this research, a new scenario-dependent version of SLEUTH is presented. In this version, some modifications are done in order to increase performance efficiency of model including modifications to address scale sensitivity, calibration statistics, decreasing memory requirements and improving processing speed.

Table A.1. (Continued)

	Research title	Application
33	A cellular automata model of land cover change to integrate urban growth with open space conservation (Mitsova et al., 2011)	A Markov chain model of land cover change at a regional scale is developed in order to integrate protection of environmentally sensitive areas into urban growth projections.
34	Detecting land-use/land-cover change in rural-urban fringe areas using extended change-vector analysis (He et al., 2011)	An extended change-vector analysis (CVA) approach that incorporates textural change information into the traditional spectral-based CVA is proposed in order to detect land-use/land-cover changes in rural–urban fringe areas.
35	Dynamic modeling of forest conversion: simulation of past and future scenarios of rural activities expansion in the fringes of the Xingu National Park, Brazilian Amazon (Maeda et al., 2011)	In this research, a spatially explicit dynamic model of land cover and land use change is used in order to simulate the expansion of agricultural and cattle raising activities within a watershed located in the fringes of the Xingu National Park, aiming to identify the role of driving forces of change in the study area.
36	Forecasting Urban Growth Based on GIS, RS and SLEUTH Model in Pune Metropolitan Area (KantaKumar et al., 2011)	The SLEUTH model, GIS and RS are integrated to anticipate urban growth in Pune Metropolitan area. The Brute force method has been adopted in calibration mode to sequentially narrow down the ranges of coefficient values with respect to the increasing spatial resolution of datasets in the three phase containing the coarse, fine and final calibration.
37	Modeling Dynamic Urban Growth Using Cellular Automata and Particle Swarm Optimization Rules (Feng et al., 2011)	A dynamic urban growth CA model is developed by using particle swarm optimization (PSO-CA) approaches with inertia weight in Fengxian District of Shanghai Municipality, eastern China.
38	Multiple scenario analyses forecasting the confounding impacts of sea level rise and tides from storm induced coastal flooding in the city of Shanghai China (Yin et al., 2011)	In this paper, two scenario-based model contain sea level rise and storm surge flooding along the Shanghai coast are developed by using previously developed inflow calculating and flood routing models.
39	Random forest classification of Mediterranean land cover using multi-seasonal imagery and multi-seasonal texture (Rodriguez-Galiano et al., 2012)	The machine learning, multi-temporal Landsat satellite image, texture variables, and spectral bands are used to quantify the urban growth annually. The Random Forest classification system has been used to determine and select the most important textural features. Incorporating the geostatistical texture in Random Forest classifiers leads to increase in accuracy.

Table A.1. (Continued)

	Research title	Application
40	Cellular automata-based model for developing land use ecological security patterns in semi-arid areas: a case study of Ordos, Inner Mongolia China (Mao et al., 2013)	A CA model is developed to optimize the land use patterns in semi-arid areas in Northern China in the context of ecological security and land use suitability.
41	The performance of random forests in an operational setting for large area Sclerophyll forest classification (Mellor et al., 2013)	In this research, a Random Forest classifier using multi-spectral satellite sensor imagery for large area feature classification is developed in order to evaluate the mapping and monitoring forest extent.
42	A GIS-based model to analyze the spatial and temporal development of oil palm land use in Kuala Langat district (Nourqolipour et al., 2014)	CA model, multi-criteria evaluation (that used to provide transition rules of CA iterations), and Markov chain analysis (that used to assign a transition probability to each single pixel at the time steps) are integrated in order to simulate the oil palm expansion.
43	Predicting Functional Role and Occurrence of Whitebark Pine (<i>Pinus albicaulis</i>) at Alpine Treelines: Model Accuracy and Variable Importance (Resler et al., 2014)	In order to predict whitebark pine's functional role, four different modeling approaches including the general linear models, classification and regression trees, random forests, and support vector machines are applied and their prediction accuracy and variable importance are compared in this research.
44	Modeling Urban Growth with GIS Based Cellular Automata and Least Squares SVM Rules: A Case Study in Qingpu–songjiang Area of Shanghai, China (Feng et al., 2015)	In the proposed model, the Least Squares SVM (LS-SVM) rules are integrated to CA and GIS in order to generate a direct solution by solving a set of linear equations instead of representing the optimization problem as one of quadratic programming. This model can dynamically update the transition rules for each iteration of the model without needs of any arbitrary definition of a transition probability threshold.
45	Simulation of land use/land cover change and its effects on the hydrological characteristics of the upper reaches of the Hanjiang Basin (Deng et al., 2015)	In order to simplify the structure of simulation models and evaluate the impact of land use/cover change on surface runoff and evapotranspiration an ANN-based CA model is developed in this research. This model can effectively reflect the complex relations between the spatial variables and significantly reduce the simulation time.

Table A.1. (Continued)

	Research title	Application
46	Simulating Urban Growth Using a Random Forest-Cellular Automata (RF-CA) Model (Kamusoko and Gamba, 2015)	In this research, a random forest-cellular automata (RF-CA) model is developed to simulate the urban growth of Harare Metropolitan Province, Zimbabwe. The proposed model can handle a large database including the thousands of input numerical and categorical variables while quantify each input variable into an importance measure.
47	Modélisation paramétrique 3D et multi-échelle du développement résidentiel : exemple du modèle SLEUTH3D (3D parametric and multiscale modeling of residential development: example of model SLEUTH3D) (Da Silva et al., 2018)	They have developed a primary 3D simulation model of residential development SLEUTH3D. In proposed model, the transportation map is automatically updated to connect the simulated urban patches to the existing roads network.
48	SLEUTH urban and land use change model (Project Gigalopolis, 2018)	The Gigalopolis project provides an open source CA urban and land use change model.

Annex B: SLEUTH Urban Growth Model Process Flow and the Scenario File Description

Contents

- B.1. Data Set Preparation
 - B.2. Scenario File Example - Toulouse Protection Scenario Level 3 (Extreme Environmental Protection - EEP)
 - B.3. Process Control and Model Execution
-

B.1. Data Set Preparation

Create Geographic Temporal Database:

- Source data: historical maps (2000, 2008, 2012 and 2017)
 - Slope (from Digital Elevation Model (DEM) of RGE ALTI with a spatial resolution of 5m, provided by IGN)
 - Land use (from BD TOPO and BD ORTHO from IGN)
 - Excluded (from BD TOPO and BD ORTHO from IGN)
 - Urban (from BD TOPO and BD ORTHO from IGN)
 - Transportation (from BD TOPO and BD ORTHO from IGN)
 - Hillshade (from Digital Elevation Model (DEM) of RGE ALTI with a spatial resolution of 5m, provided by IGN)
- Geo-registration
 - extent (lat, long)
- Resolution
 - Toulouse metropolitan → 52m*52m
 - Saint Sulpice la Pointe → 30m*30m
 - Rieucros → 20m*20m

- Naming Convention: input data → GIF image format
 - Slope data GIF: format: <location>.slope.[<user info>].gif
 - Land use data GIFs: format: <location>.landuse.<date>.[<user info>].gif
 - Excluded data GIFs: format: <location>.excluded.[<user info>].gif
 - Urban data GIFs: format: <location>.urban.<date>.[<user info>].gif
 - Road data GIFs: format: <location>.roads.<date>.[<user info>].gif
 - Background data GIF format: <location>.hillshade.[<user info>].gif

B.2. Scenario File

A scenario file contains all necessary data for run such as:

- Sets all parameters, constants
- Sets echo options
- Controls colors, etc.
- #comments to guide

Below, the Toulouse protection scenario level 3 (EEP) as an example in predict mode is represented.

B.2.1. Master Control

```
# FILE: 'scenario file' for SLEUTH land cover transition model
#   (UGM v3.0)
#   Comments start with #
#
# I. Path Name Variables
# II. Running Status (Echo)
# III. Output ASCII Files
# IV. Log File Preferences
# V. Working Grids
# VI. Random Number Seed
# VII. Monte Carlo Iteration
#VIII. Coefficients
#   A. Coefficients and Growth Types
#   B. Modes and Coefficient Settings
# IX. Prediction Date Range
# X. Input Images
# XI. Output Images
# XII. Colortable Settings
#   A. Date_Color
#   B. Non-Landuse Colortable
#   C. Land Cover Colortable
```

```
# D. Growth Type Images
# E. Deltatron Images
#XIII. Self Modification Parameters
```

B.2.2. Basic Settings

```
# I.PATH NAME VARIABLES
# INPUT_DIR: relative or absolute path where input image files and
#           (if modeling land cover) 'landuse.classes' file are
#           located.
# OUTPUT_DIR: relative or absolute path where all output files will
#           be located.
# WHIRLGIF_BINARY: relative path to 'whirlgif' gif animation program.
#           These must be compiled before execution.
INPUT_DIR=../input/Toulouse/
OUTPUT_DIR=../output/Toulouse_pre/EEP_ 2050/
WHIRLGIF_BINARY=../Whirlgif/whirlgif

# II. RUNNING STATUS (ECHO)
# Status of model run, monte carlo iteration, and year will be
# printed to the screen during model execution.
ECHO(YES/NO)=yes

# III. Output Files
# INDICATE TYPES OF ASCII DATA FILES TO BE WRITTEN TO
# OUTPUT_DIRECTORY.
#
# COEFF_FILE: contains coefficient values for every run, monte carlo
#           iteration and year.
# AVG_FILE: contains measured values of simulated data averaged over
#           monte carlo iterations for every run and control year.
# STD_DEV_FILE: contains standard deviation of averaged values
#           in the AVG_FILE.
# MEMORY_MAP: logs memory map to file 'memory.log'
# LOGGING: will create a 'LOG_#' file where # signifies the processor
#           number that created the file if running code in parallel.
#           Otherwise, # will be 0. Contents of the LOG file may be
#           described below.
WRITE_COEFF_FILE(YES/NO)=yes
WRITE_AVG_FILE(YES/NO)=yes
WRITE_STD_DEV_FILE(YES/NO)=yes
WRITE_MEMORY_MAP(YES/NO)=YES
LOGGING(YES/NO)=YES
```

B.2.3. Log Control

```
# IV. Log File Preferences
# INDICATE CONTENT OF LOG_# FILE (IF LOGGING == ON).
# LANDCLASS_SUMMARY: (if landuse is being modeled) summary of input
#           from 'landuse.classes' file
# SLOPE_WEIGHTS(YES/NO): annual slope weight values as effected
#           by slope_coeff
# READS(YES/NO)= notes if a file is read in
# WRITES(YES/NO)= notes if a file is written
# COLORTABLES(YES/NO)= rgb lookup tables for all colortables generated
# PROCESSING_STATUS(0:off/1:low verbosity/2:high verbosity)=
# TRANSITION_MATRIX(YES/NO)= pixel count and annual probability of
#           land class transitions
# URBANIZATION_ATTEMPTS(YES/NO)= number of times an attempt to urbanize
#           a pixel occurred
# INITIAL_COEFFICIENTS(YES/NO)= initial coefficient values for
#           each monte carlo
# BASE_STATISTICS(YES/NO)= measurements of urban control year data
# DEBUG(YES/NO)= data dump of igrid object and grid pointers
# TIMINGS(0:off/1:low verbosity/2:high verbosity)= time spent within
# each module. If running in parallel, LOG_0 will contain timing for
# complete job.
LOG_LANDCLASS_SUMMARY(YES/NO)=yes
LOG_SLOPE_WEIGHTS(YES/NO)=yes
LOG_READS(YES/NO)=no
LOG_WRITES(YES/NO)=no
LOG_COLORTABLES(YES/NO)=no
LOG_PROCESSING_STATUS(0:off/1:low verbosity/2:high verbosity)=1
LOG_TRANSITION_MATRIX(YES/NO)=yes
LOG_URBANIZATION_ATTEMPTS(YES/NO)=no
LOG_INITIAL_COEFFICIENTS(YES/NO)=YES
LOG_BASE_STATISTICS(YES/NO)=yes
LOG_DEBUG(YES/NO)= yes
LOG_TIMINGS(0:off/1:low verbosity/2:high verbosity)=1
```

B.2.4. Monte Carlo Iterations/Working Grids

```
# V. WORKING GRIDS
# The number of working grids needed from memory during model execution is

# designated up front. This number may change depending upon modes. If
# NUM_WORKING_GRIDS needs to be increased, the execution will be exited
# and an error message will be written to the screen and to 'ERROR_LOG'
```

```
# in the OUTPUT_DIRECTORY. If the number may be decreased an optimal
# number will be written to the end of the LOG_0 file.
```

```
NUM_WORKING_GRIDS=12
```

```
# VI. RANDOM NUMBER SEED
```

```
# This number initializes the random number generator. This seed will be
# used to initialize each model run.
```

```
RANDOM_SEED=9407
```

```
# VII. MONTE CARLO ITERATIONS
```

```
# Each model run may be completed in a monte carlo fashion.
```

```
# For CALIBRATION or TEST mode measurements of simulated data will be
# taken for years of known data, and averaged over the number of monte
```

```
# carlo iterations. These averages are written to the AVG_FILE, and
# the associated standard deviation is written to the STD_DEV_FILE.
```

```
# The averaged values are compared to the known data, and a Pearson
# correlation coefficient measure is calculated and written to the
```

```
# control_stats.log file. The input per run may be associated across
# files using the 'index' number in the files' first column.
```

```
#
```

```
MONTE_CARLO_ITERATIONS=100
```

B.2.5. Dispersion (diffusion) Coefficient Multiplier

```
# The following auxiliary values for Version D have been set to have
# no effect on computation.
```

```
AUX_DIFFUSION_MULT=0.004
```

```
AUX_DIFFUSION_COEFF=1
```

```
AUX_BREED_COEFF=1
```

```
# The following auxiliary values for Version D have been set so that
# the corresponding variables will have been initialized.
```

```
WRITE_RATIO_FILE(YES/NO)=yes
```

```
WRITE_SLOPE_FILE(YES/NO)=yes
```

```
WRITE_XYPOINTS_FILE(YES/NO)=yes
```

B.2.6. Calibration Instructions

```
# VIII. COEFFICIENTS
```

```
# The coefficients effect how the growth rules are applied to the data.
```

```
# Setting requirements:
```

```
# *_START values >= *_STOP values
```

```
# *_STEP values > 0
```

```
# if no coefficient increment is desired:
```

```
# *_START == *_STOP
```

```

# *_STEP == 1
# For additional information about how these values affect simulated
# land cover change see our publications and PROJECT GIGALOPOLIS
# site: (www.ncgia.ucsb.edu/project/gig/About/abGrowth.htm).
# A. COEFFICIENTS AND GROWTH TYPES
# DIFFUSION: affects SPONTANEOUS GROWTH and search distance along the
# road network as part of ROAD INFLUENCED GROWTH.
# BREED: NEW SPREADING CENTER probability and affects number of ROAD
# INFLUENCED GROWTH attempts.
# SPREAD: the probability of ORGANIC GROWTH from established urban
# pixels occurring.
# SLOPE_RESISTANCE: affects the influence of slope to urbanization. As
# value increases, the ability to urbanize
# ever steepening slopes decreases.
# ROAD_GRAVITY: affects the outward distance from a selected pixel for
# which a road pixel will be searched for as part of
# ROAD INFLUENCED GROWTH.
#

```

B.2.7. Calibration Settings

```

# B. MODES AND COEFFICIENT SETTINGS
# TEST: TEST mode will perform a single run through the historical
# data using the CALIBRATION_*_START values to initialize
# growth, complete the MONTE_CARLO_ITERATIONS, and then conclude
# execution. GIF images of the simulated urban growth will be
# written to the OUTPUT_DIRECTORY.
# CALIBRATE: CALIBRATE will perform monte carlo runs through the
# historical data using every combination of the
# coefficient values indicated. The CALIBRATION_*_START
# coefficient values will initialize the first run. A
# coefficient will then be increased by its *_STEP value,
# and another run performed. This will be repeated for all
# possible permutations of given ranges and increments.
# PREDICTION: PREDICTION will perform a single run, in monte carlo
# fashion, using the PREDICTION_*_BEST_FIT values
# for initialization.

```

```

CALIBRATION_DIFFUSION_START= 100
CALIBRATION_DIFFUSION_STEP= 1
CALIBRATION_DIFFUSION_STOP= 100

```

```

CALIBRATION_BREED_START= 1
CALIBRATION_BREED_STEP= 1

```

```

CALIBRATION_BREED_STOP= 1

CALIBRATION_SPREAD_START= 25
CALIBRATION_SPREAD_STEP= 1
CALIBRATION_SPREAD_STOP= 25

CALIBRATION_SLOPE_START= 25
CALIBRATION_SLOPE_STEP= 1
CALIBRATION_SLOPE_STOP= 25

CALIBRATION_ROAD_START= 1
CALIBRATION_ROAD_STEP= 1
CALIBRATION_ROAD_STOP= 1

PREDICTION_DIFFUSION_BEST_FIT= 100
PREDICTION_BREED_BEST_FIT= 1
PREDICTION_SPREAD_BEST_FIT= 25
PREDICTION_SLOPE_BEST_FIT= 25
PREDICTION_ROAD_BEST_FIT= 1

```

B.2.8. Input

```

# IX. PREDICTION DATE RANGE
# The urban and road images used to initialize growth during
# prediction are those with dates equal to, or greater than,
# the PREDICTION_START_DATE. If the PREDICTION_START_DATE is greater
# than any of the urban dates, the last urban file on the list will be
# used. Similarly, if the PREDICTION_START_DATE is greater
# than any of the road dates, the last road file on the list will be
# used. The prediction run will terminate at PREDICTION_STOP_DATE.
#
PREDICTION_START_DATE=2017
PREDICTION_STOP_DATE=2050

# X. INPUT IMAGES
# The model expects grayscale, GIF image files with file name
# format as described below. For more information see our
# PROJECT GIGALOPOLIS web site:
# (www.ncgia.ucsb.edu/project/gig/About/dtInput.htm).
#
# IF LAND COVER IS NOT BEING MODELED: Remove or comment out
# the LANDUSE_DATA data input flags below.
#
# < > = user selected fields

```

```

# [< >] = optional fields
#
# Urban data GIFs
# format: <location>.urban.<date>.[<user info>].gif
#
#
URBAN_DATA= toulouse.urban.2000.gif
URBAN_DATA= toulouse.urban.2008.gif
URBAN_DATA= toulouse.urban.2012.gif
URBAN_DATA= toulouse.urban.2017.gif
#
# Road data GIFs
# format: <location>.roads.<date>.[<user info>].gif
#
#
ROAD_DATA= toulouse.roads.2000.gif
ROAD_DATA= toulouse.roads.2008.gif
ROAD_DATA= toulouse.roads.2012.gif
ROAD_DATA= toulouse.roads.2017.gif
#
# Landuse data GIFs
# format: <location>.landuse.<date>.[<user info>].gif
#
#
LANDUSE_DATA= toulouse.landuse.2000.gif
LANDUSE_DATA= toulouse.landuse.2017.gif
#
# Excluded data GIF
# format: <location>.excluded.[<user info>].gif
#
#
EXCLUDED_DATA= toulouse.excluded.[EEP].gif
#
# Slope data GIF
# format: <location>.slope.[<user info>].gif
#
#
SLOPE_DATA= toulouse.slope.gif
#
# Background data GIF
# format: <location>.hillshade.[<user info>].gif
#
#
BACKGROUND_DATA= toulouse.hillshade.gif

```

B.2.9. Output

```

# XI. OUTPUT IMAGES
# WRITE_COLOR_KEY_IMAGES: Creates image maps of each colortable.

```

```

#           File name format: 'key_[type]_COLORMAP'
#           where [type] represents the colortable.
# ECHO_IMAGE_FILES: Creates GIF of each input file used in that job.
#           File names format: 'echo_of_[input_filename]'
#           where [input_filename] represents the input name.
# ANIMATION: if whirlgif has been compiled, and the WHIRLGIF_BINARY
#           path has been defined, animated gifs beginning with the
#           file name 'animated' will be created in PREDICT mode.
WRITE_COLOR_KEY_IMAGES(YES/NO)=yes
ECHO_IMAGE_FILES(YES/NO)=yes
ANIMATION(YES/NO)= yes

```

B.2.10. Color Tables

```

# XII. COLORTABLE SETTINGS
# A. DATE COLOR SETTING
#   The date will automatically be placed in the lower left corner
#   of output images. DATE_COLOR may be designated in with red, green,
#   and blue values (format: <red_value, green_value, blue_value> )
#   or with hexadecimal beginning with '0X' (format: <0X#####> ).
#default DATE_COLOR= 0XFFFFFF white
DATE_COLOR= 0XFFFFFF #white

# B. URBAN (NON-LANDUSE) COLORTABLE SETTINGS
# 1. URBAN MODE OUTPUTS
#   TEST mode: Annual images of simulated urban growth will be
#   created using SEED_COLOR to indicate urbanized areas.

#   CALIBRATE mode: Images will not be created.
#   PREDICT mode: Annual probability images of simulated urban
#   growth will be created using the PROBABILITY
#   _COLORTABLE. The initializing urban data will be
#   indicated by SEED_COLOR.
#
# 2. COLORTABLE SETTINGS
#   SEED_COLOR: initializing and extrapolated historic urban extent

#   WATER_COLOR: BACKGROUND_DATA is used as a backdrop for

#   simulated urban growth. If pixels in this file
#   contain the value zero (0), they will be filled
#   with the color value in WATER_COLOR. In this way,
#   major water bodies in a study area may be included
#   in output images.

```



```
#SEED_COLOR= 0XFFFF00 #yellow
SEED_COLOR= 249, 209, 110 #pale yellow
#WATER_COLOR= 0X0000FF # blue
WATER_COLOR= 20, 52, 214 # royal blue
```

B.2.11. Forecast Image

```
# 3. PROBABILITY COLORTABLE FOR URBAN GROWTH
# For PREDICTION, annual probability images of urban growth
# will be created using the monte carlo iterations. In these
# images, the higher the value the more likely urbanizaion is.
# In order to interpret these 'continuous' values more easily
# they may be color classified by range.
#
# If 'hex' is not present then the range is transparent.
# The transparent range must be the first on the list.
# The max number of entries is 100.
# PROBABILITY_COLOR: a color value in hexadecimal that indicates
# a probability range.
# low/upper: indicate the boundaries of the range.
#
# low, upper, hex, (Optional Name)
PROBABILITY_COLOR= 0, 1, , #transparent
PROBABILITY_COLOR= 1, 10, 0X00ff33, #green
PROBABILITY_COLOR= 10, 20, 0X00cc33, #
PROBABILITY_COLOR= 20, 30, 0X009933, #
PROBABILITY_COLOR= 30, 40, 0X006666, #blue
PROBABILITY_COLOR= 40, 50, 0X003366, #
PROBABILITY_COLOR= 50, 60, 0X000066, #
PROBABILITY_COLOR= 60, 70, 0XFF6A6A, #lt orange
PROBABILITY_COLOR= 70, 80, 0Xff7F00, #dark orange
PROBABILITY_COLOR= 80, 90, 0Xff3E96, #violetred
PROBABILITY_COLOR= 90, 100, 0Xff0033, #dark red
```

B.2.12. Land Use Color Table

```
# C. LAND COVER COLORTABLE
# Land cover input images should be in grayscale GIF image format.
# The 'pix' value indicates a land class grayscale pixel value in
# the image. If desired, the model will create color classified
# land cover output. The output colortable is designated by the
# 'hex/rgb' values.
# pix: input land class pixel value
# name: text string indicating land class
```

```

# flag: special case land classes
#   URB - urban class (area is included in urban input data
#       and will not be transitioned by deltatron)
#   UNC - unclass (NODATA areas in image)
#   EXC - excluded (land class will be ignored by deltatron)
# hex/rgb: hexadecimal or rgb (red, green, blue) output colors
#
#   pix, name,  flag,  hex/rgb, #comment
LANDUSE_CLASS= 0, Unclass , UNC  , 0X000000
LANDUSE_CLASS= 1, Urban   , URB  , 0X8b2323 #dark red
LANDUSE_CLASS= 2, Range  ,     , 0Xee9a49 #tan
LANDUSE_CLASS= 3, Forest ,     , 0X006400

```

B.2.13. Growth Rule Image

```

# D. GROWTH TYPE IMAGE OUTPUT CONTROL AND COLORTABLE
#
# From here you can control the output of the Z grid
# (urban growth) just after it is returned from the spr_spread()
# function. In this way it is possible to see the different types
# of growth that have occurred for a particular growth cycle.
#
# VIEW_GROWTH_TYPES(YES/NO) provides an on/off
# toggle to control whether the images are generated.
#
# GROWTH_TYPE_PRINT_WINDOW provides a print window
# to control the amount of images created.
# format: <start_run>,<end_run>,<start_monte_carlo>,
#         <end_monte_carlo>,<start_year>,<end_year>
# for example:
# GROWTH_TYPE_PRINT_WINDOW=run1,run2,mc1,mc2,year1,year2
# so images are only created when
# run1 <= current run <= run2 AND
# mc1 <= current monte carlo <= mc2 AND
# year1 <= current year <= year2
#
# 0 == first
VIEW_GROWTH_TYPES(YES/NO)=yes
GROWTH_TYPE_PRINT_WINDOW=0,0,0,0,2000,2060
PHASE0G_GROWTH_COLOR= 0xff0000 # seed urban area
PHASE1G_GROWTH_COLOR= 0X00ff00 # diffusion growth
PHASE2G_GROWTH_COLOR= 0X0000ff # NOT USED
PHASE3G_GROWTH_COLOR= 0Xffff00 # breed growth
PHASE4G_GROWTH_COLOR= 0Xffffff # spread growth

```

PHASE5G_GROWTH_COLOR= 0X00ffff # road influenced growth

B.2.14. Deltatron Behavior

```
#####  
#  
# E. DELTATRON AGING SECTION  
#  
# From here you can control the output of the deltatron grid  
# just before they are aged  
#  
# VIEW_DELTATRON_AGING(YES/NO) provides an on/off  
# toggle to control whether the images are generated.  
#  
# DELTATRON_PRINT_WINDOW provides a print window  
# to control the amount of images created.  
# format: <start_run>,<end_run>,<start_monte_carlo>,  
#         <end_monte_carlo>,<start_year>,<end_year>  
# for example:  
# DELTATRON_PRINT_WINDOW=run1,run2,mc1,mc2,year1,year2  
# so images are only created when  
# run1 <= current run <= run2 AND  
# mc1 <= current monte carlo <= mc2 AND  
# year1 <= current year <= year2  
#  
# 0 == first  
VIEW_DELTATRON_AGING(YES/NO)=YES  
DELTATRON_PRINT_WINDOW=0,0,0,0,2000,2060  
DELTATRON_COLOR= 0x000000 # index 0 No or dead deltatron  
DELTATRON_COLOR= 0X00FF00 # index 1 age = 1 year  
DELTATRON_COLOR= 0X00D200 # index 2 age = 2 year  
DELTATRON_COLOR= 0X00AA00 # index 3 age = 3 year  
DELTATRON_COLOR= 0X008200 # index 4 age = 4 year  
DELTATRON_COLOR= 0X005A00 # index 5 age = 5 year
```

B.2.15. the constants

```
# XIII. SELF-MODIFICATION PARAMETERS  
# SLEUTH is a self-modifying cellular automata. For more  
# information see our PROJECT GIGALOPOLIS web site  
# (www.ncgia.ucsb.edu/project/gig/About/abGrowth.htm)  
# and publications (and/or grep 'self modification' in code).  
ROAD_GRAV_SENSITIVITY=0.01  
SLOPE_SENSITIVITY=0.1
```

CRITICAL_LOW=0.0000097
CRITICAL_HIGH=1.9999999
CRITICAL_SLOPE=15.0
BOOM=1.1
BUST=0.90

B.3. Model Execution

To run the model, in the scenario directory:

➤ `grow.exe <mode> <scenario file>`

Allowable modes are:

- calibrate
- restart
- test
- predict

Annex C: Coefficients and Calibration

Contents

- C.1. Dispersion Coefficient Multiplier
 - C.2. Best-Fit Coefficient
-

In this Annex, an example of the 'ratio_pe_0.log' file used for calculation of dispersion coefficient multiplier and for best fit coefficients are represented. A portion of the table of the "ratio_pe_0.log" file is shown as an example in this Annex.

C.1. Dispersion Coefficient Multiplier

As discussed in chapter 2, the number of spontaneous urbanization attempts that comes from the dispersion value (D_V) depends on the calibrated value for the dispersion coefficient (D_C), a constant number as dispersion coefficient multiplier (D_M), and the number of pixels in the image diagonal. We have mentioned that the dispersion coefficient multiplier is no longer a constant in SLEUTH-3r (Jantz et al., 2010). This allows the user to modify this multiplier value interactively. To find the appropriate value of D_M , the dispersion set to 100 and other coefficients set to zero and the model perform in the calibration mode. This allows the growth coefficients to produce the maximum level of spontaneous new growth. We have tested different value for D_M with 100 Monte Carlo iteration. We have taken the D_M value which make the model to captures or even over estimates the number of urban clusters (cluster fractional difference metric). In basic SLEUTH model, the default value of dispersion multiplier is a constant equal to 0.005. The number of tested value for each scenario is between three to five times of test. Tables C.1 to C.15 illustrate the dispersion coefficient multiplier obtained from 'ratio_pe_0.log' files for Toulouse, Saint Sulpice la Pointe and Rieucros study area respectively, each according to the environmental protection scenarios separately.

Table C. 1. Dispersion coefficient multiplier, scenario protection level 0 (Nearly No Environmental Protection - NEP), Toulouse

Dispersion coefficient multiplier = 0.003 (MONTE_CARLO_ITERATIONS=25)											
diffusion	breed	spread	slp_resst	road_grav	control	area	area	area	cluster	cluster	cluster
coeff	coeff	coeff	coeff	coeff	year	diff	ratio	fract	diff	ratio	fract
100.00	1.00	1.00	1.00	1.00	2008	-206.120	0.977	-0.023	393.280	1.156	0.156
100.00	1.00	1.00	1.00	1.00	2012	-169.160	0.981	-0.019	578.320	1.226	0.226
100.00	1.00	1.00	1.00	1.00	2017	-1382.640	0.871	-0.129	723.680	1.267	0.267

Table C. 2. Dispersion coefficient multiplier, scenario protection level 1 (Limited Environmental Protection - LEP), Toulouse

Dispersion coefficient multiplier = 0.004 (MONTE_CARLO_ITERATIONS=25)											
diffusion	breed	spread	slp_resst	road_grav	control	area	area	area	cluster	cluster	cluster
coeff	coeff	coeff	coeff	coeff	year	diff	ratio	fract	diff	ratio	fract
100.00	1.00	1.00	1.00	1.00	2008	-154.320	0.983	-0.017	452.720	1.180	0.180
100.00	1.00	1.00	1.00	1.00	2012	-93.400	0.990	-0.010	662.560	1.258	0.258
100.00	1.00	1.00	1.00	1.00	2017	-1277.720	0.881	-0.119	837.360	1.309	0.309

Table C. 3. Dispersion coefficient multiplier, scenario protection level 2 (Moderate Environmental Protection - MEP), Toulouse

Dispersion coefficient multiplier = 0.004 (MONTE_CARLO_ITERATIONS=25)											
diffusion	breed	spread	slp_resst	road_grav	control	area	area	area	cluster	cluster	cluster
coeff	coeff	coeff	coeff	coeff	year	diff	ratio	fract	diff	ratio	fract
100.00	1.00	1.00	1.00	1.00	2008	-174.400	0.980	-0.020	431.800	1.172	0.172
100.00	1.00	1.00	1.00	1.00	2012	-119.160	0.987	-0.013	633.080	1.247	0.247
100.00	1.00	1.00	1.00	1.00	2017	-1304.000	0.878	-0.122	805.040	1.298	0.298

Table C. 4. Dispersion coefficient multiplier, scenario protection level 3 (Extreme Environmental Protection - EEP), Toulouse

Dispersion coefficient multiplier = 0.004 (MONTE_CARLO_ITERATIONS=25)											
diffusion	breed	spread	slp_resst	road_grav	control	area	area	area	cluster	cluster	cluster
coeff	coeff	coeff	coeff	coeff	year	diff	ratio	fract	diff	ratio	fract
100.00	1.00	1.00	1.00	1.00	2008	-182.440	0.979	-0.020	432.960	1.172	0.172
100.00	1.00	1.00	1.00	1.00	2012	-127.000	0.986	-0.014	638.680	1.249	0.249
100.00	1.00	1.00	1.00	1.00	2017	-1325.360	0.8764	-0.124	801.560	1.296	0.296

Table C. 5. Dispersion coefficient multiplier, attraction-based scenario protection level 1 (Attraction-based Limited Environmental Protection - ALEP), Toulouse

Dispersion coefficient multiplier = 0.0035 (MONTE_CARLO_ITERATIONS=25)											
diffusion	breed	spread	slp_resst	road_grav	control	area	area	area	cluster	cluster	cluster
coeff	coeff	coeff	coeff	coeff	year	diff	ratio	fract	diff	ratio	fract
100.00	1.00	1.00	1.00	1.00	2008	-104.480	0.988	-0.012	447.960	1.178	0.178
100.00	1.00	1.00	1.00	1.00	2012	-17.920	0.998	-0.002	658.760	1.257	0.257
100.00	1.00	1.00	1.00	1.00	2017	-1172.480	0.891	-0.109	836.040	1.309	0.309

Table C. 6. Dispersion coefficient multiplier, scenario protection level 0 (Nearly No Environmental Protection - NEP), Saint Sulpice la Point

Dispersion coefficient multiplier = 0.0006 (MONTE_CARLO_ITERATIONS=100)											
diffusion	breed	spread	slp_resst	road_grav	control	area	area	area	cluster	cluster	cluster
coeff	coeff	coeff	coeff	coeff	year	diff	ratio	fract	diff	ratio	fract
100.00	1.00	1.00	1.00	1.00	2008	-380.830	0.862	-0.138	56.340	1.175	0.175
100.00	1.00	1.00	1.00	1.00	2012	-362.650	0.869	-0.131	77.840	1.241	0.241
100.00	1.00	1.00	1.00	1.00	2017	-939.770	0.723	-0.277	101.220	1.309	0.3095

Table C. 7. Dispersion coefficient multiplier, scenario protection level 1 (Limited Environmental Protection - LEP), Saint Sulpice la Point

Dispersion coefficient multiplier = 0.0006 (MONTE_CARLO_ITERATIONS=100)											
diffusion	breed	spread	slp_resst	road_grav	control	area	area	area	cluster	cluster	cluster
coeff	coeff	coeff	coeff	coeff	year	diff	ratio	fract	diff	ratio	fract
100.00	1.00	1.00	1.00	1.00	2008	-384.660	0.8604	-0.139	55.460	1.172	0.172
100.00	1.00	1.00	1.00	1.00	2012	-369.210	0.867	-0.133	75.440	1.234	0.234
100.00	1.00	1.00	1.00	1.00	2017	-947.890	0.721	-0.279	97.730	1.299	0.299

Table C. 8. Dispersion coefficient multiplier, scenario protection level 2 (Moderate Environmental Protection - MEP), Saint Sulpice la Point

Dispersion coefficient multiplier = 0.0006 (MONTE_CARLO_ITERATIONS=100)											
diffusion	breed	spread	slp_resst	road_grav	control	area	area	area	cluster	cluster	cluster
coeff	coeff	coeff	coeff	coeff	year	diff	ratio	fract	diff	ratio	fract
100.00	1.00	1.00	1.00	1.00	2008	-388.170	0.8592	-0.141	53.590	1.166	0.166
100.00	1.00	1.00	1.00	1.00	2012	-373.630	0.865	-0.135	73.420	1.227	0.227
100.00	1.00	1.00	1.00	1.00	2017	-954.030	0.719	-0.281	95.440	1.292	0.292

Table C. 9. Dispersion coefficient multiplier, scenario protection level 3 (Extreme Environmental Protection - EEP), Saint Sulpice la Point

Dispersion coefficient multiplier = 0.0006 (MONTE_CARLO_ITERATIONS=100)											
diffusion	breed	spread	slp_resst	road_grav	control	area	area	area	cluster	cluster	cluster
coeff	coeff	coeff	coeff	coeff	year	diff	ratio	fract	diff	ratio	fract
100.00	1.00	1.00	1.00	1.00	2008	-390.010	0.858	-0.141	52.620	1.163	0.163
100.00	1.00	1.00	1.00	1.00	2012	-377.780	0.863	-0.136	71.590	1.222	0.222
100.00	1.00	1.00	1.00	1.00	2017	-959.590	0.717	-0.282	93.120	1.285	0.285

Table C. 10. Dispersion coefficient multiplier, attraction-based scenario protection level 1 (Attraction-based Limited Environmental Protection - ALEP), Saint Sulpice la Point

Dispersion coefficient multiplier = 0.0005 (MONTE_CARLO_ITERATIONS=100)											
diffusion	breed	spread	slp_resst	road_grav	control	area	area	area	cluster	cluster	cluster
coeff	coeff	coeff	coeff	coeff	year	diff	ratio	fract	diff	ratio	fract
100.00	1.00	1.00	1.00	1.00	2008	-376.490	0.863	-0.137	55.470	1.172	0.172
100.00	1.00	1.00	1.00	1.00	2012	-356.790	0.871	-0.129	75.980	1.235	0.235
100.00	1.00	1.00	1.00	1.00	2017	-931.280	0.726	-0.274	97.040	1.297	0.297

Table C. 11. Dispersion coefficient multiplier, scenario protection level 0 (Nearly No Environmental Protection - NEP), Rieucros

Dispersion coefficient multiplier = 0.0002 (MONTE_CARLO_ITERATIONS=100)											
diffusion	breed	spread	slp_resst	road_grav	control	area	area	area	cluster	cluster	cluster
coeff	coeff	coeff	coeff	coeff	year	diff	ratio	fract	diff	ratio	fract
100.00	1.00	1.00	1.00	1.00	2008	-6.780	0.976	-0.024	5.380	1.082	0.082
100.00	1.00	1.00	1.00	1.00	2012	-88.270	0.760	-0.240	12.090	1.186	0.186
100.00	1.00	1.00	1.00	1.00	2017	-167.450	0.634	-0.366	19.090	1.294	0.294

Table C. 12. Dispersion coefficient multiplier, scenario protection level 1 (Limited Environmental Protection - LEP), Rieucros

Dispersion coefficient multiplier = 0.0002 (MONTE_CARLO_ITERATIONS=100)											
diffusion	breed	spread	slp_resst	road_grav	control	area	area	area	cluster	cluster	cluster
coeff	coeff	coeff	coeff	coeff	year	diff	ratio	fract	diff	ratio	fract
100.00	1.00	1.00	1.00	1.00	2008	-6.930	0.975	-0.025	5.130	1.078	0.078
100.00	1.00	1.00	1.00	1.00	2012	-89.500	0.757	-0.243	11.150	1.172	0.172
100.00	1.00	1.00	1.00	1.00	2017	-169.560	0.630	-0.370	17.930	1.276	0.276

Table C. 13. Dispersion coefficient multiplier, scenario protection level 2 (Moderate Environmental Protection - MEP), Rieucros

Dispersion coefficient multiplier = 0.0002 (MONTE_CARLO_ITERATIONS=100)											
diffusion	breed	spread	slp_resst	road_grav	control	area	area	area	cluster	cluster	cluster
coeff	coeff	coeff	coeff	coeff	year	diff	ratio	fract	diff	ratio	fract
100.00	1.00	1.00	1.00	1.00	2008	-7.390	0.973	-0.027	5.010	1.076	0.076
100.00	1.00	1.00	1.00	1.00	2012	-89.820	0.756	-0.244	11.190	1.172	0.172
100.00	1.00	1.00	1.00	1.00	2017	-170.420	0.628	-0.372	17.660	1.272	0.272

Table C. 14. Dispersion coefficient multiplier, scenario protection level 3 (Extreme Environmental Protection - EEP), Rieucros

Dispersion coefficient multiplier = 0.0002 (MONTE_CARLO_ITERATIONS=100)											
diffusion	breed	spread	slp_resst	road_grav	control	area	area	area	cluster	cluster	cluster
coeff	coeff	coeff	coeff	coeff	year	diff	ratio	fract	diff	ratio	fract
100.00	1.00	1.00	1.00	1.00	2008	-8.470	0.970	-0.030	4.600	1.070	0.070
100.00	1.00	1.00	1.00	1.00	2012	-91.340	0.752	-0.248	10.630	1.164	0.164
100.00	1.00	1.00	1.00	1.00	2017	-171.580	0.625	-0.375	17.400	1.268	0.268

Table C. 15. Dispersion coefficient multiplier, attraction-based scenario protection level 1 (Attraction-based Limited Environmental Protection - ALEP), Rieucros

Dispersion coefficient multiplier = 0.0002 (MONTE_CARLO_ITERATIONS=100)											
diffusion	breed	spread	slp_resst	road_grav	control	area	area	area	cluster	cluster	cluster
coeff	coeff	coeff	coeff	coeff	year	diff	ratio	fract	diff	ratio	fract
100.00	1.00	1.00	1.00	1.00	2008	-1.610	0.994	-0.006	7.330	1.111	0.111
100.00	1.00	1.00	1.00	1.00	2012	-79.520	0.784	-0.216	15.520	1.239	0.239
100.00	1.00	1.00	1.00	1.00	2017	-155.920	0.660	-0.340	23.920	1.368	0.368

C.2. Best-Fit Coefficients

SLEUTH-3r creates new metric table that could be find in 'ratio_pe_0.log' file generated in the calibration process (see table 2.2, chapter 2). As mentioned in chapter 2, two metrics of the pixel fractional difference (PFD) and the clusters fractional difference (CFD) are used in calibration procedure of this thesis. PFD makes direct comparisons between the numbers of urban pixels in the control maps and the corresponding simulated maps. Obtaining an accurate fit for this metric ensured that the overall amount of development would be matched. The CFD focuses on the frequency of clusters in the urban system and compares the number of urban clusters. The accurate metrics indicate that the model could create the urban form and could avoid the dispersed settlement patterns (Jantz et al., 2010). In this research, the set of parameters are selected that could achieve the best goodness of the fit in both PFD and CFD. The parameters that have the minimum differences in cluster and pixel ratio are considered as the best-fit parameters. For the initial run 25 Monte Carlo trial is used. After obtaining the range of the desired value, another execution by setting 100 Monte Carlo trial is done. Since the input excluded maps of the environmental scenarios are different, for each environmental scenario the calibration process is run in order to achieve its best fit coefficient for the forecasting process.

Table C. 16. Calibration coefficients, scenario protection level 0 (Nearly No Environmental Protection - NEP), Toulouse

MONTE_CARLO_ITERATIONS=100												
run	diffusion	breed	spread	slp_resst	road_grav	control	area	area	area	cluster	cluster	cluster
number	coeff	coeff	coeff	coeff	coeff	year	diff	ratio	fract	diff	ratio	fract
2669	100	25	25	75	100	2017	2611.142	1.243	0.243	336.285	1.124	0.124

Table C. 17. Calibration coefficients, scenario protection level 1 (Limited Environmental Protection - LEP), Toulouse

MONTE_CARLO_ITERATIONS=100												
run	diffusion	breed	spread	slp_resst	road_grav	control	area	area	area	cluster	cluster	cluster
number	coeff	coeff	coeff	coeff	coeff	year	diff	ratio	fract	diff	ratio	fract
2532	100	1	25	25	50	2017	1734.57	1.161	0.161	444.428	1.164	0.164

Table C. 18. Calibration coefficients, scenario protection level 2 (Moderate Environmental Protection - MEP), Toulouse

MONTE_CARLO_ITERATIONS=100												
run	diffusion	breed	spread	slp_resst	road_grav	control	area	area	area	cluster	cluster	cluster
number	coeff	coeff	coeff	coeff	coeff	year	diff	ratio	fract	diff	ratio	fract
2534	100	1	25	25	100	2017	1690.571	1.157	0.157	458.428	1.169	0.169

Table C. 19. Calibration coefficients, scenario protection level 3 (Extreme Environmental Protection - EEP), Toulouse

MONTE_CARLO_ITERATIONS=100												
run	diffusion	breed	spread	slp_resst	road_grav	control	area	area	area	cluster	cluster	cluster
number	coeff	coeff	coeff	coeff	coeff	year	diff	ratio	fract	diff	ratio	fract
2530	100	1	25	25	1	2017	1691.00	1.157	0.157	441.48	1.163	0.163

Table C. 20. Calibration coefficients, attraction-based scenario protection level 1 (Attraction-based Limited Environmental Protection - ALEP), Toulouse

MONTE_CARLO_ITERATIONS=100												
run	diffusion	breed	spread	slp_resst	road_grav	control	area	area	area	cluster	cluster	cluster
number	coeff	coeff	coeff	coeff	coeff	year	diff	ratio	fract	diff	ratio	fract
2545	100	1	25	100	1	2017	2345.85	1.218	0.218	157.571	1.058	0.058

Table C. 21. Calibration coefficients, scenario protection level 0 (Nearly No Environmental Protection - NEP), Saint Sulpice la Point

MONTE_CARLO_ITERATIONS=100												
run	diffusion	breed	spread	slp_resst	road_grav	control	area	area	area	cluster	cluster	cluster
number	coeff	coeff	coeff	coeff	coeff	year	diff	ratio	fract	diff	ratio	fract
2544	100	1	25	75	100	2017	17.400	1.074	0.074	-0.04	0.999	-0.0006

Table C. 22. Calibration coefficients, scenario protection level 1 (Limited Environmental Protection - LEP), Saint Sulpice la Point

MONTE_CARLO_ITERATIONS=100												
run	diffusion	breed	spread	slp_resst	road_grav	control	area	area	area	cluster	cluster	cluster
number	coeff	coeff	coeff	coeff	coeff	year	diff	ratio	fract	diff	ratio	fract
2674	100	25	25	100	100	2017	21.60	1.092	0.092	-0.04	0.99	-0.0006

Table C. 23. Calibration coefficients, scenario protection level 2 (Moderate Environmental Protection - MEP), Saint Sulpice la Point

MONTE_CARLO_ITERATIONS=100												
run	diffusion	breed	spread	slp_resst	road_grav	control	area	area	area	cluster	cluster	cluster
number	coeff	coeff	coeff	coeff	coeff	year	diff	ratio	fract	diff	ratio	fract
2540	100	1	25	75	1	2017	4.92	1.021	0.021	0.04	1.0006	0.0006

Table C. 24. Calibration coefficients, scenario protection level 3 (Extreme Environmental Protection - EEP), Saint Sulpice la Point

MONTE_CARLO_ITERATIONS=100												
run	diffusion	breed	spread	slp_resst	road_grav	control	area	area	area	cluster	cluster	cluster
number	coeff	coeff	coeff	coeff	coeff	year	diff	ratio	fract	diff	ratio	fract
2670	100	25	25	100	1	2017	4.64	1.019	0.019	-0.04	0.99	-0.0006

Table C. 25. Calibration coefficients, attraction-based scenario protection level 1 (Attraction-based Limited Environmental Protection - ALEP), Saint Sulpice la Point

MONTE_CARLO_ITERATIONS=100												
run	diffusion	breed	spread	slp_resst	road_grav	control	area	area	area	cluster	cluster	cluster
number	coeff	coeff	coeff	coeff	coeff	year	diff	ratio	fract	diff	ratio	fract
2545	100	1	25	100	1	2017	22.40	1.09	0.09	-6.52	0.89	-0.10

Table C. 26. Calibration coefficients, scenario protection level 0 (Nearly No Environmental Protection - NEP), Rieucros

MONTE_CARLO_ITERATIONS=100												
run	diffusion	breed	spread	slp_resst	road_grav	control	area	area	area	cluster	cluster	cluster
number	coeff	coeff	coeff	coeff	coeff	year	diff	ratio	fract	diff	ratio	fract
2545	100	1	25	100	1	2017	3.44	1.08	0.08	2.04	1.15	0.15

Table C. 27. Calibration coefficients, scenario protection level 1 (Limited Environmental Protection - LEP), Rieucros

MONTE_CARLO_ITERATIONS=100												
run	diffusion	breed	spread	slp_resst	road_grav	control	area	area	area	cluster	cluster	cluster
number	coeff	coeff	coeff	coeff	coeff	year	diff	ratio	fract	diff	ratio	fract
2049	75	25	25	100	100	2017	4.00	1.10	0.102	1.40	1.107	0.107

Table C. 28. Calibration coefficients, scenario protection level 2 (Moderate Environmental Protection - MEP), Rieucros

MONTE_CARLO_ITERATIONS=100												
run	diffusion	breed	spread	slp_resst	road_grav	control	area	area	area	cluster	cluster	cluster
number	coeff	coeff	coeff	coeff	coeff	year	diff	ratio	fract	diff	ratio	fract
1920	75	1	25	100	1	2017	3.08	1.078	0.078	1.96	1.15	0.15

Table C. 29. Calibration coefficients, scenario protection level 3 (Extreme Environmental Protection - EEP), Rieucros

MONTE_CARLO_ITERATIONS=100												
run	diffusion	breed	spread	slp_resst	road_grav	control	area	area	area	cluster	cluster	cluster
number	coeff	coeff	coeff	coeff	coeff	year	diff	ratio	fract	diff	ratio	fract
2674	100	25	25	100	100	2017	3.76	1.096	0.096	1.16	1.089	0.089

Table C. 30. Calibration coefficients, attraction-based scenario protection level 1 (Attraction-based Limited Environmental Protection - ALEP), Rieucros

MONTE_CARLO_ITERATIONS=100												
run	diffusion	breed	spread	slp_resst	road_grav	control	area	area	area	cluster	cluster	cluster
number	coeff	coeff	coeff	coeff	coeff	year	diff	ratio	fract	diff	ratio	fract
2170	75	50	25	100	1	2017	33.36	1.855	0.855	1.52	1.116	0.116

Annex D: Weighting Urban Patches Using Predefined Urban Land Use Models

Contents

- D.1. Toulouse concentric zone model
 - D.2. Toulouse sector model
 - D.3. Toulouse multiple nuclei model
 - D.4. Toulouse particular complex model
-

In this Annex, three famous urban land use models, concentric zone model, sector model and multiple nuclei model are defined and applied on Toulouse. These models were developed to generalize the patterns of urban land use of the industrial cities of United States and they are not correspond to the geographic and social situation of Toulouse. The point is only to show how to make different patterns and weighting them.

Next, another land use model matched to Toulouse land use is created and applied. All these models will give weight to the urban patches. The weight is defined as the value of the average height of the buildings in urban area that locate in the same zone in land use pattern.

D.1. Toulouse Concentric Zone Model

The first step of weighting urban patches is creating the land use pattern. The pattern is an image containing different rings. Each ring has its own color (value). The value of the pixels that have similar color are the same. The next step is preparing the 2D prospective urban map and applying the urban land use model on it. Figure D.1 shows the concentric zone model prepared and applied on the Toulouse 2D prospective map of 2030. The different values of the weighted urban growth map represent the land use of each zone. The defined weights correspond to the average values of the height of the buildings in same zone. Assuming a height for the buildings in each zone will carry out to a very simple 3D model.

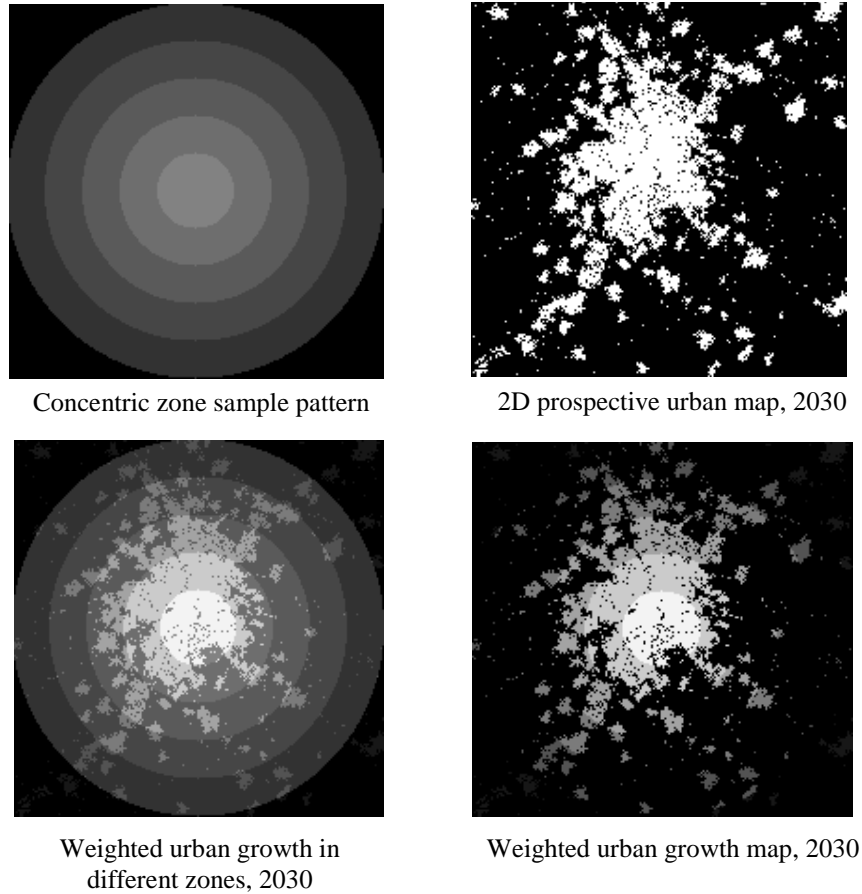
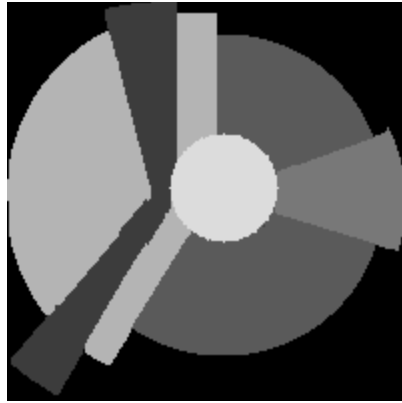


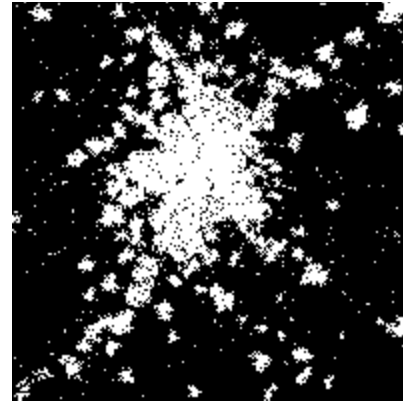
Figure D. 1. Giving weight to the urban area using concentric zone model, Toulouse

D.2. Toulouse Sector Model

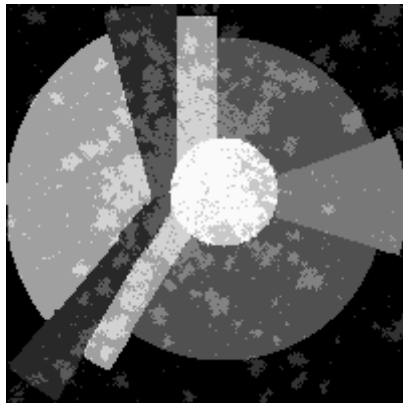
The process of the weighting urban patches by sector model is similar to the concentric zone model. Therefore, the first step is creating the sector model pattern defining different value for each sector. These values correspond to the average height of the buildings in this sector. The second step is preparing the 2D prospective urban map. The last step is applying the urban land use pattern on the prospective urban map in order to find out the land use of the growth urban area (see figure D.2).



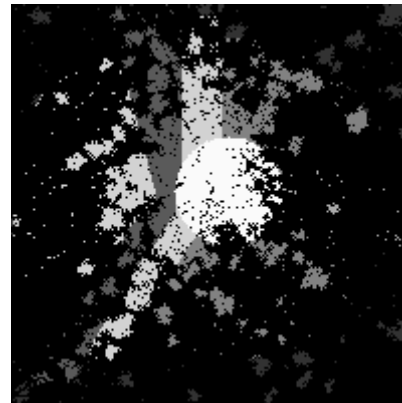
Sector sample pattern



2D prospective urban map, 2030



Weighted urban growth in different zones, 2030



Weighted urban growth map, 2030

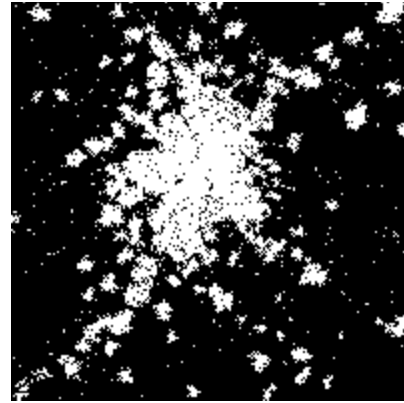
Figure D. 2. Giving weight to the urban area using sector model, Toulouse

D.3. Toulouse Multiple Nuclei Model

Similar to the previous predefined land use models, the weighting urban patches start by creating the multiple nuclei pattern. Each nuclei has its own value correspond to the average height of the buildings in that nucleus. Afterwards, the 2D prospective urban map have to be simulated. The weighting urban patches process finished by applying the urban land use pattern on the prospective urban map in order to find out the land use of the growth urban area (see figure D.3).



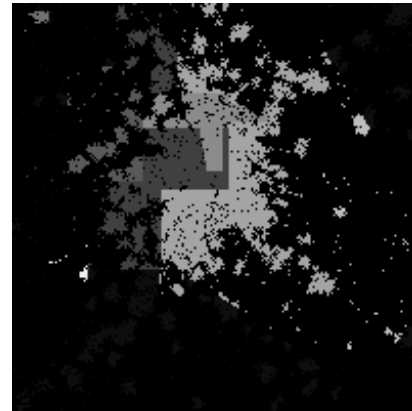
Multiple nuclei sample pattern



2D prospective urban map, 2030



Weighted urban growth in different zones, 2030



Weighted urban growth map, 2030

Figure D. 3. Giving weight to the urban area using multiple nuclei model, Toulouse

D.4. Toulouse Particular Complex Model

This proposed model is based on the multiple nuclei model. The pattern is created for Toulouse considering the information of the height. Using the building classification discussed on chapter 2, six different maps are created for the undifferentiated buildings and three maps for the industrial buildings as follow (see figure D.4):

Undifferentiated buildings:

- Individual dwellings, $h = 4\text{m}$
- Low-rise housing, $h = 7\text{m}$
- Shop top housing, $h = 15\text{m}$
- Medium height housing, $h = 20\text{m}$
- Medium / high rise housing, $h = 27\text{m}$
- High-rise housing, $h = 36\text{m}$

Industrial buildings:

- Agricultural building, $h = 8\text{m}$
- Industrial building, $h = 9\text{m}$
- Commercial building, $h = 10\text{m}$

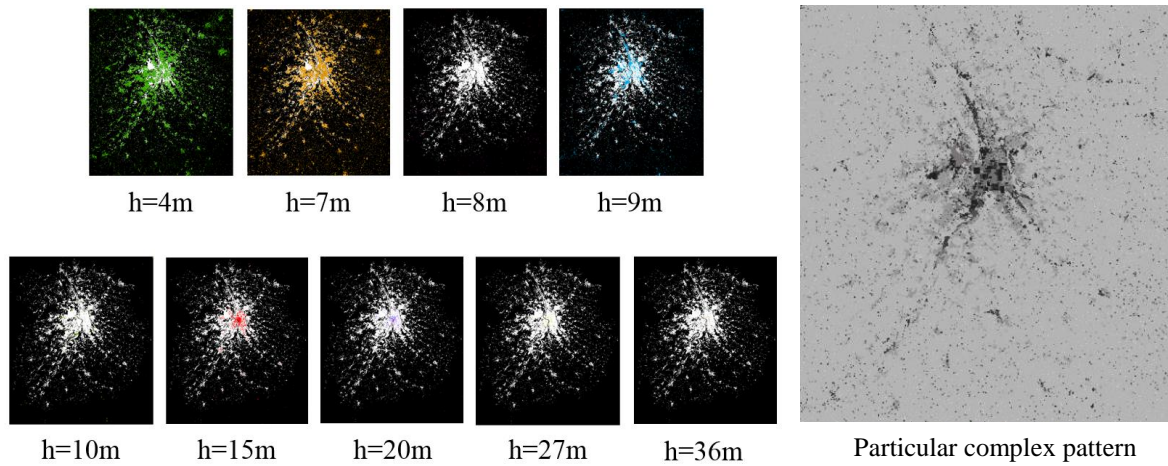


Figure D. 4. The urban maps with different height that used to create particular complex pattern. The process of weighting urban patches particular complex model starts by creating the pattern. The pattern has different height values due to the building classification. The second step is simulating the 2D prospective urban map. Applying the 2D prospective map on particular complex pattern leads to weighted urban growth map. Figure D.5 illustrates the results of weighted urban map of Toulouse for 2030. The weighted urban growth map can be used for classifying the new urban pixels.

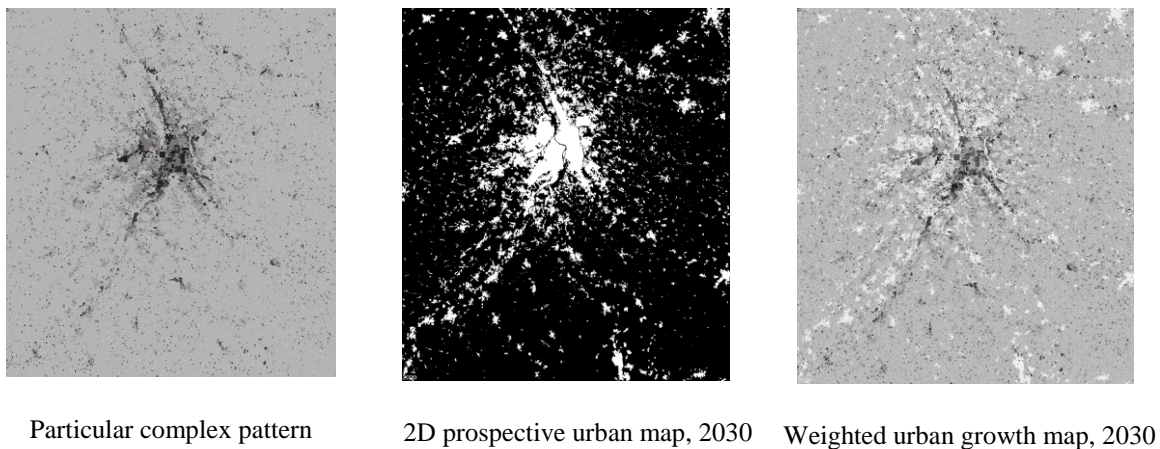


Figure D. 5. Giving weight to the urban area using particular complex pattern for Toulouse

In all patterns presented in this Annex, if we want to classify a new urban pixel, we have only one choice for it. For example, if a prospective urban pixel is located in the zones of single dwelling, means that this pixel could only be a house. However, using the new technique for creating a land use pattern that proposed in chapter 2 (Active Land Use Model), we will have different choices (with their probabilities) for each building class, which gives a great advantage for précising the urban patterns.

Annex E: INSEE Data Documentations

Contents

- E.1. Number of inhabited
 - E.2. List and description of variables - Table of tiles
 - E.3. List and description of variables - Table of rectangles
-

E.1. Number of Inhabited

- The data provided from a specific exploitation of tax files aimed at giving each household a precise geographic position. The squared population data is consistent with the data disseminated by the localized tax revenue source:
 - o Populations not referenced to the housing tax are not present: homeless people, communities;
 - o Students are usually located at the home of their parents;
 - o The concept of principal residence can be significantly different.
- Localized tax revenues (RFL) are based on the exhaustive files of the personal income tax returns and the housing tax provided to INSEE by the General Tax Directorate. INSEE reconciles these two files in order to estimate the tax revenue at finely localized geographical levels, while preserving the confidentiality of the data.
- This database includes 18 variables on the age structure of individuals, household characteristics (renter / owner, etc.) and income as of December 31, 2010.
- The data comes in two alternative forms: a DBF dBase file and a MapInfo MIF / MID transport map.
- The square estimates are in the form of two datasets, one with a resolution of 1 km, the other with a resolution of 200 m.
- The projection system used on the metropolis is the "Lambert Azimutal Equal Area (code EPSG 3035)" which conforms to the European recommendations within the framework of the INSPIRE directive

E.2. List and Description of Variables - Table of Tiles

- The geographical identifiers of the tile
- The number of inhabited tiles in the rectangle to which the tile belongs
- The geographical identifiers of the rectangle to which the tile belongs

- The number of individuals of the tile

E.3. List and Description of Variables - Table of Rectangles

- The total number of individuals
- The total number of households (i.e. of main residences)
- The total number of individuals aged 0 to 3 years
- The total number of individuals aged 4 to 5 years
- The total number of individuals aged 6 to 10 years
- The total number of individuals aged 11 to 14
- The total number of individuals aged 15 to 17
- The total number of individuals aged 25 and over
- The total number of households of 5 or more
- The total number of households present for 5 years or more in their current dwelling
- The total number of households in collective housing
- The cumulative surface area of the main residences, in square meters
- The sum of tax revenues per individuals
- The total number of individuals aged 65 and over
- The total number of individuals aged 75 and over
- The total number of households of a person
- The total number of owner households
- The total number of households whose tax revenue is below the low threshold

Publications

- Eslahi, M., El Meouche, R., Ruas, A.; " Towards the best urban growth parameterization in order to control the urban sprawl: the SLEUTH modeling improvement by integrating topographic data, urban tissue and demographic data "; (submitting in progress).
- Eslahi, M., El Meouche, R., Bing, W., Ruas, A., Doukari, O. (2019). BIM and Contribution to IFC-Bridge Development: Application on Raymond Barre Bridge, Springer CCIS - Communications in Computer and Information Science.
- Eslahi, M., El Meouche, R., and Ruas, A. (2019). Using building types and demographic data to improve our understanding and use of urban sprawl simulation, Proc. Int. Cartogr. Assoc., 2, 28, <https://doi.org/10.5194/ica-proc-2-28-2019>.
- Da Silva, G., Doukari, O., Aguejdad, R., Eslahi, M. (2018). Modélisation paramétrique 3D et multi-échelle du développement résidentiel : exemple du modèle SLEUTH3D, Edubim, 2018.
- Majid Zadeh, Heravi, F., Eslahi, M., Farazdaghi, E., Nait-Ali, A. (2016). A Morphable Model to Simulate Rejuvenation Trajectory of 3D Face Images: Preliminary Results, International Conference on Bio-engineering for Smart Technologies (BioSMART), 1-4. 2016.

Bibliography

Aguejdad, R., Doukari, O., Houet, T., Avner, P. and Viguié, V. (2016). Etalement urbain et géoprospective : apports et limites des modèles de spatialisation. Application aux modèles SLEUTH, LCM et NEDUM-2D. *Cybergeo*, No. 782.

Aguejdad, R. and Hubert-Moy, L. (2016). Suivi de l'artificialisation du territoire en milieu urbain par télédétection et à l'aide de métriques paysagères. Application à une agglomération de taille moyenne, Rennes Métropole. *Cybergeo*, No. 766.

Akbar, M., Aliabadi, S., Patel, R. and Watts, M. (2013). A fully automated and integrated multi-scale forecasting scheme for emergency preparedness. *Environ. Model. Softw.* 39, 24–38. 10.1016/j.envsoft.2011.12.006.

Alkheder, S., Wang, J., and Shan, J. (2008). Fuzzy inference guided cellular automata urban-growth modelling using multi-temporal satellite images. *International Journal of Geographical Information Science*. 22. 1271-1293. 10.1080/13658810701617292.

Almeida, C. M., Gleriani, J. M., Castejon, E. F., and Soares-Filho, B. S. (2008). Using neural networks and cellular automata for modelling intra-urban land-use dynamics. *International Journal of Geographical Information Science*, 22(9), 943–963. 10.1080/13658810701731168.

Al-shalabi, M., Billa, L., Pradhan, B., Mansor, S. and Al-Sharif A.A.A. (2013). Modelling urban growth evolution and land-use changes using GIS based cellular automata and SLEUTH models: the case of Sana'a metropolitan city Yemen. *Environ Earth Sci*, 70(1):425–437

Antoni, J.P., Vuidel, G., Omrani, H. and Klein, O. (2019). Geographic cellular automata for realistic urban form simulations: How far should the constraint be contained? 10.1007/978-3-030-12381-9_7.

Antoni, J.P. (2010). L'étalement urbain. Gabriel Wackermann. *La France en villes*, Ellipses, pp.164-176, 2010. hal-01075776

Antoni, J.P. (2003). Modélisation de la dynamique de l'étalement urbain - aspects conceptuels et gestionnaires - application à Belfort, Thèse, l'Université Louis Pasteur, Strasbourg I

Antrop, M. (2004). Landscape change and the urbanization process in Europe. *Landscape and Urban Planning*, 67 (1-4): 9-26. [http://dx.doi.org/10.1016/s0169-2046\(03\)00026-4](http://dx.doi.org/10.1016/s0169-2046(03)00026-4)

Arsanjani, J. J., Helbich, M. and Noronha Vaz, E. (2013). Spatiotemporal simulation of urban growth patterns using agent-based modeling: The case of Tehran. *Cities*. 32. 33–42. 10.1016/j.cities.2013.01.005.

Autodesk (2019), <https://www.autodesk.fr/products/autocad/features>

Badariotti, D., Banos, A. and Moreno, D. (2007). Conception d'un automate cellulaire non stationnaire à base de graphe pour modéliser la structure spatiale urbaine: le modèle Remus. *CyberGeo*. 10.4000/cybergeo.10993.

Barredo J. I., Kasanko M., McCormick N. and Lavallo C. (2003). "Modelling Dynamic Spatial Processes: Simulation of Urban Future Scenarios through Cellular Automata," *Landscape and Urban Planning*, Vol. 64, No. 3, 2003, pp. 145-160. doi:10.1016/S0169-2046(02)00218-9

Batty M., Besussi E. and Chin N., (November 2003). *Traffic, Urban Growth and Suburban Sprawl*. UCL Centre for Advanced Spatial Analysis Working Papers Series. 70. ISSN 1467-1298. Retrieved May 17, 2015.

Batty, M. and Xie, Y. (1994). *From Cells to Cities*. *Environment and Planning B: Planning and Design*, 21(7), S31–S48. <https://doi.org/10.1068/b21S031>

Batty, M., Xie, Y., and Sun, Z., (1999). Modeling urban dynamics through GIS-based cellular automata. *Computers Environment and Urban Systems*, 1999, 23, 205–233.

Benning, P. (2017). *Contribution to IFC-Bridge Development: Missing Concepts and New Entities*, Edu-BIM, 2017.

Béchet B., Le Bissonnais Y., Ruas A. (pilotes), Aguilera A., Andrieu H., Barbe E., Billet Ph., Cavailhès J., Cohen M., Cornu S., Dablanc L., Delolme C., Géniaux G., Hedde M., Mering C., Musy M., Polèse M., Weber C., Frémont, A., Le Perchec, S., Schmitt, B., c Savini, I., Desrousseaux, M. (2017). *Artificialized land and land take; drivers, impacts and potential responses*. Synthesis of the collective scientific expert report, Ifsttar-Inra (France), 121 p.

Béchet B. (coord.), Le Bissonnais Y. (coord.), Ruas A. (coord.), Aguilera A., André M., Andrieu H., Ay J.-S., Baumont C., Barbe E., Beaudet-Vidal L., Belton-Chevallier L., Berthier E., Billet Ph., Bonin O., Cavailhès J., Chancibault K., Cohen M., Coisson T., Colas R., Cornu S., Cortet J., Dablanc L., Darly S., Delolme C., Fack G., Fromin N., Gadal S., Gauvreau B., Géniaux G., Gilli F., Guelton S., Guérois M., Hedde M., Houet T., Humbertclaude S. (expert technique), Jolivet L., Keller C., Le Berre I., Madec P. (expert technique), Mallet C., Marty P., Mering C., Musy M., Oueslati W., Paty S., Polèse M., Pumain D., Puissant A., Riou S., Rodriguez F., Ruban V., Salanié J., Schwartz C., Sotura A., Thébert M., Thévenin T., Thisse J., Vergnès A., Weber C., Wery C., Desrousseaux M. (2017). *Sols artificialisés et processus d'artificialisation des sols, Déterminants, impacts et leviers d'action*. INRA (France), 609 pages.

Bétaille, D., Peyret, F., Ortiz, M., Miquel, S. and Fontenay, L. (2013). A New Modelling based on Urban Trenches to Improve GNSS Positioning Quality of Service in Cities. *Intelligent Transportation Systems Magazine*, in *IEEE Intelligent Transportation Systems Magazine*, vol. 5, no. 3, pp. 59-70, Fall 2013. doi: 10.1109/MITS.2013.2263460.

Biljecki F (2017). *Level of detail in 3D city models*. PhD thesis, TU Delf, 353 pp. doi:10.4233/uuid:f12931b7-5113-47ef-bfd4-688aae3be248

Biljecki, F., Ledoux, H., and Stoter, J. (2017). Generating 3D city models without elevation data. *Computers Environment and Urban Systems*. 64. 1-18. [10.1016/j.compenvurbsys.2017.01.001](https://doi.org/10.1016/j.compenvurbsys.2017.01.001).

Biljecki, F., Stoter, J., Ledoux, H., Zlatanova, S. and Çoltekin, A. (2015). Applications of 3D City Models: State of the Art Review. *ISPRS Int. J. Geo-Inf.* 2015, 4, 2842-2889; doi:10.3390/ijgi4042842

Billen, R., Carre, C., Delfosse, V., Hervy, B., Laroche, F., Lefèvre, D., Servièrès, M. and Ruymbeke, M. (2012). 3D historical models: the case studies of Liege and Nantes. <http://hdl.handle.net/2268/126687>

Billen, R., Cutting-Decelle, Af., Marina, O., Duarte de Almeida, J., Caglioni, M., Falquet, G., Leduc, T., Métral, C., Moreau, G., Perret, J., Rabino, G., García, R., Yatskiv, I., and Zlatanova, S., (2014). 3D City Models and urban information: Current issues and perspectives. 10.1051/TU0801/201400001.

Billen, R., Zaki, C., Servièrès, M., Moreau, G. and Hallot, P. (2012). Developing an ontology of space: Application to 3D city modeling. 02007. 10.1051/3u3d/201202007.

Blaauboer, J., Goos, J., Ledoux, H., Penninga, F., Reuvers, M., Stoter, J., & Vosselman, G. (2012). 3D Pilot Eindrapport werkgroep Technische specificaties voor de opbouw van 3D IMGeo-CityGML. Tech. rep., Kataster.

Brasebin Mickaël , Christophe Sidonie , Jacquinod Florence , Vinesse A. and Mahon, H. (2016). 3D geovisualization and stylization to manage comprehensive and participative local urban plans. 10.5194/isprs-annals-IV-2-W1-83-2016.

BuildingSMART (2019), International home of openBIM, Infrastructure; <http://www.buildingsmart-tech.org/infrastructure/projects>

Caglioni Matteo, Pelizzoni Mattia and Rabino Giovanni. (2006). Urban sprawl: A case study for project gigalopolis using SLEUTH model. 4173. 436-445. 10.1007/11861201_51.

Candau, J. (2002). Temporal calibration sensitivity of the SLEUTH urban growth model. Master's thesis, Department of Geography, University of California, Santa Barbara, C.A.

Chaturvedi Kanishk , Smyth Carl , Gesquière Gilles, Kutzner Tatjana and Kolbe Thomas. (2017). Managing Versions and History Within Semantic 3D City Models for the Next Generation of CityGML. 10.1007/978-3-319-25691-7_11.

Chaudhuri G. and Clarke K.C. (2013). The SLEUTH Land Use Change Model: A Review. International Journal of Environmental Resource Research

Chaudhuri, G. and Clarke K.C. (2014). Temporal Accuracy in Urban Growth Forecasting: A Study Using the SLEUTH Model. Transactions in GIS. 10.1111/tgis.12047.

Chen, R. (2011). The development of 3D city model and its applications in urban planning. In Proceedings of the 19th International Conference on Geoinformatics, Shanghai, China, 26 June 2011; pp. 1–5.

Cheng J. and Masser I. (2003). Urban growth pattern modeling: A case study of Wuhan City, PR China. Landscape and Urban Planning. 199-217. 10.1016/S0169-2046(02)00150-0.

CII - Construction Industry Institutes of USA. (1986), Constructability: A Primer, Austin.

CIRIA - Construction Industry Research and Information Association. (1983), Buildability: An assessment, London.

Clarke K.C., Gaydos L. and Hoppen S. (1997). A self-modifying cellular automaton model of historical urbanization in the San Francisco Bay area. *Environment and Planning B* 24: 247-261

Clarke K. C. (2008). A Decade of Cellular Urban Modeling with SLEUTH: Unresolved Issues and Problems. In Brail R.-K. (eds.), *Planning Support Systems for Cities and Region*, Lincoln Institute of Land Policy, Cambridge, MA, 47–60.

Clarke K. C. and Gaydos L. J. (1998). Loose-coupling of a cellular automaton model and GIS: Long-term growth prediction for the San Francisco and Washington/ Baltimore. *International Journal of Geographical Information Science*, 1998, 12, 699–714.

Clarke, K. C., Gazulis, N., Dietzel, C.K., Goldstein, N.C.(2007) A decade of SLEUTHing: Lessons learned from applications of a cellular automaton land use change model. Chapter 16 in Fisher, P. (ed) *Classics from IJGIS. Twenty Years of the International Journal of Geographical Information Systems and Science*. Taylor and Francis, CRC, Boca Raton, FL. pp. 413–425.

Clarke, K. C., Hoppen, S. and Gaydos, L. (1996). Methods and techniques for rigorous calibration of a cellular automation model of urban growth. In: *Proceedings of the Third International Conference/Workshop on Integrating GIS and Environmental Modelling*, Santa Fe, New Mexico, January 21–25, 1996.

Clarke K.C., Parks B. O., Crane M. P., and Parks B. E. (2001). *Geographic Information Systems and Environmental Modeling*, Prentice Hall; 1 edition (July 5, 2001)

College of Liberal Arts & Sciences, Department of Geography & Earth Sciences, (2017). <https://geoearth.uncc.edu/people/hcampbell/landuse/3models.html>

Construction elements classification (Sydenham to Banks town Urban Renewal Corridor, Draft Urban Renewal Corridor Strategy, Department of Planning and Environment-NSW Government, Sydney, Australia, (2017). <http://www.planning.nsw.gov.au/Plans-for-your-area/Priority-Growth-Areas-and-Precincts/Sydenham-to-Bankstown-Urban-Renewal-Corridor>

Content description of BD TOPO version 2.1, IGN; 73 avenue de Paris 94165 Saint-Mandé Cedex www.ign.fr

Contrada. F., (2019). L'apport de la constructibilité au pré-design. Analyse et support au choix des solutions techniques Ph.D Thesis in Science de l'Ingénieur Université Paris Est.

Coors V., Holweg D., Matthias E., Petzold B. and Broschüre, (2013). *3D-Stadtmodelle*, Ingeoforum: Darmstadt, Germany, p. 20.

CORINE Land Cover (2006, 2012), <https://land.copernicus.eu/pan-european/corine-land-cover>

Couclelis H. (1985). Cellular Worlds: A Framework for Modeling Micro—Macro Dynamics. *Environment and Planning A: Economy and Space*, 17(5), 585–596. <https://doi.org/10.1068/a170585>

- Cox, S., Daisey, P., Lake, R., Portele, C. and Whiteside, A. (2004). Geography Markup Language (GML) Encoding Specification v3.1.1. 10.13140/2.1.2846.2401.
- Crooks A., Castle C. and Batty M. (2008). Key challenges in agent-based modelling for geospatial simulation. *Computers, Environment and Urban Systems*, 2008, 32(6), 417–430.
- Curie, F., Mas, A., Perret, J., Puissant, A. and Ruas, A. (2011). Simulation d'un processus de densification du tissu urbain à base d'agents, *Revue Internationale de Géomatique*, vol. 21, n. 4, pp. 489--513, doi:10.3166/rig.21.489-511
- Curie, F., Perret, J. and Ruas, A. (2010). Simulation of urban blocks densification, 13th AGILE International Conference on Geographic Information Science.
- Da Silva G., Doukari O. and Aguejdad, R. (2016). Towards a BIM-based 3D Modeling of Urban Growth: Application to the SLEUTH Cellular-automata Model, BAFConf16.
- Da Silva, G., Doukari, O., Aguejdad, R. and Eslahi, M. (2018). Modélisation paramétrique 3D et multi-échelle du développement résidentiel: exemple du modèle SLEUTH3D, EduBIM, France
- Dahal, K.J. and Chow, T.E. (2014). A GIS toolset for automated partitioning of urban lands. *Environmental Modeling and Software*, vol. 55, 222–234.
- Deng, Z., Zhang, X., Li, D., and Pan, G. (2015). Simulation of land use/land cover change and its effects on the hydrological characteristics of the upper reaches of the Hanjiang Basin. *Environmental Earth Sciences*. 73. 10.1007/s12665-014-3465-5.
- Dietzel, C., and Clarke, K. C. (2004). Spatial differences in multi-resolution urban automata modeling. *Transactions in GIS* 8:479-492. <https://doi.org/10.1111/j.1467-9671.2004.00197.x>
- Dietzel, C., and Clarke, K. C. (2007). Toward Optimal Calibration of the SLEUTH Land Use Change Model. *T. GIS*. 11. 29-45. 10.1111/j.1467-9671.2007.01031.x.
- Doukari, O., Aguejdad, R. and Houet, T. (2016). SLEUTH* : un modèle d'expansion urbaine scénario-dépendant. *Revue Internationale de Géomatique*. 26. 7-32. 10.3166/RIG.26.7-32.
- Dubos-Paillard, E. and Langlois, P. (2018). Simulation et validation de la dynamique urbaine par automate cellulaire, halshs-01694570
- Dubos-Paillard, E., Guermond, Y. and Langlois, P. (2003). Analyse de l'évolution urbaine par automate cellulaire. *Le modèle SpaCelle*, Conference Proceedings DOI:10.3917/eg.324.0357
- EL Meouche, R., Rezoug, M., Hijazi, I. and Maes, D. (2013). Automatic Reconstruction of 3D Building Models from Terrestrial Laser Scanner Data. *ISPRS Annals of Photogrammetry, Remote Sensing and Spatial Information Sciences*. II-4/W1. 7-12. 10.5194/isprsannals-II-4-W1-7-2013.
- ESCo (L'expertise scientifique collective) (2017), Ifsttar-Inra « Sols artificialisés et processus d'artificialisation des sols »

- Ewing, R.H. (1994). Causes, characteristics, and effects of sprawl: A literature review. *Environmental and Urban Issues*, 21 (2): 1-15.
- Fan, Y., Yu, G., He, Z., Yu, H., Bai, R., Yang, L., Wu, D. (2017). Entropies of the Chinese Land Use/Cover change from 1990 to 2010 at a County level. *Entropy* 19 (2), 51. <http://dx.doi.org/10.3390/e19020051>.
- Feng, Y., Liu, Y. and Batty, M. (2015). Modeling Urban Growth with GIS Based Cellular Automata and Least Squares SVM Rules: A Case Study in Qingpu–songjiang Area of Shanghai, China, Springer-Verlag Berlin Heidelberg, DOI 10.1007/s00477-015-1128-z.
- Feng, Y., Liu, Y., Tong, X., Liu, M. and Deng, S. (2011). Modeling Dynamic Urban Growth Using Cellular Automata and Particle Swarm Optimization Rules, *Landscape and Urban Planning* 102 188– 196.
- Ferber, Jacques. (1995) *Les Systèmes Multi Agents : vers une intelligence collective*, InterEditions.
- Fosset, P., Banos, A., Beck, E., Chardonnel, S., Lang, C., Marilleau, N., Piombini, A., Leysens, T., Conesa, A. and André-Poyaud, I. (2016). Exploring Intra-Urban Accessibility and Impacts of Pollution Policies with an Agent-Based Simulation Platform: GaMiroD. *Systems*. 4. 5. 10.3390/systems4010005.
- Frankhauser Pierre, Tannier Cécile, Vuidel Gilles and Houot Hélène. (2007). *Approche fractale de l'urbanisation - Méthodes d'analyse d'accessibilité et simulations multi-échelles*.
- Frankhauser, Pierre. (1990). Aspects fractals des structures urbaines. *Espace géographique*. 19. 10.3406/spgeo.1990.2943.
- Frankhauser, Pierre. (1994). *La fractalité des structures urbaines*. Economica, Anthropos, collection « Villes », Paris, 291 pp.
- Frankhauser, Pierre. (2005). La Morphologie des tissus urbains et périurbains à travers une lecture fractale, *Revue Géographique de l'Est*, no 45,p. 145-160 ,2005
- Galiano, V. F., Chica-Olmo, M., Abarca-Hernandez, F., Atkinson, P. M. and Jeganathan, C. (2012). Random forest classification of Mediterranean land cover using multi-seasonal imagery and multi-seasonal texture. *Remote Sens. Environ*, 121, 93–107.
- Galster G, Hanson R, Ratcliffe MR, Wolman H, Coleman S, Freihage J (2001) Wrestling sprawl to the ground: defining and measuring an elusive concept. *Hous Policy Debate* 12:681–717
- Gelan, A., Shannon, P. and Aitkenhead, M. (2008). Sustainable local land use policy: Rhetoric and reality. *Local Environment*, 13(4): 291-308. <http://dx.doi.org/10.1080/13549830701803331>
- Geniaux, G. and Napoléone, C. (2011). Évaluation des effets des zonages environnementaux sur la croissance urbaine et l'activité agricole. *Economie et Statistique*, 444 (1): 181-199. <http://dx.doi.org/10.3406/estat.2011.9650>

- Gober, P. and Burns, E.K. (2002). The size and shape of Phoenix's urban fringe. *Journal of Planning Education and Research*, 21 (4): 379-390. <http://dx.doi.org/10.1177/07356X021004003>
- Goldstein, N.C., Candau, J.T., and Clarke, K.C. (2004). Approaches to simulating the “March of Bricks and Mortar”. *Comput. Environ Urban Syst.* 28, 125-147.
- Gong, J.Z., Liu, Y.S., Xia, B.C. and Zhao, G.W. (2009). Urban ecological security assessment and forecasting, based on a cellular automata model: a case study of Guangzhou China. *Ecol Model*, 220(24):3612–3620. DOI:10.1016/j.ecolmodel.2009.10.018
- Gonzva, M., Barroca, B., Gautier, P.E. and Diab, Y. (2015). A modelling of disruptions cascade effect within a rail transport system facing a flood hazard. 48th ESReDA Seminar on Critical Infrastructures Preparedness: Status of Data for Resilience Modelling, Simulation and Analysis, ESReDA, May 2015, Wroclaw, Poland. pp.53-59. fhal-01430921f
- Gröger, G. and Plümer, L. (2012). CityGML – Interoperable semantic 3D city models. *ISPRS Journal of Photogrammetry and Remote Sensing*. 71. 12–33. 10.1016/j.isprsjprs.2012.04.004.
- Gröger, G., Kolbe, T.H., Nagel, C. and Häfele, K.H. (2012). OGC City Geography Markup Language (CityGML) Encoding Standard, Version 2.0.0. Open Geospatial Consortium, OGC Doc. No. 12–019.
- Guan, Q., and Clarke, K. C. (2010). A general-purpose parallel raster processing programming library test application using a geographic cellular automata model, *International Journal of Geographical Information Science*, Volume 24, Issue 5, May 2010, pages 695 - 722
- Haala, N., Kada, M., (2010). An update on automatic 3D building reconstruction. *ISPRS Journal of Photogrammetry and Remote Sensing*. 65. 570-580. 10.1016/j.isprsjprs.2010.09.006.
- Han, J., Yoshitsugu, H., Cao, X., and Imura, H. (2009). Application of an integrated system dynamics and cellular automata model for urban growth assessment: A case study of Shanghai, China. *Landscape and Urban Planning*. 91. 133-141. 10.1016/j.landurbplan.2008.12.002.
- Hanwei Xu, Rami Badawi, Xiaohu Fan, Jiayong Ren and Zhiqiang Zhang, (2009). Research for 3D visualization of digital city based on SketchUp and ArcGIS. *International Symposium on Spatial Analysis, Spatial-Temporal Data Modeling, and Data Mining*. Vol. 7492. International Society for Optics and Photonics, 2009.
- Harris, C.D. and Ullman, E.L. (1945). Building the Future City. *Annals of the American Academy of Political and Social Science* Vol. 242, pp. 7-17.
- He, C., Okada, N., Zhang, Q., Shi, P., and Li, J. (2008). Modelling dynamic urban expansion processes incorporating a potential model with cellular automata. *Landscape and Urban Planning*. 86. 79-91. 10.1016/j.landurbplan.2007.12.010.
- He, C., Wei, A., Shi, P., Zhang, Q., and Zhao, Y. (2011). Detecting land-use/land-cover change in rural-urban fringe areas using extended change-vector analysis. *Int. J. Applied Earth Observation and Geoinformation*. 13. 572-585. 10.1016/j.jag.2011.03.002.

He, Shuang, Perret, Julien, Brasebin, Mickaël and Brédif, Mathieu. (2014). A Stochastic Method for the Generation of Optimized Building Layouts Respecting Urban Regulations. 10.1007/978-3-319-19950-4_16.

Hegde N.P, Muralikrishna I.V., & Chalapatirao K.V. (2008). Settlement Growth Prediction Using Neural Network And Cellular Automata. Journal of Theoretical and Applied Information Technology (JATIT), 4 (5) : 419-428.

Herold M., Scepan J. and Clarke K. C. (2002). The Use of Remote Sensing and Landscape Metrics to Describe Structures and Changes in Urban Land Uses. Environment and Planning A. 34. 1443-1458. 10.1068/a3496.

Hervy, B., Billen, R., Laroche, F., Carre, C., Servières, M., Ruymbeke, M., Tourre, V., Delfosse, V. and Kerouanton, J. L. (2012). A generalized approach for historical mock-up acquisition and data modelling: Towards historically enriched 3D city models. 02009. 10.1051/3u3d/201202009.

Hijatzi, I., Ehlers, M., Zlatanova, S., Adolphi, T. and Berleo, L. (2011). Initial Investigations for Modeling Interior Utilities Within 3D Geo Context: Transforming IFC-Interior Utility to CityGML/UtilityNetworkADE. 10.1007/978-3-642-12670-3_6.

Homer Hoyt (1939). The Structure and Growth of Residential Neighborhoods in American Cities Washington, Federal Housing Administration.

Houet, T, Aguejdad, R., Doukari, O., Battaia, G., Clarke, K.(2016). Description and validation of a “non path-dependent” model for projecting contrasting urban growth futures. CyberGeo. 759. 10.4000/cybergeogeo.27397.

INSEE (2011), <https://www.insee.fr/fr/accueil>

Isikdag U. and Zlatanova S. (2009) Towards Defining a Framework for Automatic Generation of Buildings in CityGML Using Building Information Models. In: Lee J., Zlatanova S. (eds) 3D Geo-Information Sciences. Lecture Notes in Geoinformation and Cartography. Springer, Berlin, Heidelberg, ISBN: 978-3-540-87394-5, DOI: https://doi.org/10.1007/978-3-540-87395-2_6

Itami, M. Robert. (1994). Simulating spatial dynamics: cellular automata theory. Landscape and Urban Planning - LANDSCAPE URBAN PLAN. 30. 27-47. 10.1016/0169-2046(94)90065-5.

Jantz, C. A., Goetz, S. J. and Shelley, M. K., (2004). Using the SLEUTH urban growth model to simulate the impacts of future policy scenarios on urban land use in the Baltimore/Washington metropolitan area. Environment and Planning B 31: 251–71

Jantz, C.A., Drzyzga, S. A. and Michael, M. (2014). Calibrating and Validating a Simulation Model to Identify Drivers of Urban Land Cover Change in the Baltimore, MD Metropolitan Region. Land. 3. 1158-1179. 10.3390/land3031158.

Jantz, C.A. and Goetz S.J., (2005). Analysis of scale dependencies in an urban land-use change model. International Journal of Geographical Information Science, vol. 19, No. 2, 217–241.

Jantz, C.A., Goetz, S. J., Donato, D. and Claggett P. (2010). Designing and Implementing a Regional Urban Modeling System Using the SLEUTH Cellular Urban Model, *Computers, Environment and Urban Systems*, Vol. 34, No. 1, 2010, pp. 1-16. doi:10.1016/j.compenvurbsys.2009.08.003

Julin, A., Jaalama, K., Virtanen, J., Pouke, M., Ylipulli, J., Vaaja, M., Hyyppä, J. and Hyyppä, H., (2018). Characterizing 3D city modeling projects: Towards a harmonized interoperable system, *ISPRS Int. J. Geo-Inf.* 2018, 7(2), 55; <https://doi.org/10.3390/ijgi7020055>.

Kamusoko, C. and Gamba, J. (2015). Simulating Urban Growth Using a Random Forest-Cellular Automata (RF-CA) Model, *ISPRS Int. J. Geo-Inf.* 2015, 4, 447-470.

KantaKumar, N., Sawant, N. G. and Kumar, S. (2011). Forecasting urban growth based on GIS, RS and SLEUTH model in Pune metropolitan area. *International Journal of Geomatics and Geosciences*. 2. 568-579.

Kapoor, M., Khreim, J.F., El Meouche, R., Bassit, D., Henry, A., Ghosh, S. (2010). Comparison of techniques for the 3D modeling and thermal analysis, x Congreso Internacional Expresión Gráfica aplicada a la Edificación Graphic Expression applied to Building International Conference, APEGA 2010

Kobayashi, Y. (2006). Photogrammetry and 3D city modelling. 209-218. 10.2495/DARC060211.

Kolbe, T.H. and Gröger, G. (2003). Towards unified 3D city models. In *Proceedings of the ISPRS Commission IV Joint Workshop on Challenges in Geospatial Analysis, Integration and Visualization II*, Stuttgart, Germany, 8–9 September 2003.

L'Her, G., Servières, M., and Siret, D. (2018). La Cartopartie, une nouvelle forme de balade urbaine déployée par les villes. *Cahiers de la recherche architecturale, urbaine et paysagère*. 3. 10.4000/craup.1003.

L'Her, G., Servières, M., and Siret, D. (2017). Participer et transformer les territoires: Interactions entre habitants, techniques et milieux à partir de la notion de « citoyen-capteur ». *Netcom*. 31. 153-174. 10.4000/netcom.2668.

Ledoux, H. and Meijers, M. (2011). Topologically consistent 3D city models obtained by extrusion. *Int. J. Geogr. Inf. Sci.* 2011, 25, 557–574.

Lee, D. R. and Sallee, G. T., (1970). A method of measuring shape. *The Geographical Review* 60: 555–63

Legal populations 2016, Municipality of Saint-Sulpice-la-Pointe (81271), <https://www.insee.fr/fr/statistiques/3681328?geo=COM-81271>

Lhomme, S., Serre, D., Diab, Y. and Laganier, R. (2011). Domino effect analysis of interdependent systems with risk analysis methods. Application to urban networks facing flood events.

- Li, X. and Yeh, A. G. O. (2001). Calibration of cellular automata by using neural networks for the simulation of complex urban systems, *Environment and Planning A*, 2001, 33 (4), 1445–1462.
- Li, X. and Yeh, A. G. O. (2002). Neural-network based cellular automata for simulating multiple land use changes using GIS. *International Journal of Geographical Information Science*, 2002, 16(4), 323–343.
- Maeda, E., Almeida, C.M., Ximenes, A.C., Formaggio, A.R., Shimabukuro, Y.E. and Pellikka, P. (2011). Dynamic modeling of forest conversion: Simulation of past and future scenarios of rural activities expansion in the fringes of the Xingu National Park, Brazilian Amazon. *Int. J. Applied Earth Observation and Geoinformation*. 13. 435-446. 10.1016/j.jag.2010.09.008
- Mandelbrot B. B. (1983). *The Fractal Geometry of Nature*, W. H. Freeman and Company, New York, 1983.
- Manson, S. M. (2005). Agent-based modeling and genetic programming for modeling land change in the Southern Yucatán Peninsular Region of Mexico. *Agriculture, Ecosystems & Environment*, 2005, 111(1–4), 47–62.
- Mao, X., Meng, J. and Xiang, Y. (2013). Cellular automata-based model for developing land use ecological security patterns in semi-arid areas: A case study of Ordos, Inner Mongolia, China. *Environmental Earth Sciences*. 70. 10.1007/s12665-012-2125-x.
- Martinez, C. (2007). Analyse du dispositif français des aires protégées au regard du Programme de travail «Aires protégées» de la Convention sur la diversité biologique. Etat des lieux et propositions d'actions. Paris : Comité français de l'UICN, 92 p. http://uicn.fr/wpcontent/uploads/2016/09/UICN_France_-_aires_protegees_francaises_et_CDB.pdf
- Mellor, A., Haywood, A., Stone, C. and Jones, S. (2013). The Performance of Random Forests in an Operational Setting for Large Area Sclerophyll Forest Classification. *Remote Sensing*, vol. 5, issue 6, pp. 2838-2856. 5. 2838-2856. 10.3390/rs5062838.
- Mitsova, D., Shuster, W. and Wang, X. (2011). A cellular automata model of land cover change to integrate urban growth with open space conservation. *Landsc Urban Plan*, 2011, 99(2):141-153
- Mohammady, S., Delavar, M. R., Pahlavani, P. (2014). Urban growth modeling using an artificial neural network, a case study of Sanandaj city, Iran, *The International Archives of the Photogrammetry, Remote Sensing and Spatial Information Sciences*, The 1st ISPRS International Conference on Geospatial Information Research, Tehran, Iran.
- Moreno, D., Badariotti, D. and Banos, A. (2012). Un automate cellulaire pour expérimenter les effets de la proximité dans le processus d'étalement urbain : le modèle Raumulus. *CyberGeo*. 10.4000/cyberge0.25353.
- Neng Chen, S., & Xu, L., and Li, H., (2005). Research on 3D modeling in scene simulation based on Creator and 3dsmax. *Journal of Computer and System Sciences - JCSS*. 1736 - 1740 Vol. 4. DOI:10.1109/ICMA.2005.1626821.

Nourqolipour, R., Shariff, A., Balasundram, S.K., Ahmad, N.B., Sood, A.M., Buyong, T. and Amiri, F. (2014). A GIS-based model to analyze the spatial and temporal development of oil palm land use in Kuala Langat district. *Environ Earth Sci*, DOI 10.1007/s12665-014-3521-1.

OECD, 2017. OECD Publishing. http://dx.doi.org/10.1787/reg_glance-2013-fr , https://eeas.europa.eu/diplomatic-network/organisation-economic-co-operation-and-development-oecd_en

Park, R. E., Burgess, E. W. and McKenzie, R. D. (1925). *The city Chicago, Illinois: The University of Chicago Press* 1925.

Parker, D. (2006). A Demonstration That Large-Scale Warming Is Not Urban. *Journal of Climate*. 19. 10.1175/JCLI3730.1.

Pedrinis, Frédéric and Gesquière, Gilles. (2017). Reconstructing 3D Building Models with the 2D Cadastre for Semantic Enhancement. 10.1007/978-3-319-25691-7_7.

Perez, L., and Dragicevic, S. (2012). Landscape-level simulation of forest insect disturbance: Coupling swarm intelligent agents with GIS-based cellular automata model. *Ecological Modelling*, 231, 53–64.

Perret, J., Curie, F., Gaffuri, J. and Ruas, A. (2010). A Multi-Agent System for the simulation of urban dynamics, 10th European Conference on Complex Systems (ECCS'10).

Pijanowski, B.C, Tayyebi, A., M. R., Delavar, and M. J, Yazdanpanah (2009). Urban Expansion Simulation Using Geospatial Information System and Artificial Neural Networks, *Int. J. Environ., Res.*, 3(4):493-502.

Pijanowski, B.C., Brown, D.G., Shellito, B., and Manik, G.A. (2002). Using neural networks and GIS to forecast land use changes: a land transformation model. *Comput. Environ. Urban*, 26 (6), 553–575.

Pollock P. (2008). *Urban Growth Management Strategies; Sustainable Community Development Code*, Research Monologue Series, Urban Form, Transportation. The Rocky Mountain Land Use Institute.

Pontius Jr, R. G. and Schneider. L. C. (2001). Land-cover change model validation by an ROC method for the Ipswich watershed, Massachusetts, USA. *Agriculture, Ecosystems & Environment*, 85(1-3), 239-248. DOI:10.1016/S0167-8809(01)00187-6

Pontius Jr., R.G., Boersma, W., Castella, J.C., Clarke, K., de Nijs, T., Dietzel, C., Zengqiang, D., Fotsing, E., Goldstein, N., Kok, K., Koomen, E., Lippitt, C.D., McConnell, W., Pijanowski, B., Pithadia, S., Sood, A.M., Sweeney, S., Trung, T.N., Veldkamp, and A.T., Verburg, P.H. (2008). Comparing the input, output, and validation maps for several models of land change, *Annals of Regional Science*, 42: 11 – 47.

Project Gigalopolis. (2018). <http://www.ncgia.ucsb.edu/>

Pumain, D., and Reuillon, R. (2017). *Urban Dynamics and Simulation Models*, Springer, Alessandro Sarti, CAMS Center for Mathematics, CNRS-EHESS, Paris, France

- Rafiee, R., Mahiny, A. S., Khorasani, N., & Darvisefat, A. A. (2009). Simulating urban growth in Mashad City, Iran through the SLEUTH model. *Cities*, 26.
- Resler, L., Shao, Y., Tomback, D. and Malanson, G. (2014). Predicting Functional Role and Occurrence of Whitebark Pine (*Pinus albicaulis*) at Alpine Treelines: Model Accuracy and Variable Importance. *Annals of the Association of American Geographers*. 104. 10.1080/00045608.2014.910072.
- Robinson, D. T., Murray-Rust, D., Rieser, V., Milicic, V. and Rounsevell, M. (2012). Modelling the impacts of land system dynamics on human well-being: Using an agent-based approach to cope with data limitations in Koper, Slovenia. *Computers, Environment and Urban Systems*. 36. 10.1016/j.compenvurbsys.2011.10.002.
- Rodriguez-Galiano, V.F., Chica-Olmo, M., Abarca-Hernandez, F., Atkinson, P.M. and Jeganathan, C. (2012). Random Forest Classification of Mediterranean Land Cover Using Multi-Seasonal Imagery and Multi-Seasonal Texture. *Remote Sensing of Environment*, 121, 93-107. <https://doi.org/10.1016/j.rse.2011.12.003>
- Ross, L. (2010). Virtual 3D City Models in Urban Land Management—Technologies and Applications. Ph.D. Thesis, Technische Universität Berlin, Germany, 2010.
- Rousseaux, Frederic & Long, Nathalie & Renouard, Antoine. (2011). Vers une simulation de l'évolution des structures urbaines à partir d'une modélisation multi-agents. *Vertigo*. Volume 11. 10.4000/vertigo.11561.
- Russell, S. and Norvig, P. (2003). *Artificial Intelligence, A Modern Approach*. Second Edition.
- Santé, I., García, A. M., Miranda, D. and Crecente, R. (2010). Cellular automata models for the simulation of real-world urban processes: A review and analysis. *Landscape and Urban Planning*. 96. 108-122. 10.1016/j.landurbplan.2010.03.001.
- Schiff, Joel L. (2011). *Cellular Automata: A Discrete View of the World*. Wiley & Sons, Inc. p. 40. ISBN 9781118030639.
- Schone, K. (2010). *Stratégies d'influences et politiques de maîtrise de la croissance locale*. Thèse de Doctorat en Sciences Economiques. Faculté de science économique et de gestion, Université de Bourgogne, Dijon. 290p. <https://nuxeo.ubourgogne.fr/nuxeo/site/esupversions/08912051-3bb2-40af-859e-d5ecdb343d41>
- Servières, M. and Gesquière, G., *MAGIS (Méthodes et Applications pour la Géomatique et l'Information Spatiale - Methods and Applications for Geomatic and Spatial Information)*, (2019), Données 3D géospatiales, <http://gdr-magis.imag.fr/>
- Shiode, N. (2000). 3D urban models: Recent developments in the digital modelling of urban environments in three-dimensions. *GeoJournal*. 52. 263-269. 10.1023/A:1014276309416.
- Silva, E. A. and Clarke, K. C. (2002). Calibration of the SLEUTH urban growth model for Lisbon and Porto, Portugal. *Computers, Environment and Urban Systems* 26: 525–52

Singh, S., Jain, K. and Mandla, V.R. (2014). Image based Virtual 3D Campus modeling by using CityEngine. *American Journal of Engineering Science and Technology Research* 2.1 (2014): 01-10.

SketchUp (2019), <https://www.sketchup.com/fr>

Slak M.-F., Vidal C. (1995). Ter-Uti, indicateur de paysage', Agreste, cahiers n°21

SOeS, MTES, <https://www.statistiques.developpement-durable.gouv.fr/>

Sridhar, K. S. (2007). Density gradients and their determinants: Evidence from India. *Regional Science and Urban Economics*, 37, 314–44. doi: 10.1080/01944360208977191,ISSN: 0194-4363.

Ruas, A., Perret, J., Curie, F., Mas, A., Puissant, A., Skupinski, G., Badariotti, D., Weber, C., Gancarski, P., Lachiche, N., Lesbegueries, J. and Braud, A. (2011). Conception of a GIS-Platform to simulate urban densification based on the analysis of topographic data. 10.1007/978-3-642-19214-2_28.

Tabourin, E. (1995). Les formes de l'étalement urbain. La logique du modèle de Bussière appliquée à l'agglomération lyonnaise. *Persée-Portail des revues scientifiques en SHS (Les Annales de la recherche urbaine)*. <http://dx.doi.org/10.3406/aru.1995.1875>

Taillandier, P., Banos, A., Drogoul, A., Gaudou, B., Marilleau, N. and TRUONG Chi, Q. (2016). Simulating Urban Growth with Raster and Vector Models: A Case Study for the City of Can Tho, Vietnam. 154-171. 10.1007/978-3-319-46840-2_10.

Tang, M., (2014). *Parametric building design using Autodesk Maya*. Routledge, New York, NY, 10001 ©2014.

Tayyebi, A., Pijanowski, B.C. and Tayyebi, A.H. (2011). An urban growth boundary model using neural networks, GIS and radial parameterization: An application to Tehran, Iran. *Landscape and Urban Planning*. 100. 35-44. 10.1016/j.landurbplan.2010.10.007.

Tayyebi, A., Pijanowski, B.C., Delavar M. R. and Yazdanpanah, M.J. (2009). Urban expansion simulation using geospatial information system and artificial neural networks. *International Journal of Environmental Research*. 3. 493-502.

Teruti-Lucas, (2014). <http://agreste.agriculture.gouv.fr/enquetes/territoire-prix-des-terres/teruti-lucas-utilisation-du/>

Tobler, W.R. (1970). A computer movie simulating urban growth in the Detroit region. *Econ Geogr* 46(2):234-240

Tobler, W.R. (1979). Cellular geography. In: Gale, S., Olsson, G. (Eds.), *Philosophy in Geography*. Reidel, Dordrecht.

Tomljenovic, I., Höfle, B., Tiede, D. and Blaschke, T. (2015). Building Extraction from Airborne Laser Scanning Data: An Analysis of the State of the Art. *Remote Sensing*. 7. 3826-3862. 10.3390/rs70403826.

Triantakonstantis, D. (2012). Urban Growth Prediction Modelling Using Fractals and Theory of Chaos. *Open Journal of Civil Engineering*. 02. 10.4236/ojce.2012.22013.

Union Internationale pour la conservation de la nature – UICN (International Union for the Conservation of Nature); <https://www.iucn.org/fr>

United Nations, World urbanization prospects: Department of Economic and Social Affairs, Population Division, 2018. <https://archive.is/wOOs1>

Varma, G. (2016). An Analysis on the Concept of Urban Densification and its Implications on Transportation. *Linkedin*. <https://www.linkedin.com/pulse/analysis-concept-urban-densification-its-implications-gautham-varma/>

Vemuri, V.R. and Rogers, R.D. (1994). *Artificial Neural Networks: Forecasting Time Series*, IEEE Computer Society Press, Los Alamitos, CA.

Wagner, D. F. (1997). Cellular Automata and Geographic Information Systems. *Environment and Planning B: Planning and Design*, 24(2), 219–234. <https://doi.org/10.1068/b240219>

Weisner C. and Cowen D. J. (1997). Modeling urban dynamics with artificial neural networks and GIS, *Ram mobile data USA*, Department of geography & liberal arts computing lab university of South Carolina, USA.

Weng, Q. (2002). Land use change analysis in the Zhujiang delta of China using satellite remote sensing, GIS, and stochastic modeling. *Journal of Environmental Management*, 64. 273-84. 10.1006/jema.2001.0509.

White, R. and Engelen, G. (1993). Cellular automata and fractal urban form: a cellular modelling approach to the evolution of urban land use patterns. *Environment and Planning A*, 1993, volume 25, pages 1175-1199.

Wolfram, S. (1983). Statistical Mechanics of Cellular Automata. *Reviews of Modern Physics*. 55 (3): 601–644. Bibcode: 1983RvMP.55.601W.

Wu, J.J., Adams, R.M. and Plantinga, A.J. (2004). Amenities in an urban equilibrium model: Residential development in Portland, Oregon. *Land Economics*, 80 (1): 19-32. <http://dx.doi.org/10.2307/3147142>

Yang, Q., Li, X. and Shi, X. (2008). Cellular automata for simulating land use changes based on support vector machines. *Computers & Geosciences*. 34. 592-602. 10.1016/j.cageo.2007.08.003.

Yang, X. and Lo, C. P. (2003). Modelling urban growth and landscape change in the Atlanta metropolitan area. *International Journal of Geographical Information Science* 17: 463–88

Yin, J., Yin, Z., Hu, X., Xu, S., Wang, J., Li, Z., Zhong, H. and Gan, F. (2011). Multiple scenario analyses forecasting the confounding impacts of sea level rise and tides from storm induced coastal flooding in the city of Shanghai, China. *Environmental Earth Sciences*. 63. 407-414. 10.1007/s12665-010-0787-9.

Youssoufi, S. and Antoni, J.p. (2009). Simulation as a prospective tool in urban planning, *Territoire, Images de franche-comté* - N° 39 - JUIN 2009

Zhao, Y., Yan, C., Zhou, X., Zhu, Q., Wang, S. and Guo. W., (2013). The research and development of 3D urban geographic information system with Unity3D. 21st International Conference on Geoinformatics. IEEE.

Zhu, Q., Hu, M., Zhang, Y. and Du, Z. (2009). Research and practice in three-dimensional city modeling. *Geo-spatial Information Science*. 12. 18-24. 10.1007/s11806-009-0195-z.

Zhuang, Xinyu & Zhao, Shichen. (2014). Effects of land and building usage on population, land price and passengers in station areas: A case study in Fukuoka, Japan. *Frontiers of Architectural Research*. 3. 10.1016/j.foar.2014.01.004.